

**Clinical, laboratory, and genetic studies of families with Charcot-
Marie-Tooth type 2C disease**

Guida Landouré

**A thesis submitted to the University College London for the degree of
Doctor of Philosophy**

August 2011

**Department of Medicine
University College London**

‘I, Guida Landouré, confirm that the work presented in this thesis is my own. Where information has been derived from other sources, I confirm that this has been indicated in the thesis.’

Dedication and acknowledgements

I dedicate this work to:

GOD the Almighty, the clement and merciful who gave me the chance and courage to accomplish this work, and to his Prophet Muhammad, Peace upon Him.

My parents: thanks for your unshakable love and support throughout my life.

All my relatives and friends: thanks for being there whenever I needed you.

My wife and son for their love and support.

My friend Addis Taye and our patient Kelly Clever (*in memoriam*).

First, my thanks to my supervisor Professor Robert Kleta. You have given me the chance to accomplish a dream that would be unlikely in other situations. It has sometimes been hard, but you have been patient and understanding to make this happen. Your sense of good and high standard work is remarkable.

I am thankful to my supervisor Professor John Hardy. Your guidance and encouragement throughout this work were most helpful.

To my scientific Godfather Dr. Kenneth Fischbeck: I met you when I did not know that a gene was made of exons and introns, but you have trusted me from the beginning and gave me an opportunity that not many would give to unskilled people like me. Thank you for your continued support. I will always be grateful to you.

To my mentor Dr. Charlotte Sumner: I still remember the day you handed me this project, and I was wondering why to a layperson as me. Thank you for all the knowledge learned.

Thank you for all your teaching, and above all for your friendship.

A special thanks to Professor Moussa Traoré for his continued support.

Many thanks to my co-workers at UCL and NIH, in particular Horia Stanescu and Barrington Burnett. Your presence and support helped me pass difficult moments.

I thank all the other people who worked in this project from the beginning to the end: Dr. Michael Caterina, Shelly Choo, Dr. Rachelle Gaudet, Dr. Henry Houlden, Hitoshi Inada, Lingling Kong, Dr. Christy Ludlow, Tara Martinez, Clare Munns, Rima Paudel, Christopher Phelps, Yijun Shi, and Dr. Anselm Zdebik.

Abstract

Charcot-Marie-Tooth disease type 2C (CMT2C) is an autosomal dominant neuropathy characterized by limb, diaphragm, and laryngeal muscle weakness. We studied five unrelated families with CMT2C, of which two showed significant linkage to chromosome 12q24.11. Linkage analysis excluded this locus in one of the remaining families, suggesting genetic heterogeneity within this CMT subtype. SNP genotyping of samples from affected individuals in the three linked families did not reveal any deletion or copy number variation. All genes in this region were sequenced and two heterozygous missense mutations were identified in the transient receptor potential, subfamily V, member 4 (*TRPV4*), at positions c.805C>T and c.806G>A in two families, predicting the amino acid substitutions R269C and R269H, respectively. Two other mutations (R186Q, R232C) and one change of uncertain significance (D584N) were subsequently identified. The R269C and R269H variants were not present in more than 200 controls. *TRPV4* is a well known member of the TRP superfamily of cation channels. We confirmed that it is expressed in motor and sensory neurons. The R186, R232, and R269 residues are located in the intracellular N-terminal portion of the *TRPV4* protein in the ankyrin repeat domain (ARD); functional domains known to mediate protein-protein interactions. When expressed in HEK293 cells and *Xenopus* oocytes, R269C and R269H *TRPV4* trafficked normally to the cell surface, but caused increased cell toxicity and increased constitutive and activated channel currents compared to wild-type *TRPV4*. Other mutations in *TRPV4* have been previously associated with inherited forms of skeletal dysplasia. When mapped onto the crystal structure of the *TRPV4* ARD, the mutations found in bone diseases lie on the opposite face of the domain compared to those causing neuropathy. Our findings indicate that *TRPV4* mutations cause a degenerative disorder of peripheral nerves. Thus, there is striking phenotypic variability with different mutations in this important channel protein.

Table of contents

1	Introduction.....	10
1.1	The nervous system.....	10
1.1.1	Neuron.....	10
1.1.2	The central nervous system.....	12
1.1.3	The peripheral nervous system	17
1.1.4	Histopathological responses of peripheral nerves to injury.....	21
1.1.5	Diseases of the peripheral nervous system	22
1.1.6	Approach to evaluation of peripheral neuropathies.....	26
1.1.7	Treatment of peripheral neuropathies	29
1.2	Charcot-Marie-Tooth disease (CMT)	29
1.2.1	Historical notes.....	29
1.2.2	General findings.....	30
1.2.3	Classification	30
1.2.4	Therapeutic approaches.....	47
1.3	Transient Receptor Potential (TRP) Channels.....	48
1.3.1	The canonical transient receptor potential channels (TRPC).....	52
1.3.2	Transient receptor potential vanilloid channels (TRPV).....	54
1.3.3	Transient receptor potential melastatin channels (TRPM)	58
1.3.4	Transient receptor potential ankyrin channel (TRPA)	61
1.3.5	Transient receptor potential polycystin channels (TRPP).....	62
1.3.6	Transient receptor potential mucolipin channels (TRPML).....	64
1.4	Objectives	65
2	Materials and Methods.....	66
2.1	Patients.....	66
2.2	Laboratory studies.....	72
2.2.1	Muscle and nerve biopsy.....	72
2.2.2	Nerve conduction studies (NCS) and electromyography (EMG).....	72
2.2.3	Fiberoptic nasolaryngoscopy.....	74
2.2.4	Radiological evaluation	75
2.2.5	DNA extraction	75
2.2.6	Skin biopsy	75
2.2.7	Immortal cell lines establishment	75

2.3 Genetic analysis	76
2.3.1 Linkage analysis/Fine mapping	76
2.3.2 Single Nucleotide Polymorphism (SNP) array analysis	77
2.3.3 Selection of candidate genes	77
2.3.4 Mutation detection	78
2.3.5 Exome sequencing	79
2.4 Functional studies of mutants TRPV4	80
2.4.1 TRPV4 expression in the nervous system.....	80
2.4.2 Expression of WT and mutant TRPV4 in <i>Xenopus</i> oocytes and mammalian cells	81
2.4.3 TRPV4 blockers	82
2.4.4 Cell death quantification.....	82
2.4.5 Immunohistochemistry	83
2.4.6 Cell surface biotinylation.....	83
2.4.7 Endoplasmic Reticulum (ER) stress experiment	84
2.4.8 Intracellular calcium measurement.	85
2.4.9 Electrophysiology	86
2.4.10 Protein structure determination.....	88
2.4.11 TRPV4-ARD expression and purification.....	88
2.4.12 Co-immunoprecipitation	89
2.4.13 Protein binding assays	90
2.5 Statistical analysis	90
3 Results.....	91
3.1 Patients.....	91
3.1.1 General findings.....	91
3.1.2 Case presentations:.....	102
3.2 Genetic analysis:	109
3.2.1 Linkage analysis/Fine mapping	109
3.2.2 SNP arrays analysis	115
3.2.3 Selection of candidate genes	116
3.2.4 Mutation detection by Sanger sequencing	120
3.2.5 Exome sequencing	122
3.3 Functional studies	123

3.3.1	<i>Expression analysis</i>	123
3.3.2	<i>Analysis of WT and mutant TRPV4 in transfected mammalian cells</i>	125
3.3.4	<i>Cell calcium measurement</i>	137
3.3.5	<i>Chicken TRPV4-ARD structure determination</i>	139
3.3.6	<i>Protein binding assays and co-immunoprecipitation</i>	140
4	Discussion.....	142
4.1	Clinical and laboratory findings.....	142
4.2	Genetic analysis.....	152
4.3	Gene sequencing.....	154
4.4	Functional studies.....	160
4.5	Calcium and neurodegeneration.....	169
4.6	TRP channels and diseases.....	172
4.7	Channelopathies and therapeutic future.....	177
4.8	Conclusion.....	178
4.9	Future directions.....	179
5	References.....	180
6	Publications that have arisen from the thesis.....	198

Table of figures

Figure 1 Diagram representing a myelinated motor neuron.	11
Figure 2 Representation of different parts of the brain. (Crossman A. R. 2010b).....	14
Figure 3 Representation of a transverse section of the spinal cord. (Crossman 2010c)	17
Figure 4 Anatomy of a peripheral nerve (Felten D. L. 2010).	18
Figure 5 Typical thoracic spinal nerve and its branches (Parent 1996).	19
Figure 6 Diagram showing the brachial plexus and peripheral nerves of the forearm.	20
Figure 7 Diagram of basic pathologic processes affecting peripheral nerves.	22
Figure 8 CMT genes involved in the peripheral nerve structure and function (Patzko and Shy 2011).	47
Figure 9 Structures of the mammalian TRP subfamilies.	52
Figure 10 Pedigree of family F1.	67
Figure 11 Pedigree of family F2.	68
Figure 12 Pedigree of family F3.	69
Figure 13 Pedigree of family F4.	70
Figure 14 Pedigree of family F5.	71
Figure 15 Phenotypic characteristics of family F1.	92
Figure 16 Muscle and nerve biopsy.	93
Figure 17 Haplotype reconstruction for family F1.	111
Figure 18 Haplotype reconstruction for family F2.	112
Figure 19 Haplotype reconstruction for family F4.	113
Figure 20 LOD score curve for family F1 and F2.	114
Figure 21 Summary of linked regions in family F1, F2, and F4.	115
Figure 22 Part of the haplotype reconstruction in family F5.	116

Figure 23 Chromatographs representing the mutations found by Sanger sequencing.	121
Figure 25 Quantification of TRPV4 transcript by quantitative RT-PCR.	124
Figure 26 TRPV4 expression in mouse spinal cord ventral horn motor neuron.	125
Figure 27 The CMT2C mutations do not change TRPV4 trafficking.	127
Figure 28 Staining of transfected HeLa cells with ER and Golgi markers.....	128
Figure 29 Immunodetection of TRPV4 proteins in HeLa cells.	129
Figure 30 Mutant TRPV4 is not retained in the ER.	130
Figure 31 Mutant TRPV4 causes cell toxicity in non-neuronal and in neuronal cells.	131
Figure 32 CMT2C mutations cause cell death that is prevented by TRPV channel blockers.	132
Figure 33 Mutant TRPV4 toxicity in <i>Xenopus</i> oocytes is blocked by ruthenium red.	133
Figure 34 The R269C and R269H mutations cause increased TRPV4 channel activity in <i>Xenopus</i> oocytes.	135
Figure 35 The R269C and R269H mutants cause increased TRPV4 channel activity in HEK293 cells.	136
Figure 36 HEK293 cells expressing mutant TRPV4 have higher basal calcium levels than WT expressing cells.	138
Figure 37 Localization of CMT2C and skeletal dysplasia TRPV4 mutations in the chicken Trpv4 ankyrin repeat domain crystal structure.....	139
Figure 39 Surface representation of the chicken TRPV4 ARD showing neurological and bone diseases mutations.	166
Figure 40 Comparisons of the chicken TRPV4 ARD structures to that of other TRPV proteins.....	168

List of tables

Table 1 Symptoms and signs seen in peripheral neuropathies	26
Table 2 Genetic and clinical features of CMT types	46
Table 3 Classification and pathogenesis of TRP channels	51
Table 4 Summary of the clinical features in CMT2C patients.	99
Table 5 Summary of laryngological examination findings in CMT2C patients.....	100
Table 6 Summary of nerve conduction studies findings in CMT2C patients.....	101

1 Introduction

1.1 The nervous system

The human nervous system consists of a central nervous system, the brain and spinal cord; and a peripheral nervous system, including cranial and spinal nerves. The autonomic or involuntary system is considered to be part of the peripheral nervous system.

1.1.1 Neuron

Neurons are the basic constituents of the nervous system, which include brain, the spinal cord, and the peripheral ganglia. There are motor, sensory, and inter neurons, each divided into three parts: a cell body called soma, dendrites that are filaments that arise from cell body and receive the input of the neuron, and an axon that carries the nerve signals away from the cell body (Figure 1). Neurons are electrically excitable cells, allowing them to produce and conduct the regenerative electrical signals called action potentials.

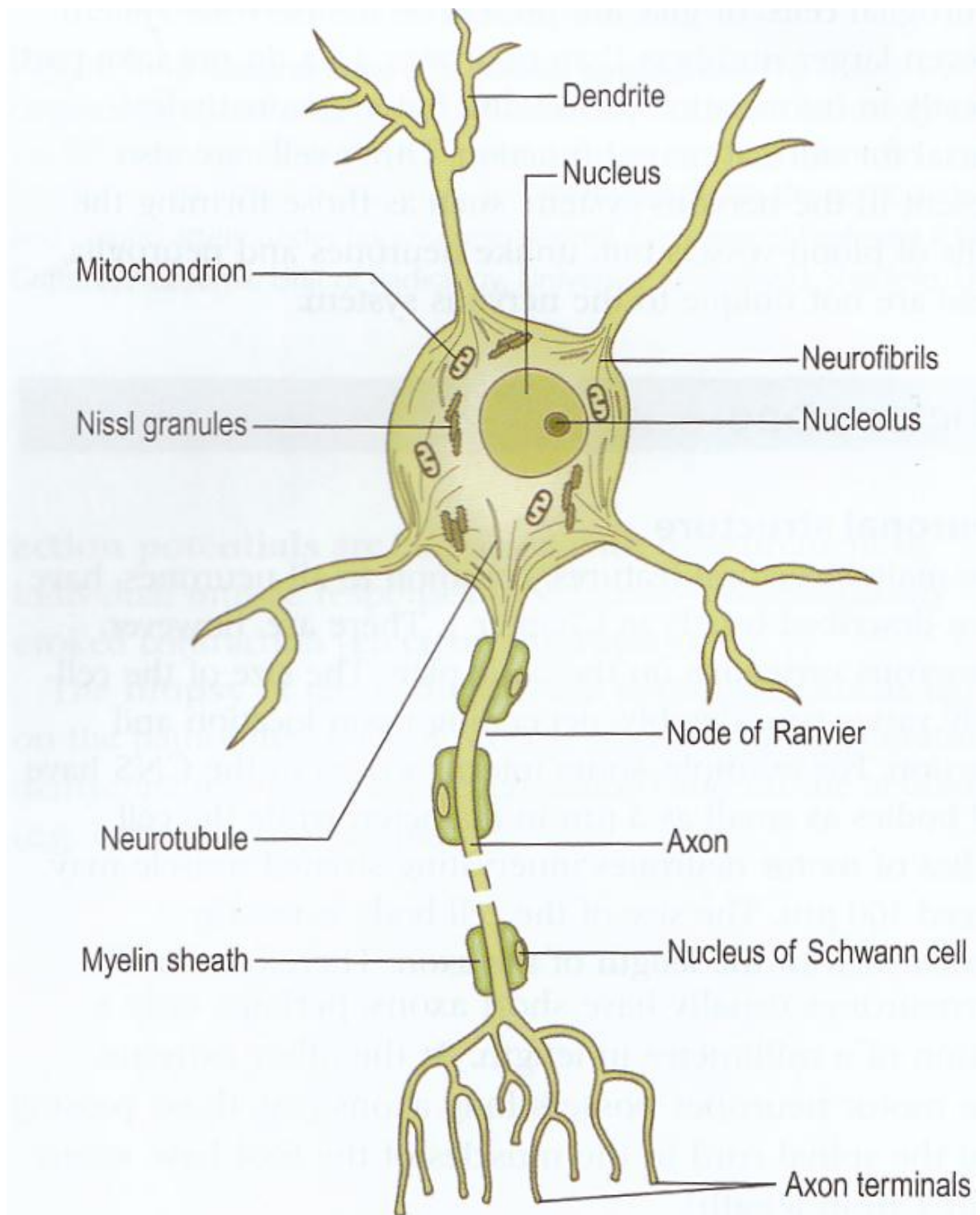


Figure 1 Diagram representing a myelinated motor neuron.
(Crossman 2010a)

1.1.2 The central nervous system

The central nervous system (CNS) consists of the brain and the spinal cord.

The brain

Human brain consists of six parts: the telencephalon (cerebral hemispheres), the diencephalon (thalamus and hypothalamus), mesencephalon (midbrain), the cerebellum, the pons, and the medulla oblongata.

The cerebral cortex

The cerebral cortex contains sensory areas and areas concerned with motor activity.

Sensory areas include primary sensory areas and secondary sensory areas. The primary sensory areas are constituted with the cortical regions to which impulses that convey specific sensory modalities are projected. These areas play the role of integrating the sensory experience and the discriminative qualities of sensation. Primary sensory areas include the somesthetic area that consists of the postcentral gyrus and its medial extension in the paracentral lobule, the visual or striate area located along the lips of the calcarine sulcus, the auditory area located on the two transverse gyri, the gustatory area localized to most ventral part of the postcentral gyrus, the olfactory area that consists of the allocortex of the prepyriform and the periamygdaloid regions.

Motor areas convey impulses related to motor function, modification of muscle tone and reflex activity, modulation of sensory impulses, and the alteration of the sense of awareness. Motor areas include the primary motor area, the premotor area, the supplementary motor area, and the cortical eye fields. The primary motor area or area 4 of Brodmann is located on the anterior wall of the central sulcus and adjacent portions of the precentral gyrus. Lesions of the primary motor area produce flaccid paralysis of the contralateral limbs, marked hypotonia, and loss of superficial and myotatic reflexes.

The diencephalon

Consisting of the thalamus and hypothalamus, the diencephalon is the most rostral part of the brain stem. The thalamus consists of three separate nuclei; the ventral posterior nucleus, the ventral lateral nucleus, and the ventral anterior nucleus. All sensory impulses terminate in the gray masses of the thalamus, except the olfactory impulses. The hypothalamus is involved in the visceral, autonomic and endocrine functions.

The mesencephalon

Also known as midbrain, the mesencephalon is divided into three parts: the tectum, the tegmentum, and the crura cerebri. The tegmentum and crura cerebri are separated by the substantia nigra, a large nucleus in the midbrain. Two cranial nerves, the trochlear and oculomotor nerves arise in the midbrain. But, the midbrain contains important relay nuclei for the auditory and visual systems.

The cerebellum

The cerebellum is the organ of coordination, equilibrium and muscle tone. The cerebellum contains a median portion, cerebellar vermis, and two lateral lobes, cerebellar hemispheres. The cerebellar vermis controls mostly the posture and the cerebellar hemispheres control the equilibrium.

The pons

Also known as metencephalon, the pons represents the rostral part of the hindbrain. It is divided into two parts: a dorsal portion, the pontine tegmentum, and a ventral portion or the proper pons. Nuclei of cranial nerves including the facial, the abducens, the trigeminal and the cochlear are found in this part of the brain stem.

The medulla

The medulla or myelencephalon is the most caudal brain stem segment. It is the part that links the spinal cord to the brain. The medulla is home of some cranial nerves, including the hypoglossal, the spinal accessory, the vagus, and the glossopharyngeal.

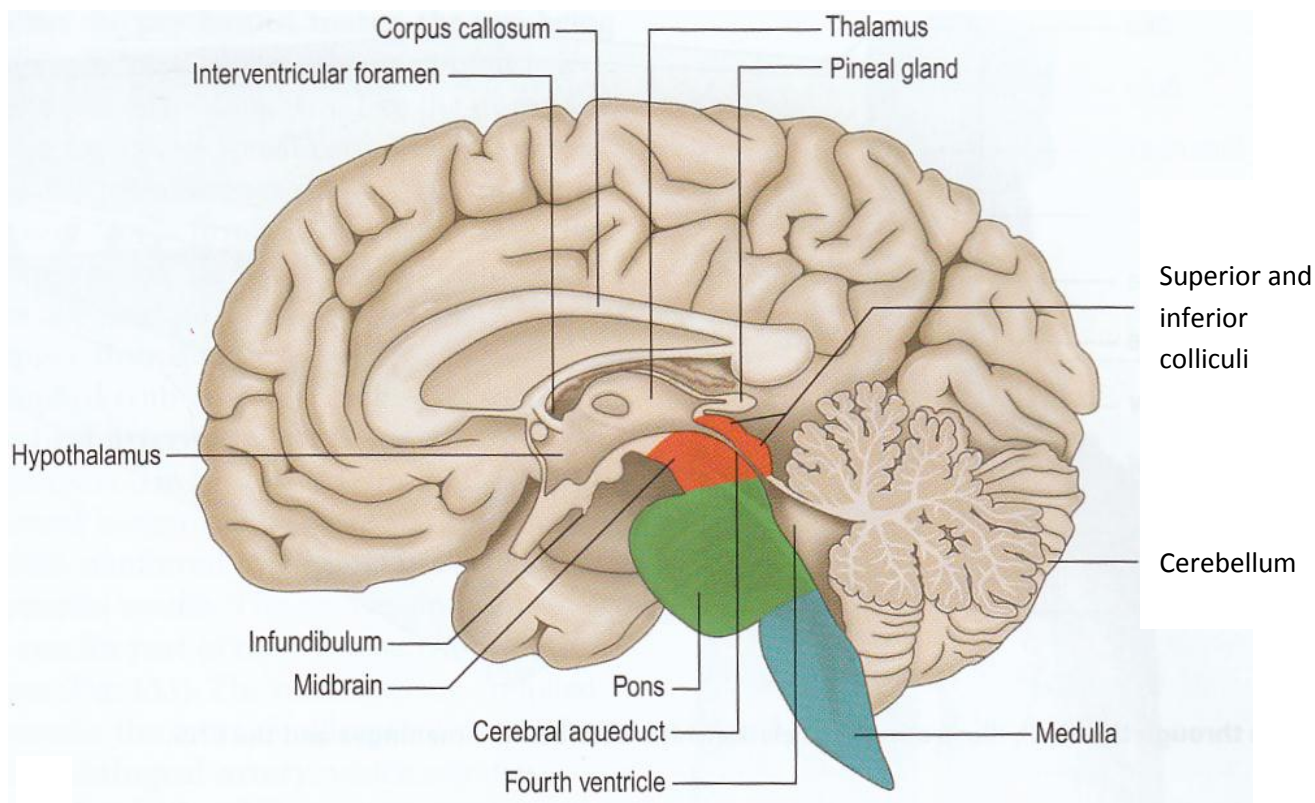


Figure 2 Representation of different parts of the brain. (Crossman A. R. 2010b)

The spinal cord

The spinal cord, like all of the central nervous system, is derived from the embryonic neural tube. It is the main pathway for information connecting the brain to the peripheral nervous system. The spinal cord is surrounded by three layers, dura mater, pia mater, and arachnoid mater; and lies loosely in the vertebral canal. It is about 45 cm long in men and 43 cm in women and extends from the foramen magnum to the first or second lumbar vertebra. The spinal cord has an ovoid shape, and has two spindle-shaped swellings located in the cervical (C4 to T1) and lumbar (T9 to T12) regions. The spinal cord contains 33 segments corresponding to the 31 nerve pairs. The last 3 coccygeal segments come together to form a single segment. The cord furnishes dorsal and ventral root filaments to form a single pair of nerves. There are 8 cervical, 12 thoracic, 5 lumbar, 5 sacral and usually 1 coccygeal spinal nerves.

In transverse section, the spinal cord consists of a peripheral region made of the neuronal white matter containing sensory and motor neuron axons and myelin (it is white because of the myelin). The central part consists of butterfly-shaped gray

substance made of nerve cell bodies and their processes, and surrounds the central canal; which is an extension of the ventricles located in the brain.

The gray substance consists of cell columns which have a posterior (dorsal) column or horn, an anterior column, and, in the thoracic segments, a small pointed lateral horn.

The white matter is divided into three paired funiculi: posterior funiculus (between posterior horn and posterior median septum), lateral funiculus (between dorsal root entry zone and the ventral root fibres emerging site), and the anterior funiculus (between the anterior median fissure and the emerging ventral root filaments). The white matter contains ascending and descending fibre bundles called tracts or fascicles occupying its particular regions.

Ascending spinal tracts

Posterior white columns and medial lemniscus tract convey touch, proprioception and vibration sense impulses. In this pathway, a primary neuron's axon enters the spinal cord and then enters column. Lesions involving the posterior columns diminish or abolish discriminating tactile sense and kinesthetic sense, mostly in the distal parts of extremities. Loss of position in lower limbs impairs gait, and is called posterior column ataxia.

The anterior spinothalamic tract conveys light touch impulses. This is closely associated with the medial lemniscus in the pons and midbrain, and terminates upon cells of the ventral posterolateral nucleus (VPL) of the thalamus.

The lateral spinothalamic tract transmits impulses associated with pain and thermal sense. This tract sends branches in the brain stem whereas its main fibres terminate in the VPL of the thalamus. Unilateral section of this tract leads to loss of pain and thermal sense on the opposite side of the body beginning about one segment below the level of the lesion.

The posterior spinocerebellar tract arises from the large cells of the dorsal nucleus of Clarke and does not cross; it ascends along the posterolateral periphery of the spinal cord. Impulses transmitted via this tract are related to touch and pressure receptors in skin. Impulses conveyed by this tract do not reach the conscious level.

The anterior spinocerebellar tract ascends along the lateral periphery of the spinal cord anterior to the posterior spinocerebellar tract. Other spinal tracts are usually involved during anterior spinocerebellar tract injury, making it difficult or impossible to clinically differentiate its injury.

Descending spinal tracts

The descending spinal tracts mediate motor function, visceral innervations, muscle tone, segmental reflexes, and central transmission of sensory impulses. These tracts consist of fibres arising mostly from the cerebral cortex (corticospinal system), the midbrain (tectospinal, interstitiospinal, and rubrospinal tracts), and the pons (vestibulospinal and reticulospinal tracts).

The corticospinal system consists of the largest and most important tracts. These tracts pass through the medullary pyramid and enter and descend in the spinal cord. The corticospinal tract undergoes an incomplete decussation at the junction of medulla and spinal cord and divides into three separate tracts: the lateral corticospinal tract, the anterior corticospinal tract, and the anterolateral corticospinal tract. The lateral corticospinal tract is crossed and is the largest tract. It descends the length of the spinal cord, gives off fibres to spinal gray at all levels, and progressively diminishes in size at more caudal levels. The anterior corticospinal tract is smaller and is uncrossed. It is located in an area adjacent to the anterior median fissure and is mostly visible in cervical segments. The anterolateral corticospinal tract is the smallest tract descending in a more anterior position than the lateral corticospinal tract. Its fibres do not cross and terminate in the base of the posterior horn, the intermediate gray and central parts of the anterior horn. The corticospinal tract is considered the descending pathway conveying voluntary, discrete, skilled movements. Lesions of parts of this tract at any level lead to paresis of variable degrees associated with loss of muscle tone followed by gradually increased tone, increased tendon reflexes, loss of superficial abdominal and cremasteric reflexes, and the Babinski sign (the appearance of an extensor toe response on stroking the sole of the foot).

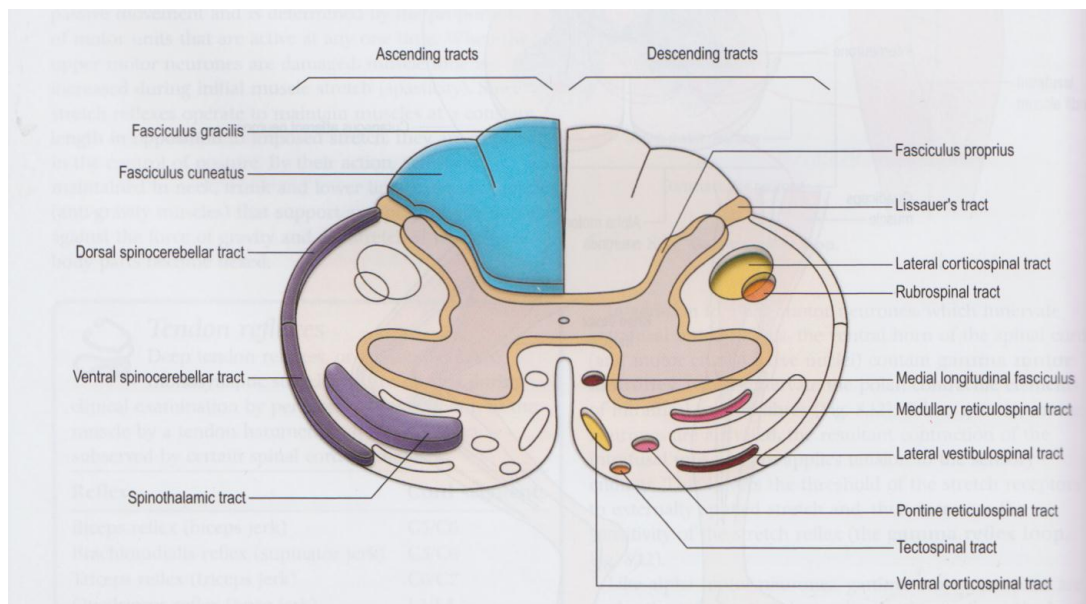


Figure 3 Representation of a transverse section of the spinal cord. (Crossman 2010c)

1.1.3 The peripheral nervous system

The peripheral nervous system (PNS), in anatomical terms, consists of those parts of the nervous system in which neurons or their processes are related to the peripheral satellite cell, the cell of Schwann. It thus comprises the cranial nerves (except for the second nerve), the spinal nerve roots, the dorsal root ganglia, the peripheral nerve trunks and their terminal ramifications and the peripheral autonomic system. Peripheral nerves are divided into two main groups: the somatic nerves and autonomic nerves. Somatic nerves comprise of motor nerves that control muscles and sensory nerves that carry sensations such as heat, pain, and touch to the central nervous system. Autonomic nerves are divided into sympathetic and parasympathetic nerves that control autonomic functions including blood pressure, digestion, and bladder function.

Structurally, a peripheral nerve or nerve consists of many axons surrounded by a layer called endoneurium. Axons are grouped in a fascicle wrapped in a layer called perineurium. Externally, the whole nerve is surrounded by another layer called epineurium (Figure 4) (Felten D. L. 2010).

Axon

An axon is a wiring of a neuron that conducts electrical impulses away from the neuron's cell body. Axons are thin in diameter, about 1 μm , but long, attaining in some cases several feet. They make contact with other cells such as other neurons,

muscles and glands through junctions called synapses. Axons are sheathed in myelin, but also contain unmyelinated segments called nodes of Ranvier. Action potentials are amplified at the nodes of Ranvier and transmitted down the axon. Myelinated axons appear in white, making up the “white matter”.

Myelin

Myelin is an electrically insulating material that forms a layer called myelin sheath around the axon. In the peripheral nerves it is formed by a type of glial cells called Schwann cells, and contributes to a rapid propagation of electrical impulses by a mechanism called saltation. The role of the myelin is to increase the speed at which an impulse is propagated.

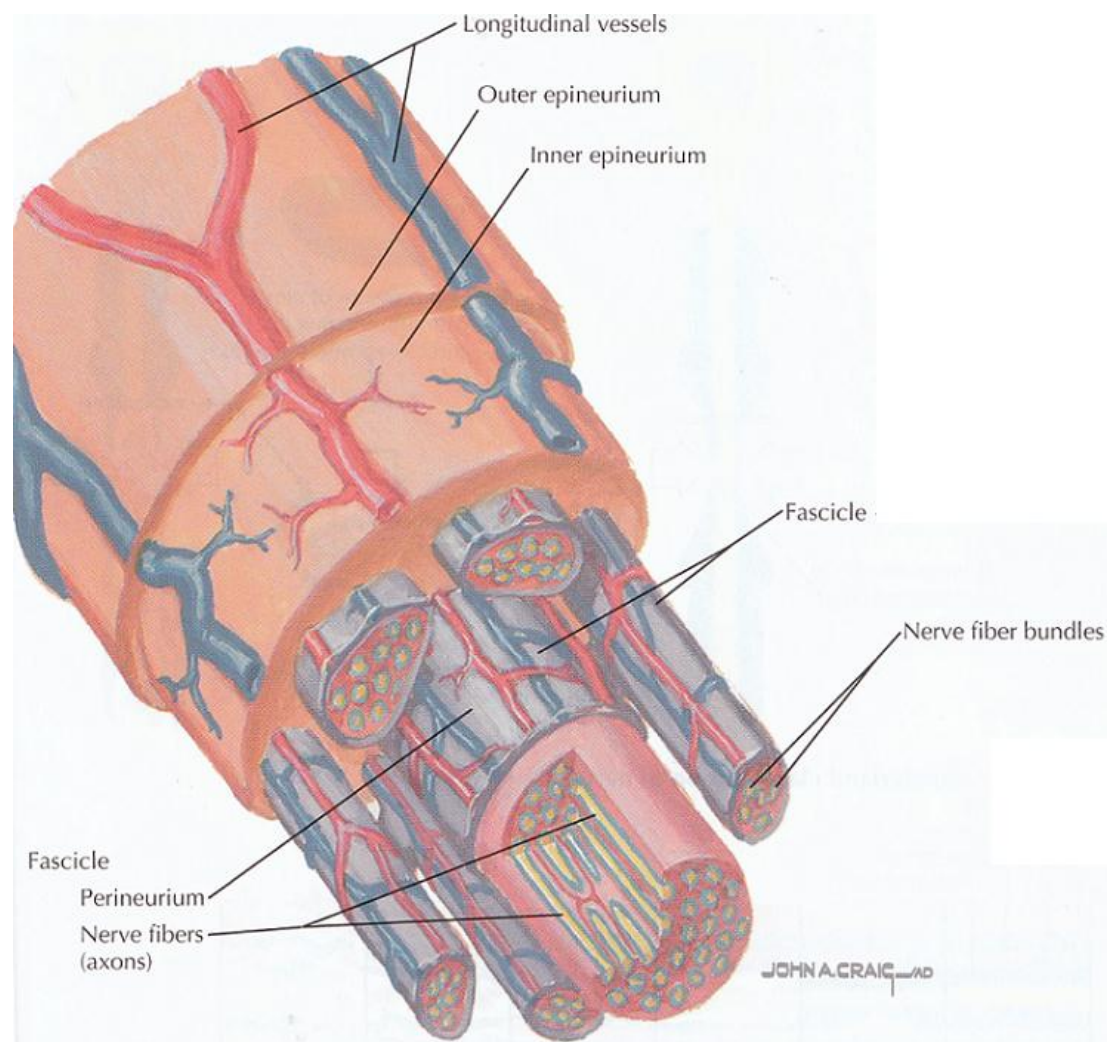


Figure 4 Anatomy of a peripheral nerve (Felten D. L. 2010).

Peripheral nerves are categorized into groups based on the direction they transmit signals and based on where they connect to the central nervous system. Based on the direction they conduct signals there are afferent nerves that conduct signals from sensory neurons to the central nervous system and efferent nerves that conduct signals from central nervous along motor neurons to the peripheral organs such as muscles and glands. However, there are also mixed nerves that play both afferent and efferent functions.

Based on where they connect to the central nervous system there are spinal nerves that originate from the spinal cord and are formed by the joining of ventral roots (motor) and dorsal roots (sensory) (Figure 5) (Parent 1996) and cranial nerves that connect directly to the brain, mostly the brain stem. While spinal nerves are numbered according to the vertebra through which they connect to the spinal cord, cranial nerves are assigned numerals (1 to 12) and have also descriptive names according to the muscle they innervate or the function they perform.

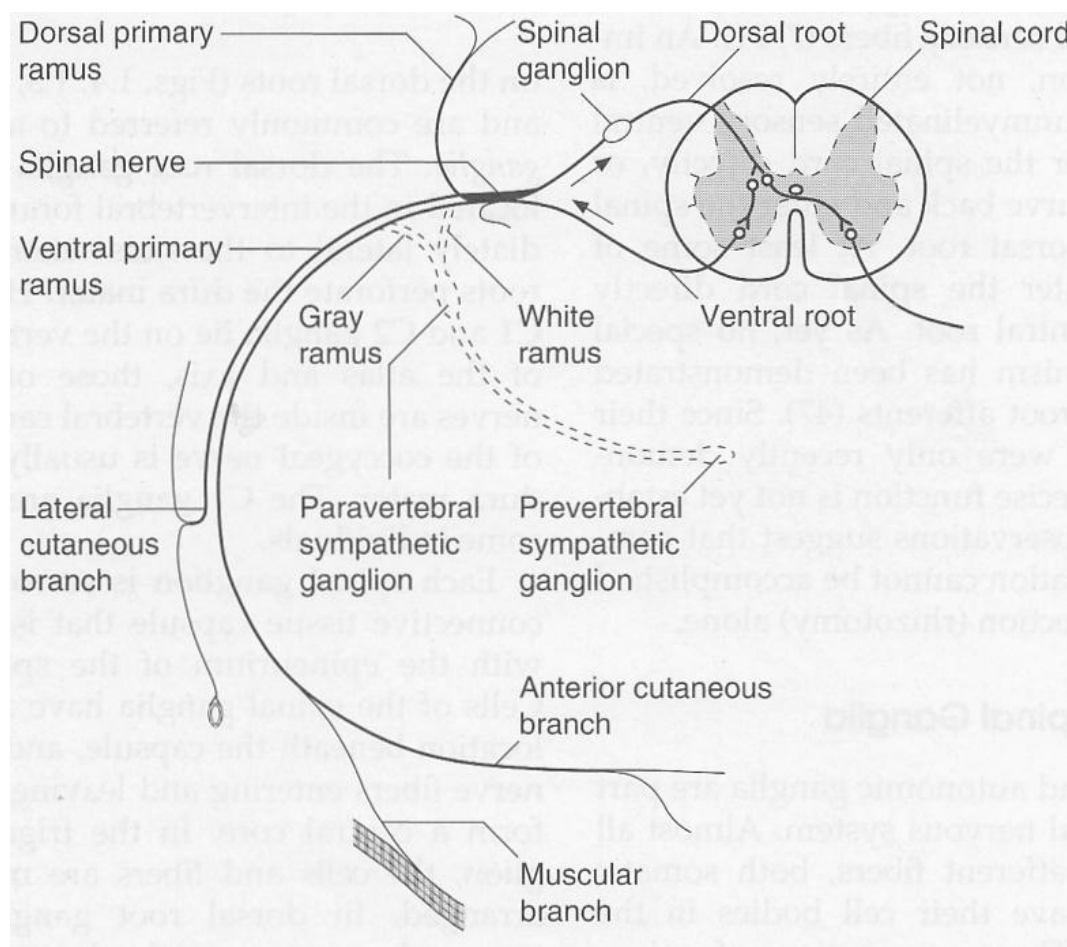


Figure 5 Typical thoracic spinal nerve and its branches (Parent 1996).

At cervical and lumbar levels, the spinal nerves combine to form a network of intersecting nerves called brachial and lumbosacral plexus. Distal to the plexus, nerve fibres branch to form individual peripheral nerves such as median, ulnar and radial nerves of the forearm and peroneal and tibial nerves of the lower leg (Figure 6) (Parent 1996).

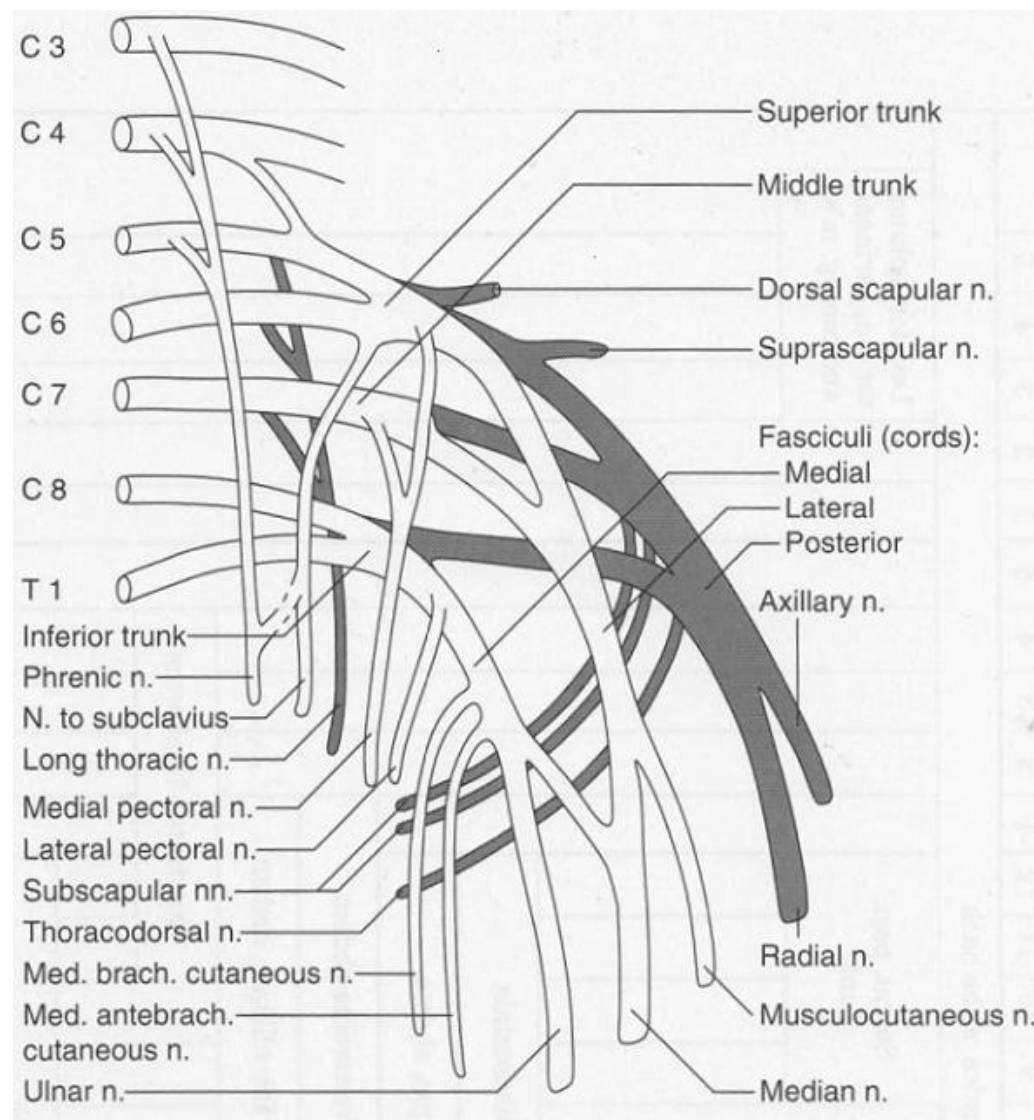


Figure 6 Diagram showing the brachial plexus and peripheral nerves of the forearm. The posterior divisions, posterior cords, and peripheral nerves formed from the posterior divisions are shaded. Cords and peripheral nerves formed from the anterior divisions of the ventral primary rami are in white (Parent 1996).

1.1.4 Histopathological responses of peripheral nerves to injury

Diverse mechanisms lead to nerve injury: inflammatory, metabolic, toxic, ischemic, infectious, traumatic, compressive, inherited, and paraneoplastic. The motor nerves, the sensory nerves or both can be affected and either the myelin sheaths or axons, separately or concurrently, can be at fault (Figure 7) (Adams 1993). This results in axonal degeneration or demyelination or both.

Wallerian degeneration

Wallerian degeneration is a sequence of axonal and myelin degeneration. It was named after Augustus Holney Waller who, in 1850, observed axonal degeneration and myelin disintegration when he severed the glossopharyngeal and hypoglossal nerves in frogs. Wallerian degeneration occurs distal to the site of injury, usually within 24-36 hours after an axonal injury. The part of the axon separated from the cell body degenerates distally to the site of injury leading to a phenomenon called anterograde degeneration. Within hours, accumulation of organelles and mitochondria in paranodal regions near the injury takes place. There is a loss of structure of the endoplasmic reticulum and a degradation of neurofilaments associated with calcium influx and activation of calpain. The axon becomes fragmented and phagocytosed. The myelin sheath does not degenerate and remains as an empty tube towards which nerve fibres send out sprouts. Schwann cells proliferate and produce growth factors that attract these sprouts until they reach the target tissue which they innervate at a pace of 1 mm a day. However, Schwann cells atrophy and disappear in the absence of axonal regeneration. The regeneration is faster in the peripheral nervous system than in the central nervous system because in the central nervous system, myelin sheaths are produced by oligodendrocytes and not Schwann cells.

Axonal degeneration

Axonal degeneration can occur independently of Wallerian degeneration such as in distal axonopathy. This is seen in polyneuropathies where distal parts of axons are first affected leading to the condition called “dying back” axon; leading to symptoms in the distal part of the body (stocking-glove). Here too neurofilaments and organelles accumulate in the axon, leading to axonal atrophy and breakdown, eventually. As axonal degeneration advances, axons will lose their myelin leading to demyelination

Segmental demyelination

As it is called, in segmental demyelination there is a breakdown and loss of myelin over a few segments while the axon and neuronal body remain intact. However, a long-lasting severe demyelination may lead to axonal loss. Because myelin is responsible for salutatory conduction propagation, segmental demyelination leads to reduced conduction velocity and conduction block. Repetitive segmental demyelinations can lead to formation of concentric layers of Schwann cells and collagen around the axon called “onion bulbs”, and thickening of peripheral nerves also known as hypertrophic neuropathy. Both processes are histological hallmarks of hereditary neuropathies including some Charcot-Marie-Tooth disease sub-types.

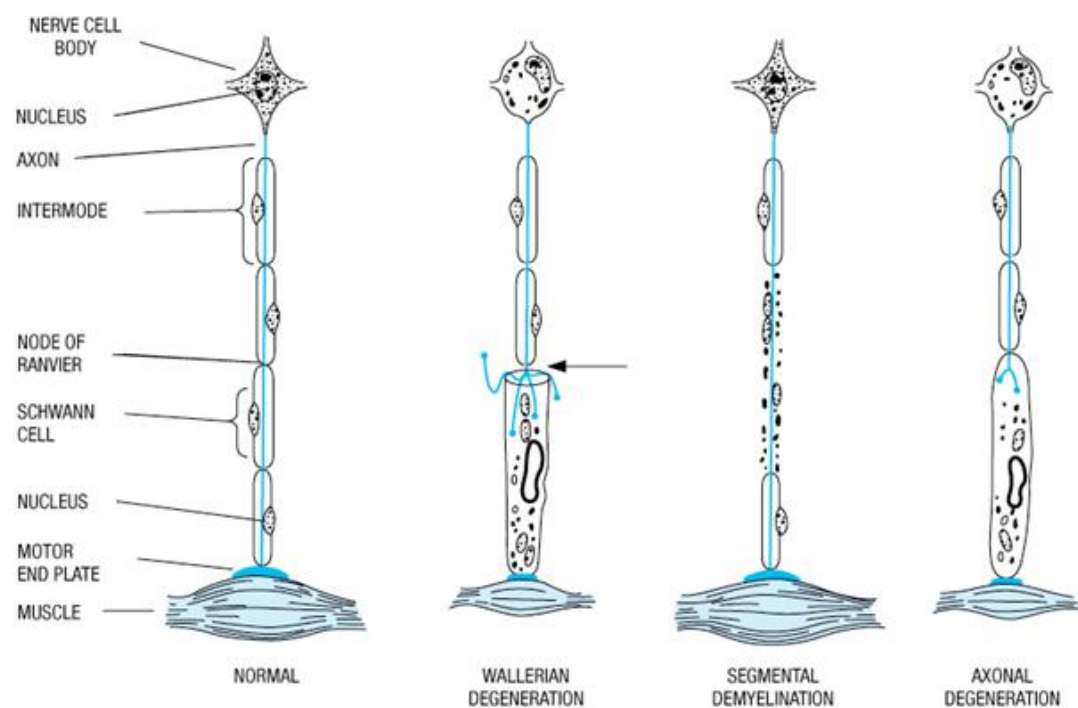


Figure 7 Diagram of basic pathologic processes affecting peripheral nerves.

In Wallerian degeneration, the arrow is showing the site of axonal interruption distal to which there is degeneration of the axis cylinder and myelin, and central chromatolysis. In segmental demyelination, the axon is spared. Axonal degeneration leads to distal degeneration of myelin and axis cylinders resulting to a neuronal disease. As seen in the diagram, both Wallerian degeneration and axonal degeneration lead to muscle atrophy (Adams 1993).

1.1.5 Diseases of the peripheral nervous system

Technically, a peripheral neuropathy can be any disorder, either focal or generalized, that causes damage to the nerve fibres within the PNS. The definition is not always

clear as disorders that lead to primary degeneration of the anterior horn cells such as spinal muscular atrophy are sometimes referred to as motor neuropathies. Conditions that lead to loss of the whole neuron (cell body and axons) are referred to as neuronopathies.

There are numbers of ways in which the PNS can malfunction: as part of an isolated peripheral nerve disorder (mononeuropathy or mononeuropathy multiplex), a general neurological disorder or a systemic condition (polyneuropathy). These conditions can be acquired (diabetic, infectious, toxic, and metabolic) or, of interest to our study, genetic (inherited motor or sensory neuropathies and inherited motor and sensory neuropathies). Symptoms and signs linked to motor fibres involvement are muscle weakness and atrophy, fasciculations and muscle cramp, and loss of motor functional abilities including walking and fine motor skills. In sensory fibres involvement, symptoms and signs differ according to the type of fibres affected. Large fibre involvement leads to numbness, inability to determine joint position sense with resulting incoordination and ataxia, poor vibration sensibility, and loss of tendon reflexes whereas damage to small fibres manifests with paresthesias, numbness, burning or cold sensations, “lightening” pains, loss of pinprick and temperature sensibility. Because the autonomic nervous system controls involuntary and semi-involuntary function, damage to autonomic fibres manifests with abdominal bloating, constipation, diarrhea, dizziness and fainting associated with a fall of blood pressure, urinary hesitancy, sexual dysfunction, decreased sweating and dry mouth.

Peripheral neuropathies can be classified according to the pattern of their occurrence (mono or polyneuropathy), the type of fibre involved (motor, sensory, autonomic), the time course (acute, subacute, chronic, very chronic), the pathological features (axonal, demyelinating), and the aetiology (diabetic, inflammatory, infectious, toxic, genetic).

Mononeuropathy

Mononeuropathy is damage to a single nerve or nerve group, and results in loss of movement, sensation or other functions of regions innervated by the nerve or nerve group. The most common cause of mononeuropathy is compression also known as compression neuropathy. Single nerves susceptible to entrapment or compression are the median nerve causing neuropathy called “carpal tunnel syndrome” at wrist, and characterized by pain, numbness, and weakness in hand in the 1st three digits, the ulnar nerve causing neuropathy at elbow, and characterized by pain, numbness and

weakness in hand in the 4th and 5th digits, the radial nerve causing radial palsy, and characterized by wrist drop commonly called “Saturday night palsy”, the peroneal nerve causing neuropathy at the fibular head and leading to foot drop, and the lateral cutaneous femoral nerve causing the so-called “meralgia paresthetica”. Although mononeuropathies can be caused by chronic stress at the nerve crossing or route, mononeuropathies can also be caused by traumatic injuries.

Traumatic neuropathies are examples of mononeuropathies. They can be complete leading to total loss of motor and sensory function or incomplete with some sparing of nerve function. Some examples of traumatic neuropathies are stretch brachial plexus injury during birth or motorcycle accident, fracture of humerus resulting in radial nerve palsy, fracture or dislocations of hip resulting in sciatic nerve palsy, and fracture of fibula resulting in femoral palsy.

Mononeuropathy multiplex

Mononeuropathy multiplex is damage to at least two individual nerve distributions serially or concurrently in a multifocal pattern. It usually presents with acute or subacute loss of sensory and motor function of individual nerves, and is often associated with pain. At the beginning, symptoms present in an asymmetrical pattern, but become more confluent and symmetrical later as the disease progresses; thus, making it difficult to differentiate from polyneuropathy. Mononeuropathy multiplex are often axonal neuropathies, and are caused or associated with diverse medical conditions, including diabetes mellitus, vasculitides (polyarteritis nodosa, Sjögren’s syndrome, Wegener granulomatosis), infectious diseases (leprosy, HIV), immune-mediated diseases (sarcoidosis, lupus erythematosus), and genetic disorders (hereditary neuropathy with liability to pressure palsy). Leprous neuropathy is an example of mononeuropathy multiplex.

Leprous neuropathy

Leprosy is an infectious disease caused by *Mycobacterium leprae*, and leprosy neuropathy is a leading cause of neuropathy worldwide. It is characterized by an early involvement of unmyelinated cutaneous nerve fibres and their Schwann cells resulting to a superficial loss of sensation and numbness. If not treated, the disease becomes debilitating leading to shortened extremities such as fingers, toes or nose.

Polyneuropathy

Polyneuropathy is a generalized disorder in which many nerve fibres of different parts of body are affected. However, not all nerve cells are affected altogether in any case of polyneuropathy. For example in distal axonopathy, the most common pattern of polyneuropathy, while cell bodies remain intact, only axons are affected in proportion to their length. This results in symptoms that occur first and most severely in feet, and, eventually, in a “stocking-glove” pattern of symptoms. The second pattern is demyelinating neuropathies in which the myelin sheath around axons is affected. Although axons are not damaged, their ability to transmit electrical impulses will be impaired. In the third pattern, cell bodies are directly affected, leading to situations called motor neuron disease or sensory neuronopathy. Polyneuropathies cause diffuse often symmetrical symptoms resulting in weakness, atrophy and sensory loss in more than one body part. The aetiology of polyneuropathies are diverse, including diabetic, toxic (pharmaceuticals, toxins, industrial agents), nutritional or metabolic (e.g., alcoholic, vitamin deficiency or excess, uremia, porphyria), infectious (HIV or HIV drug-induced neuropathy), inflammatory (Guillan-Barré syndrome) and inherited (hereditary motor and sensory neuropathy or Charcot-Marie-Tooth disease). In this section, we will review diabetic polyneuropathy and the Guillan-Barré syndrome, and in the next section we will review Charcot-Marie-Tooth diseases.

Diabetic polyneuropathy

Diabetic polyneuropathy is the most common polyneuropathy affecting up to 50 % of patients with polyneuropathy. It can manifest as pure small fibres neuropathy or sensorimotor axonal neuropathy. Diabetic polyneuropathy can also occur in the pre-diabetes status such as in the impaired glucose tolerance. The onset is insidious, and distal parts of the body are first affected. Sensory symptoms including numbness, sensory loss, dysesthesia and night time pain appear early in a glove-stockings distribution fashion while motor ones occur later, and autonomic involvement can sometimes be noticed.

Guillan-Barré Syndrome

Guillan-Barré syndrome is an acute inflammatory demyelinating neuropathy caused by an autoimmune attack against peripheral nerves. It is the most common cause of acute neuromuscular paralysis. The disease can be triggered by preceding viral infection that may pass unnoticed. Most commonly, the disease progresses in an

ascending flaccid paralysis fashion over days. Large fibres are most affected leading to loss of tendon reflexes, vibratory sense and proprioception, and conserved temperature and pain sensibility. Nerve conduction studies show evidence of segmental demyelination at nerve root and peripheral nerve. Most patients make a full or substantial recovery.

1.1.6 Approach to evaluation of peripheral neuropathies

As reviewed in Adams and Victor's Principles of Neurology (Adams 1993), the diagnosis of a peripheral neuropathy is based on certain points:

- Determine whether the central or peripheral nervous systems are affected. History, the most important part of the evaluation, contributes to 85 % of a correct diagnosis. History taking should be directed at elucidating the anatomical location of the complaints, central versus peripheral and systemic versus focal.
- Determine based on symptoms and signs which nerve fibres are affected; motor or sensory (small or large) or autonomic (Table 1). This requires both history and examination.

Table 1 Symptoms and signs seen in peripheral neuropathies

Affected fibres	Positive symptoms	Negative symptoms
Sensory Small fibres	Pain, paresthesias	Numbness/lack of sensation
Sensory Large fibres	Not concerned	Poor balance
Motor	Cramps, fasciculations	Weakness, atrophy
Autonomic	Diarrhea, hyperhidrosis	Orthostatic hypotension, impotence, anhidrosis

- Localize which part of the peripheral nerve system is affected. Examination can conclude to a radiculopathy, plexopathy, mononeuropathy or peripheral neuropathy.

- Determine the time course. Here also history is very useful in determining the acute pattern of a peripheral neuropathy that occurs in days, the subacute peripheral neuropathy that occurs in days to weeks, chronic peripheral neuropathy that occurs in months or years, or very chronic peripheral that occurs insidiously in several years.
- Determine the primary pathological process that led to the peripheral neuropathy. This will determine whether it is axonal damage or a demyelinating neuropathy. History and examination, except in certain unusual cases such as enlarged nerves in some CMT cases, are not useful. Important evaluations are nerve conduction studies or nerve biopsy.
- Determine important contributing factors, including medical history (diabetes mellitus, HIV, other immune diseases), medications (vitamins), and family history (history of high arches or hammer toes).
- Characterize neuropathy by further testing such as nerve conduction studies, electromyography, skin biopsy, nerve and muscle biopsy, quantitative sensory testing, and laboratory testing that include genetic testing. We will be reviewing some important diagnostic testing here.

Nerve conduction studies (NCS)

Nerve conduction studies are commonly used tests that evaluate the electrical conduction ability of motor and sensory nerves. NCS consists of three major components; motor NCS, sensory NCS, and F-wave study. Motor NCS measures the time an electrical impulse takes from a stimulation site of peripheral nerve to a recording site, which is the muscle it supplies. This value is called latency and measured in millisecond (ms). The size of the response called motor amplitude is also measured, and in millivolts (mV). The velocity of the impulse called nerve conduction velocity (NCV) can also be determined by stimulating the same nerve in two or more sites. The distance between the different stimulating electrodes and the difference in latencies are used for calculations. Measurement of sensory NCS isn't different except that recording is performed in a purely-sensory portion such as finger. In addition, sensory amplitudes are smaller than the motor ones. NCS measures large diameter motor and sensory fibres, and can distinguish axonal versus demyelinating neuropathy and polyneuropathy versus mononeuropathy. As stated above, axons transmit the amplified action potentials and myelin plays a role in the rapid propagation of

electrical impulses. As result, damage to axons results in low action potentials while demyelinating neuropathy leads low nerve conduction velocity. Routine studies include sural, median, ulnar, and radial sensory nerve action potentials, and peroneal, tibial, median and ulnar compound motor action potentials. F-wave study also record action potentials from a muscle by supramaximal stimulation of the motor nerve that supplies it. While motor and sensory nerve conduction velocity evaluates conduction in the segment of the limb, F-wave can be used to assess conduction between nerve and spine.

Electromyography (EMG)

EMG is another electrodiagnostic procedure that measures electrical signals transmitted by motor nerves at the muscle. When performing EMG electrical activities of muscles can be recorded at the surface or at intramuscular level by inserting a needle electrode into the muscle tissue. Measurement is done at rest and at smooth muscle contraction. The activity of several motor units and at different locations is measured to have an accurate study. EMG is used to evaluate radiculopathies, plexopathies, and mononeuropathies.

Skin biopsy

Skin biopsy is used for a quantitative evaluation of epidermal innervation (small sensory nerve fibres). Three main techniques are used: a shave biopsy, an excisional biopsy, and now commonly used punch biopsy. Skin sample is stained with pan-axonal marker to determine their number.

Nerve biopsy

Nerve biopsy plays a small role in diagnosing peripheral neuropathy. However, it is important in confirming demyelinating neuropathies, and may play a role in the cellular pathology and the diagnosis in some diseases including vasculitis, amyloid neuropathy, giant axonal neuropathy, and leprous neuropathy.

Laboratory studies

Although not always specific, laboratory testing may contribute to the diagnosis or understanding of peripheral neuropathies such as vitamin deficiencies or intoxication, Guillan-Barré syndrome, and metabolic disorders. Routine tests include blood glucose, vitamin B12 levels, lipid profile, homocysteine, and thyroid function. In cases where a particular disease is suspected, specific testing can be performed, e.g.,

anti-nuclear antibodies, anti-neutrophilic cytoplasmic antibodies, HIV, Lyme disease, and most importantly in our case genetic testing.

In conclusion, the diagnosis of a peripheral neuropathy is mainly based on history and examination. Blood testing can identify acquired causes of neuropathy as well as testing of the cerebrospinal fluid (CSF), which is important to identify inflammatory neuropathies. Neurophysiology is very important to identify which part of the peripheral nerve is affected. Nerve biopsy is usually the final test carried out but it is often the most important in identifying the more unusual types of neuropathy. The advance in the molecular genetics of inherited neuropathy has allowed many patients and families to be diagnosed without having to undergo many of these invasive investigations.

1.1.7 Treatment of peripheral neuropathies

Currently there is no proven disease modifying treatment for peripheral neuropathies except for some inflammatory neuropathy types including Guillan-Barré Syndrome for which plasmapheresis and/or intravenous immunoglobulins are used. In most cases peripheral neuropathies are managed by identifying and treating the underlying cause. Symptomatic treatment using non-steroidal anti-inflammatory drugs for back pain, and anti-epileptic drugs or tricyclic anti-depressants for neuropathic pain can be used to improve patients' quality of life. Because peripheral neuropathies often lead to disability, it is important to help patients gain maximum independence and self-care ability through physical therapy to prevent contractures and falls, and occupational therapy. In addition, orthopaedic devices can be used to improve gait and reduce falls.

1.2 Charcot-Marie-Tooth disease (CMT)

1.2.1 Historical notes

In 1886, Jean-Marie Charcot and Pierre Marie in Paris, France (Charcot 1886) first described a "particular form of progressive muscular atrophy". At the same time in London, England, Howard Henry Tooth (Tooth 1886) independently described patients with a peroneal type of progressive muscular atrophy and contrasted this with a "classical" progressive muscular atrophy. Tooth was first to attribute the symptoms to a neuropathy rather than a myopathy as physicians had done in earlier descriptions. These descriptions led to the term CMT or progressive muscular atrophy being used

to describe what was initially thought to be one disease. Over the last century, clinical, electrophysiological and pathological descriptions have shaped the classification of inherited peripheral neuropathy from the original description of CMT to a spectrum of peripheral nerve degenerative disorders known to occur in several inherited neuromuscular and central nervous system disorders.

1.2.2 General findings

Charcot-Marie-Tooth disease is the most common inherited disorder of the peripheral nervous system. The prevalence of CMT disease (all types) has been reported to be between 4.7 cases per 100,000 in Newcastle-Upon-Tyne (Davis, Bradley et al. 1978) and 36 cases per 100,000 in Western Norway (Brust, Lovelace et al. 1978). The estimated prevalence based on several studies is one case per 2,500 individuals (Skre 1974). The mode of inheritance can be autosomal dominant, autosomal recessive or X-linked. The classical clinical presentation of CMT is distal weakness involving first the lower limbs, extending to the upper limbs during the disease course; sensory loss, decreased reflexes and foot deformities; and the most common presenting symptoms are walking difficulties with steppage gait (Shy, Jani et al. 2004). Sensory symptoms are usually less prominent than motor ones (Harding and Thomas 1980; Shy, Jani et al. 2004). Other less frequent signs include cranial nerve impairment, scoliosis, vocal fold and diaphragm paralysis and glaucoma (Dyck, Litchy et al. 1994; Azzedine, Bolino et al. 2003; Senderek, Bergmann et al. 2003; Hirano, Takashima et al. 2004). Although variable between and within families (Garcia, Malamut et al. 1995; Pareyson, Scaioli et al. 2006), symptom onset usually occurs during first decades of life, and the disease course is very slowly progressive over decades (Pareyson, Scaioli et al. 2006); initial symptoms may occur in infancy (Thomas, Marques et al. 1997; Pareyson 2004) or late (Harding and Thomas 1980; Shy, Jani et al. 2004).

1.2.3 Classification

CMT disease was thought to be one disease until almost a century after the first descriptions. But, with advances in electrophysiological, pathological and genetic investigations of this disorder, it is now classified into many different subtypes. The differentiation of this heterogeneous condition into two predominant types came with Dyck and Lambert's work (Dyck and Lambert 1968). In 1968, they found clinical, pathological, electrophysiological and genetic heterogeneity among patients with

CMT. In their series they found that patients were divided into two main groups and then into subgroups: (i) those with diffusely low nerve conduction velocities with hypertrophic neuropathy and demyelination (CMT1), and (ii) those with normal or borderline abnormal nerve conduction velocities and without hypertrophic neuropathy, but peripheral nerve axonal degeneration (CMT2). They also introduced the term hereditary motor and sensory neuropathy (HMSN) that includes a broader group of inherited neuropathies. Both terms are used interchangeably, but CMT is now preferred. Subsequent studies done by Thomas and Calne (Thomas, Calne et al. 1974) and Harding and Thomas (Harding and Thomas 1980) reinforced this classification. This differentiation was based on the median motor nerve conduction velocity, with 38 m/s being the cut-off value to differentiate between the two types (conduction velocity (CV) <38 m/s in CMT1 patients, whereas it is >38 m/s in CMT2 patients). But, both axonal and demyelinating CMT eventually result in loss of axons and in reduction of compound motor action potential (CMAP) and sensory nerve action potential (SNAP) amplitudes (Lewis, Sumner et al. 2000). Forms of CMT with intermediate values have also been described (Verhoeven, Villanova et al. 2001; Jordanova, Thomas et al. 2003; Zuchner, Nouredine et al. 2005).

It is often impossible to distinguish CMT1 and CMT2 based on neurological examination because clinical features are similar. As genetic and clinical investigation of CMT has continued to improve in recent years, the classification of CMTs has continued to evolve and there are now a total of about 40 recognized subtypes.

1.2.3.1 CMT1

The disorder that Charcot, Marie and Tooth described in their original papers best fits the phenotype of CMT1. Based on the mode of inheritance, and according to the data in the Inherited Peripheral Neuropathies Mutation Database (IPNMD, Department of Molecular Genetics, University of Antwerp, Antwerpen, Belgium), there are 2 subtypes of demyelinating CMT: the dominant forms that are divided into two subgroups (autosomal dominant: CMT1 and X-linked dominant: CMT1X) and the recessive forms also divided into two subgroups (autosomal recessive: CMT4 and X-linked recessive: CMT4X).

Dominant forms of CMT1

Autosomal dominant (CMT1)

Six sub-forms have been characterized in this sub-type, and five genes have been identified (IPNMD, accessed January 2011). We will review here the two most common sub-types: CMT1A and CMT1B. This type is the most common of all CMTs in general and CMT1 in particular, with CMT1A alone representing 40-50 % of all CMT cases (Nelis, Van Broeckhoven et al. 1996; Dubourg, Tardieu et al. 2001; Boerkoel, Takashima et al. 2002). The majority of cases in this type develop symptoms during the first decade (Harding and Thomas 1980). Symptoms begin insidiously with muscle weakness and atrophy in the foot and leg muscles, especially the intrinsic muscles; leading to a gait abnormality or clumsiness in running and foot deformities. Later, calf, intrinsic hand, and thigh muscles may become affected. The atrophy tends to affect the distal part of the gastrocnemius, soleus, and distal quadriceps muscle, giving the characteristic appearance of “inverted champagne bottle” of lower limbs seen only in thin patients with fully expressed disease. Fasciculations and cramps after exercise are common. Sensory dysfunction affecting all modalities can be seen (Dyck P. J. *et al.*, 1993), though less prominent than the motor signs. Tendon reflex changes are seen and more marked in this type than the type 2. Harding and Thomas found 58 per cent of their patients with HMSN type 1 had total tendon areflexia (Harding and Thomas 1980).

Hypertrophic neuropathy characterized as hard enlargement of peripheral nerves is usually seen in nerve biopsies (Dyck P.J. 1993).

CMT 1A

CMT1A represents the typical form of CMT with an early onset, but milder course compared to other types of CMT. About 60 % of patients with CMT1A have a positive family history. Symptoms include a childhood or adolescent disease onset, slowly progressive disease course, symmetrical demyelinating polyneuropathy, variable degree of distal muscle weakness and atrophy, and sensory disturbances. In 10 % of cases, proximal limbs become affected in late teenage years. Slow nerve conduction velocities ranging between 20-25 m/s is a 100 % penetrant phenotype independent of age, and may appear within the first months of life (Krajewski, Lewis

et al. 2000). Histological studies show hypertrophic neuropathy and “onion bulb” formations.

CMT1A is due to mutations in the peripheral myelin protein 22 gene (*PMP22*) on chromosome 17. Both duplication and point mutation in the *PMP22* gene cause CMT1A. However, the majority of CMT1A cases are caused by a 1.4-Mb duplication in band 17p11.2 (Lupski, de Oca-Luna et al. 1991), although the disease course is more severe in point mutation cases. Pentao et al. were first to suggest that unequal crossing over due to misalignment at the CMT1A-REP (repetitive elements) repeat sequences during meiosis was the cause of de novo duplication in CMT1A (Pentao, Wise et al. 1992).

PMP22 encodes an integral membrane protein, and is mainly expressed in Schwann cells. It constitutes the major component of compact myelin in peripheral nerves where it plays a role during Schwann cell growth and differentiation (Snipes, Suter et al. 1992). CMT1A is suggested to be caused by *PMP22* overexpression that leads to accumulation in the late Golgi-cell membrane compartment and uncouples myelin assembly from the underlying program of Schwann cell differentiation (Niemann, Sereda et al. 2000).

CMT 1B

The first CMT1B case was reported in 1952 in a family with six individuals in 3 generations (England and Denny-Brown 1952). These individuals presented with footdrop, distal leg weakness, and loss of deep tendon reflexes.

Although clinically similar to CMT1A, CMT1B appears more severe, and many cases are sporadic. In addition, motor NCV, especially in the early-onset cases, are slower, in the range of 5-15 m/s. But due to the variability seen in all CMT cases, it can be difficult to clearly differentiate CMT1B from CMT1A cases. Onion bulb formation and excessive myelin folding and thickness are reported in histological studies.

CMT1B is caused by mutations in the myelin protein-zero (*MPZ* or *P0*) gene (Hayasaka, Himoro et al. 1993). Mutations in *MPZ* account for 5 % of all CMT1 cases (Nelis, Van Broeckhoven et al. 1996). *MPZ* is the major structural protein of the peripheral myelin, and is expressed in Schwann cells. It accounts for 50 % of the protein present in the myelin sheath. *MPZ* is also an integral membrane glycoprotein that is thought to join adjacent lamellae, thus stabilizing the myelin assembly. The

MPZ protein contains a highly conserved extracellular domain which plays this role and where most of the mutations are located. Animal models have shown that a strict dosage of MPZ is required for normal peripheral nerve myelination (Wrabetz, Feltri et al. 2000). Mutations in MPZ are predicted to alter myelin adhesion or produce an unfolded protein response (Wrabetz, D'Antonio et al. 2006). In transfected cells, Grandis et al. found that mutations associated with late-onset disease show partial loss of protein function while those associated with an early-onset disease show an abnormal gain of function (Grandis, Vigo et al. 2008).

Other variants of this sub-type include CMT 1C caused by mutations in the lipopolysaccharide-induced tumor necrosis factor-alpha factor (*LITAF*) gene (Street, Bennett et al. 2003), CMT 1D caused by mutations in the early growth response protein 2 gene (*EGR2*) (Warner, Mancias et al. 1998), CMT 1E caused by point mutations in the *PMP22* gene (Kovach, Lin et al. 1999), and the CMT1F/CMT2E complex caused by mutation in the neurofilament protein, light chain gene (*NEFL*) (Jordanova, De Jonghe et al. 2003).

X-linked dominant (CMT1X)

CMT1X is the second most common variant of all CMTs. This subtype is characterized by weakness and wasting in distal limbs. The onset occurs before 20 years of age with gait disorder. Sensory loss is more often described, and absent tendon reflexes are noted most often at the knees and ankles. Patients also develop hearing loss. Females present with milder signs consistent with absent hypertrophic nerves and mildly slow or normal NCVs or are asymptomatic. Some studies have reported transient central nervous system symptoms including numbness and paresis in the left face and arm with an abnormally increased T2 signal and reduced diffusion in the posterior portion of the centrum semiovale bilaterally as well as in the splenium of the corpus callosum in MRI (Sakaguchi, Yamashita et al. 2010). Some patients show both demyelinating and axonal features.

CMT1X is due to a mutation in the connexin-32 gene (*CX32*) also called Gap Junction protein Beta-1 (*GJB1*) (Bergoffen, Scherer et al. 1993). Connexins are proteins that span along the cell membrane and assemble to form gap junction channels that play a role in facilitating transfer of ions and molecules between cells. *CX32* is highly expressed in kidney and peripheral nerves. In peripheral nerve *CX32*

is found at the nodes of Ranvier and Schmidt-Lanterman incisures where it may form intracellular gap junctions that connect to the folds of Schwann cell cytoplasm; allowing the transfer of nutrients, ions, and molecules to the innermost myelin layers (Meier, Dermietzel et al. 2004). While some studies proposed a nonfunctional chimeric connexin formation by mutant CX32 with wildtype connexins (Omori, Mesnil et al. 1996), others have found a trafficking defect that leads to retention of mutant proteins in the Golgi apparatus, therefore failure to form gap junctions (Kleopa, Zamba-Papanicolaou et al. 2006).

Recessive forms of CMT1

Autosomal recessive (CMT4)

Eleven different clinical forms have been characterized in this sub-type, and ten genes have been identified. Although the clinical presentation is quite similar to the dominant CMT1 form, the disease course appears to be more severe. Harding and Thomas found that autosomal recessive type I cases had more severe weakness in the lower limbs, more frequent scoliosis, and a significantly lower motor nerve conduction velocities than those with autosomal dominant inheritance (Harding and Thomas 1980). Here we will review some of the most frequent forms.

CMT 4A

This sub-type is frequent in Hispanic population, Northern Africa and Eastern Europe. Symptoms start in childhood, before 2 years, and are characterized by weakness, sensory loss, and reduced to absent tendon reflexes. Weakness is rapidly progressive; involves distal limbs with lower limbs being more affected, and affects the left more than right vocal fold. Because of vocal fold paralysis, patients present with breathing difficulties and hoarse voice. There is an earlier involvement of upper extremities and proximal muscle weakness. Nerve conduction studies and pathology show the same patterns seen in demyelinating CMT.

CMT4A is caused by mutations in the ganglioside-induced differentiation-associated protein 1 (*GDAP1*) gene (Baxter, Ben Othmane et al. 2002; Cuesta, Pedrola et al. 2002), and accounts for about 25 % of all CMT4. *GDAP1* is a protein that forms a homodimer, and contains 2 N-terminal GST domains and 2 C-terminal transmembrane domains. It is highly expressed in brain, spinal cord, and dorsal root ganglia. In the peripheral nerve, *GDAP1* is expressed in both Schwann cells and

neurons where it may regulate mitochondrial dynamics that are critical for the proper function of myelinated peripheral nerves (Niemann, Ruegg et al. 2005). The same study showed that truncating GDAP1 mutations led to mitochondrial targeting defect and loss of mitochondrial fragmentation activity, whereas missense mutations in GDAP1, although targeted to mitochondria, showed some impaired ability to induce fragmentation.

CMT 4C

CMT4C affects families from different ethnic background (Kessali, Zemmouri et al. 1997; Gabreels-Festen, van Beersum et al. 1999; Colomer, Gooding et al. 2006),. Skeletal deformities are the main presenting features. Symptoms include delayed walking, distal muscle weakness and atrophy, early cutaneous sensory and late vibration and joint position loss. Some patients present with cranial nerve involvement causing deafness, nystagmus, facial and pupil unresponsiveness, and unilateral tongue atrophy. Laboratory studies show similar features to those seen in CMT1.

This sub-type is caused by mutations in the SH3 domain and tetratricopeptide repeat domain-2 (*SH3TC2*) gene (Senderek, Bergmann et al. 2003). The protein encoded by *SH3TC2* is expressed in the Schwann cells, and localized to the plasma membrane and the perinuclear endocytic recycling compartment, which suggest a possible function in myelination and/or in regions of axoglial interactions (Arnaud, Zenker et al. 2009). The suggested mechanism leading to CMT4C is endocytic and membrane trafficking pathway defect. Studies postulate that missense mutations impair communication between Schwann cells and axon, leading to myelin malformation (Lupo, Galindo et al. 2009).

Other variants of CMT4 include CMT 4B1 due to mutation in the myotubularin-related protein 2 (*MTMR2*) (Bolino, Muglia et al. 2000), CMT 4B2 caused by mutations in the SET binding factor-2 (*SBF2*) gene (Senderek, Bergmann et al. 2003), CMT 4D caused by mutations in the N-myc Downstream-Regulated Gene 1 (*NDRG1*) (Kalaydjieva, Gresham et al. 2000), CMT 4F caused by mutations in the periaxin gene (*PRX*) (Guilbot, Williams et al. 2001), CMT 4G due to mutations in the Hexokinase 1 (*HK1*) gene, CMT 4H due to mutations in the FYVE, RhoGEF and PH domain containing 4 (*FGD4*) gene (Delague, Jacquier et al. 2007), and CMT 4J which is due

to mutations in the *FIG4* homolog, SAC1 lipid phosphatase domain containing (*S. cerevisiae*) (Chow, Zhang et al. 2007).

X-linked recessive (CMT4X)

Four families have been described in this subtype with at least 3 loci. The clinical findings are not much different from the typical CMT presentation except that some of these patients have spastic paraparesis, pain and paresthesia. NCS showed both demyelination and axonal involvement.

1.2.3.2 CMT2

In 1968 Dyck and Lambert (Dyck and Lambert 1968) showed that many CMT patients had nerve conduction studies with a normal or borderline conduction velocities ($CV > 38$ m/s), but reduced compound motor and sensory action potentials. In addition, pathological studies of nerve biopsies in these patients have showed axonal degeneration and regeneration, leading to progressive loss of available nerve fibres (Zuchner, De Jonghe et al. 2006). CMT2 is thus defined as forms of CMT characterized primarily by axonal loss without demyelination. Like CMT1, CMT2 is also clinically and genetically heterogeneous with over fifteen different subtypes described, and a disease-causing gene identified in eleven of these subtypes; leaving five with no identified gene defect, although regions of interest have been found through linkage (IPNMDDB). As seen in most CMT cases, the age of onset and the severity of the disease in CMT2 cases are variable between and within families. The clinical presentation in this type is similar to the type I with some differences: the peak age of onset is in the second decade with some developing symptoms even much later (seventh or eighth decade) (Harding and Thomas 1980; Klein, Cunningham et al. 2003), distal weakness in the upper limbs occurs less frequently, sensory loss, foot deformity, and scoliosis are less prominent and less common, and nerve enlargement is almost always absent (Harding and Thomas 1980; Dyck P.J. 1993). Some studies have reported a mean age of onset of 20 years (median 13, range 1-63) (Bienfait, Baas et al. 2007). Symptoms more often start in legs with foot deformities and difficulty walking (Gemignani and Marbini 2001; Santoro, Manganelli et al. 2002; Bienfait, Baas et al. 2007). Based on the mode of inheritance, the classification found in the IPNMDDB website has this type also divided in 2 subtypes: dominant and recessive (autosomal and X-linked) forms.

Autosomal dominant forms of CMT2

Ten genetically different entities have been described in this subtype, and a causative gene was identified for 8 of them. We will review the most frequent form, CMT2A2 and the subtype we are interested in, CMT2C.

CMT 2A2

This subtype represents the majority of CMT2A families (Saito, Hayashi et al. 1997), and CMT2A2 constitutes 19 to 23 % of all CMT2 cases. The mean age of onset is 15 years, and symptoms start with weakness in lower limbs and walking difficulties. Patients have absent tendon reflexes and mild distal sensory loss. Optic atrophy, tremor, pain, and hearing loss may be associated with the disease. CNS involvement can be seen in some patients. NCS shows normal NCV but low action potentials. Nerve biopsy is consistent with loss of myelinated large fibres with intact myelin.

CMT2A2 is caused by mutation in the Mutofusin 2 gene (*MFN2*) (Zuchner, Mersiyanova et al. 2004). Mutofusins mediate the fusion of mitochondria contributing to the dynamic balance between fusion and fission that determines mitochondria morphology (Santel and Fuller 2001). *MFN2* is expressed in almost all tissues but its highest expression was seen in heart and skeletal muscle. It contains an N-terminal GTPase domain and transmembrane domain close to the C-terminal region. In transfected cells, *MFN2* was shown to colocalize with mitochondrial markers. Studies in cells derived from CMT2A2 patients showed that mutations lead to uncoupling of mitochondria oxygen consumption and reduced oxygen utilization efficiency, though ATP production was normal (Guillet, Gueguen et al. 2010).

CMT 2C

CMT2C is a rare, autosomal dominant form of CMT with five families reported in the literature, at the time of the start of this study, (two in the United States of America, one in New Zealand, one in the United Kingdom and one in Italy) (Dyck, Litchy et al. 1994; Donaghy and Kennett 1999; Santoro, Manganelli et al. 2002; McEntagart, Reid et al. 2005). The disease initially causes distal limb muscle weakness and limb atrophy with later involvement of proximal muscles. These symptoms are associated with diaphragm, vocal fold and intercostal muscles paralysis; which together are distinguishing features of this subtype of CMT, although vocal fold paralysis has been reported in other types of CMT, including CMT4A, and CMT2K (Baxter, Ben

Othmane et al. 2002; Cuesta, Pedrola et al. 2002; Birouk, Azzedine et al. 2003; Zuchner, De Jonghe et al. 2006). Consequently, patients experience hoarseness of voice, stridor and shortness of breath aggravated by exertion. Some patients have been noted to have facial weakness (Dyck, Litchy et al. 1994). Sensory symptoms are often mild and seen more often in most severely affected individuals and include loss of touch, vibration sense, and joint position sense in the hands and feet. Some patients complain of pain, numbness and paresthesias. Decreased or absent tendon reflexes, typical in all CMT types, are seen in this subtype, including mildly affected patients. Unlike in most of CMT2 cases, CMT2C manifests more often in the first decade; although the age of onset is variable within and between families. This striking variability in the disease severity within and between families constitutes another characteristic feature of the CMT2C sub-type. Autonomic symptoms have not been reported in previous reports of CMT2C. NCS show a pattern of axonal involvement, with normal or borderline low nerve conduction velocities and decreased amplitudes. Laryngoscopy shows vocal fold paralysis, with the left side being more affected early in disease. Chest X-ray shows diaphragm paralysis which affects the left more than right side.

The gene for CMT2C was mapped to 12q23-24 in a large Caucasian-American family (Klein, Cunningham et al. 2003). This region was further narrowed down by another study that studied two families, one from New Zealand and another from England (McEntagart, Reid et al. 2005).

At the time of this study the gene for this CMT2 subtype had not been identified. Three independent studies including the one described here identified the transient receptor potential vanilloid superfamily member 4 (*TRPV4*) as the disease-causing gene for this CMT2 sub-type (Auer-Grumbach, Olschewski et al. 2010; Deng, Klein et al. 2010; Landoure, Zdebik et al. 2010). We will review this gene in the next section.

A few other autosomal dominant CMT2 subtypes have been described in the literature. These include CMT 2A1 caused by mutation in the Kinesin family member 1 β (*KIF1B*) gene (Zhao, Takita et al. 2001), CMT 2B caused by mutations in RAB7A, member RAS oncogene family gene (*RAB7*), CMT 2D due to mutations in the Glycyl tRNA Synthetase (*GARS*) gene (Antonellis, Ellsworth et al. 2003), CMT 2F due to mutations in the heat shock 27 kDa protein 1 gene (*HSPB1*) (Evgrafov, Mersianova

et al. 2004), CMT 2G that links to chromosome 12q12-12q13.3 (Nelis, Berciano et al. 2004), CMT 2L caused by mutation in the heat shock 22kDa protein 8 gene (*HSPB8*) (Tang, Zhao et al. 2005), CMT 2M due to mutations in the dynamin 2 (*DNM2*) gene (Zuchner, Nouredine et al. 2005), and CMT 2N caused by mutation in the Alanine tRNA synthetase (*AARS*) gene (Latour, Thauvin-Robinet et al. 2010).

Recessive forms of CMT2

This subtype is divided into two subforms: autosomal and X-linked recessive. Four autosomal recessive subtypes of CMT2 are listed in the IPNMDDB website, and causative genes were identified in two of them, while about three X-linked recessive axonal forms were listed in the same website. Although symptoms are similar to those in the dominant form, the disease course and clinical signs in the recessive forms are more severe.

AR-CMT 2A

Also called CMT2B1, this disease was characterized in Northern Africa families who presented with weakness in the legs within the second decade (Bouhouche, Benomar et al. 1999). Scapular weakness was also seen. The disease progresses rapidly, and can lead to prominent disability over 4 years.

This sub-type is caused by mutations in the lamin A/C (*LMNA*) gene (De Sandre-Giovannoli, Chaouch et al. 2002). Lamins are proteins that compose the structure of the nuclear lamina, and form a protein network that constitutes the inner nuclear membrane determining the nuclear shape and size.

AR-CMT 2B

This sub-type, also known as CMT2B2, was described in a single family (Leal, Morera et al. 2001). The mean age of onset is 32 years, and initial symptoms are weakness in the ankles. In addition to the classical CMT2 presentation, patients can present with cramps and paresthesias.

This disease is caused by mutations in the mediator complex subunit 25 gene (*MED25*) (Leal, Huehne et al. 2009). MED25 is ubiquitously expressed but highest expression was seen in dorsal root ganglia, cerebellum, cortex, and optic nerve, and contains an SD1 domain, and a SD2 domain which contains two putative CAM kinase

phosphorylation sites. Heterologous expression studies suggest that mutant MED25 lose SH3 domain binding specificity.

AR-CMT 2C is another recessive CMT2 that was mapped to chromosome 8q21.3 (Barhoumi, Amouri et al. 2001). However, the disease-causing gene is not identified yet.

CMT 2K occurs in both autosomal recessive and dominant patterns, and is caused by mutations in the *GDAP1* gene (Birouk, Azzedine et al. 2003). The disease starts around 2 years with feet weakness and deformities. Some patients present with vocal fold paralysis; leading to hoarseness of voice in the second decade of life (Birouk, Azzedine et al. 2003).

X-linked CMT2

Five sub-types have been described in the literature.

CMT X-linked Type 1: caused by mutations in the connexin-32 (*GJB1*) gene (Bergoffen, Scherer et al. 1993), this sub-type is semi-dominant. Symptoms are similar to the classical CMT associated with hearing loss. NCS show both myelin and axonal loss.

CMT X-linked Type 2: linked to chromosome Xp22.2 (Ionasescu, Trofatter et al. 1991), this sub-type is recessive, and is associated with mental retardation.

CMT X-linked Type 3 is linked to chromosome Xq26.3-q27.1 (Huttner, Kennerson et al. 2006), and is recessively inherited. The disease starts between age 3 and 13, and is characterized by pain and paresthesias in legs. NCS show an axonal-type CMT.

CMT X-linked Type 4, also called Cowshock syndrome, is recessive and linked to chromosome Xq24-q26.1 (Priest, Fischbeck et al. 1995). Symptoms are axonal-type neuropathy, and associated with mental retardation and deafness by age 5.

CMT X-linked Type 5 is recessive, and is caused by mutations in the Phosphoribosylpyrophosphate synthetase I (*PRPS1*) (Kim, Sohn et al. 2007). The disease starts at early age and is associated with sensorineural hearing loss. However, sensation is normal. An optic neuropathy starts between 7 and 10 years (Rosenberg and Chutorian 1967).

1.2.3.3 Charcot-Marie-Tooth disease with intermediate nerve conduction velocities

This type of CMT can be inherited in both dominant and recessive pattern. As indicated, nerve conduction velocities show intermediate values, between 24 and 50 m/s.

Dominant intermediate CMT

DI-CMT, Type B (CMTDIB)

In addition to typical CMT findings, patients may present with tremor, and none of them never use wheelchair (Kennerson, Zhu et al. 2001).

This sub-type is due to mutations in the dynamin 2 gene (*DNM2*) (Zuchner, Nouredine et al. 2005). *DNM2* is a member of a GTPase family, and contains 9 consensus motifs for CDC2 phosphorylation, making it an important element for the G2/mitosis transition. The protein is expressed in a wide range of tissues, but highest expression was found in heart and skeletal muscle. *DNM2* is thought to regulate actin reorganization at the immunologic synapse and links to VAV1 and its downstream signalling pathway after TCR engagement (Gomez, Hamann et al. 2005).

DI-CMT, Type C (CMTDIC)

This sub-type was described in two families from German and Bulgarian origin (Jordanova, Thomas et al. 2003). The age of onset ranges from 7 to 54 years, and many patients never need to use a wheelchair.

CMTDIC is due to mutations in the Tyrosyl-tRNA synthetase (*YARS*) gene (Jordanova, Irobi et al. 2006). Aminocyl-tRNA synthetases catalyze the aminoacylation of tRNA by their cognate amino acid. They play an important role in linking amino acids with nucleotide triplets contained in tRNAs, suggesting that they are among the first proteins that appeared in evolution.

DI-CMT, Type A (CMTDIA) is another dominant intermediate described in one Italian family, the gene for this sub-type was mapped to chromosome 10q24.1-q25.1 (Verhoeven, Villanova et al. 2001). The disease starts within the first or second decade, and manifests like classical CMT. Many of the patients never become wheelchair-bound.

Recessive intermediate CMT

RI-CMT, Type A (CMTRIA)

This sub-type is due to mutations in the Ganglioside-induced differentiation-associated protein 1 (*GDAP1*) gene (Nelis, Erdem et al. 2002), and is a variant of the CMT 2K form. The disease starts at early childhood with gait disorder.

RI-CMT, Type B (CMTRIB)

Due to mutations in the Lysyl-tRNA Synthetase (*KARS*) gene (McLaughlin, Sakaguchi et al. 2010), this sub-type can be dominant or recessive. Symptoms may include developmental delay, self abuse, and dysmorphic features.

1.2.3.4 Other subtypes

Other subtypes have been added later after Dyck and Lambert's initial classification.

HMSN type III:

This type was described by Dejerine and Sottas as severe hypertrophic demyelinating neuropathy with early onset (Déjérine J. 1893). The clinical features include delayed motor development in infancy, generalized muscle weakness and atrophy affecting predominantly the distal limbs, areflexia, and sensory loss affecting the touch-pressure, joint position, and vibration modalities. Difficulties with walking occur in childhood and patients become wheelchair-bound by the third decade. Nerve biopsy shows lamellar protuberances (the so called onion bulbs; whose origin are the Schwann cells) along the axons and segmental demyelination and remyelination thereof (Dyck P.J. 1993).

HMSN type IV:

Seen in Refsum's disease, this subtype is an autosomal recessive hypertrophic neuropathy associated with phytanic acid excess. The diagnosis is made with the finding of a tetrad of retinitis pigmentosa, peripheral neuropathy (muscle atrophy and weakness in the distal parts of lower limbs leading to foot drop, areflexia, sensory disturbances), cerebellar signs (ataxia, nystagmus, intention tremor), and increased cerebrospinal fluid protein content. Other findings include sensorineural hearing loss, anosmia, skin changes, skeletal malformations, cardiac abnormalities, and ophthalmologic abnormalities other than the retinitis pigmentosa. The age at onset varies from early childhood to the fourth decade, but most of the patients seem to have symptoms by the age of 20 years (Ola H Skjeldal 1993).

HMSN type V:

First described as inherited spastic paraplegia with distal limb weakness by Strümpell in 1883 (Strümpell 1883), HMSNV is characterized by peroneal atrophy and spastic paraplegia. The mode of inheritance is believed to be autosomal dominant. Patients manifest symptoms usually in the second decade or later, and the disease course is insidiously progressive over many years. Initial stiffness of the legs makes walking and running difficult. Later, the spasticity may be so severe that a scissoring-type of gait may develop. Although they present difficulty with walking, many patients are never confined to a wheelchair and those who are, only are so in the fourth decade or later. Clinical examination will show hyperreflexia mainly in the lower limbs, and the Babinski sign. Sensory symptoms are absent. NCS show normal conduction velocities of motor nerves in the upper limbs and either low normal or only slightly below the normal in the lower limbs, and a decrease in amplitude or an absence of the sural nerve action potential (Dyck P.J. 1993).

HMSN type VI:

In 1879, Vizioli described a family with optic atrophy in association with peroneal muscular atrophy (Vizioli 1889). The disease manifests with muscle atrophy and weakness first in legs and later in hands, loss of visual acuity progressing to blindness, and lancinating pains. The reflexes were normal or decreased.

HMSN type VII:

This type is characterized by pigmentary retinopathy associated with distal limb muscle atrophy and weakness. Cutaneous sensation was recorded as normal. Vibration was decreased at the malleolus, and myotatic reflex of the gastrocnemius and soleus muscles could not be obtained (Massion-Verniory L 1946).

As our knowledge grows there is more and more evidence about clinical, laboratory and genetic heterogeneity of CMT disease with about forty different clinical types characterized and around twenty six genes reported to cause CMT thus far (IPNMDB) (Table 2). Genes implicated in CMTs are involved in the peripheral nerve development or function, directly or indirectly (Figure 8) (Patzko and Shy 2011). There are genes involved in the structural formation of myelin (PMP22 and MPZ) or axonal transport (NEFL) or radial transport (CX32) or Schwann cell differentiation (EGR2) or mitochondrial function (MFN2, GADP1) or signal transduction pathways

(MTMR2, PRX, SBF2, NDGR1) or endosomal proteins (RAB7) or molecular chaperones (HSP22, HSP27) or involved in protein translation (GARS, YARS). With all the advances done in understanding the function of these proteins, how mutations in these genes cause degeneration of the peripheral nerve is still not known; making it difficult to find a treatment.

However, studying new genes and understanding the process of the disease mechanism remains critical to developing therapy for not only these disorders but also for the other more common forms of peripheral neuropathy (e.g., leprosy neuropathy or diabetes neuropathy).

Because different forms are often clinically indistinguishable in a single patient, the diagnostic approach to the identification of the CMT subtype is complex and should be based on inheritance pattern, careful clinical examination, electrophysiological examination and nerve biopsy together (Pareyson 1999; Pareyson 2003).

Table 2 Genetic and clinical features of CMT types

Type	Inheritance	Subtype	Locus	Gene	Age of onset	Specific features
Demyelinating	Dominant	CMT 1A	17p11	PMP22	1 st decade	Classical phenotype
		CMT 1B	1q22	MPZ (P ₀)	1 st decade	Classical severe phenotype
		CMT 1C	16p13	LITAF	2 nd decade	Classical phenotype
		CMT 1D	10q21	EGR2	2 nd decade	Ptosis
		CMT 1E	17p11, 1q22	PMP22, P ₀	1 st decade	Deafness
		CMT 1F	8p21	NEFL	1-40 years	Ataxia
	Recessive	CMT 4A	8q21	GADP1	Childhood	Vocal fold paralysis
		CMT 4B	11q22	MTMR2	2-4 years	Proximal weakness
		CMT 4B2	11p15	SBF2	< 20 years	Glaucoma
		CMT 4C	5q32	SH3TC2	5-15 years	Delayed walking, cranial nerves
CMT 4D		8q24	NDRG1	1-10 years	Hearing loss	
CMT 4E		10q21	EGR2	Birth	Infant hypotonia	
CMT 4F		19q13	Periaxin	1-3 years	Motor delay	
CMT 4G		10q22	HK1	8-16 years	Classical phenotype	
CMT 4H		12q12	FGD4	10-24 months	Motor delay	
CMT 4J	6q21	FIG4	Congenital	Asymmetric, proximal involvement		
X-linked	CMT 1X	Xq13	GJB1	2 nd decade	Encephalopathy, deafness	
Axonal	Dominant	CMT 2A1	1p36	KIF1B	7 years	Classical phenotype
		CMT 2A2	1q36	MFN2	10 years	CNS, hearing loss
		CMT 2B	3q13-q22	RAB7	2 nd decade	Acromutilation
		CMT 2C	12q24	TRPV4	<1 to 50 years	Vocal fold, diaphragm, urinary incontinence
		CMT 2D	7p15	GARS	16-30 years	Arms>legs
		CMT 2E	8p21	NEFL	1-40 years	Classical phenotype
		CMT 2F	7q11-q21	HSPB1	6-54 years	Classical phenotype
		CMT 2G	12q12	Unknown	15-25 years	Classical phenotype
		CMT 2I	1q22	P ₀	>30 years	Deafness, photophobia
		CMT 2J	1q22	P ₀	>50 years	Deafness, photophobia
		CMT 2K	8q21	GADP1	Infant	Vocal fold paralysis
		CMT 2L	12q24	HSPB8	15-33 years	Classical phenotype
		CMT 2M	19p12	DNM2	0-50 years	Ophthalmoparesis
		CMT 2N	16q22	AARS	6-54 years	Classical phenotype
	Recessive	AR-CMT2A	1q21	Lamin A/C	2 nd decade	Scapular weakness
		AR-CMT2B	19q13	MED25	30-40 years	Classical phenotype
		AR-CMT2	9q33	LRSAM1	2 nd -5 th decade	Autonomic symptoms
		AR-CMT2 (CMT 2B5)	8p21	NEFL	<2 years	Early hypotonia
		AR-CMT2C (CMT 2H)	8q21.3	Unknown	4-8 years	Pyramidal involvement
		AR-CMT2 (CMT 2K)	8q21	GADP1	<2 years	Vocal fold paralysis
AR-CMT2	7q11-q21	HSPB1	6-54 years	Fasciculations		
X-linked	CMT X1	Xq13	GJB1	<20 years	Hearing loss, females	
	CMT X2	Xp22.2	Unknown	1 st decade	Mental retardation	
	CMT X3	Xq26	Unknown	3-13 years	Pain, paresthaesia	
	CMT X4 (Cowchock)	Xq24	Unknown	<5 years	Mental retardation, deafness	
	CMT X5	Xq22	PRPS1	8-13 years	Hearing loss	
Intermediate	Dominant	CMT DIA	10q24	Unknown	1 st -2 nd decade	Classical phenotype
		CMT DIB	19p12	DNM2	1 st -2 nd decade	Neutropenia in some patients
		CMT DIC	1p34	YARS	7-54 years	Classical phenotype
		CMT DID	1q22	P ₀	>30 years	Photophobia, deafness
	Recessive	CMT RIA	8q21.1	GADP1	2 nd decade	Vocal fold paralysis
		CMT RIB	16q23	KARS	Birth	CNS, dysmorphic features

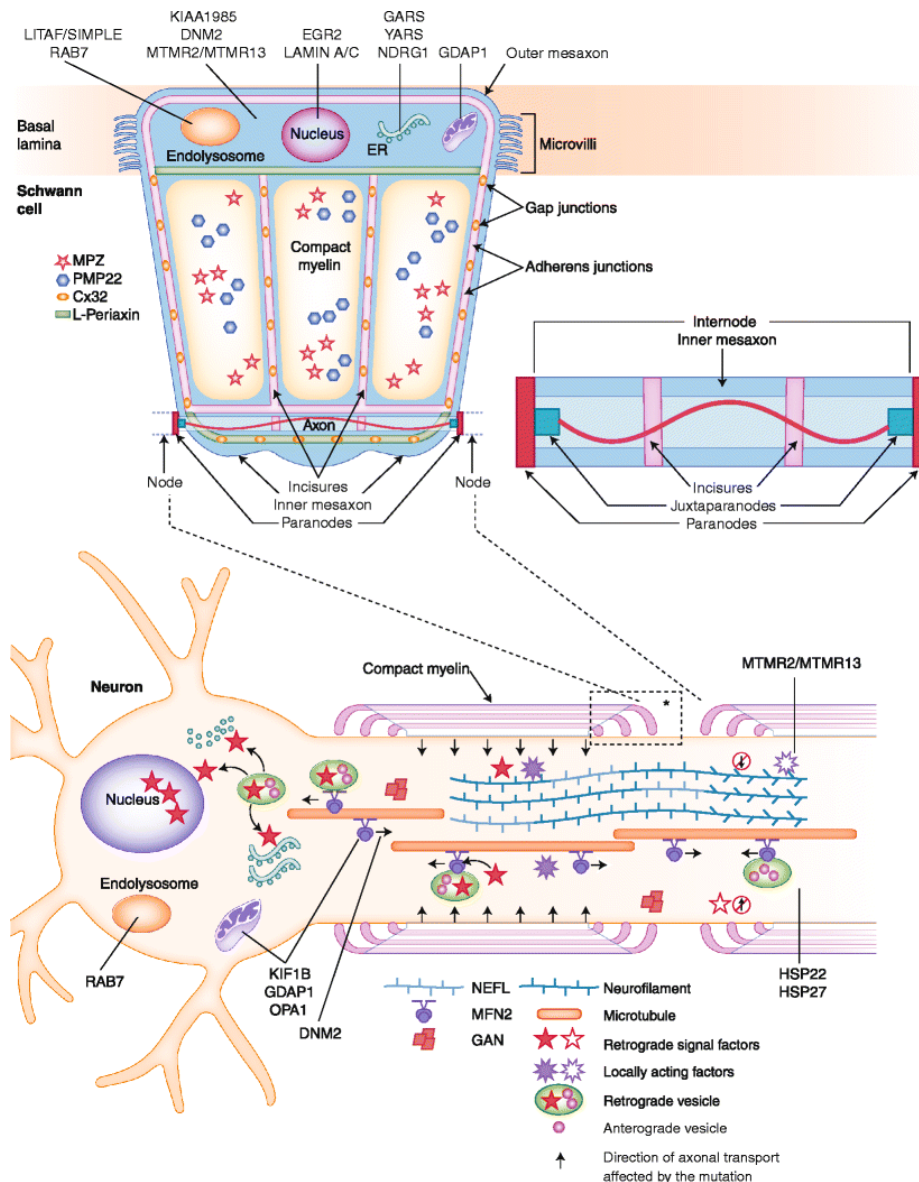


Figure 8 CMT genes involved in the peripheral nerve structure and function (Patzko and Shy 2011).

1.2.4 Therapeutic approaches for CMT

To date, no disease modifying treatment has been found for the many CMTs described so far because the proteins involved are difficult to target for therapeutics. However, therapeutic developments that target the molecular pathway of the proteins causing CMTs are underway.

Transcriptional regulation has been tried as treatment in CMT1A by *PMP22* gene dosage. In animal models, two compounds have been shown to alter *PMP22* mRNA levels. The first one, progesterone is produced by both neurons and Schwann cells, and has been shown to worsen the disease in *PMP22* cDNA overexpressing rats while

selective progesterone receptor antagonist, onapristone, reduced the disease and PMP22 levels (Sereda, Griffiths et al. 1996). Because onapristone is toxic in humans, developing a less toxic progesterone antagonist is ongoing. The second compound, ascorbic acid (vitamin C), necessary for peripheral nerve myelination, led to improvement in myelination and reduction of PMP22 levels in CMT1A transgenic mouse (Passage, Norreel et al. 2004); prompting several studies with different vitamin C doses.

Ions including sodium, calcium, and more importantly potassium play a role in depolarization at the nodes of Ranvier. In addition, calcium influx plays a major role in axonal degeneration. Therapeutic approaches targeting these ion channels may open the road for new treatment of CMTs. Although the first studies that used potassium channel blockers did not show improvement in CMT1 patients (Russell, Windebank et al. 1995), there is still hope that finding more specific ion channel blockers may reverse the disease course in CMT patients.

Therapeutic approach targeting Schwann cell-axonal signal transduction pathways based on the fact that overexpression of neuregulin-1 type III, a protein that expresses in axons and binds to ErbB receptors on Schwann cells to initiate myelination, induces Schwann cell hypermyelination (Michailov, Sereda et al. 2004).

Other potential therapeutic approaches include targeting the mitochondrial function because genes involved in the mitochondrial function (MFN2, GADP1) cause CMT, protein misfolding, membrane trafficking, and gene therapy.

1.3 Transient Receptor Potential (TRP) Channels

TRP channels are a superfamily of cation channels that are mostly permeable to both monovalent and divalent cations. The first TRP channel was identified in *Drosophila* as a phospholipase C-dependent process gene (Hardie and Minke 1993). The name *transient receptor potential* is based on the transient response pattern of flies carrying a mutant in the *trp* locus to light (Montell and Rubin 1989). Seven TRP-related proteins subfamilies have been described based on their amino acid sequence similarities: the transient receptor potential canonical (TRPC), the transient receptor potential vanilloid (TRPV), the transient receptor potential melastatin (TRPM), the transient receptor potential polycystin (TRPP), the transient receptor potential mucolipin (TRPML), the transient receptor potential ankyrin (TRPA), and the no

mechanoreceptor potential C (TRPN); which is present only in tunicates, flies, and worms. About twenty eight mammalian TRP channels grouped into six main subfamilies have been cloned in recent years, and many of them are conserved in flies, worms, fish and tunicates. However, only a single TRP-related gene, *yvc1*, has been identified in yeast, and none in plants, thus far.

These subfamilies are subdivided into several members except TRPA that has only one member (TRPA1). The TRPC subfamily consists of seven channels (TRPC1-7), TRPV has six channels (TRPV1-6), TRPM comprises eight members (TRPM1-8), and TRPP and TRPML each contain three members (Table 3). There is approximately 90 % amino acid sequence similarity among members of one subfamily, but this degree of amino acid sequence similarity cannot be found among members of different subfamilies. This similarity accounts for heteromerization of TRP channels members of one subfamily in native tissues and primary cells. Assembly of channel subunits as homo- or heterotetramers results in the formation of cation-selective channels. TRP channels are expressed in almost every tissue and cell type including peripheral nerves, and play an important role in the regulation of various cell functions. Each TRP channel subunit consists of six putative transmembrane spanning segments (S1–6), a pore-forming loop between S5 and S6, and intracellularly located NH₂ and COOH termini. Among other structural features of TRP proteins are ankyrin repeats domain (ARD) within the NH₂-terminal and coiled-coil domains within the C-terminal cytoplasmic regions of TRPCs, TRPVs, TRPMs, and TRPA1 (Figure 9) (Flockerzi 2007). These structural domains are absent in TRPPs or TRPMLs subfamilies. In addition to these structural features, four short amino acid sequence motifs, M1-M4, are present in the proteins of some TRP subfamilies. Thus, the M1 motif, consisting of 38 amino acids is present in TRPC1-7 at the upstream region of S1. An alternative M1 motif consisting of 52 to 63 amino acid residues is detectable in TRPV1-6, at the corresponding position. The M2 motif resides within the cytosolic loop between S4 and S5 of TRPC1-7, and is fairly conserved in the TRPVs and TRPMs subfamilies. Motif M3 (consensus sequence ILLLNLM-LIAMM) is part of S6 of all TRPCs, TRPVs, and TRPMs. Finally, the M4 motif which consists of highly conserved 26 amino acids and contains the TRP-box domain (WKFQR) follows immediately the transmembrane segment S6.

The M4 motif is located within the C-terminal cytosolic tail of most TRPs, and is followed by proline-rich sequences in some TRP channels (Flockerzi 2007).

Except TRPM4 and TRPM5, which are only permeable to monovalent cation, all TRP channels are permeable to Ca^{2+} . Of all TRP channels, only TRPV5 and TRPV6 are highly Ca^{2+} -selective, with permeability ratio relative to sodium ($P_{\text{Ca}}/P_{\text{Na}}$) > 100 whereas this ratio is between 0.3 and 10 in the other Ca^{2+} -permeable TRP channels (Nilius 2007).

Different stimuli have been shown to trigger TRP channel gating. These stimuli include the binding of intracellular and extracellular messengers, changes in temperature, and chemical (e.g., vanilloid compounds, endocannabinoid lipids, IGF-1, camphor, 4-alpha-Phorbol) and/or mechanical (hypotonicity) stress. Chemical components including ruthenium red, capsazepine, gadolinium, and spermine and pharmaceutical molecules (RN1734 and RN1747) have also been described to inhibit some TRP channel activity (Flockerzi 2007; Vincent, Acevedo et al. 2009).

TRP proteins have been shown to play a role in sensory processes such as thermosensation, osmosensation, olfaction, taste, mechanosensation, vision, and pain perception. Recently, the role of TRP proteins in non-excitabile cells including endothelial and smooth muscle cells was demonstrated in knock-out mice.

Table 3 Classification and pathogenesis of TRP channels

Subfamily	Member	Locus	Agonists	Antagonists	Thermo-sensitive	Human disease	References
Canonicals	TRPC1	3q22-q24	↓Ca ²⁺	Gd ³⁺ , CaM	No	NR	(Reiser, Polu et al. 2005; Winn, Conlon et al. 2005)
	TRPC3	4q27	DAG, PLC, IP ₃	Gd ³⁺ , La ³⁺	No	NR	
	TRPC4	13q13.3	PLC, ↓Ca ²⁺	Gd ³⁺ , La ³⁺	No	NR	
	TRPC5	Xq23	Gd ³⁺ , La ³⁺ , ↓Ca ²⁺	2APB	No	NR	
	TRPC6	11q21-22	CaM, FFA, 20-HETE	Gd ³⁺ , La ³⁺	No	Focal segmental glomerular sclerosis	
	TRPC7	5q31.1	DAG/PLC, ↓Ca ²⁺	Gd ³⁺ , La ³⁺	No	NR	
	Vanilloids	TRPV1	17p13.2	Heat, Capsaicin	Capsazepine, RR, A-425619	Yes	
TRPV2		17p11.2	Heat, IGF-1, 2APB	RR, La ³⁺	>52 °C	NR	
TRPV3		17p13.2	Heat	RR	22-40 °C	NR	
TRPV4		12q24	Heat, 4αPDD, hypotonicity	RR, RN1734	24-32 °C	Skeletal dysplasias, peripheral neuropathies	
TRPV5		7q35	Calcitropic hormones	RR	No	NR	
TRPV6		7q33-q34	PIP ₂	Mg ²⁺	No	NR	
Melastatins	TRPM1	15q13.3\	Constitutively ADPR, NAD, AMP SPH, ↓Ca ²⁺	Gd ³⁺ , La ³⁺	No	Congenital stationary night blindness	(Audo, Kohl et al. 2009)
	TRPM2	21q22.3		Fenamates, La ³⁺	No		
	TRPM3	9q21.11		RR, Gd ³⁺ , La ³⁺	No		
	TRPM4	9q13.33		Clotrimazole, flufenamic acid	15-37 °C		
	TRPM5	11p15.5	Ca ²⁺ /PLC	Acid pH	No	NR	(Schlingmann, Weber et al. 2002) (Hermosura, Nayakanti et al. 2005)
	TRPM6	9q21.13	↓Mg ²⁺	RR	No	Hypomagnesaemia with hypocalcaemia	
	TRPM7	15q21	Free Mg ²⁺	Muscarinic	No	ALS-Parkinsonism/Dementia Complex of Guam	
	TRPM8	2q37.1	Cold, menthol	Capsazepine	23-28 °C	NR	
Ankyrin	TRPA1	8q13	Pungent, irritants, bradykinin	Gentamicin, amiloride, RR, Gd ³⁺	17 °C (?)	NR	
Polycystins	TRPP1	16p13.3	NR	NR	No	Polycystic kidney disease, type 1	(Peral, Gamble et al. 1995) (Mochizuki, Wu et al. 1996)
	TRPP2	4q21-23	Vasopressin, EGF, ATP	↑[H ⁺]	No	Polycystic kidney disease, type 2	
	TRPP3	10q24-q25	[Ca ²⁺] _{ic} , ec	NR	No	NR	
	TRPP5	5q31	NR	NR	No	NR	
	Mucolipins	TRPML1	19q13.2	[Ca ²⁺] _{ic}	[Ca ²⁺] _{ic}	No	
TRPML2		1q22	[Ca ²⁺] _{ic}	[Ca ²⁺] _{ic}	No	NR	
TRPML3		1q22.3	[Ca ²⁺] _{ic}	[Ca ²⁺] _{ic}	No	NR	

Gd³⁺: gadolinium, CaM: calmodulin, DAG: diacylglycerol, PLC: phospholipase C, IP₃: inositol 1,4,5-trisphosphate, La³⁺: lanthanum, 2APB: 2-aminoethoxydiphenyl borate, FFA: flufenamate, 20-HETE: 20-hydroxyeicosatetraenoic acid, RR: ruthenium red, PIP₂: phosphatidylinositol bisphosphate, ADPR: adenosine 5'-diphosphoribose, NAD: nicotinamide adenine dinucleotide, AMP: adenosine monophosphate, SPH: D-erythro-sphingosine, EGF: epidermal growth factor, NR: not reported.

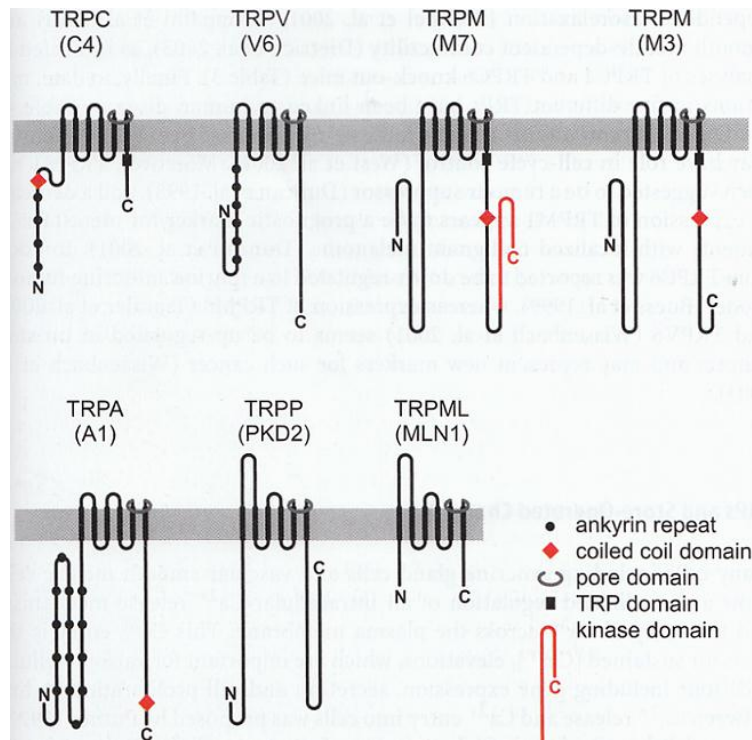


Figure 9 Structures of the mammalian TRP subfamilies. Brackets indicate representatives of subfamilies. Protein domains (ankyrin repeats, coiled-coil domain, protein kinase domain, and TRP domain) are indicated (Flockerzi 2007).

1.3.1 The canonical transient receptor potential channels (TRPC)

TRPC channels are nonselective, Ca^{2+} -permeable cation channels, but the permeability ratio ($P_{\text{Ca}}/P_{\text{Na}}$) varies significantly between different members of the family. There are seven mammalian TRPC channels (TRPC1-7). We will review one member that was implicated in human disease. TRPC channel family can be subdivided into three major subfamilies: TRPC1/4/5 activated by calcium store depletion; and TRPC3/6/7 activated by diacylglycerol (DAG) (Vazquez, Wedel et al. 2004). All TRPCs share a structural motif in the COOH-terminal tail called “TRP box”. This motif is located close to the intracellular border of S6, and contains the invariant sequence EWKFAR. TRPC channels also contain three or four ankyrin repeats located in the NH2-terminal (Philipp S 2000).

TRPC6

The canonical transient receptor potential 6 gene was first cloned in mouse brain (Boulay, Zhu et al. 1997), and later in human placenta (Hofmann, Obukhov et al.

1999). The human *TRPC6* gene is localized on chromosome 11q21-q22 and has 13 exons coding for 931 amino acids.

TRPC6 structural features are similar to those of the other TRP channels with intracellular N- and C- terminal regions, six transmembrane helices (S1-S6) and a predicted pore forming loop (P) between S5 and S6. Three ankyrin domains are found in the amino terminus. The TRPC6 protein also contains an EWKFAR TRP box, which is a conserved motif in the TRPC family, and two inositol 1,4,5-trisphosphate (IP3) receptor binding domains. The second domain overlaps with a calmodulin binding site (Boulay, Brown et al. 1999). Two glycosylation sites were identified in the first and second extracellular loop (Asn473, Asn561). The glycosylation sites are important determinants for the tightly receptor-operated behaviour of TRPC6 (Dietrich, Mederos y Schnitzler et al. 2003).

TRPC6 channels form heteromeric complexes in native environments, but functional TRPC6 tetrahomomers were characterized in over-expression studies. As discussed earlier in other TRPC channels, over-expression studies and observation in native tissues revealed that TRPC6 can form homo- and heterotetramers with TRPC1, TRPC3, TRPC4/TRPC5 and TRPC7.

In human TRPC6 appears to be expressed at higher levels in lung, placenta, ovary and spleen (Hofmann, Schaefer et al. 2000). While TRPC6 is found in numerous tissues enriched with smooth muscle cells including lung, stomach, colon, oesophagus and myometrium (Beech, Muraki et al. 2004), its functional roles were only described in vascular and pulmonary arteries. TRPC6 expression in brain is lower than that of other TRPCs.

Gain-of-function mutations of the TRPC6 channel were identified in families with focal and segmental glomerulosclerosis (FSGS) by two groups (Reiser, Polu et al. 2005; Winn, Conlon et al. 2005). These studies showed TRPC6 expression in the glomeruli and the tubuli as well as the podocytes. TRPC6 was also implicated in other diseases including cardiac hypertrophy (Bush, Hood et al. 2006), idiopathic pulmonary hypertension (Yu, Keller et al. 2009), and infantile hypertrophic pyloric stenosis (Everett, Chioza et al. 2009). TRPC6 properties show that TRPC6 displays double rectification with single-channel conductance of 28-37 pS. The ion permeability ratio P_{Ca}/P_{Na} is approximately 6 (Hofmann, Obukhov et al. 1999), distinguishing it from its closely related channel, TRPC3, which has a significant low Ca^{2+} selectivity values, 1.1, and a higher single-channel conductance, 60-66 pS

(Owsianik, Talavera et al. 2006). In contrast to TRPC3, TRPC6 is a receptor-operated channel (ROC) and shows little basal activity.

TRPC6 was the first ion channel identified that is activated by diacylglycerol (DAG) in a membrane delimitation fashion, independently of PKC. Ca^{2+} /calmodulin has a stimulatory impact on TRPC6 channel activity (Zhang and Saffen 2001). TRPC6 ions channels are also regulated by protein serine and tyrosine phosphorylation. Although the PKC activator phorbol 12-myristate 13-acetate (PMA) has no effect on basal TRPC6 activity it inhibits carbachol-induced TRPC6 activation by more than 90 % (Estacion, Li et al. 2004). Fyn, a member of the Src family of protein tyrosine kinase, increases TRPC6 channel activity.

There are no specific inhibitors for TRPC6. Lanthanum and gadolinium block TRPC6 at IC₅₀ of 4-6 μ M and 1.9 μ M, respectively. An arachidonic acid metabolite, 20-hydroxyeicosatetraenoic acid (20-HETE) and flufenamate (FFA; 100 μ M) were shown to activate TRPC6.

1.3.2 Transient receptor potential vanilloid channels (TRPV)

This family comprises of six members that share the same structural organization consisting of an N-terminal region where is located ankyrin repeat domain and a transmembrane domain containing six segments. TRPV channels are expressed in a wide range of tissues and organs such as sensory neurons (TRPV1, TRPV2, TRPV4, TRPV5), smooth muscle cells of blood vessels (TRPV2, TRPV4), kidney, bladder, keratinocytes (TRPV4, TRPV5), and digestive apparatus (TRPV4, TRPV6). Some of these channels (TRPV1/TRPV2, and TRPV5/TRPV6) interact to form heteromers. We will review TRPV1; the first discovered and most studied vanilloid channel, and TRPV4 that causes the disease we are studying here.

TRPV1

Also called capsaicin receptor, the transient receptor potential vanilloid member 1 gene was first cloned in rat dorsal root ganglia (DRG) (Caterina, Schumacher et al. 1997), and was named VR1, for vanilloid receptor subtype 1. This receptor was subsequently identified to be a member of the transient receptor potential (TRP) family of cation channels, and was thus named TRPV1. TRPV1 has been later cloned from human, guinea pig, rabbit, mouse, and porcine tissues. Significant differences

are noted in TRPV1 orthologs from different species in their sensitivity to various agonists and antagonists.

TRPV1 is expressed in diverse tissues but high levels are detected in DRG, trigeminal ganglia, and nodose ganglia. TRPV1 is predominantly expressed in small- and medium-sized peptidergic and non-peptidergic neurons. Peptidergic neurons are important in the development of neurogenic pain and inflammation while non-peptidergic neurons play a critical role in mediating chronic pain. Other regions of the brain where TRPV1 is expressed are the hypothalamus, cerebellum, cerebral cortex, striatum, midbrain, olfactory bulb, pons, medulla, hippocampus, thalamus, and substantia nigra. In non-neuronal tissues, TRPV1 is detected in keratinocytes of the epidermis, bladder urothelium and smooth muscles, glial cells, liver, and polymorphonuclear granulocytes, mast cells, and macrophages.

TRPV1 is localized on chromosome 17p13.2 with 17 exons encoding for 839 amino acids that form a 95-kDa protein. Mouse *Trpv1* has two splice variants, *Trpv1 α* and *Trpv1 β* . *Trpv1 β* is not functional by itself, and has a dominant-negative effect on *Trpv1* by inhibiting *Trpv1 α* function during co-expression (Wang, Hu et al. 2004). Human TRPV1 has four transcript variants encoding for the same protein but different in their 5' untranslated region (UTR). Human TRPV1b splice variant, expressed in trigeminal ganglion neurons, is unresponsive to capsaicin or protons, but can be activated by high temperature (>47 °C) (Lu, Henderson et al. 2005). TRPV1 consists of six transmembrane domains containing a short pore-forming region between the fifth and sixth transmembrane domains, 400-amino-acid N-terminus containing three ankyrin-repeat domains, and a carboxy-terminus containing a TRP domain. TRPV1 channels can function as homo- or heteromultimers, and homotetramer TRPV1 channels are the predominant forms of expression (Kedei, Szabo et al. 2001). TRPV1 can form with TRPV2 or TRPV3 functional heteromers (Smith, Gunthorpe et al. 2002; Liapi and Wood 2005). This ability to form functional heteromers with different TRPV channels is, at least in part, responsible for the variable responses to agonists and antagonists.

TRPV1 is a non-selective cation channel with near equal selectivity for Na⁺, K⁺, Li⁺, Cs⁺, and Rb⁺ ions (Caterina, Schumacher et al. 1997) but moderate selectivity for divalent cations. The permeability of Mg²⁺ and Ca²⁺ relative to Na⁺ is higher when activated by capsaicin than when activated by heat, 5 and 10 versus 3 and 4.

TRPV1 currents exhibit significant outward rectification due to a combined effect of voltage on both channel conductance and open probability (Nilius, Talavera et al. 2005). Upon activation, TRPV1 undergoes desensitization; a phenomenon that can occur rapidly during application of an agonist or slowly following repeated agonist application.

TRPV1 is activated by increases in temperature in the noxious range, suggesting that it functions as a transducer of painful thermal stimuli *in vivo*. TRPV1 activates at positive potentials and deactivates at negative potentials. These phenomena depend on temperature and ligand concentration, in the absence of which large membrane depolarisations are required to activate the channel. TRPV1 is also activated by capsaicin, the pungent component of hot chili peppers. Several endogenous fatty acids that share structural similarity with capsaicin also activate TRPV1. Those include endocannabinoid anandamide, N-arachidonoyl dopamine (NADA) and oleoyl-dopamine, the 12 hydroperoxyeicosatetraenoic acid (12-HPETE), and 18-20 carbon N-acylethanolamines (Movahed, Jonsson et al. 2005). Other TRPV1 regulators include extracellular protons and cations, protein kinase A and C, Ca^{2+} /calmodulin-dependent kinase II (CaMKII) or Src kinase.

Several TRPV1 inhibitors have been described. Capsazepine, which has structural similarity with capsaicin, is a competitive antagonist for TRPV1. Ruthenium red also blocks TRPV1 activity, though not specific.

The biological relevance of TRPV1 was shown in some pathological processes such as inflammatory pain that can be induced by sensitization of TRPV1, and other physiological processes like regulation of normal body temperature. The role of TRPV1 in several tissues was reported in several studies. TRPV1 is important in regulating normal lower urinary tract function, and maintains mucosal homeostasis, and protects against mucosal injury in the gastrointestinal tract. Moreover, in human, inflammatory bowel disease is associated with up-regulation of TRPV1 in nerve fibres of the colon (Yiangou, Facer et al. 2001). Other tissues and organs where TRPV1's important role was demonstrated include the vascular system, brain, ear, respiratory tract, and skin.

TRPV4

The transient receptor potential vanilloid subfamily, member 4 was found by screening expressed sequence tag databases for sequences with similarity to other

TRPV channels including TRPV1 and TRPV2, and the *Caenorhabditis* TRPV isoform Osm-9. TRPV4 was cloned from kidney, hypothalamus and the auditory epithelium. Different names were given to this newly cloned TRPV: Osm-9-like TRP channel 4 (OTRPC4) (Strotmann, Harteneck et al. 2000), vanilloid receptor-related osmotically activated channel (VR-OAC) (Liedtke, Choe et al. 2000), transient receptor potential channel 12 (TRP12) (Wissenbach, Bodding et al. 2000), and vanilloid receptor-like channel 2 (VRL-2) (Delany, Hurle et al. 2001). The human TRPV4 is located on chromosome 12q23-q24.1. Five TRPV4 splice variants have been described (Arniges, Fernandez-Fernandez et al. 2006). The full-length splice variant named TRPV4A encodes an 871-amino acids protein. TRPV4B lacks exon 7 ($\Delta 384-444$), TRPV4C lacks exon 5 ($\Delta 237-284$), TRPV4D has a small deletion inside exon 2 ($\Delta 27-61$), while TRPV4E lacks both exon 5 and 7. Studies have shown that only two of these variants, TRPV4A and TRPV4D, traffic to the membrane (Arniges, Fernandez-Fernandez et al. 2006). The other TRPV4 variants are retained in the endoplasmic reticulum (ER). This lack of trafficking was explained by the loss of parts of the ankyrin domains consecutive to the splicing. Ankyrin domains are important for TRP channels oligomerization that is a pre-requisite for trafficking. The glycosylation site Asn⁶⁵¹ has been also shown to influence trafficking (Xu, Fu et al. 2006). Mutation of Asn⁶⁵¹ to Gln prevented glycosylation and increased both cell surface expression of TRPV4 and functional responses mediated by TRPV4.

As all TRP channels, TRPV4 contains six transmembrane segments (S1-S6) with a pore-forming loop between S5 and S6, and intracytoplasmic N- and C-termini. There are six ankyrin repeat domains in the N-terminus region. TRPV4 channels are believed to form homotetramers.

TRPV4 is expressed in many tissues with various physiological functions. TRPV4 mRNA was detected in heart, endothelium, brain, liver, placenta, lung, trachea, and salivary gland (Liedtke, Choe et al. 2000; Strotmann, Harteneck et al. 2000; Wissenbach, Bodding et al. 2000; Delany, Hurle et al. 2001), but it is in kidney and cartilage that TRPV4 has been detected at highest levels. TRPV4 was also found in the stria vascularis of the cochlea, in the inner and outer hair cells of the organ of Corti, and in the peripheral nervous system (Liedtke, Choe et al. 2000; Suzuki, Mizuno et al. 2003; Facer, Casula et al. 2007).

Heterologous experiments demonstrated that TRPV4 forms a Ca²⁺-permeable, non-selective cation channels. TRPV4 acts as an outwardly rectifying channel, but has a

higher proportion of inward current to outward current than other TRPV channels such as TRPV1 and TRPV2. The outward rectification function in physiological solutions results from a block by extracellular Ca^{2+} ions resulting from binding to negatively charged amino acids, Asp⁶⁷² and Asp⁶⁸², in the pore loop.

TRPV4 can be activated by a numerous stimuli including heat, extracellular osmolarity, mechanical and chemical stimuli. Some studies have shown spontaneous TRPV4 activity in some type of cells. Changes in extracellular osmolarity were the first TRPV4 modulator found. Increases in osmolarity from 300 mosmol/l reduced TRPV4 activity (Nilius, Prenen et al. 2001), whereas hypotonic solutions led to an increase in TRPV4 activity (Nilius, Droogmans et al. 2003). Activation of TRPV4 by 4 α -phorbol ester derivatives was shown by several studies. In fact, TRPV4 is strongly activated by 4 α -PDD, especially in higher than room temperature (Watanabe, Davis et al. 2002). Temperature, especially above 25 °C, strongly activates TRPV4. Ca^{2+} controls both activation and inactivation of TRPV4.

General TRP channel blockers that block TRPV4 include but not limited to ruthenium red and lanthanides. Replacement of Met680 residue by a negatively charged lysine reduced TRPV4 divalent permeability. Recently, two TRPV4 blockers were discovered (RN-1734 and RN-1747), with one being a specific TRPV4 blocker (Vincent, Acevedo et al. 2009).

TRPV4 plays a role in the mechanosensation, the osmosensation, and nociception (Tabuchi, Suzuki et al. 2005; Gevaert, Vriens et al. 2007).

Prior to our study, TRPV4 had not been implicated in the pathogenesis of a neurological disorder. During our study, the gene was involved in inherited skeletal dysplasias (Rock, Prenen et al. 2008), and was also associated with hyponatremia (Tian, Fu et al. 2009).

1.3.3 Transient receptor potential melastatin channels (TRPM)

The mammalian TRPM family consists of eight genes of which three (TRPM2, TRPM6, TRPM7) differ from the other ion channels by their C-terminal region that contains enzyme domains. The C-terminal region of TRPM2 contains a NUDT9 domain that has an ADP-ribose pyrophosphatase activity, whereas those of TRPM6 and TRPM7 contain a serine/threonine protein kinase domain. We will review some of the melastatin channels here.

TRPM1

The transient receptor potential melastatin subfamily, member 1, also called melastatin 1, is the founding member of the melastatin subfamily of TRP channels. Originally discovered as a melanocyte-specific gene that is silenced in aggressive mouse melanoma cells (Duncan, Deeds et al. 1998), TRPM1 is expressed in normal tissues primarily in the melanin pigment-producing cells melanocytes of the skin and eye. *TRPM1* is conserved in a wide range of species from mammals to worm. The *TRPM1* gene is located on chromosome 15q13.3, and contains 27 exons of which 26 encode a 1,603-amino acids long protein.

Heterologous experiments have demonstrated that TRPM1 preferentially transports Ca^{2+} but the permeability ratio ($P_{\text{Ca}}/P_{\text{Na}}$) is not determined yet.

TRPM1 is thought to be constitutively active in overexpression systems and inhibited by trivalent ions such as lanthanum (La^{3+}) and gadolinium (Gd^{3+}) (Xu, Moebius et al. 2001).

TRPM1 has been also shown to express in cells responsible for transmitting signals from the retina to the ganglions, and mutations in TRPM1 have been associated with congenital stationary night blindness (Audo, Kohl et al. 2009; Li, Sergouniotis et al. 2009; van Genderen, Bijveld et al. 2009; Nakamura, Sanuki et al. 2010).

TRPM4

The human TRPM4 is located on chromosome 9q13.33, and consists of 25 exons spanning 54 kb. Splicing occurring within TRPM4 leads to two variants, TRPM4a and TRPM4b, with TRPM4b being the longest. TRPM4 has the six membrane-spanning segments with the pore region between S5 and S6, as seen in other TRP channels. However, no ankyrin repeats are present in the N-terminal region of TRPM4. Nevertheless, TRPM4 variants have important domains or sites, including a putative calmodulin binding sites in the N- and C-termini, phosphorylation sites for protein kinase A (PKA) and C (PKC), four Walker B motifs, a phosphatidylinositol biphosphate (PIP_2) binding site (Nilius, Prenen et al. 2005). TRPM4 channels homotetramerize to form functional channels.

Human TRPM4 expresses almost ubiquitously except in brain. Northern blot studies have found TRPM4 in a wide range of tissues, including placenta, spleen, prostate, skeletal muscle, heart, kidney, pancreas, small intestine, colon, lung and thymus (Xu, Moebius et al. 2001; Launay, Fleig et al. 2002; Nilius, Prenen et al. 2003).

TRPM4 protein was shown to function as a Ca^{2+} -activated channel. In addition to Ca^{2+} -dependent activation, TRPM4 currents are also strongly voltage-dependent (Nilius, Prenen et al. 2003). TRPM4 channel is activated at positive potentials whereas it closes at negative potentials.

TRPM4b constitutes a cation-selective pore that is poorly and selectively permeable to monovalent cations (Na^+ , K^+ , Cs^+ , Li^+), and impermeable to Ca^{2+} (Launay, Fleig et al. 2002; Nilius, Prenen et al. 2003). This selectivity filter feature is unique to TRPM4b, and was attributed to a 6-amino acids stretch (EDMDVA) found between S5 and S6.

TRPM4b activity is modulated by PKC activity, temperature, and binding of intracellular ATP, PIP_2 and decavanadate to the channel. Recent studies showed that TRPM4b is also a heat-activated channel.

Among TRPM4 blockers are intracellular spermine and flufenamic acid, and extracellular clotrimazole. But these compounds are not selective.

TRPM4 has been shown to be expressed in the Purkinje fibres of the heart and plays an important role in the human heart conductance. Moreover, mutations in TRPM4 have been implicated in progressive familial heart block, type 1B (Kruse, Schulze-Bahr et al. 2009).

TRPM6

The human TRPM6 is located on chromosome 9q21.13. This gene has 3 splice variants containing 39 exons. The longest variants encodes for 2,022 amino acids. The TRPM6 gene was first cloned when screening for homologues of elongation factor-2 kinase (Riazanova, Pavur et al. 2001). TRPM6 is Mg^{2+} and Ca^{2+} -permeable channel. Structural analysis showed that TRPM6, as most TRP channels, has six transmembrane domains with a pore region between S5 and S6. In addition, TRPM6 has kinase domains at its C-terminal end, conferring it a serine/threonine kinase activity. The Mg^{2+} permeability coupled with the kinase activity confers TRPM6 a unique status in TRP channels. TRPM6 has highest similarity with TRPM7, and the sequence identity increases to more than 80 % in the pore-forming region.

TRPM6 is predominantly expressed in kidney and intestine, where it might play a role in the Mg^{2+} re/absorption.

TRPM6 channels were shown to homomerize but also to heteromerize with its closest TRP channels, TRPM7. Heterologous experiments using *Xenopus* oocytes suggested

that interaction between TRPM6 and TRPM7 is required in order for TRPM6 to be trafficked to the cell membrane. But there was no sign that TRPM6 increased TRPM7 expression (Chubanov, Waldegger et al. 2004).

TRPM6 is activated by a decrease in the intracellular Mg^{2+} concentration. TRPM6 channels show outwardly rectifying currents, and reverse close to 0 mV.

Only one unspecific blocker was identified for TRPM6. In fact, TRPM6 inward monovalent currents are strongly inhibited by ruthenium red (10 μ M) whereas the outward currents remain unaffected (Voets, Nilius et al. 2004).

Mutations in TRPM6 were shown to cause hypomagnesaemia with secondary hypocalcaemia (Schlingmann, Weber et al. 2002).

TRPM7

The transient receptor potential melastatin-related subfamily member seven is located on chromosome 15q21 and contains 39 exons that encode for 1,865 amino acids. Like TRPM6, TRPM7 is also a bifunctional protein that contains both ion channel and protein kinase domains (Ryazanova, Dorovkov et al. 2004). TRPM7 has very strong outward rectification currents with little inward current in the physiological range of -70 mV to 0 mV. Its currents are characterized by a reversal potential of approximately 0 mV.

TRPM7 activity is controlled by intracellular free Mg^{2+} . Other TRPM7 activity controllers are magnesium-complexed nucleotides. The role of the kinase domain in TRPM7 gating was speculated on in different studies. Others have suggested a receptor stimulation of TRPM7 activity.

TRPM7, unlike TRPM6, is ubiquitously expressed, although expressed in variable amounts in different cells. Reports have implicated TRPM7 in the susceptibility for Amyotrophic Lateral Sclerosis-Parkinsonism/Dementia Complex of Guam (Hermosura, Nayakanti et al. 2005).

1.3.4 Transient receptor potential ankyrin channel (TRPA)

There is only one TRPA channel in human known so far, the transient receptor potential cation channel, subfamily A, member 1. Also called ankyrin-like with transmembrane domains 1 or transformation-sensitive protein p120, TRPA1 is located on chromosome 8q13 and contains 27 exons encoding for 1,119-amino acids long protein with a molecular weight of 127.4 kDa. As for most TRP proteins, TRPA1 has

six transmembrane domains with a presumed pore region between S5 and S6. Two potential N-linked glycosylation sites are located in the predicted extracellular four short loops. TRPA1 has up to 18 predicted ankyrin repeats domain in its N-terminal region. This feature distinguishes the human TRPA1 from the other TRP channels since most of them have zero to eight ankyrin repeat domains.

The expression of TRPA1 was detected in dorsal root, trigeminal, and nodose ganglia, and in the inner ear in the vestibular and auditory sensory epithelia. In these tissues, TRPA1 mediates pain.

Many stimuli have been reported to activate TRPA1 channels. These stimuli include pungent compounds and environmental irritants (e.g., mustard, wasabi, and cinnamon), bradykinin via bradykinin receptor. The role of cold in TRPA1 activation is still debated.

Four antagonist compounds, including gentamicin, ruthenium red, gadolinium, and amiloride, have been identified for TRPA1. However, as mentioned earlier, these chemicals block other channels.

1.3.5 Transient receptor potential polycystin channels (TRPP)

This family is divided into two groups, the polycystic kidney disease 1-like proteins and the polycystic kidney disease 2-like proteins. TRPP2, TRPP3 and TRPP5 are members of the polycystic kidney disease 2-like group and are called TRPP2-like proteins. They are cation-permeable channels with a calcium to sodium ratio ($P_{Ca^{2+}}/P_{Na^{+}} > 1$). They do not contain TRP domain nor do they contain ankyrin repeats. We will review two of the polycystin channels implicated in diseases.

TRPP1

The transient receptor potential polycystin member 1, also called polycystic kidney disease gene 1 (PKD1) is localized on chromosome 16p13.3 and encodes for two splice variants. The longest splice variant contains 46 exons that encode for 4303 amino acids with a 460 kDa molecular mass protein. This gene encodes for glycoprotein that contain a large extracellular N-terminal region, 11 transmembrane domains, and a cytoplasmic C-terminal region.

TRPP1 is thought to interact with TRPP2 and other TRP channels including TRPC1 and TRPC4 (Kottgen, Buchholz et al. 2008). Other interactors include cytoskeletal proteins. TRPP1 and TRPP2 co-localize at the membrane of the primary cilia of renal

epithelial cells and endothelial cells. In these cells, the two genes are proposed to transducer luminal shear stress into a calcium signal (Nauli, Kawanabe et al. 2008). PKD1 is a membrane integral protein that functions as a regulator of calcium permeable cation channels and intracellular calcium homeostasis. This channel is also involved in cell-cell/matrix interaction and may modulate G-protein-coupled signal-transduction pathways. Studies showed that this gene plays a role in renal tubular development.

Mutations in this gene were shown to cause autosomal dominant polycystic kidney disease type 1 (ADPKD1) (Peral, Gamble et al. 1995).

TRPP2

Also called the polycystic kidney disease gene 2 (PKD2), the transient receptor potential polycystin subfamily member 2 is located on chromosome 4q21-23 and contains 15 exons that encode for 968 amino acids protein with a molecular weight of 110 kDa. Structurally, TRPP2, as all other TRP channels contains six membrane-spanning segments with a pore region between S5 and S6, and intracytoplasmic N- and C-terminus regions. There are two predicted motifs in the C-terminal region, a coiled-coil domain and a Ca^{2+} -binding EF-hand (E and F helices motifs).

TRPP2 channels are thought to homomerize but also interaction with TRPP1 and TRPC1 was also demonstrated in studies. This interaction is mediated by the C-terminal region (Qian, Germino et al. 1997). This region mediates interaction with other proteins including α -actinin, troponin I, IP_3 receptor, and PACS-1/PACS-2 among others. Several studies have established that TRPP2 is a non-selective cation channel with a large conductivity averaging 100 pS. TRPP2 is permeable to divalent and monovalent ions such as Ca^{2+} , Na^+ , and Cs^+ but not to Cl^- . Heterologous experiments of mouse *Trpp2* in *Xenopus* oocytes showed that most of the protein localizes in the intracellular membranes, and its trafficking is induced by chaperones and proteasome inhibitors (Vassilev, Guo et al. 2001).

Several factors directly or indirectly modulate TRPP2 activity. Among those factors are interaction with TRPP1, the pH, vasopressin, ATP, hydro-osmotic pressure, and the epidermal growth factor (EGF). In fact, TRPP2 activity is inhibited by an increased hydrogen ions concentration $[\text{H}^+]$. Other non-specific TRPP2 inhibitors are lanthanum (La^{3+}), high Ca^{2+} concentrations, gadolinium (Gd^{3+}), and amiloride.

PKD2 is mutated in patients with autosomal dominant polycystic kidney disease Type 2 (Mochizuki, Wu et al. 1996). Mutations in PKD2 have been identified in around 15 % of these patients (Peters and Sandkuijl 1992).

1.3.6 Transient receptor potential mucolipin channels (TRPML)

This family contains three members of which one, TRPML1, has been associated with a disease.

TRPML1

Also called *MCOLN1*, this gene encodes the protein mucolipin 1 (MLN1). MLN1 is a non-specific Ca^{2+} channel that has a similar putative structure to the TRP superfamily for which it was called TRPML1 (Delmas 2004). TRPML1 is located on chromosome 19p13.2, and contains 14 exons that encode for a 580-long protein. TRPML1, like most TRP channels has six transmembrane segments with a pore region between S5 and S6. However, TRPML1 does not contain ankyrin domains. The MLN1 protein functions as calcium channel regulated by cations concentration. But, MLN1 function is also regulated by monovalent cations (Na^+ and K^+) (LaPlante, Falardeau et al. 2002) and pH changes (Raychowdhury, Gonzalez-Perrett et al. 2004). MLN1 contains a serine-lipase domain in the amino part of the protein between the first two transmembrane domains. Studies have localized MLN1 in late endosomal-lysosomal organelles (Luzio, Poupon et al. 2003). In addition, MLN1 contains two di-leucine motifs, one in the N-terminal region and another in the C-terminal region. The C-terminal di-leucine motif is responsible for targeting TRPML1 from the plasma membrane to early endosomes (Vergarajauregui and Puertollano 2006). Studies have shown that TRPML1, TRPML2, and TRPML3 can interact to form functional channels that traffic from Golgi to lysosomes. Although TRPML1 and TRPML2 can independently transport to lysosomes, TRPML3 requires one of the first two to traffic. Heterologous experiments have shown that TRPML1 generates robust outwardly rectifying currents.

Mutations in this gene result in patients with mucopolidosis type IV (Bargal, Avidan et al. 2000).

1.4 Objectives

The gene for CMT2C has been mapped in a large Caucasian-American family to chromosome 12q23-24 (Klein, Cunningham et al. 2003) spanning about 5 Mb between markers *D12S105* and *D12S1330*. This region contains 81 annotated genes. Subsequently, two other European families were studied, and their trait showed linkage to the same region; they narrowed the region to 3.9 Mb between markers *D12S105* and *D12S1340* (McEntagart, Reid et al. 2005); reducing the number of genes to 63.

However, at the time of this study, the gene causing CMT2C was not yet identified. We identified five families with a CMT2C-like phenotype. One of these families is a branch of the first large family in which the region was first mapped by Klein et al. (Klein, Cunningham et al. 2003). Our goals were to study these new families with the following objectives:

- a. Clinical and laboratory characterization of these additional CMT2C families to confirm their similarity with the classical CMT2C phenotype.
- b. Perform linkage analysis by fine mapping to see if the trait in these families links to the previously published region and moreover to narrow this region.
- c. Compare the haplotypes of these families to see whether there is a common haplotype.
- d. Find the gene causing this disease by sequencing all the genes in the region found by linkage. Eventually use high-through-put sequencing technology to find the gene when it becomes available.
- e. Study the cellular and molecular biology of the causative gene defect by heterologous expression comparing mutant to wild-type versions of the gene.

2 Materials and Methods

2.1 Patients

We evaluated five unrelated families who presented with clinical and laboratory findings consistent with CMT 2C disease. All adult subjects and parents or guardian for minors gave written consent before participation in studies at the National Institute of Neurological Disorders and Stroke (NINDS) at the National Institutes of Health (NIH), Bethesda, Maryland (United States of America) and the University College London Research Ethics Committee research protocols (London, United Kingdom). Permission was obtained from all participating individuals to share their samples with other researchers. A separate consent to take and publish pictures for scientific purposes was signed by patients. All subjects provided a detailed medical and family history, and underwent neurological evaluations and genetic counselling. A subset of patients and normal individuals underwent electrophysiological, radiological, laryngological, or audiological evaluations.

Medical and family history

Family F1 (Figure 10)

This is a Caucasian American family with German ancestors. Twenty five individuals were examined and had peripheral blood collected. Eight members were seen in the Neurogenetics Clinic at NIH. The rest of the individuals were seen during field trips in their homes. Overall, seven individuals identified themselves as being affected in this family based on the symptoms they were experiencing, and/or previous electrophysiological and laryngoscopic findings. Fifteen family members did not complain of any symptom suggestive of CMT, and three were unaffected, unrelated spouses. Of the seven affected, five underwent neuro-electrophysiological studies and laryngoscopy during this study. Nerve conduction studies and laryngoscopy were performed in one unaffected member who had raspy voice, and revealed no abnormalities except vocal cord inflammation; which may explain her raspy voice. Two patients who were complaining of hearing loss underwent audiological examination. Muscle and peripheral nerve biopsy of the gastrocnemius muscle and sural nerve was performed in one patient.

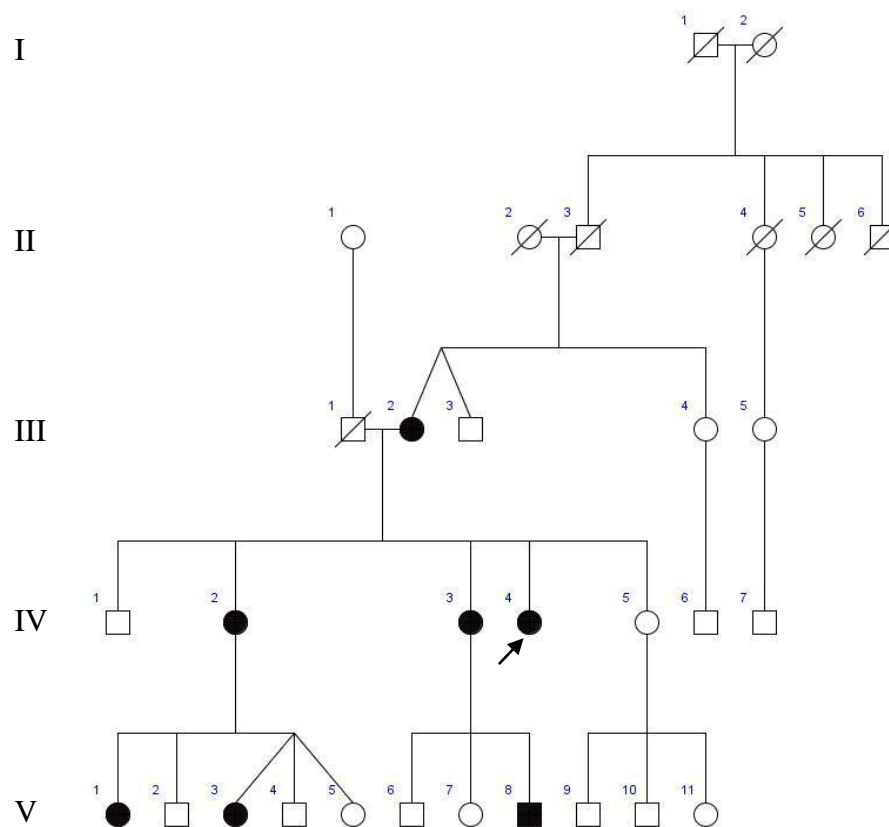


Figure 10 Pedigree of family F1.

Note that there is at least one affected in generations III to V. The arrow denotes the proband.

Family F2 (Figure 11)

Currently living in the United States, this family has Scottish ancestors. Twenty-four individuals of which six were seen in the Neurogenetics Clinic and the Laboratory of Speech and Language at the National Institutes of Health (NIH) were studied. The rest of family members were seen during field trips. Ten individuals had symptoms consistent with a peripheral neuropathy. Nine described themselves as unaffected and five were designated as unknown because of their young age or insufficient symptoms or lack of previous neurophysiological and laryngoscopic evaluation for those with suspicious symptoms. Of the six individuals seen at the Neurogenetics Clinic at NIH, three were affected and three unaffected. Neurological examination, nerve conduction studies and laryngoscopy were performed on them.

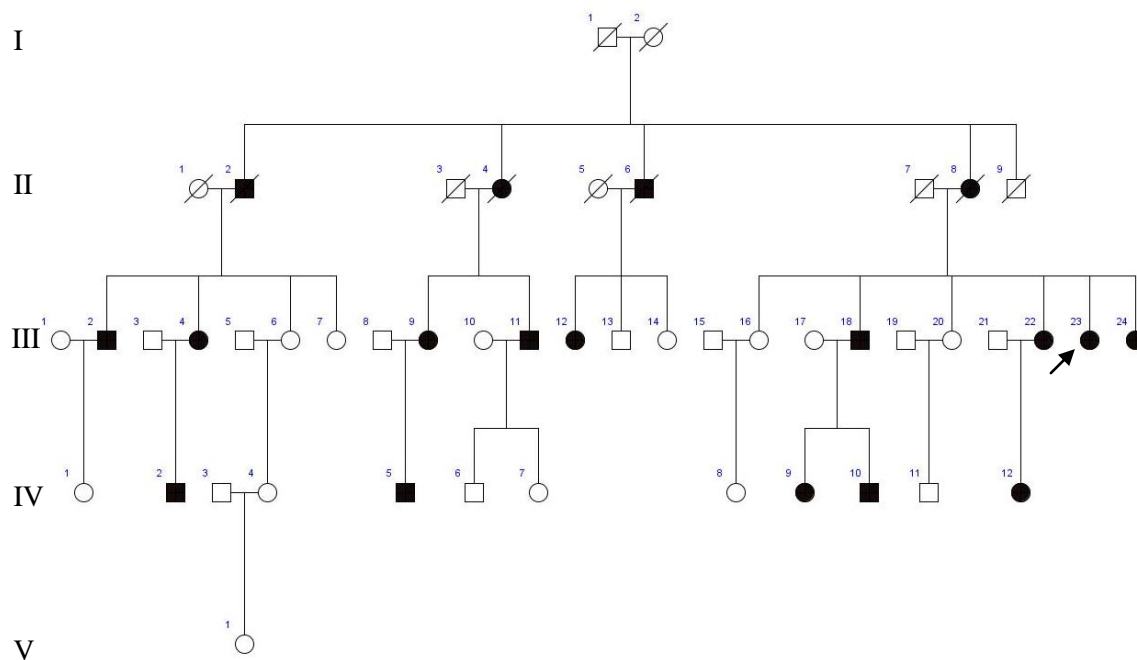


Figure 11 Pedigree of family F2.

Note that there is at least one affected in generations II to IV, and two cases of male to male transmission. The arrow indicates the proband.

Family F3 (Figure 12)

This also is a Caucasian family of which 9 individuals were seen in the Neurogenetics Clinic at NIH. Three family members identified themselves as being affected or showed obvious symptoms of peripheral neuropathy and laryngeal involvement. One individual complained of cramps in calves, numbness in hands, and sleep apnea. All individuals underwent a complete neurological examination. Laryngoscopy was performed in the three people who presented with weakness and breathing difficulties. Nerve conduction studies were done in all but one. That individual had clear symptoms of CMT, but was too young at time of study to undergo NCS. An audiological examination was performed in the most affected patient (IV.3) because of complaints of hearing loss.

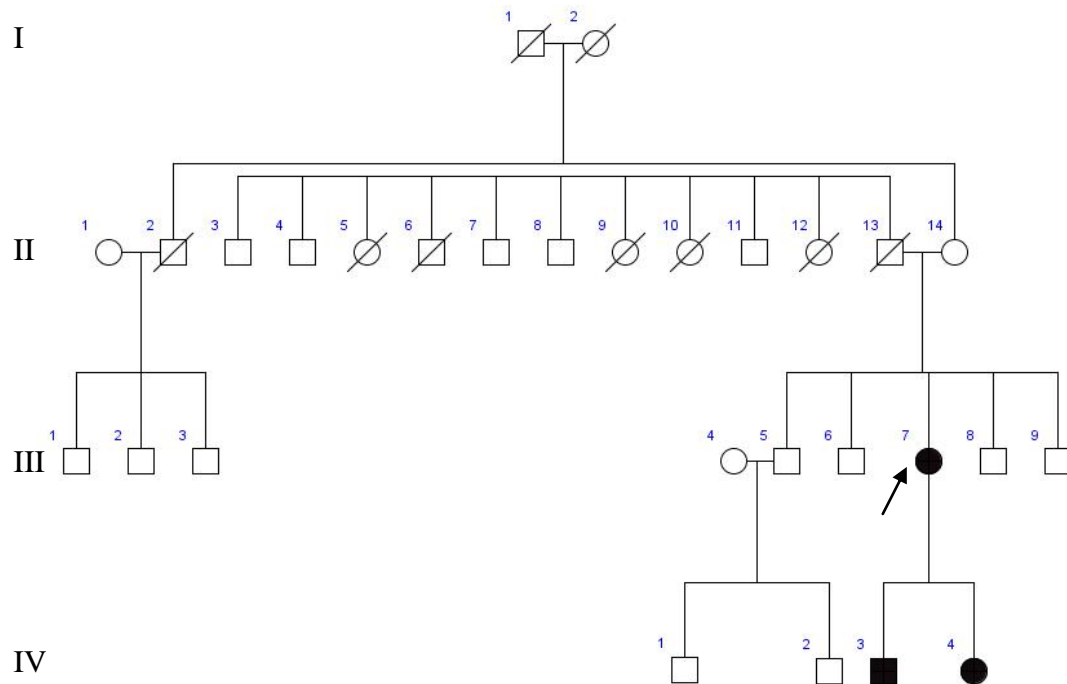


Figure 12 Pedigree of family F3.

Note the vertical transmission pattern of the disease. The black arrow indicates the initial proband.

Family F4 (Figure 13)

Also living in the United States, this family has European ancestors. All individuals were seen in the Neurogenetics Clinic at NIH. Four presented with weakness and breathing difficulties. Two family members had no complaints (one unaffected sibling and one unaffected unrelated spouse). All four affected family members were seen in the Clinic of Speech and Voice department at NIH because of their laryngeal symptoms, and neuro-electrophysiological studies and laryngoscopy were performed.

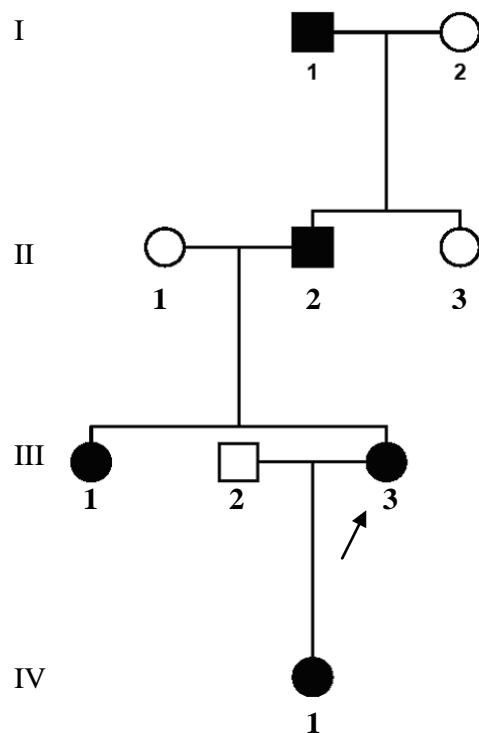


Figure 13 Pedigree of family F4.

Note the vertical transmission of the disease with a male to male transmission. The initial proband is indicated by the arrow.

Family F5 (Figure 14)

This is a small family that is originally from Iran collected by our collaborator Dr Henry Houlden in the Institute of Neurology at the University College London, London, United Kingdom. Five individuals in this family were affected or reportedly had symptoms suggesting that they are affected, a mother and her four children. The disease onset was variable, and symptoms included distal weakness and atrophy associated with shortness of breath on exertion and hoarseness of voice. No hearing loss or urinary incontinence was reported in any of the affected individuals.

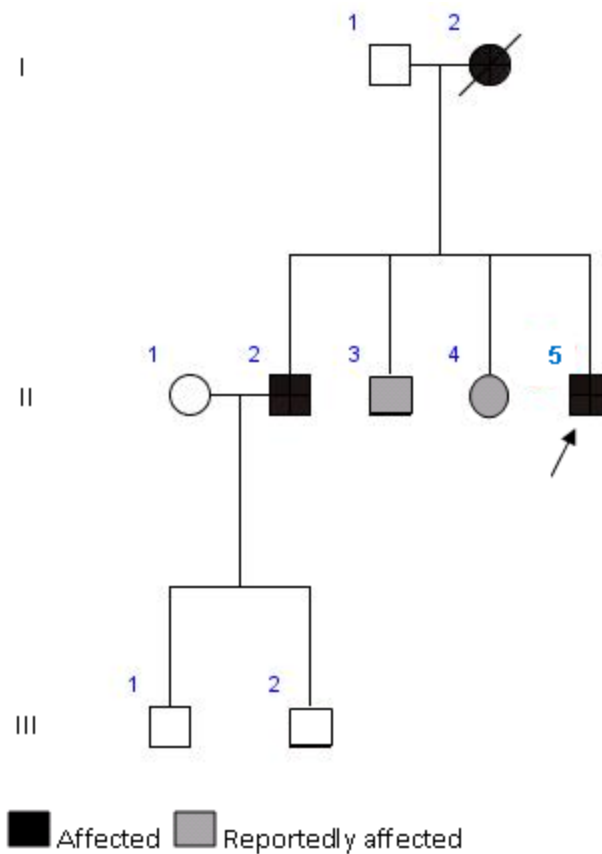


Figure 14 Pedigree of family F5.

Note the vertical pattern of the disease transmission. Individuals II.3 and II.4 are reportedly affected but were not seen in clinic.

In all five families at least one affected was seen in each generation that followed the founder. In two families (F4 and F2), there was evidence of male to male transmission, excluding X-linked mode of inheritance. Families F1 and F3 had fewer males, and the only affected male does not have offspring. We concluded that this is most likely an autosomal dominant disease and the analyses were done accordingly.

Phenotypic characterization

The affected status was determined based on clinical findings consistent with a CMT 2C-type phenotype, with vocal fold and diaphragm involvement being the key features. In addition, nerve conduction studies and electromyogram findings consistent with axonal degeneration were also considered. However, electrophysiological studies and laryngoscopy were not performed in some of the individuals we evaluated during our field trips and some individuals declined these evaluations.

Because of the high variability of the disease in term of age at onset and disease severity, we could not completely exclude people without symptoms, and revisited them occasionally after the first examination.

2.2 Laboratory studies

2.2.1 Muscle and nerve biopsy

This procedure was performed in an affected individual (Family F1 IV.4) in 1978 when she was 13 years old. The right gastrocnemius muscle and the right sural nerve were biopsies using standard techniques at the Cleveland General Hospital. The muscle fragment measured approximately 0.7 x 0.5 x 0.3 cm, the nerve fragment measured 0.7 cm in length and 0.2 cm in cross diameter. The muscle fragment was put in Zinker's solution while the nerve fragment was put in formalin. Samples were frozen in dry-ice-cooled isopentane for conservation. For the current study, fragments of the first biopsies were requested for further analysis. Samples were sectioned transversely in a cryostat for pathology. For muscle general morphology assessment, serial sections of 10 μm were picked up on poly-lysinated slides, and stained with hematoxylin and eosin. Nerve sections were stained with toluidine blue. Both muscle and nerve sections were visualized using a light microscope. In addition, sural nerve sections were examined by electron microscopy. My contribution in this part of the study was to identify the laboratory where the biopsy was done, obtain material release consent from the patient and organize the shipment.

2.2.2 Nerve conduction studies (NCS) and electromyography (EMG)

These laboratory examinations were performed in available affected and unaffected family members in the Electromyography Section at NIH by Drs. Mary Kay Floeter and Tanya J. Lehky or in their local clinics for those who could not make it to NIH or had previously had the testing prior to enrolling in this study. My contribution in this part of the study was to organize the evaluation and help with interpreting the results based on clinical findings. NCS of motor nerves and sensory nerves were obtained using standard surface recording techniques.

Compound motor action potential (CMAP), conduction velocity (CV), and distal latency (DL) were recorded at the ulnar and median nerves for upper extremities, the peroneal and tibial nerves for lower extremities, and the phrenic nerve.

For the ulnar nerve, motor action potentials were recorded at the abductor digiti minimi (ADM) muscle, with stimulation sites at wrist, below elbow, and above elbow, the conduction velocity was recorded at segments wrist-below and below elbow-above elbow while distal latencies were recorded at all segments.

For the median nerve, motor action potentials were recorded at abductor pollicis brevis muscle with the stimulation sites being the wrist and elbow, conduction velocity was recorded at the wrist-elbow segment, and the distal latency at all segments. For the peroneal nerve, motor action potentials were recorded at the extensor digitorum brevis with the ankle being the stimulation site, conduction velocity was recorded at segments ankle-fibula neck and fibula neck-popliteal fossa, and distal latencies at all sites. Motor action potentials for the tibial nerve were recorded at the abductor hallucis muscle and stimulated from the ankle, the conduction velocity at the ankle-popliteal fossa segment, and the distal latencies at all sites. For the phrenic nerve, motor action potentials and distal latencies were recorded at the chest and stimulated from the neck while conduction velocity was not usually recorded. In some patients the CMAP and DL of the phrenic nerve were recorded during laryngoscopy by fluoroscopy. F-wave studies were also performed. For these studies, F-latency and M-latency were recorded at median, ulnar, peroneal and tibial nerves.

Sensory nerve action potential (SNAP), CV, and DL were also recorded from median, radial, ulnar, and sural nerves. For the median nerve, sensory amplitude was first recorded at the index and stimulated at the wrist, and then at wrist-elbow and elbow-axilla segments. Conduction velocity was recorded at the index-wrist segment while distal latencies were recorded at all segments. The radial nerve sensory amplitude was recorded at the base of the thumb and stimulated from the forearm. Conduction velocity and distal latency were recorded at the same segment. For the ulnar nerve, sensor action potentials were recorded at the little finger and stimulated at the wrist. Both conduction velocity and distal latency were recorded at the same site. Sural nerve sensory action potentials as well as conduction velocity and distal latency were recorded at the ankle and stimulated at the lower leg.

A concentric needle EMG study was performed in the biceps brachii, the first dorsal interosseus, the tibialis anterior, the vastus lateralis, the gastrocnemius (medial head), and the diaphragm muscles. Parameters assessed include but not limited to the insertional state of muscle fibres including the spontaneous activity (fibrillation,

positive waves, fasciculations, and phases), the volitional activity (amplitude, duration, and configuration), and the recruitment of motor units (at maximum effort, and the maximum pattern). In addition, an interference pattern analysis was performed in selected muscles. Not all motor and sensory nerves amplitudes were recorded in all individuals that underwent this evaluation nor was needle EMG performed in all.

In addition, short exercise test and a quantitative sensory testing estimating the cold and warmth detection threshold and using the CASE IV machine (WR Medical Electronics CO., Stillwater, MN) with the 4-2-1 algorithm were done in a subset of patients.

2.2.3 Fiberoptic nasolaryngoscopy

This laboratory examination was performed by Dr. Christy Ludlow at the National Institutes of Health in the Speech and Language Department. Here too I helped organize patient visit, and identify those we needed undergo this examination. Otolaryngological examinations were performed using a Pentax PNL-10RP3 fiberoptic nasolaryngoscope (Pentax Precision Instruments, Orangeburg, NY) interfaced with the Kay Elemetrics Digital Stroboscope system (Kay Elemetrics Corporation, Lincoln Park, NJ) to evaluate the structure and function of the laryngeal mechanism. All available patients and unaffected family members with suspicious altered voice underwent this examination which included the following gestures to examine the vocal folds integrity:

- a. Alternating between sniff and phonation three times to examine for asymmetry in abduction and adduction.
- b. Pitch-glide up and pitch-glide down to examine for vocal fold lengthening.
- c. Rapid repetition of syllables containing glottal stops and vowels for speed and completion of hyper-adduction.
- d. Rapids repetition of syllables containing voiceless consonants and vowels for speed and completion of phonation offset and abduction.
- e. Whistling “Happy Birthday” to examine for symmetry for movement for rapid abduction and adduction during non-speech.
- f. Stroboscopy during extended vowel production to examine the symmetry of the mucosal wave during vocal fold vibration.

2.2.4 Radiological evaluation

Chest X-rays during inspiration and expiration were performed in a subset of patients to look for diaphragmatic movement abnormalities. Vertebral column, long bones, hands, and wrists X-rays were also done to evaluate skeletal deformities which are seen in CMT patients, and to examine bone morphology and density. Antero-posterior and lateral radiographs were obtained for this evaluation.

2.2.5 DNA extraction

Peripheral blood was taken from available patients and unaffected relatives for DNA extraction. I extracted DNA using the Qiagen PAXgene Blood DNA kit protocol or the Puregene Blood Core Kit C (Qiagen, Valencia, CA, USA) per manufacturer's protocol for genetic analysis. Eight millilitres (ml) of peripheral blood were collected in a tube provided by the manufacturer that contains 2 ml of buffer for the PAXgene blood DNA Kit whereas blood was collected in a heparin tube for the Puregene Blood Core Kit C.

2.2.6 Skin biopsy

Skin biopsies were performed by Dr Sumner with my assistance using a 3-mm punch. Selected areas of biopsy were cleaned with providone-iodine solution. The areas were anesthetized using a subcutaneous injection of 2 percent lidocaine. A 30-gauge needle was used to administer the anesthetic to limit discomfort. The skin surrounding the biopsy site was stretched with the thumb and index finger of the nondominant hand. The punch biopsy instrument was held vertically over the skin and rotated downward using a twirling motion created by the first two fingers on the dominant hand. Once the instrument had penetrated the dermis into the subcutaneous fat, or once the instrument reached the hub, it was removed. This created a cylindrical skin specimen which was removed. Scissors held in the dominant hand cut the specimen free from the subcutaneous tissues. The cut was made below the level of the dermis. Each specimen was placed in a formalin container. In selected patients, skin sections were analyzed to look for possible abnormalities.

2.2.7 Immortal cell lines establishment

To establish lymphoblast cell lines, peripheral blood was collected in heparin tubes and sent to Georgetown University (Washington D.C., USA) for EBV transformation.

Skin samples from some patients and unaffected individuals were used to establish fibroblast cell lines.

2.3 Genetic analysis

We performed fine mapping using STS markers and SNP arrays analysis for whole genome scan.

We then proceeded with the editing, quality control and analysis of the linkage format of pedigree, marker and map files (pedigree file .ped, marker data file .dat and mapfile .map) on a software installed (and where necessary compiled) on a Windows XP workstation and a Unix / Linux (CentOS 5) server.

2.3.1 Linkage analysis/Fine mapping

Linkage analysis was done in Professor Robert Kleta's laboratory by Dr Horia Stanescu. My role was to draw pedigrees, help design the model to use, and data interpretation. This analysis involved three families (F1, F2 and F4). Twenty five individuals were collected from family F1, 24 from family F2, and 6 from family F4. Samples from the three families were combined and sent to deCODE (Reykjavik, Iceland) for genotyping. Twelve highly informative STS markers spaced at about 0.04 to 1.6 cM intervals covering the previously reported region (Klein, Cunningham et al. 2003) were used to perform fine mapping. Di-, tri-, and tetra-microsatellite loci were used in multiplex PCR with fluorescently-labelled primers. The analysis was done in capillary electrophoresis ABI 3730 DNA analyzers (Applied Biosystems, Foster City, CA USA). Multipoint analysis was performed using both: a parametric model (assuming autosomal dominant mode of inheritance with complete penetrance and disease allele frequency of 0.001) and a nonparametric model (with no assumptions regarding the mode of inheritance) followed by haplotype reconstruction. The software used for the analysis was: Genehunter 2.0 (Kruglyak, Daly et al. 1996) and Simwalk2 v2.91 (Sobel, Sengul et al. 2001). Mendelian inconsistencies were checked using PedCheck (version 1.1). Genotyping data was formatted for Simwalk2 using mega2 (v4.0) which is based on a Markov Chain Monte Carlo simulation. The haplotypes were reconstructed with Genehunter and Simwalk, and visualized using HaploPainter (v.029.5). Data from previously reported studies on this disease were compared with our results to re-define the region of interest.

2.3.2 Single Nucleotide Polymorphism (SNP) array analysis

SNP array analysis was also performed to track for possible deletion or duplication in the region of interest found through linkage analysis using families F1, F2 and F4, and to perform whole genome scan in another family.

Copy number analysis in the linked region

The Illumina Infinium II HumanHap550 SNP chips (Illumina Inc., San Diego, CA, USA) were used in the families where linkage analysis was done with microsatellite markers for this analysis. Samples from one affected individual from each of the 3 families (F1, F2, and F4) were genotyped. These chips assay 555,352 tagging SNPs derived from phase I and II of the international HapMap project. Genotyping was performed as per the manufacturer's protocol using 750 ng of genomic DNA. Briefly, each DNA sample was amplified in an overnight step. The amplified product was then enzymatically fragmented, precipitated, and resuspended. The resulting product was then hybridized to the chip overnight. The amplified and fragmented DNA samples anneal to locus-specific 50-mers during the hybridization step. Each allele at each locus is represented by one of two bead-types fixed to the chip. Following hybridization, allelic specificity is conferred by enzymatic extension. Products were fluorescently stained and visualization of the resulting signal and localization of the SNPs was performed with the BeadStation scanner and data collection software (v2.3.25, Illumina Inc, San Diego, CA, USA).

Whole genome scan

GeneChip Human Mapping 10K array XBa142 2.0 Affymetrix (Affymetrix UK Ltd, United Kingdom) was used to perform this analysis. DNA from family F5 was genotyped according to manufacturer's instruction. Unlikely genotypes were filtered using the Merlin software (version 1.1 alpha3). Genotypes were examined as described above (linkage analysis).

2.3.3 Selection of candidate genes

To select candidate genes I considered different criteria, including the level of expression of genes in the nervous system by *in situ* hybridization or expression prediction based on homology with other known CMT genes, and their interaction or homology with other known CMT-causing genes. Another criterion considered was

the effect on the development, morphology or functioning of the nervous system of animal models of the genes in the region of interest.

Genes that fulfilled all or most of these criteria were considered first. To do this work we used different bioinformatics tools and databases including the Online Mendelian Inheritance in Man (OMIM) from the National Center for Biotechnology Information, NCBI (NIH, Bethesda, MD USA) and the McKusick-Nathans Institute of Genetic Medicine (Johns Hopkins University School of Medicine, Baltimore MD USA), Unigene and Aceview from NCBI, EMBL-EBI (Hinxton, Cambridge UK), Gene Sorter from UCSC (Santa-Cruz, CA USA) and GNF SymAtlas v1.2.4 (San Diego, CA USA). Genomic sequences of candidate genes were taken from the NCBI Entrez database (RefSeq) but cross-compared with other nucleotide sequences databases, e.g., Ensembl (EMBL-EBI and Sanger Institute) and the UCSC genome browser.

2.3.4 Mutation detection

I designed intronic primers flanking the donor and acceptor sites up to about 200 bp of all exons of candidate genes by visual inspection. The specificity of these primers to the chosen genes was checked using NCBI's nucleotide BLAST search (Basic Local Alignment Search Tool). Coding regions and flanking intronic regions up to about 200 bp of candidate genes in the region of interest were sequenced to look for eventual sequence variants. From each family, genomic DNA was amplified from an affected and an unaffected individual sharing the non-disease-bearing allele in the linked region for sequence comparison. Polymerase Chain Reaction (PCR) using 25- μ l total volume containing 25 ng genomic DNA and 10 pmol of each primer were processed in PuReTaq Ready-to-go beads (GE Healthcare, Buckinghamshire, HP7 9NA, UK). PCR was done according to the following protocol: five minutes at 95 °C for the first step, followed by 35 cycles of 95 °C for 30 seconds, 55 °C to 60 °C for 30 seconds, and 72 °C for 30 seconds to 1 minute, followed by a final 10 minutes extension step at 72 °C. All reactions were performed in a DNAEngine thermocycler from Bio-Rad (Hercules, CA USA). DNA fragments were separated by electrophoresis on 1 per cent agarose gels (150 ml TAE buffer for 1.5 g of agarose) containing 1.5 μ g of ethidium bromide. The gels were cast in 1x TAE buffer, and ran at a constant voltage of 140V for 45-60 minutes. A size marker of 200 bp ladder (Hyperladder I from Bioline, London, UK) was electrophoresed alongside the samples to allow identification of correct DNA fragments.

The DNA fragments were purified using GENECLAN Spin Kit from MP Biomedicals, Inc. (Illkirch, France). Sequencing PCR was set up in the same thermocycler according to the manufacturer's protocol (Beckman Coulter, Fullerton, CA USA), and by using their Quick Start Kit. Direct genomic DNA sequencing from both forward and the reverse primers was done by dye terminator cycle sequencing from Beckman Coulter. Sequences were aligned and compared with the NCBI reference sequences using the nucleotide BLAST software. When a sequence variant not seen in the NCBI and Ensembl SNP databases was found in the affected individual only, segregation was checked within the families, and conservation of the mutated amino acid or nucleotide among all available species was checked by alignment using the MultAlin software. In addition at least 200 ethnically matched controls were sequenced to exclude SNPs.

2.3.5 Exome sequencing

This experiment was performed by Dr Bryan Traynor's group at the National Institute of Aging (NIH). Two families, F4 that linked to the chromosome 12q24 locus but was negative for all genes within the region and F3 that was negative for TRPV4 screening, were used for this analysis. DNA from one affected individual (III:1 for family F4 and IV:3 for family F3) was enriched using SureSelect Exome target enrichment technology according to the manufacturer's protocol (version 1.0, Agilent, CA). The enriched DNA was paired-end sequenced on a Genome Analyzer Iix (Illumina, CA). Sequence alignment and variant calling were performed against the reference human genome (UCSC hg 18) using the Genome Analysis Toolkit (http://www.broadinstitute.org/gsa/wiki/index.php/The_Genome_Analysis_Toolkit). PCR duplicates were removed prior to variant calling using Picard software (<http://picard.sourceforge.net/index.shtml>). Based on the hypothesis that the mutation underlying this rare familial disease was not present in the general population, SNPs identified in the 1000 Genomes project (www.1000genomes.org/) or in dbSNP (<http://www.ncbi.nlm.nih.gov/projects/SNP/>, Build 131) were removed. Next, synonymous changes were identified and filtered from the variant list using SIFT software (version 4.0, <http://sift.jcvi.org/>). Sanger sequencing using customized primers was performed to confirm the variant and determine its presence in the other affected family members as well as the unaffected family members to check for segregation.

As an additional step, variants and indels detected in the genotyped families were filtered against exome data generated for 200 neurologically normal control subjects. My contribution in this part of the study was to draw pedigrees, help design the approach, confirm sequence variants, and check co-segregation.

2.4 Functional studies of mutants TRPV4

2.4.1 TRPV4 expression in the nervous system

- Quantitative Reverse Transcriptase-Polymerase Chain Reaction (qRT-PCR)

Frozen human spinal cord and trachea tissues isolated at autopsy were obtained from the Maryland Brain and Tissue Bank (Baltimore, MD). Human knee cartilage primary chondrocytes isolated at the time of knee surgery were a kind gift of Jennifer Eisenhoff at John Hopkins University. Spinal cord dorsal horn and ventral horn and tracheal cartilage was dissected from the whole tissues and homogenized. RNA was isolated from tissues using TRIZol reagent and purified using the QIAGEN RNeasy mini kit. RNA was converted to cDNA by using the High Capacity cDNA RT kit (Applied Biosystems) as previously described. Primers to amplify different exons of the TRPV4 transcript (exons 3-4, exons 5-6, exons 7-8, exon 5, and exon 7) and 18S (as internal control) were purchased from Applied Biosystems (ABI). Reactions were run in triplicate using the ABI Prism 7900 Sequence Detector System as previously described. Data were analyzed in an excel spreadsheet.

- Standard Polymerase Chain Reaction

Studies have shown that TRPV4 have five splice variants, some lacking exon number 5 or exon number 7, and some lacking both. I then designed primers covering exon 5 and 7 of TRPV4 within exon number 4 and 8 in the human and mouse cDNA sequence. These primers were ordered from Integrated DNA Technologies (Leuven, Belgium). Human cDNAs from different tissues including lung, brain, trachea, spinal cord, heart, and kidney were purchased from Clontech (Mountain View, CA). Mouse spinal cord, peripheral nerves and cartilage cDNAs were also ordered. A regular PCR using the protocol described above (mutation detection) was processed. PCR products were run on a 1 % agarose gel to identify bands characterizing different splice variants. Bands were identified, cut, purified and sequenced to verify the presence or absence of exon number 5 and/or exon number 7.

2.4.2 Expression of WT and mutant TRPV4 in *Xenopus* oocytes and mammalian cells

Xenopus oocytes experiments were completed by Dr Anselm Zdebik in our laboratory at UCL. I helped selecting healthy oocytes, inject them, and performed western blot to check equal expression. For expression in *Xenopus* oocytes, cDNA constructs were obtained by recombinant PCR from mouse cDNA prepared using Superscript III (Invitrogen) primed with polydT according to manufacturer's instructions. A recombinant 5' fragment carrying the R269C mutation was combined with a 3' fragment carrying the R269H mutation to obtain WT, R269C and R269H through proofreading activity. The full-length fragment was then inserted into pTLB via ClaI and XbaI sites test digested, and fully sequenced. These mouse WT and mutant TRPV4 cDNAs were also subcloned into a modified pIRES-CD8 for transfection in mammalian cells.

Mammalian expression constructs (pcDNA3.1 and pcDNA3.1-FLAG), expressing human TRPV4 cDNA, were a gift from Miguel Angel Valverde. I generated the R269C and R269H TRPV4 mutants using the QuickChange Site-Directed Mutagenesis kit (Stratagene) as per the manufacturer's instructions. For the R269C sequence variant we used the following primers: forward primer 5'-CCACGCCCCAGGCC**T**GTGGGCGCTTCTTCCAGCCC-3' and reverse primer 3'-GGGCTGGAAGAAGCGCC**C**AC**A**GGCCTGGGCGTGG-5'. For the R269H sequence variant we used the following primers: forward primer 5'-CCACGCCCCAGGCC**C****A**TGGGCGCTTCTTCCAGCCC-3' and reverse primer 3'-GGGCTGGAAGAAGCGCC**C****A**TGGGCGCTGGGCGTGG-5'. A PCR reaction using 50 µl total volume containing 1µg of plasmid DNA, 125 pmol of each primer, 2 µl of enzyme, 2 µl of DMSO, 1 µl dNTPs, was completed with water and processed in a 200-µl tube. PCR was done according to the following protocol: 95 °C for 30 seconds followed by 16 cycles of 68 °C for 3 minutes. The PCR product was test-digested with DPN1 for up to 6 hours to eliminate wild-type version and purified using the Qiagen PCR purification kit as directed. To transform TOP10 supercompetent cells (Invitrogen), 5 µl of the PCR product were used. Transformed cells were plated in ampicillin-containing agar overnight. Plasmid DNA was isolated from three random colonies using the Qiagen Miniprep DNA kit and mutagenesis confirmed by DNA sequencing. Mutant plasmid DNA was first used to transfect cells to check for

transfection efficiency before transforming Maxi Efficiency DH5 α (Invitrogen) for maxiprep plasmid DNA extraction.

Human epithelial cervical cancer cells (HeLa), Human Embryonic Kidney (HEK) 293 were grown and plated in high glucose DMEM supplemented with fetal bovine serum (FBS) (Hyclone) (10 %) and penicillin/streptomycin/glutamine (PSG) (1 %) at 37 °C in 5 % CO₂, and DRG cell lines were grown in neurobasal medium supplemented with glucose (20 %), L-glutamine (0.2 M), FBS (10 %), B-27 supplement (Invitrogen) (5 %), and blasticidin (Invitrogen) (1 %). HeLa cells were transfected with the mouse cDNA using polyethyleneimine (1 mg/ml) in Optimem I (Invitrogen). HEK 293 and DRG cells were transfected with the Human cDNA using lipofectamine 2000 (Invitrogen).

2.4.3 TRPV4 blockers

TRPV4 is an ion channel that is regulated by different stimuli including chemical compounds and structural changes. A pore domain mutant M680K, shown to be a TRPV4 inhibitor (Voets, Prenen et al. 2002), was generated in WT, R269C and R269H mutants TRPV4 using the QuickChange Site-Directed Mutagenesis kit (Stratagene) as described above.

RN1734 is a chemical compound that was shown to be a specific TRPV4 blocker (Vincent, Acevedo et al. 2009). This compound is commercially available, and was purchased from Menai Organics Ltd. (catalogue number NC1207) (Bangor, United Kingdom).

2.4.4 Cell death quantification

Part of cell death assays was performed in Dr Charlotte Sumner and I performed part of it in our laboratory. HEK 293 cells were grown on cover slips and transfected as described above. For indicated samples, ruthenium red (Sigma) or RN1734 (10 μ M) was added to the media 4 hours after transfection at a concentration of 10 μ M. Twenty four or 48 hours after transfection, cells were washed once with PBS and incubated with 2 μ M Calcein AM and 4 μ M of ethidium homodimer-1 (EthD-1) (Invitrogen) for 30 minutes at room temperature. EthD-1 is used to label and detect nucleotides and nucleic acids. Because EthD-1 is highly positively charged and cannot cross cell membrane of living cells, it is used to stain dead or dying cells. Cover slips were then immediately mounted using ProLong Gold antifade reagent

(Invitrogen) and imaged immediately using a Zeiss AxioImager Z1 microscope. Each experiment was performed in triplicate and digital pictures were taken at 40X magnification of each sample at random. The number of dead cells (red) and live cells (green) were counted in each picture using the Zeiss Axiovision 4.6 software, and the average percentage of dead cells for 3 separate experiments was quantified. Equal expression of TRPV4 was confirmed by protein blot of cells transfected under identical conditions.

2.4.5 Immunohistochemistry

This experiment was done in Dr Charlotte Sumner's laboratory. Cells were transfected as above and after 24-48 hours were fixed with 4 % paraformaldehyde (PFA)/0.05 % NP-40. They were stained with the following antibodies: polyclonal rabbit anti-TRPV4 antibody 1:300 (Sigma reference number T9075), polyclonal rabbit anti-TRPV4 1:1000 (gift from Michael Catarina, Johns Hopkins), monoclonal anti-Flag 1:500 (Sigma), monoclonal anti-calnexin 1:50 (BD), and acetylated tubulin (Sigma). Alexa Fluor conjugated 488, 546, or 594 (Molecular Probes) secondary antibodies were used at 1:1000 dilution. Nuclei were counterstained with TOTO-3 (Molecular Probes) at 1:3000 dilution or mounted in ProLong gold anti-fade reagent with or without DAPI (Invitrogen). Images were obtained using a Zeiss LSM-510 META confocal microscope. Z-stack projections were made from serial scanning every 0.5 μm .

Adult mice (strain C57/B6) were transcardially perfused with 4 % PFA and spinal cords and DRGs were isolated, post-fixed in 4 % PFA for 6h, cryoprotected in 30 % sucrose, and cut into transverse sections on a cryostat at 50 μm thickness. Polyclonal rabbit anti-TRPV4 1:1000 (gift from Michael Caterina, Johns Hopkins) (Guler, Lee et al. 2002), anti-Choline acetyltransferase (ChAT) (Chemicon), and anti-Tuj1 (Covance) were used followed by the appropriate Alexa Fluor-conjugated 488, 546, or 594 secondary antibodies (Molecular Probes). Images were obtained with an inverted Zeiss LSM 510 META confocal microscope as above.

2.4.6 Cell surface biotinylation

This experiment was also done by Dr Anselm Zdebik. For surface biotinylation, cells were transfected as above, washed with PBS, and incubated with SulfoLink NHS Biotin from Pierce (0.5 mg/ml in PBS+2 mM MgCl_2) for 1 h at 4 °C. Cells were

washed with PBS and TBS to block unincorporated biotin, and harvested into 0.1x TBS+300 mM Mannitol, 1 % Triton X-100 supplemented with a complete protease inhibitor cocktail (Roche). Cells were incubated on ice for 10 min, centrifuged at 1000 g for 10 min, and an aliquot of the supernatant saved for Western blotting of the input fraction.

The remaining was incubated with streptavidin-covered agarose beads for 60 min at room temperature with gentle shaking. Beads were pelleted at 500 g for 2 min for a total of 4-wash steps using TBS 1 % Triton-X100, 0.05 % SDS, 0.1 % sodium desoxycholate. Protein was recovered from the beads by incubation with 100 µl 1x LDS loading buffer (Invitrogen) supplemented with 100 mM DTT. Five per cent input and biotinylated protein was separated on 4-12 % ready-made gels using MOPS run buffer (Invitrogen), transferred to PVDF membrane using a Biorad TransCell semidry blotter and protein visualized using Sigma anti-TrpV4 (reference number T9075) and mouse anti-actin antibodies. Secondary antibodies were from Amersham and diluted 1:3000 in block containing 5 % non-fat dry milk and 0.05 % NP-40 in TBS. Blots were visualized using homemade ECL reagent on a Syngene cooled CCD imaging station.

2.4.7 Endoplasmic Reticulum (ER) stress experiment

This work was completed in Dr Charlotte Sumner's laboratory. The endoplasmic reticulum (ER) is a central organelle of each eukaryotic cell as the place of lipid synthesis, protein folding and protein maturation. Proteins of the plasma membrane, secreted proteins as well as proteins of the Golgi apparatus and lysosomes fold into their tertiary and quaternary structure in the ER. The ER is the major signal transducing organelle that senses and responds to changes of the homeostasis. Conditions interfering with the function of ER are collectively called ER stress. ER stress is induced by accumulation of unfolded protein aggregates (unfolded protein response, UPR) or by excessive protein traffic usually caused by viral infection (ER overload response, EOR). Several genes including HSPA5 (Grp78), HSP90B1 (Grp94), and GADD45A have been implicated in protecting against ER stress. As a result these genes become over expressed during ER stress. To investigate whether TRPV4 mutants induce ER stress, we have measured the expression of these genes in WT compared to mutants-expressed HEK293T cells. To measure the expression RNA was extracted in cultured HEK293T cells expressing WT and mutants TRPV4, and

converted to cDNA by using the High Capacity cDNA RT kit (Applied Biosystems) as previously described. Primers to amplify different exons of the Grp78, Grp94 and GADD45A transcripts, and 18S were purchased from Applied Biosystems (ABI). Reactions were run in triplicate using the ABI Prism 7900 Sequence Detector System as previously described.

2.4.8 Intracellular calcium measurement.

In this experiment I provided mutant and wild-type constructs.

Cell calcium imaging

Calcium imaging was done in Dr Michael Caterina's laboratory at Johns Hopkins' University. HEK293 cells were transfected with 0.1 µg wild type or mutant TRPV4 + 0.4 µg pcDNA3, or 0.5 µg pcDNA3 alone, plus fluorescent marker (0.02 µg mCherry), using Lipofectamine 2000, according to the manufacturer's instructions. Cells were replated onto polyornithine-coated coverslips approximately 4.5 hours after transfection and were maintained at 37 °C in 5 % CO₂ until use. A subset of cells was cultured in the presence of 10 µM ruthenium red which is a TRP channels blocker. Calcium imaging was started approximately 22-24 hours post-transfection.

Cells were loaded with Fura 2-AM (10 µM Fura + 0.02 % pluronic acid diluted in extracellular buffer; Molecular Probes, Eugene, OR) for 1 hour at 37 °C. Coverslips were positioned on an inverted microscope (Nikon, Melville, NY), and solutions were delivered via a gravity-driven perfusion system using electronically controlled valves (Warner Instruments, Hamden, CT). Standard extracellular buffer contained (in mM): 130 NaCl, 3 KCl, 2.5 CaCl₂, 0.6 MgCl₂, 10 HEPES, 10 sucrose, 1.2 NaHCO₃, pH 7.4 (NaOH), 295 ± 5 mOsm. Baseline Fura 2 fluorescence was assessed over a period of 90 seconds and was used as a measure of intracellular calcium levels. Ratiometric images were captured at 340 and 380 nm excitation at 2 second intervals, using a fluorescent light source (DG4, Sutter Instruments, Santa Rosa, CA), cooled CCD camera (Roper, Tucson, AZ) and RatioTool software (ISee Imaging, Raleigh, NC). All experiments were done at room temperature. Only transfected (mCherry-positive) cells were included in the subsequent analysis.

Plate-based intracellular calcium assay

This assay was performed in Dr. Charlotte Sumner's laboratory at Johns Hopkins' University. Intracellular calcium levels were determined using a calcium assay kit

according to manufacturer's instructions (catalogue number R8041, Molecular Devices). The assay was performed with the use of a Fluorometric Imaging Plate Reader (FLIPR) calcium assay kit, according to the recommendations of the manufacturer (Molecular Devices). HEK293 cells were transfected with wild-type and mutants TRPV4 constructs. At 4 h, RN1734 was added at 10 μ M, and at 24 h, media was removed. Cells were washed once in Hanks balanced saline supplemented with 2.5 mM probenecid (pH 7.4), and 50 μ l of Calcium Assay Reagent was added, and cells were incubated at 37 °C for 1 h. After incubation, cells were placed immediately in a FlexStation plate fluorometer equipped with a multichannel injector (Molecular Devices) and set at $\lambda_{\text{ex}} = 485$ nm, $\lambda_{\text{em}} = 520$ nm. Agonist or a vehicle was added in a volume of 50 μ L/well at an injection speed of 80 μ L/ s. Fluorescence measurements were taken at 1.52 s intervals before and after agonist addition for a total of 60 s per well. Each assay plate included a mock-transfected control, wild-type receptor and a test mutant all transfected at the same time and seeded at the same cell density. The raw data were analyzed with the SoftmaxPro software package (Molecular Devices). The baseline was defined as the average of the first five recordings on each curve. Functional responses were measured as peak fluorescence levels after subtraction of the baseline. Basal (spontaneous) receptor activity was determined by subtracting the baseline in the mock-transfected control from that of the test sample also measured on the same assay plate. All measurements were derived from at least three separate experiments each performed in sets of three to four replicates.

2.4.9 Electrophysiology

Xenopus oocytes whole-cell currents measurement

This work was done in our laboratory by Dr. Anselm Zdebik. Whole-cell membrane current was measured using *Xenopus oocytes*. Mouse TrpV4 cRNA was transcribed from templates linearized with MluI using mMessageMachine Sp6 kits (Applied Biosciences) according to manufacturer's instructions. We injected 0.5-5 ng of cRNA into oocytes prepared according to standard protocols (Thiemann, Grunder et al. 1992). Oocytes were incubated in nominally Ca^{2+} free solution containing 100 mM NaCl, 4 mM MgCl_2 , 2 mM KCl and 5 mM HEPES, pH 7.5 after injection to prevent degradation. Oocyte currents were measured using a npj Tec01 TEVC amplifier (npj, Tamm, Germany) in the same solution supplemented with 20 mM CaCl_2 after 24-48 h. Currents were activated by increasing temperature from 17 °C to 38 °C using a

Peltier-based CL-100 solution cooler/heater (Harvard Apparatus, Kent, UK) or by preincubation with 4- α -phorbol 12,13-didecanoate (4- α -PDD) (Watanabe, Davis et al. 2002) obtained from LC laboratories (Woburn, USA) predissolved at 5 mM in DMSO at a final concentration of 5 μ M. Temperature activated currents were measured initially and when the bath had reached 38 °C. Pre-incubation with 4- α -PDD rather than acute application was used due to the observed slow activation of TRPV4 currents in oocytes. A ramp or pulse protocol was used in clamping oocytes from -100 to +100 mV, and currents from WT and the two mutants compared at -100 mV. Each experimental condition was replicated in at least 3 to 4 different oocyte batches. Recordings were performed in a solution containing 100 mM sodium gluconate, 20 mM calcium gluconate, 4 mM MgSO₄ and 5 mM HEPES, pH 7.5.

Human Embryonic Kidney cells (HEK293T cells) whole-cell currents measurement

This experiment was completed in Dr. Rachelle Gaudet's laboratory at Harvard University, Cambridge by Dr Hitoshi Inada.

HEK293 cells were transfected using Opti-MEM and Lipofectamine2000. Cells were prepared in 3.5-cm dishes at a cells density of about 1×10^6 . Four μ g of DNA was added into a tube containing 250 μ l of Opti-MEM and mixed well. Ten μ l of Lipofectamine2000 was added into another tube. Samples were incubated for 5 min at room temperature. Solutions were combined and incubated for 25 min at room temperature. After incubation, 500 μ l of DNA/Lipofectamine2000 were added in the cells and incubated at 37 °C for 4 to 5 hours. Media was removed by aspiration and 2 ml of warm PBS was added to wash cells. Cells were resuspended in 2 ml of DMEM containing 10 % Fetal Bovine Serum (FBS), and 500 μ l of cells were dispersed in 6-cm dishes, and incubated at 37 °C for 24 to 36 hours. For visual selection of transfected cells pNEGFP was added to the cells.

Whole-cell currents were measured at 25 °C with Axopatch 200B (Molecular Devices) using a repeated ramp protocol (-100 to +100 mV, 400 ms, every two seconds). The solutions were: standard extracellular, 150 mM NaCl, 5 mM KCl, 1 mM MgCl₂, 2 mM CaCl₂, 10 mM glucose, 10 mM HEPES, pH 7.4 with NaOH; hypotonic (200 mOsm), NaCl reduced to 80 mM; isotonic (320 mOsm), 120 mM mannitol added to hypotonic solution; and pipette solution, 140 mM CsCl, 5 mM EGTA, 10 mM HEPES, pH 7.2 with CsOH.

2.4.10 Protein structure determination

This experiment was completed in Dr Rachele Gaudet's laboratory. TRPV4-ARD (132-383) was amplified from avian cDNA (provided by Stefan Heller) and cloned into pET21-C6H (Jin, Touhey et al. 2006), providing a C-terminal AAAHHHHHHH-tag.

The protein was expressed in BL21 (DE3) at room temperature, inducing with 0.75 μ M IPTG at OD₆₀₀=0.6. Cells were lysed in 20 mM Tris pH 8.0, 300 mM NaCl, 20 mM imidazole pH 8.0, 1 mM PMSF, 7 mM β -mercaptoethanol (β -ME), 0.1 % Triton X-100, 0.4 mg/mL lysozyme, 0.05 mg/mL RNase A and 0.02 mg/mL DNase I. The clarified lysate was loaded onto Ni-NTA agarose (Qiagen), eluted with a stepwise imidazole gradient; 7 mM β -ME and 10 mM EDTA were added after elution. TRPV4-ARD was further purified on an SP FF column (GE Healthcare) with a NaCl gradient in 20 mM HEPES pH 8.0 and 5 mM DTT, dialyzed against 10 mM Tris pH 8.0, 300 mM NaCl, 5 mM DTT, and 10 % glycerol, concentrated to 7-10 mg/mL with a centrifugal concentrator (10,000 MWCO; VivaScience), and stored at -80 °C.

TRPV4-ARD crystals were grown in hanging drops at 4 °C in 0.1 M sodium citrate pH 5.0, 10 % MPD, 2 % PEG8000, 4.3 % trifluoroethanol and frozen in reservoir with 20 % PEG4000 (crystal form I), or 0.025 M KH₂PO₄, 7 % MPD, 7 % PEG8000, and 5 mM DTT and frozen in reservoir with 25 % PEG400 (crystal form II). Data were collected at 110 K and 1.54 Å on a Micromax007/R-Axis IV++ system (Rigaku/MSI Inc) and processed with HKL2000. The structures were determined by molecular replacement using TRPV2-ARD (Jin, Touhey et al. 2006) as search model in MOLREP, model building in COOT, and refinement using REFMAC. Data and refinement statistics are in Table 7. The coordinates were deposited in the Protein Data Bank with entry codes 2JXI and 2JXJ (crystal forms I and II, respectively). Crystal form I chain A was used for structural analyses unless otherwise noted. Figures were generated using PyMOL.

2.4.11 TRPV4-ARD expression and purification

This experiment was also done in Dr. Rachele Gaudet's laboratory. The chicken TRPV4-ARD (132-383) was generated by amplification of the cDNA (provided by Stefan Heller) and cloned into the Nde I and Not I sites of pET21-C6H, providing a C-terminal AAAHHHHHHH-tag for purification. The resulting protein construct was expressed in BL21(DE3) at room temperature after induction with IPTG at an

OD(600 nm) of 0.6. Cells were resuspended in lysis buffer [20 mM Tris pH 8.0, 300 mM NaCl, 20 mM imidazole pH 8.0, 1 mM PMSF, and 7 mM β -mercaptoethanol (β -ME)] with 0.1 % Triton X-100, 0.4 mg/mL lysozyme, 0.05 mg/mL RNase A and 0.02 mg/mL DNase I and lysed by sonication. The clarified lysate was loaded onto Ni-NTA agarose (Qiagen) and eluted with a stepwise imidazole gradient of 50 mM, 100 mM, 150 mM, 200 mM, and 300 mM imidazole. β -ME and EDTA (7 mM and 10 mM, respectively) were immediately added to each elution fraction. Fractions containing TRPV4-ARD were diluted 1:5 with 20 mM HEPES pH 8.0 and 5 mM DTT, and loaded onto a HiPrep 16/10 S FF column (GE Healthcare) and eluted with a NaCl gradient. Relevant fractions were pooled, and dialyzed against 10 mM Tris pH 8.0, 300 mM NaCl, 5 mM DTT, and 10 % glycerol. The TRPV4-ARD protein was concentrated to 7-10 mg/mL with a Vivaspin centrifugal concentrator (10,000 MWCO; VivaScience), and stored at -80 °C.

2.4.12 Co-immunoprecipitation

These experiments were completed in our laboratory at the Neurogenetics Branch (NINDS, NIH, Bethesda). HEK293 cells were co-transfected with 0.5 μ g of pcDNA3 expressing human PACSIN1, PACSIN2 or PACSIN3 (gifts of M. Plomann, Cellular Neurobiology Research Group, Center for Biochemistry, University of Cologne, Cologne, Germany) and 0.5 μ g Flag-TRPV4. The transfection was performed using the Fugene6 (Roche) and Optimem. The Fugene6 was added to Optimem and let sit for 5 minutes. This amount of DNA was then added, and the solution was incubated at room temperature for at least 20 but no longer than 40 minutes, and was then added to the cells. Each construct was done in duplicate. At 24 h, cells were washed once and harvested after with 1 ml of PBS and cleared. Cell pellets were obtained after spinning the harvested solution for 3 minutes. Cell pellets were re-suspended in 200 μ l of lysis buffer containing a protease. An aliquot of 20 μ l was taking out for the input, and the remaining cell lysates were incubated with anti-Flag M2 (Sigma) for 6 h followed by overnight incubation with Dynabeads Protein G (Dynal). The beads were washed 3 times with 500 μ l lysis buffer, and proteins were denaturated by adding 4X dye and heating at 95 °C for 5 min. Bound proteins were separated by SDS-PAGE, and analyzed by immunoblotting with antibodies to PACSIN3, PACSIN2 and PACSIN1 (gifts of M. Plomann), respectively. TRPV4 immunoprecipitation was verified by immunoblotting with anti-Flag M2.

2.4.13 Protein binding assays

This experiment was performed in Dr. Rachele Gaudet's laboratory. Wild-type and mutant human TRPV4-ARDs, including the N-terminal proline-rich region (residues 136–397), were expressed and purified as the chicken Trpv4-ARD.

Mouse Pacsin3-Sh3 domain (residues 361–424; single difference between mouse and human PACSIN3-SH3 is V362A; cDNA provided by S. Heller) was cloned into NdeI and NotI sites of pET21-C6H, expressed in BL21 (DE3) cells induced with 0.4 mM isopropyl- β -d-thiogalactopyranoside at room temperature. Cells were lysed by sonication in lysis buffer (20 mM Tris-HCl, pH 8.0, 300 mM NaCl, 20 mM imidazole, pH 7.0, and 1 mM phenylmethylsulfonyl fluoride) with 0.1 % Triton X-100, 0.2 mg/ml lysozyme, 50 μ g/ml RNase A and 25 μ g/ml DNase I. The cleared lysate was loaded onto Ni-NTA (Qiagen) and eluted with steps of 25, 50, 100, 150 and 250 mM imidazole pH 7 in lysis buffer, adding 10 mM EDTA at pH 8.0 and 1 mM dithiothreitol (DTT) after elution. Relevant fractions were pooled, dialyzed, purified on Superdex75 (GE Healthcare) in 10 mM Tris-HCl, pH 8.0, 50 mM NaCl, 1 mM DTT, and concentrated to >20 mg/ml in centrifugal filters. For PACSIN3-SH3 interaction assays, samples contained 25 nmol TRPV4-ARD with or without 37.5 nmol PACSIN3-SH3 in 125 μ l pre-incubated for >30 min, and 100 μ l were loaded onto a Superdex75 10/30 column (GE Healthcare) in 20 mM Tris, pH 7.0, 150 mM NaCl, 1 mM DTT at 4 °C. Calmodulin-agarose binding assays were performed essentially as described (Phelps, Wang et al. 2010).

2.5 Statistical analysis

Data were analyzed using Excel (Microsoft) and the Strathclyde electrophysiology suite (University of Strathclyde, Glasgow). Data significance was estimated using paired and unpaired student's *t*-Tests, where appropriate. Data are reported as means or standard error of the mean.

3 Results

3.1 Patients

3.1.1 General findings

Family F1

From the 25 family members evaluated, seven were found to be affected. The mode of inheritance was vertical, suggesting a dominant model, but no male-to-male transmission was seen. This may be explained by the fact that the founder, a female, had only one son who is unaffected and four daughters. In addition, from her eight grandchildren born from affected parents, four were males, and only one was affected. This affected grandson had no offspring.

Clinical findings

The age of onset was highly variable, with the earliest occurring before one year and the latest yet known at 44 years of age. This variability was seen in the disease course, and no relationship was seen between the age of onset and disease severity (as shown in the case presentations below). The clinical variability between the proband and her mother can be appreciated in Figure 15. Weakness and atrophy in lower extremities were the first reported symptoms in all but one. Altered voice and shortness of breath with stridor in variable degree were seen in all the affected individuals. These symptoms were worse on exertion or excitement. Absent or reduced tendon reflexes were seen in all patients. Minimal to moderate sensory loss was seen in all but one, and was more prominent in the most affected family members. All sensory modalities, including pin-prick, light touch, temperature sense, vibration sense, and proprioception were affected. However, vibration sense was the most affected modality. Five patients reported bladder urgency or urinary incontinence, and two complained of progressive hearing loss. The most affected patient had subtle facial weakness consistent with orbicularis oculi and oris muscle weakness. None of the patients presented with upper motor neuron involvement or memory decline. Two of them underwent tracheotomy (at 20 months and 18 years of age) because of the seriousness of the symptoms resulting from the laryngeal muscles paralysis. One unaffected individual (IV.5) of 41 year-old was complaining of raspy voice which she said started few months prior her visit, but had no other neurological symptoms such as muscle weakness or atrophy or breathing difficulties. Her neurological exam was

normal. In addition, her other family members had also normal neurological examination.



Figure 15 Phenotypic characteristics of family F1.

Marked variability of disease severity is demonstrated by mild, late-onset weakness with mild atrophy in hands and feet in subject F1.III.2, but severe quadriplegia, generalized muscle atrophy, scoliosis, and respiratory failure in her daughter, subject F1.IV.4. Written consent was obtained to publish these photographs.

Laboratory findings

Muscle/nerve biopsy

The biopsy was done in individual IV.4 when she was at age 13 (Figure 16), about five years after disease onset. The source of the specimen was the right gastrocnemius muscle and sural nerve, a sensory nerve in the leg easily accessible to biopsy. Tissue sections were stained with hematoxylin, eosin, toluidine blue, and visualized by light and electron microscopy. Findings are detailed below in the figure legend.

Muscle sections showed severe denervation atrophy, and near end-stage muscle. Type I and type II fibres were both involved, and there was fibre type grouping.

Peripheral nerve sections of the sensory sural nerve showed a slight decrease of myelinated fibres with apparently well preserved axons indicating much more severe

involvement of motor nerves innervating muscles than sensory nerves. Endoneural connective tissue was mildly increased. There were occasional axonal swellings.

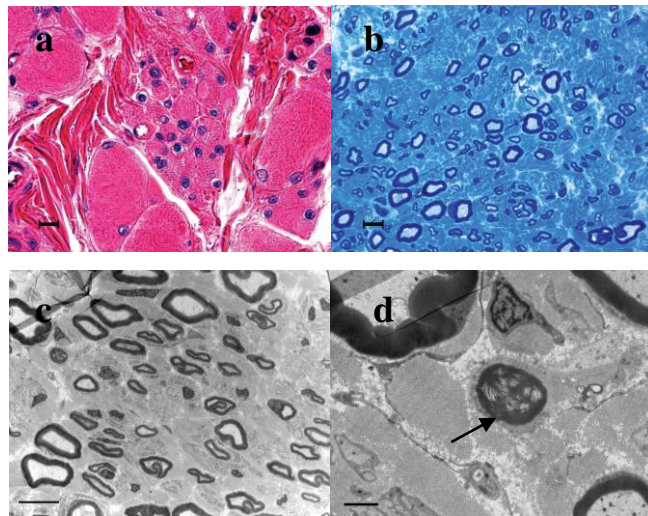


Figure 16 Muscle and nerve biopsy.

a) Light microscope images of hematoxylin and eosin-stained sections of gastrocnemius muscle biopsy from subject F1 IV.4 demonstrating profound denervation atrophy of muscle. Scale bar, 10 μm . **b)** Toluidine blue-stained section of sural nerve shows mild loss of large, myelinated sensory axons. Scale bar, 10 μm . **c)** Electron microscopy of sural nerve confirms mild loss of large and small myelinated axons and unmyelinated axons. Scale bar, 10 μm . **d)** Arrow demonstrates a rare axon undergoing Wallerian-like axonal degeneration. Scale bar, 2 μm .

Nerve conduction studies and Electromyogram

In general, NCS showed normal conduction velocities (above 38 m/s at all recorded sites), but low compound motor and sensory action potential amplitudes in all affected individuals who underwent this evaluation. The wide range of variability seen in the disease severity was reflected in the NCS by the fact that the more affected patients also had the lower amplitudes. NCS were consistent with the phrenic nerve involvement in all patients except the youngest patient who showed the mildest limb weakness and sensory symptoms. Individual IV.5, whose clinical examination was normal, also had normal NCS and normal EMG. Needle EMGs showed muscle membrane instability and motor unit remodelling, which is consistent with an active and chronic denervation/reinnervation of peripheral muscles.

Laryngoscopy

Five of the patients underwent laryngoscopy that showed bilateral laryngeal muscles paralysis with the left side being more affected in most cases. Generally, both abductor and adductor muscles were affected with a variable degree of severity. Laryngoscopy performed in the unaffected family member (IV.5) with raspy voice showed no vocal fold paralysis, but revealed inflammation of her vocal cords, which likely accounted for her raspy voice.

Audiological examination

Ear-Nose-Throat (ENT) examination was performed in two patients who were complaining decreased hearing acuity. Findings were consistent with grossly intact hearing to loudly spoken voice and Weber was midline. Rinne was inverted bilaterally suggesting conductive hearing loss. A superior retraction pocket with squamous debris was found in the left ear in one individual. A middle ear effusion with opaque TM was also noted on the left. Her audiogram showed bilateral reduced hearing in high frequencies compatible with a sensorineural hearing loss and a cholesteatoma on the left as confirmed by flattened tympanograms.

Family F02

Clinical findings

Five individuals were seen in the Neurogenetics clinic at NIH. Three of them had a history of distal atrophy and weakness, hoarseness of voice and/or breathing difficulties with stridor on exertion. These symptoms were variable in term of severity. The clinical exam confirmed the motor symptoms, and showed reduced vibration and pin-prick senses and disturbance in the proprioception. These signs were more prominent in the distal limbs, and the legs appeared to be more affected than the arms. Scoliosis and high arches were noted in some patients. Two patients reported bone abnormalities including osteoarthritis and frequent fractures. They were put on calcium supplement because of poor bone density. Bladder urgency or incontinence was reported by four affected subjects. Eight complained of progressive hearing loss that was documented by an audiological examination.

Three other unaffected members were examined in our neurogenetics clinic at NIH, and had normal neurological examination.

Laboratory findings

Nerve conduction studies/EMG

In this family, NCS showed normal conduction velocities at all recorded sites (>38 m/s in general), but low compound motor and sensory action potentials amplitudes. As expected, the peroneal nerve was the most affected. When both phrenic nerves were evaluated, the left side nerve was almost always more affected than the right side. The involvement of the phrenic nerve was seen in all patients. Fluoroscopic and EMG studies of the diaphragm was performed in two patients, and revealed that the movement of one or both hemidiaphragms was impaired.

Unaffected individuals who underwent this exam had normal electrophysiological examination.

Laryngoscopy

Laryngoscopy showed bilateral laryngeal muscle paresis with the left side more affected. The abductor muscle appeared to be paralyzed in most patients, but in some patients both the abductor and adductor were paralyzed, explaining the stridor and hoarseness of voice reported by patients. In most of the patients, laryngeal videoendoscopy noted no observable movements of the left vocal fold which remained stationary in an “off-centre” (paramedian) position. The right vocal fold had reduced, but present, opening (abductor) and closing (adductor) function. In addition, the airway was reduced up to 60 % in size.

Audiogram

The audiological exam showed bilateral hearing loss involving high frequencies in all affected individuals with a wide range of severity. Patients who complained of progressive hearing loss were not able to hear at 500Hz and 4000Hz bilaterally, when tested at both 25dB and 40dB. Acoustic emittance indicated normal middle ear mobility and pressure with normal acoustic reflexes bilaterally. Grossly, all examined patients with reduced hearing had good speech discrimination.

Family F03

This is a family in which three individuals, a mother and her son and daughter, presented with limb weakness and atrophy, breathing difficulties, and skeletal deformities. No affected individual was reported in earlier generations. However, the proband's father died when he was 35 year-old. The cause of death was reported to be tuberculosis.

Clinical findings

The mother (III.7) and daughter (IV.4) first presented with shortness of breath and stridor at age 2 and 12, respectively, whereas the son (IV.3) had gait abnormality as first symptom at age 3. They all presented with muscle weakness and atrophy in extremities later (at age 7 for the mother and son, and age 12 for the daughter) with a variable severity, and hoarseness of voice. They had high arches and hammer toes. The mother and her son developed scoliosis. The mother underwent tracheostomy at age 3, and a laser ablation surgery on vocal folds was done on her son and daughter at age 13. The disease course has been slowly progressive. One patient (IV.3) reported a bilateral progressive decrease in his hearing, whereas his mother (III.7) was complaining of right ear hearing loss. None of the affected individuals reported urinary symptoms.

Another family member (III.5) of 51 of age was seen recently in our Neurogenetics clinic, and his physical examination showed minor signs of peripheral neuropathy including high arches, twitching in calves muscles, and minimal reduction in his vibration sense and pin-prick in lower extremities. He was not actively dyspneic during the examination and did not report any breathing difficulties on exertion but was diagnosed with sleep apnoea for which he is being followed up.

Laboratory findings

Nerve conduction studies

Motor and sensory nerves amplitude potentials were decreased with normal distal latencies and conduction velocities. Like the other families, the peroneal nerve was most affected, and phrenic nerve was involved. EMGs revealed significant muscle membrane instability in a distal predominant pattern. Myotonic discharges were present, particularly in the tibialis anterior muscle. Motor units action potentials were of prolonged duration and increased amplitudes, consistent with a neurogenic process. Nerve conduction studies of the individual III.5 were overall normal except for a drop in his sural nerve action potentials from 14 to 7 over 10 years.

Laryngoscopy

Laryngeal muscles weakness was seen in all the affected individuals who underwent this examination with various level of severity. Findings ranged from breathiness to limited inspiration abduction bilaterally with no adduction on the left, and restriction of the airway. Laryngoscopy was done on individual III.5 when he was 40 years old, and was within normal limits.

Audiogram

Audiological examination of the mother showed normal hearing for speech, slight conductive hearing loss, hypomobile middle ear system on left consistent with healed tympanic membrane perforation. Individual IV.3 was complaining of bilateral hearing loss, and his audiological examination confirmed a bilateral reduction in high frequencies hearing which is consistent with a sensorineural hearing loss.

Radiological evaluation

Spine radiographs of individual IV.3 showed convex left thoracic scoliosis of about 40 degrees between the thoracic vertebra T3 and T9. Chest X-ray of individual III.5 was consistent with an elevation of the left hemi-diaphragm with sub-diaphragmatic air distended bowel. His inspiration and expiration films showed no movement of either diaphragm. The heart is displaced to the right from the elevated left hemi-diaphragm. Although he was complaining of sleep apnoea and has hemidiaphragmatic paralysis, his phrenic NCS were normal, suggesting that this symptom that this symptom may be of different origin. Another patient, IV.4, had a slightly less right diaphragmatic excursion noted during inspiration and expiration. The mother, III.7, had normal chest X-ray. No evidence of bone deformation to suggest abnormality of development was seen in these patients nor did we see abnormal bone density.

Family F4

Clinical findings

The clinical examination of this family showed weakness and atrophy in extremities, though milder than in the families described above. Two patients in the younger generation presented scoliosis and high arches. Sensory loss affecting vibration, touch, cold and pin-pick sensation were very mild. All patients had difficulties with breathing on exertion and this constituted the predominant symptom. The high variability in the disease severity between different family members seen in the other families was also observed in this family. Patients reported no bladder symptoms. One patient was complaining of unilateral hearing loss.

Laboratory findings

Nerve conduction studies and EMG

NCS were limited to the peroneal and sural nerves. The peroneal motor conduction studies were significant for reduced amplitude on the right side and a prolonged distal

motor latency in the left side, with normal conduction velocities. On the right side, the minimal F latency was also prolonged. The sural sensory conduction studies were significant for the presence of borderline reduced amplitude for age on both sides, but peak latencies and sensory conduction velocities were within normal limits. This is consistent with a diffuse axonal peripheral neuropathy, although focal neuropathy is possible, especially given the findings on the left. However, there was no phrenic nerve involvement in any of the affected individuals.

EMG studies performed in the tibialis anterior muscle only showed chronic partial denervation/reinnervation of distal muscles.

Laryngoscopy

Speech recording indicated the presence of stridor upon inhalation, and intermittent breathiness and intermittent raspiness during phonation. Flexible fiberoptic nasolaryngoscopy of affected individuals revealed bilateral vocal fold paralysis, especially with regard to abduction, which was more pronounced in the left side. The airway was reduced to 3-4 mm. Under examination via stroboscopic lighting, normal mucosal waves and vocal fold vibration were also noted.

Audiogram

Audiological examination of the patient who was complaining of hearing loss showed mild hearing loss in the right ear and features consistent with a tympanic perforation.

Radiological evaluation

Chest X-rays comparing inspiratory and expiratory films were done in one patient, and showed symmetric motion of the diaphragm, suggesting no diaphragm paralysis. However, a thoracic levoscoliosis was noted. In addition, an asymmetry of the upper ribs, particularly the second and third anterior ribs on the left, was also seen.

In summary, all five families presented with clinical and laboratory findings consistent with an axonal neuropathy as well as other clinical features seen in CMT 2C. However, none of the patients in family F3, F4 and F5 presented with urinary incontinence. In addition, families F4 and F5 did not present clinical or laboratory findings consistent with bilateral sensorineural hearing loss or diaphragm involvement as seen in the other families. The clinical, laryngological and electrophysiological findings of some family members are summarized in Tables 4, 5 and 6.

Table 4 Summary of the clinical features in CMT2C patients.

Patient	Clinical examination findings										
	Age (yr)	Sex	Age of onset (yr)	First symptom	Arm weakness		Leg weakness		Sensory loss	Hearing loss	Skeletal deformities
					Proximal	Distal	Proximal	Distal			
F1 III.2	71	F	44	Foot weakness	None	Mild	None	Moderate	Minimal	Yes	HT
F1 IV2	48	F	5	Foot weakness	Mild	Severe	Mild	Severe	Mild	No	HT, PC
F1 IV3	46	F	5	Stridor	Mild	Moderate	Mild	Moderate	Mild	No	HT, PC
F1 IV4	44	F	3	Foot weakness	Severe	Severe	Severe	Severe	Moderate	Yes	Scoliosis, PC
F1 V1	24	F	7	Foot weakness	None	Mild	None	Mild	Mild	No	HT, PC
F1 V3	20	F	5	Stridor	None	Mild	None	Mild	Mild	No	HT, PC
F1 V8	18	M	2	Stridor	None	Mild	None	Mild	Minimal	No	Slight HT
F2 III11	65	M	57	Hearing loss	None	Mild	None	Mild	Minimal	Yes	HT, PC
F2 III18	61	M	34	Foot weakness	Mild	Moderate	Mild	Moderate	Minimal	Yes	HT, PC
F2 III22	64	F	35	Foot weakness	Mild	Moderate	Mild	Severe	Minimal	Yes	HT, PC
F2 III23	57	F	22	Foot weakness	None	Mild	None	Mild	Minimal	Yes	HT, PC
F2 III24	49	F	<2	Stridor	Mild	Moderate	Mild	Moderate	Mild	No	HT, PC
F2 IV2	50	M	16	Hoarseness	Mild	Moderate	Mild	Moderate	Mild	Yes	HT, PC
F2 IV5	53	M	28	Hoarseness	None	Mild	None	Mild	Minimal	Yes	HT, PC
F2 IV9	31	F	5	Stridor	None	None	None	Mild	None	No	HT, PC
F2 IV10	29	M	5	Hoarseness	None	Mild	None	Mild	Minimal	Yes	HT, PC
F2 IV12	29	F	2	Stridor	Moderate	Severe	Moderate	Severe	Mild	No	Scoliosis, HT, PC
F3 III7	50	F	2	Stridor	Minimal	Moderate	Minimal	Severe	Mild	No	Scoliosis, HT, PC
F3 IV3	24	M	3	Foot weakness	None	Mild	None	Moderate	Minimal	Yes	Scoliosis, HT, PC
F3 IV4	22	F	12	Stridor	None	Minimal	None	Minimal	Minimal	No	HT, PC

HT: hammer toes, PC: pes cavus

Table 5 Summary of laryngological examination findings in CMT2C patients.

Patients	Age (y)	Dyspnea	Aspiration	Dysphonia	Vocal fold adduction		Vocal fold abduction		Comments
					Left	Right	Left	Right	
					F1 III2	71	-	+	
F1 IV2	48				0	1	0	1	
F1 IV3	46	+	+	+	0	1	0	1	High-pitched voice
F1 IV4	44	+	+	+	0	0	0	0	Tracheostomy at age 18, permanent ventilation
F1 V8	19	+	-	+	0	0	0	1	Husky voice, arytenoidectomy at age 2
F2 III11	65				1	2	1	2	
F2 III18	61				>1	>1	1	1	
F2 III22	64	+	+	+	>1	>1	<1	1	High-pitched reduced volume voice
F2 III23	57	+	+	+	0	1	0	1	Stridor
F2 III24	49	+	+	+	0	1	0	1	High-pitched voice with tremor, faint stridor
F2 IV2	50				1	2	1	2	
F2 IV5	53				0	1	0	1	
F2 IV9	31				0	1	0	1	
F2 IV10	29				1	2	0	1	
F2 IV12	29	+		+	0	0	0	0	
F3 III7	50	+	-	+	0	0	0	0	Tracheostomy at age 3, arytenoid tie-back age 14
F3 IV3	24	+	-	+	0	0	0	0	Laser ablation surgery at age 13
F3 IV4	22	+	-	+	1	1	1	1	Laser ablation surgery at age 13

Vocal fold movement: 2 = normal, 1 = impaired mobility, 0= immobile; +: present, -: absent

Table 6 Summary of nerve conduction studies findings in CMT2C patients

Patients	Median		Ulnar		Peroneal	Sural	Phrenic
	SNAP Amp (uV) (N≥15)	APB CMAP Amp (mV) (N≥4.5)	SNAP Amp (uV) (N≥15)	ADM CMAP Amp (mv) (N≥4.5)	EDB CMAP Amp (mV) (N≥2.5)	SNAP Amp (uV) (N≥6)	Right Amp (mV) (N> 0.6)
F1 III2	13	4.9	18	7.0	2.1	ND	0.5
F1 IV3	5	0.4	3	0.1	Absent	9	Absent
F1 IV8	20	12.4	ND	ND	4.1	13	0.6
F2 III22	11	8.5	ND	ND	0.2	4	Absent
F2 III23	10	5.1	17	ND	1.3	6	Absent
F2 III24	ND	ND	ND	0.9	1.2 (TA)	ND	Absent
F2 IV2	ND	ND	ND	ND	ND	ND	Absent
F3 III7	3	4.5	2	1.5	0.3	Absent	Absent
F3 IV3	7	2.2	ND	ND	ND	7	ND
F3 IV4	ND	7.1	ND	ND	ND	ND	ND

Amp: amplitude; **SNAP:** sensory nerve action potential; **CMAP:** compound motor action potential; **APB:** abductor pollicis brevis;

ADM: abductor digiti minimi; **EDB:** extensor digitorum brevis; **uV**=microvolts, **mV**=millivolts, **ND:** not done, **TA:** tibialis anterior; **N**= normal

3.1.2 Case presentations:

Patient IV.4, Family F1 (Figure 10): Proband of family F1, this 43-year old wheelchair bound woman was the most severely affected in her family. Her past medical records showed that pregnancy, labour, delivery, and her early developmental milestone histories were normal including the fact that she walked at 11 months. At the age of 6, however, she first began having problems running, keeping up with the other children, going upstairs and performing other motor tasks involving mainly the lower extremities. Since onset, she has experienced progressive weakness involving all four extremities, lower extremities slightly greater than the upper extremities, and distal limb slightly greater than proximal. At that time she had no numbness or tingling, and no bowel or bladder problems. She was losing weight, fatiguing easily, and progressively developed scoliosis. At age 13, she was hospitalized for acute pneumonitis, and went into respiratory distress for which she underwent surgery for tracheal and bronchial aspiration. However, her chest x-ray was completely normal. The same year she was hospitalized in a neurology department where her examination revealed marked and diffuse muscle wasting, weakness more pronounced distally and mild sensory loss. Her voice was hypophonic and high-pitched with slight inspiratory stridor. She was also noted to have some fasciculations of her tongue. Tendon reflexes were absent throughout. Her NCS showed low sensory and especially motor nerve responses, but normal conduction velocities, suggestive of an axonal type of peripheral neuropathy. Electromyography revealed widespread chronic neurogenic atrophy. Her muscle biopsy showed severe denervation, atrophy and near end stage muscle. Both type I and type II fibres were involved. Peripheral nerve sections showed slight decrease of myelinated fibres with apparently well preserved axons but occasional axonal swelling. Laryngoscopy revealed a left vocal fold paralysis. These findings led her physician to the diagnosis of Charcot-Marie-Tooth type 2 disease.

She was hospitalized for another episode of acute pneumonitis at age 15, and her chest X-ray showed left lower lobe pneumonia.

At age 16 she was seen by an orthopedic surgeon for her progressive scoliosis. A left low thoracic curve measured forty degrees, which was worse compared to what had been seen three years earlier when it was seventeen and later twenty-two degrees.

On examination, she was slightly cachectic and appeared to have marked weakness of both distal and proximal musculature including trunk and hip musculature. She had slight *cavus* and *varus* deformities of her feet. Her speech was noticed to be quite abnormal. Her walking was unsteady, and a cane had been advised.

At age 18, her general examination showed her to be very slender with minimal subcutaneous tissue. She had a mid-thoracic and lumbar spine scoliosis with lumbar lordosis. Her neurological examination showed a hoarse voice and intermittent stridor while talking. There was obvious atrophy of the margins of her tongue and quite prominent fasciculations. She had bilateral foot drop, and she could not dorsiflex her feet against gravity, and a bilateral *pes cavus* foot deformity was noted. A progression of the scoliosis was noted from forty degrees two years earlier to forty three degrees. Her vocal fold paralysis became bilateral. Because of her progressive laryngeal disease and repetitive pulmonary infections, a tracheostomy was recommended and was performed a few months later. She was put on ventilator as needed, but relied on it more and more over time. In 2000, she was hospitalized for 6-8 weeks, and was given a jejunal tube after swallowing test showed severe dysphagia. Since then, she noticed a dramatic loss of weight and became very weak. In the last two years, since her father's death, she has had to be in bed more, which she believed made her weaker because he was her care-giver.

During her recent evaluation she complained of having to stay longer than usual on ventilation. She could get off the ventilator just for a couple of hours during the day, and had to stay on it all night. She noticed urinary incontinence and diarrhoea. Her voice was barely audible, therefore she uses an amplifier. Her neurological examination showed a very weak patient with no movement in the limbs. Pin-prick, temperature, light touch and vibration, although difficult to assess because of the patient's condition, seemed to be reduced in the distal part of the limbs. Tendon reflexes were absent throughout. She wore a chest brace without which we see a marked scoliosis.

She had slight weakness of facial muscles, and some fasciculations in her tongue and *mentalis*. Her cognition was intact. Her neck muscles were strong enough to allow her to use her computer with her head.

Late in 2006, she was seen by an ENT for decreasing hearing, aural fullness, and occasional tinnitus since irrigations for cerumen disimpaction on the left ear. An audiogram was performed and showed significant bilateral conductive hearing loss

and flattened tympanograms on the left. A conductive hearing loss was noticed on sensorineural testing.

Placement of bilateral myringotomy tubes was performed after which she noticed an improvement in her hearing. No NCS were done because she was seen at home.

Patient III.2, Family F1 (Figure 10): A 73-year old woman, mother of the proband, was found to have areflexia, but normal strength and sensory tests at age 44 when she was being evaluated because of her family's disease. Prior to that time she had no complaints. Her EMG was abnormal. The NCS were normal, but the needle examination showed diffuse neurogenic abnormalities. A moderate decrease in distal vibratory sense in addition to a raspy voice was additionally noticed at the age of 53 during another physical exam. Over the past few years, she developed hoarseness of voice, difficulty of breathing on exertion, and pain in the distal legs after a long day of activity. She noticed weakness in extremities and increasing number of falls. Her recent neurological examination showed mild weakness and wasting in distal muscles. Tendon reflexes were absent at the ankles and reduced elsewhere. There was no skeletal deformity, and the facial muscles were intact. Her NCS showed axonal type abnormalities (normal nerve conduction velocity and low CMAP and SNAP) more prominent in lower limbs with mild prolonged distal latency in the right phrenic nerve. She had poor heel and toe walking, and Romberg sign was positive. EMG showed active denervation in the tibialis anterior muscle and the first dorsal interosseus muscle in addition to chronic denervation changes in the proximal arm and legs muscles. Her laryngological examination showed vocal fold paresis more prominent on the left than on the right side.

Patient IV.3, Family F1 (Figure 10): A 46-year old woman who had shortness of breath and stridor in her childhood. At 18 years old, she had NCS and EMG that showed normal conduction velocities and low to borderline amplitude in motor responses, and very prominent chronic neurogenic motor unit discharges. The lower limbs were more affected. The sensory responses were within normal limits, including the sural and forearm median nerves. At age 22, while pregnant with her second child, she had a check-up that showed she had bilateral vocal fold paresis with the left side completely paralyzed. A tracheotomy was suggested for the delivery because she has been very short of breath and had to be given oxygen during her first delivery.

In 2006, at age 46, her neurological examination showed weakness in all limbs, worse distally, and wasting in forearms, hands and feet. She had slightly high arches and hammer toes. Her shortness of breath was noticeable and worse on exertion. Her NCS showed evidence of diffuse sensorimotor polyneuropathy due to axonal loss with phrenic nerve involvement. Laryngoscopy showed bilateral vocal fold paralysis.

Patient V.8, Family F1 (Figure 10): A 19-year old young man whose birth and neonatal histories were normal. He was admitted in the hospital at 20 months of age when his parents became aware of stridor and difficulty of breathing present with excitement and vigorous activity. These symptoms became prominent over ten months. A laryngoscopy showed that the vocal folds were in a keyhole type position with the anterior tips of the vocal fold processes touching each other, leaving space anteriorly as well as posteriorly. The general examination was normal and the child was let go home. Two months later, he was brought back to the hospital because the stridor was becoming permanent with several gasping episodes. The respiratory rate was 55/s and the stridor was audible, worse with excitement. He weighed 10.7 kg. Neurological examination did not reveal any weakness or atrophy. His EMG reportedly showed a spinal muscular atrophy process. Another laryngoscopy was performed and it revealed a bilateral vocal folds paralysis in a paramedian position with an approximately 2 mm glottic opening. Following this procedure a tracheotomy tube was placed. At age 2 he had an arytenoidectomy and 2 months later the tracheotomy tube was removed. Since then he has not been complaining of any major symptoms, but X-ray done later showed a mild scoliosis.

In 2006, at 19 years old, his neurological examination showed only mild weakness in foot dorsiflexion bilaterally, high arches and slight hammer toes, and some wasting of hand intrinsic and the EDB (extensor digitorum brevis). Sensory signs were minor, with only slight decrease in proprioception and vibration in toes. Tendon reflexes were absent throughout. He had poor heel walking, but normal toe and tandem walk. His NCS was borderline normal, but the EMG showed muscle denervation and reinnervation that the examiner interpreted to be due to an early stage polyneuropathy. The laryngoscopy showed bilateral vocal fold paralysis affecting the left side more than the right.

Patient V.1, Family F1 (Figure 10): This is a 24-year old woman who complained of hoarseness of voice and weakness in the extremities. These symptoms started at 7

year old and have evolved progressively over time. She becomes short of breath and has loud breathing in inspiration on exertion. She has difficulties with running and taking stairs. Her physical examination showed slight to moderate weakness in extremities and neck flexors. Atrophy in the thenar and hypothenar eminences were noticed in addition to high arches. Sensory loss to cold, vibration and pin-prick was noticed in the extremities up to the level of the wrists and knees. Reflexes were absent throughout. She was unable to walk on the heels or the toes, and a slight sway was seen at Romberg. Because she was seen at home, no electrophysiological or laryngological studies were done.

Patient III.23, Family F2 (Figure 11): A 64-year old woman who was first seen in the neurogenetics clinic at NIH in 2000 for weakness and atrophy in extremities and speech difficulties. Her symptoms began around age 38 with weakness and wasting of the muscles in her hands and distal lower extremities. She has noticed shortness of breath with exertion over the past five years. She has difficulties climbing stairs. She was noticed to have osteoporosis and scoliosis at age 20, and has been on calcium supplementation since. She has had two fractures in her left leg. Her neurological examination showed good facial strength, moderate muscle weakness and atrophy more marked in extremities, and reduced vibration sensation in toes. Tendon reflexes were absent throughout. Her nerve conduction studies showed low amplitude but normal motor nerve conduction velocity in the ulnar and peroneal nerves. The radial sensory nerve conduction had borderline conduction velocity, but low amplitude. The sural sensory nerve action potential was absent. The right phrenic nerve conduction was also absent. Her audiological examination was consistent with bilateral sensorineural hearing loss. Her ENT examination showed a high pitched voice with reduced volume. Laryngoscopy showed a reduced abduction of both vocal folds (the left side greater than right). The adductor function of her vocal folds was also affected to a lesser degree.

Patient III.22, Family F2 (Figure 11): A 49-year old woman who was first seen in the neurogenetics clinic at NIH in 2000 reported to having difficulty breathing while nursing, and history of stridor as a child. As a child her running was slow, and she would quickly become short of breath. She presented with weakness in legs that became progressively bothersome over years, and later developed weakness in the hands. Her voice has also become weaker over time. She also has a history of

osteoarthritis, and is on calcium supplementation. Her neurological examination showed high arches, and hammer toes. She was noted to have weakness and atrophy of the limbs, with the distal parts being more affected. She had decreased vibratory and pin-prick sensation at toes. Her nerve conduction studies and laryngological examination were quite similar to her aunt's (F2 III.22).

She has a 29-year old daughter (Patient IV.12, Figure 11) who is severely affected. She is very weak and needs to use a negative pressure ventilator at night because of her laryngeal paralysis. She had severe scoliosis at age 3, and underwent spine surgery because of that.

Patient III.7, Family F3 (Figure 12): This is a 50-year old woman who developed stridor and falls at age 2. She underwent a tracheostomy at age 3, which remained in place until age 14 when she had a right vocal fold tie back surgery. She was left with a breathy voice, but denies significant change in her voice since then. She has had distal limb weakness since the age of 7. Over the years there has been slow progression. She has worn ankle-foot orthoses (AFOs) braces for 13 years, but admits to ongoing tripping and falling once a week. Although she has hand weakness, she can button, open jars and turn keys, unless her hands are cold at which point she feels her hands become completely paralyzed. She develops intermittent paraesthesias and numbness in the right second and third fingers. Otherwise, she denies sensory symptoms. She has a mild scoliosis. She has mild right-sided hearing loss.

Her neurological examination showed facial weakness. She had mild upper thoracic curvature. There was an atrophy and weakness in forearms and legs, but worse in the lower limbs. She was unable to walk on her heels or her toes and the Romberg sign was present. Cold sensation was absent below the knees and 5 % reduced in the hands. Vibration was moderately and slightly reduced at the toes and hands, respectively. Pin-prick was reduced to midshin and slightly in hands. Tendon reflexes were absent throughout.

Patient III.3, Family F4 (Figure 13) (proband): A 35-year old woman who was first seen in the neurogenetics clinic at NIH in 1998. Shortly after delivery, she was noticed to have a breathing problem for which she stayed in Intensive Care Unit for a few days. She has noticed that for all her life she has suffered from loud breathing sounds as well as from raspier voice than her peers. She did not notice limb weakness, although she does complain of difficulty with inclines and climbing stairs, but

primarily due to her breathing problem. She complains of twitching in her muscles, mainly in legs, arms, and face. She gives a history of having scoliosis and having to wear foot orthotics due to high arches. Her physical exam was consistent with a mild degree of thoracic levoscoliosis. Examination of extremities revealed thin feet with borderline elevated foot arch. The neurological examination showed mild weakness in the neck flexors, but no facial weakness was observed. There was only mild degree of weakness in the very distal foot muscles with toe extension and flexion. She had mildly decreased vibratory sensation in the toes. The rest of the sensory examination was normal. Deep tendon reflexes were absent. Her nerve conduction studies showed significantly reduced amplitudes in the peroneal motor nerve conduction, but normal conduction velocities. The sural sensory conduction studies were borderline-reduced amplitude for age. The phrenic nerve was not shown to be affected. Her laryngological examination showed bilateral vocal fold motion impairment, especially with regard to abductory motion in both sides (the left side appearing to be more affected). Her chest X-ray showed normal symmetric diaphragm motion.

Her 60-year old father (Patient II.2, Figure 13) has a history of shortness of breath since childhood, but never sought a medical evaluation until his daughter developed more severe symptoms. His neurological examination revealed very mild weakness in the very distal parts of hand and feet, and discrete pin-prick, temperature and vibration sensation loss in the distal parts of lower limbs. Reflexes were diminished or absent throughout. His laryngological examination showed a left vocal fold paralysis. His chest X-ray showed no asymmetry in the diaphragm motion. Audiological examination was normal.

Patient IV.1, Family F4 (Figure 13): A 5-year old girl who presented breathing difficulties and stridor at birth. Subsequently, she was intubated and at one month of age she had a tracheostomy tube inserted. She later developed scoliosis, for which she wears a brace. The neurological examination showed generalized hypotonia, reduced to absent sensory loss, and absent reflexes throughout. Her laryngoscopy showed bilateral vocal fold paralysis.

3.2 Genetic analysis:

3.2.1 Linkage analysis/Fine mapping

As stated above, the gene for CMT2C was previously mapped to chromosome 12q24. To confirm that the families we report here also map to this locus, we performed a genetic analysis using 12 polymorphic markers covering the previously described region between polymorphic markers *D12S84* and *D12S1023*. We performed a parametric and nonparametric analysis of the genotyped data, and found linkage to this region in three of the four families.

Family F1: The region of linkage was located at 12q24.11 with a genetic distance of 118-119 cM (Marshfield). The LOD score without the three unaffected who had the disease haplotype was 3.6, which shows a significant linkage. The haplotype reconstruction matched the disease status except in three supposedly unaffected individuals who carry the disease haplotype (Figure 17). The haplotype of one of them was inferred since that individual was not genotyped. The region of linkage in this family spanned from markers *D12S84* to *D12S1343* with a recombination occurring in the telomeric region between markers *D12S1343* and *D12S1023*. This recombination took place in the second genotyped generation, between the affected founder and one of her affected daughters. No further recombination occurred in the subsequent generation. This region spans 2.8 Mb, and has 46 labelled genes according to NCBI.

Genotyping for one individual did not work; therefore he is not represented on the haplotype in Figure 17.

Family F2: This is a branch of a family analyzed in a previous study (Klein, Cunningham et al. 2003). The region of linkage in this family was located at 12q24.11-12q24.21 with a genetic position of 118-123 cM. The LOD score for this family was close to 7. The haplotype reconstruction matched the disease status except for two supposedly unaffected family members who had the disease-bearing allele. They were not considered affected because of inconclusive findings in their neurological examination in addition to a lack of neuro-electrophysiological and laryngological studies to confirm those minor findings. A review of their medical records showed that they had reduced to absent reflexes and questionable weakness in the extremities, suggesting that they may be affected.

The haplotype analysis showed that two recombinations had occurred in this family. The first one took place in the downstream region in the second generation of one branch of the family, between markers *D12S1341* and *D12S1023*. This recombination was also seen in the third generation of another branch. The second recombination took place in the upstream region in the second generation of another branch of the family, between markers *D12S84* and *D12S105*. This recombination appeared also in the fourth generation of another branch. By taking the recombinations into account in this family the region of linkage spanned from markers *D12S105* to *D12S1341* (Figure 18). There were 86 annotated genes in this region which is 5.5 Mb large (NCBI). A review of the analysis reported in this family showed that region has been slightly narrowed; this may be due to the rearrangement of the markers we noticed in this region since the first report (Klein, Cunningham et al. 2003).

Family F4: the region of linkage was located at 12q24.11-12q24.13 with a genetic position at 118-120 cM (Marshfield). The LOD score was estimated to about 1, which was the maximum one could get because of the small number of analyzed samples. The haplotype reconstruction matched the disease status with the disease-linked haplotype seen in the affected members only. A recombination occurred in the telomeric region of the chromosome in the second genotyped generation between markers *D12S811* and *D12S1023*. This region spanned from markers *D12S84* to *D12S811* (Figure 19). This region is about 5 Mb, and has 84 labelled genes (NCBI).

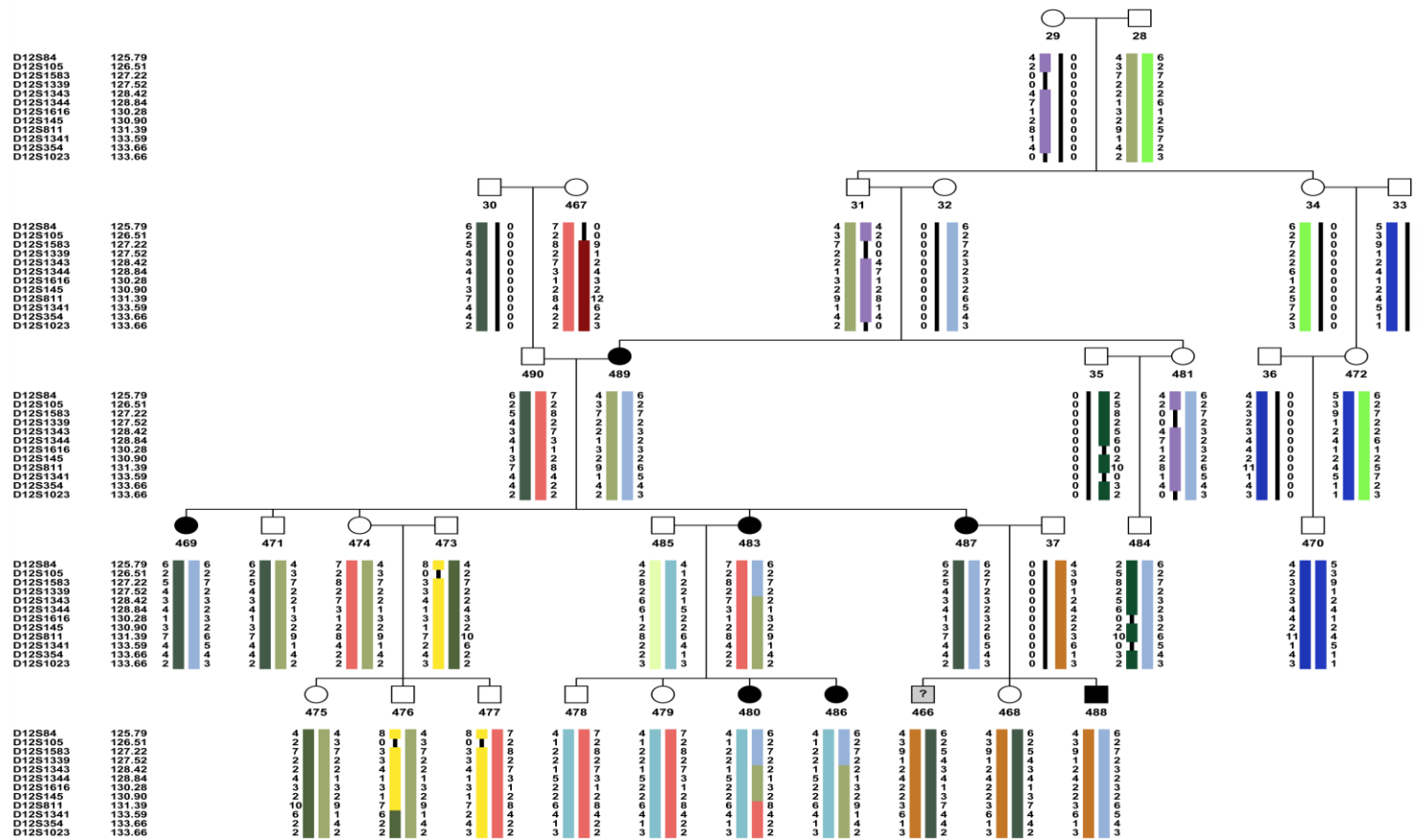


Figure 17 Haplotype reconstruction for family F1.

Note that all the patients have the disease allele (light blue). Three unaffected have also the disease allele (illustrating incomplete penetrance in individual III.2 and her mother (see Figure 10) or new mutation from individual 32 to 489).

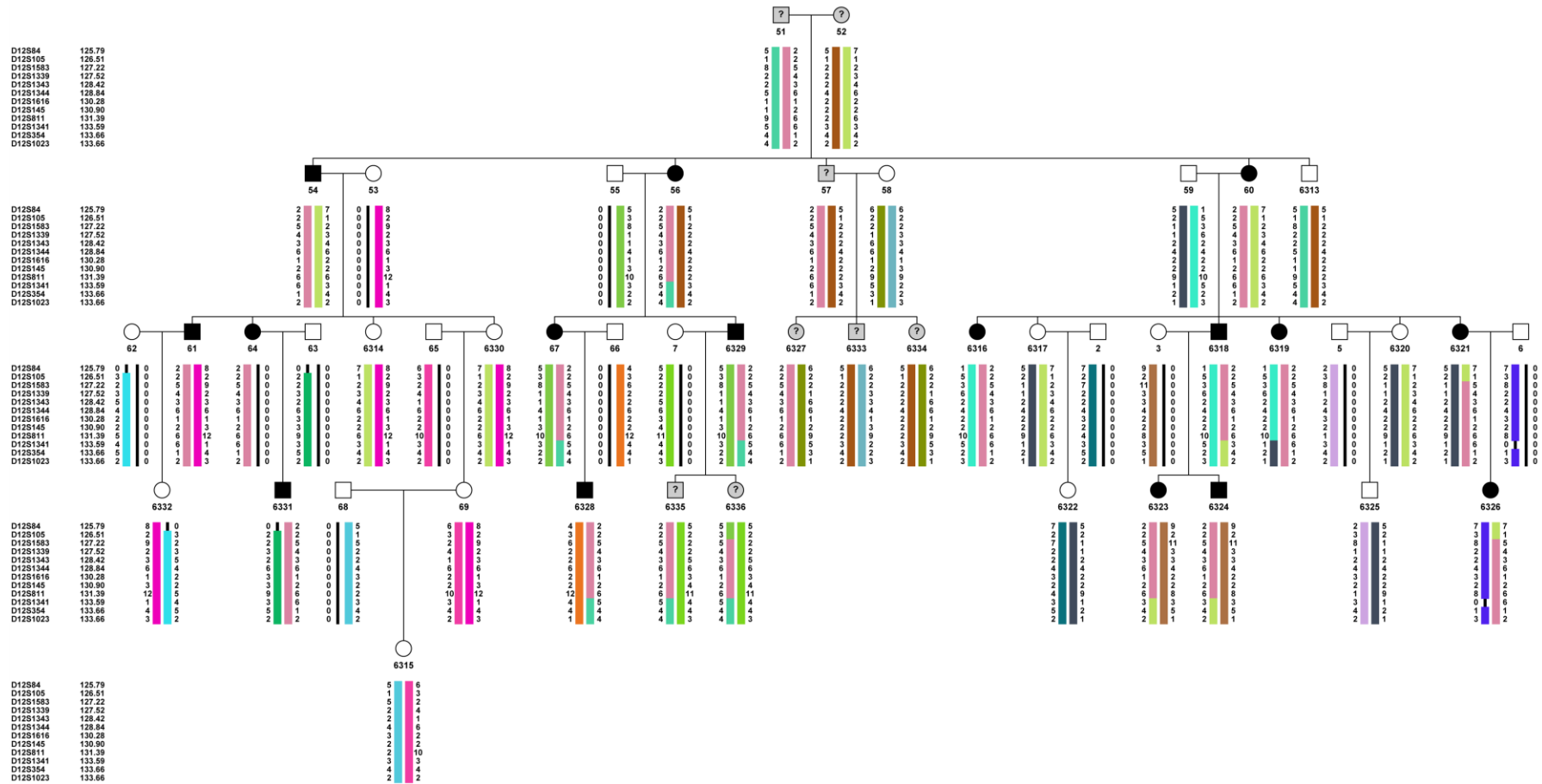


Figure 18 Haplotype reconstruction for family F2.

The disease allele (pale pink) segregates according to the disease status. Three individuals carrying this allele (6327, 6335, and 6336) were found later to be clinically affected.

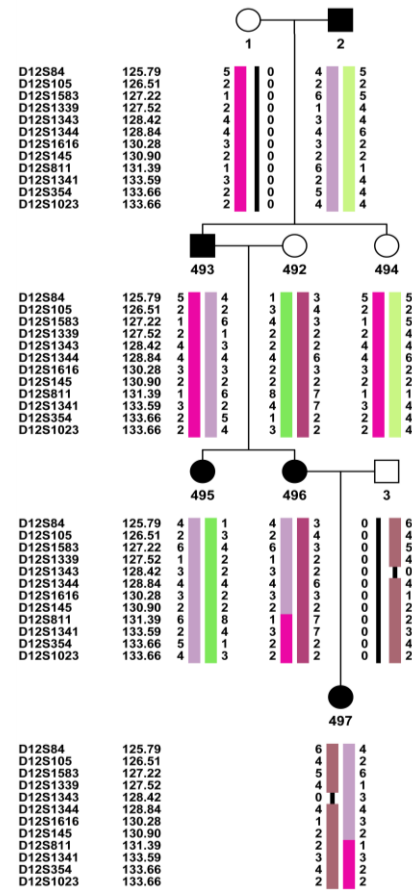


Figure 19 Haplotype reconstruction for family F4. Note that all the affected have the disease allele (pale purple).

The additive LOD score from the analysis of all three families was about 11 (Figure 20), giving us strong evidence that this locus is likely to contain the disease-causing gene for CMT2C.

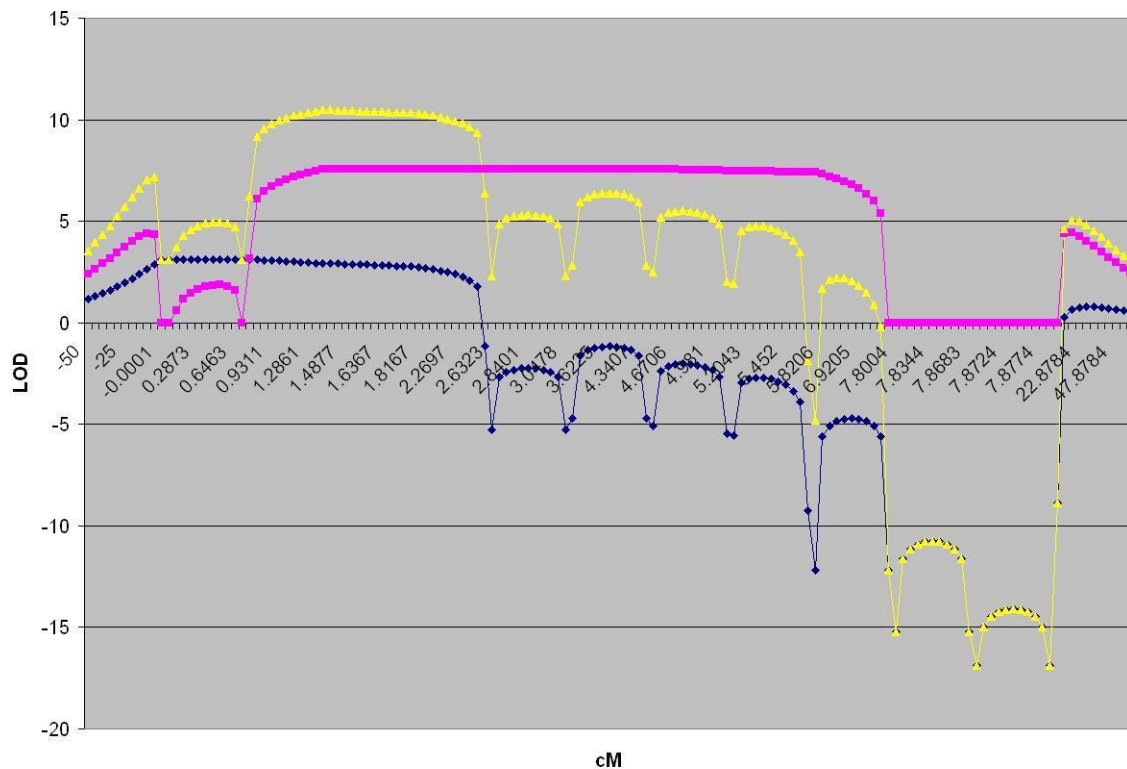


Figure 20 LOD score curve for family F1 and F2.

The plateau blue curve represents family F1 and the plateau pink curve represents family F2. The yellow curve represents the combined LOD score for these two families. Note that family F4 that has a LOD score of about 1 is not represented here. X axis: the region covered by markers D12S84 and D12S1023, Y axis: LOD score.

When data from all three families were combined, the haplotype reconstruction narrowed down the region of interest to about 2.6 Mb, between markers *D12S105* and *D12S1343* (Figure 21). Family F2 defines the upper border and F1 defines the lower border. This region contains 40 annotated genes of which 38 are protein-coding (NCBI Mapviewer), and 35 are, in various levels, expressed in the nervous system. Twenty eight of these expressed genes have a known function, and four of them are involved in diseases, but none of them is of interest for the nervous system. The

ataxin 2 gene (*ATXN2*) was excluded by this analysis as did previous studies through fine mapping as well as sequencing.

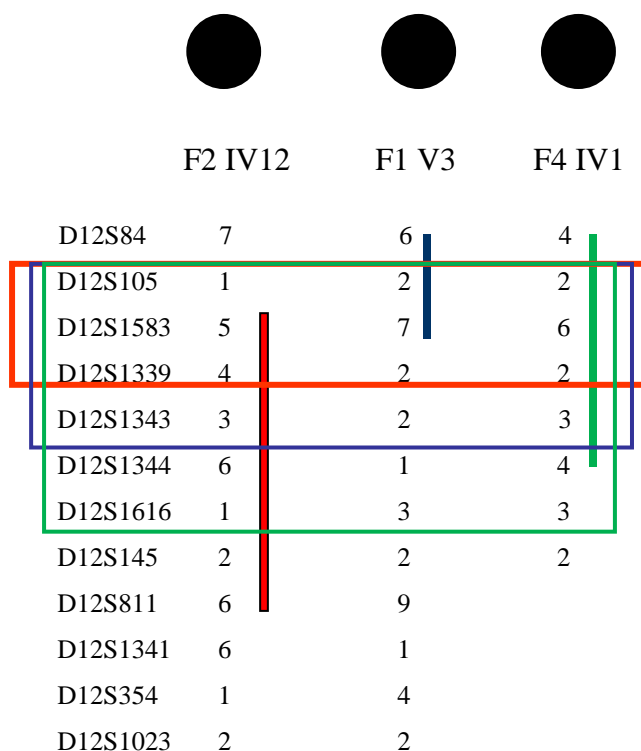


Figure 21 Summary of linked regions in family F1, F2, and F4.

Only the disease allele is represented here. Note that family F2 defines the upper border (marker D12S105) and family F1 defines the lower border (marker D12S1343). Family F4, apart from being linked, did not narrow the previous region of linkage. The green square represents the region from the first linkage study (Klein, Cunningham et al. 2003), the blue represents the region from the second linkage study in different families (McEntagart, Reid et al. 2005), and red represents our results.

3.2.2 SNP arrays analysis

SNP arrays analysis was performed to look for possible duplications or deletions in the two families (F1 and F2) where linkage with microsatellite markers was used. This analysis was focused on the region of interest found with the linkage analysis, and no copy number variation was seen.

Whole genome scan using SNP array in family F5 excluded the 12q24.11 locus (Figure 22). In fact the affected mother passed on different alleles to her affected sons for the same markers (SNP). This is not consistent with disease status in this family

because the affected sons should inherit the same allele from their mother.

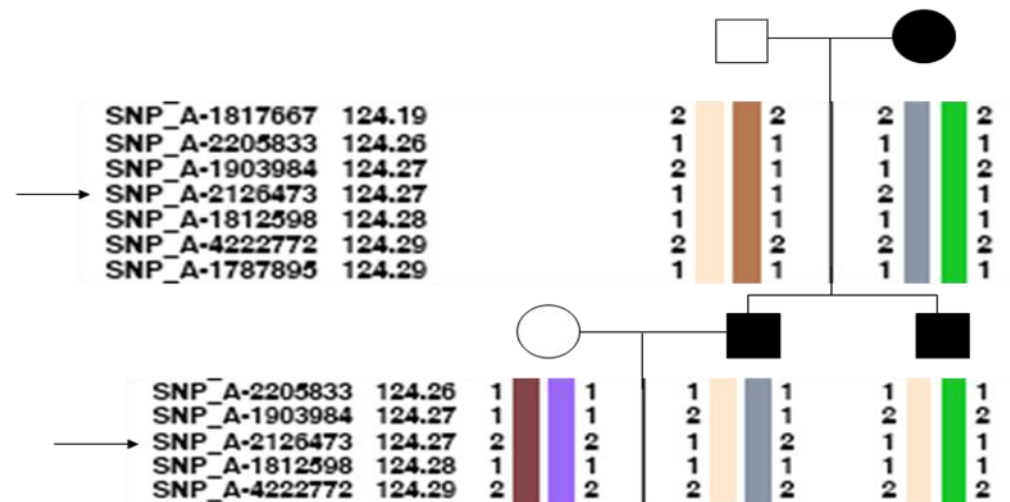


Figure 22 Part of the haplotype reconstruction in family F5.

The haplotype reconstruction is showing that the TRPV4 locus was excluded in family F5. Note that the arrow is showing one of the SNPs for which the affected mother gave a different allele to her affected sons at the same marker position.

3.2.3 Selection of candidate genes

The candidate genes selection approach within the mapped region defined earlier allowed us to choose a first set of candidate genes to be sequenced.

CUTL2

The first gene that was considered as primary candidate was the cut-like homeobox 2 gene (*CUTL2* or *CUX2*). It has three conserved domains: homeodomains that are DNA binding domains involved in the transcriptional regulation of key eukaryotic developmental processes (transcription repressor activity), an Smc domain that functions as chromosome segregation ATPases that play a role in cell division and chromosome partitioning, and CUT domains that are DNA-binding motifs which can bind independently or in cooperation with the homeodomain, often found downstream of the CUT domain (Gene Ontology Annotation [GOA] Database, EMBL-EBI). *CUX2* spans a 316528 bp long genomic region, is transcribed into a 6841 bp long mRNA, and has 22 exons that code for 1486 amino acids (NCBI, Entrez Nucleotide database).

Arguments for *CUX2* being a candidate gene:

- Expression: *Cux-2* in mouse is expressed exclusively in the central and peripheral nervous system and may encode a transcription factor that is involved in neural

specification in mammals (Quaggin, Heuvel et al. 1996; Gingras, Cases et al. 2005). Another study has found that CUX-2 functions at multiple levels during the spinal cord neurogenesis.

- Interaction and homology: CUX2 has a common cellular localization with the ataxin 1 (*ATXN1*) gene (NCBI, Aceview), and some homology with dynactin 1 (*DCTN1*) and the neurofilament light polypeptide (NEFL) genes (UCSC Human Gene Sorter) which are known to cause spinocerebellar ataxia, distal hereditary motor neuropathy with vocal fold paralysis and both axonal and demyelinating hereditary motor and sensory neuropathies, respectively.

The possibility of CUX-2 for being a candidate gene for susceptibility to bipolar disorder was also suggested (Jacobsen, Elvidge et al. 2001).

TCTN1

The tectonic 1 gene encodes a member of the tectonic family of secreted and transmembrane proteins. This gene has one conserved domain (DUF1619 superfamily) of unknown function. TCTN1 has three transcript variants that code for different length of proteins. The total genomic DNA is 35056 bp, and the longest isoform codes for 592 amino acids. The orthologous gene in mouse is required for formation of most ventral cell types.

Arguments for TCTN1 being a candidate gene:

- TCTN1 is expressed in both the central and peripheral nervous systems, though this expression is not the highest when compared to other organs.
- Studies in *Tectonic* mutant mice showed that *Tectonic* is required for formation of the *Sim1*-expressing V3 interneurons, and *Tectonic* mutants also display a variable reduction in the number of Islet1/2-positive motor neurons (Reiter and Skarnes 2006).

VPS29

The vacuolar protein sorting 29 homolog (*S. cerevisiae*) gene belongs to a group of vacuolar protein sorting (VPS) genes that, when functionally impaired, disrupt the efficient delivery of vacuolar hydrolases. The protein encoded by this gene is a component of a large multimeric complex, termed the retromer complex, which is involved in retrograde transport of proteins from endosomes to the trans-Golgi network. This VPS protein may be involved in the formation of the inner shell of the retromer coat for retrograde vesicles leaving the prevacuolar compartment. Other

functions of this gene include metal ion binding, phosphoserine phosphatase activity and zinc ion binding (NCBI, Entrez Gene).

Arguments for VPS29 being a candidate gene:

- Expression: this gene is expressed in brain, nerve and spinal cord, though the expression is not higher than in other organs including parathyroid, bladder and bone marrow (NCBI, Unigene). But no expression data is available in the GNF SymAtlas v1.2.4 for this gene.
- Although no animal model is available to date to show the implication of this gene in the nervous system phenotype, it seems to be sharing the same function as another gene (DCTN1) involved in hereditary peripheral neuropathy with vocal fold paralysis; which is, as stated above, the retrograde transport of proteins from endosomes to the trans-Golgi network.

GIT2

The G protein-coupled receptor kinase interacting ADP-ribosylation factor (ARF) GTPase-activating protein (GAP) 2 (ArfGAP 2) encodes a member of the GIT protein family, which interact with G protein-coupled receptor kinases and possess ARF GAP activity. GIT proteins traffic between cytoplasmic complexes, focal adhesions, and the cell periphery, and interact with Pak interacting exchange factor beta (PIX) to form large oligomeric complexes that transiently recruit other proteins. GIT proteins regulate cytoskeletal dynamics and participate in receptor internalization and membrane trafficking. This gene has been shown to repress lamellipodial extension and focal adhesion turnover, and is thought to regulate cell motility.

Arguments for GIT2 being a candidate gene:

- Expression: GIT2 is expressed in the nervous system; however this expression does not exceed the median seen in other organs (NCBI Unigene, GNF SymAtlas v1.2.4).
- Studies have suggested pathogenic roles for GIT proteins in Huntington's disease, a disease due to a damage of nerve cells of basal ganglia and cerebral cortex (Hoefen and Berk 2006).

ACACB

Acetyl-CoA carboxylase (ACC) is a complex multifunctional enzyme system. ACC is a biotin-containing enzyme which catalyzes the carboxylation of acetyl-CoA to malonyl-CoA, the rate-limiting step in fatty acid synthesis. ACC-beta is thought to control fatty acid oxidation by means of the ability of malonyl-CoA to inhibit

carnitine-palmitoyl-CoA transferase I, the rate-limiting step in fatty acid uptake and oxidation by mitochondria. ACC-beta may be involved in the regulation of fatty acid oxidation, rather than fatty acid biosynthesis. ACACB also functions as ATP binding.

Arguments for ACACB being a candidate gene:

- Expression: ACACB is expressed in the central and peripheral nervous system although not at higher level than the other organs.
- ACACB is expressed in hypothalamus neurons, but mutant Acetyl-CoA Carboxylase 2 mice did not show obvious neurological abnormalities other than those seen in hypothalamus damage (feeding control) (Loftus, Jaworsky et al. 2000; Abu-Elheiga, Matzuk et al. 2001). However this does not rule out a presence of neurological signs in these mice because more often investigators are focused on the organs and symptoms of their particular interest.

ANKRD13A

The ankyrin repeat domain 13A gene contains a conserved domain that is made up of ankyrin repeats which mediate protein-protein interactions in very diverse families of proteins. This gene is made of 15 exons, is transcribed into an mRNA that is 3910 bp long which is translated into a protein that consists of 590 amino acids.

Arguments for ANKRD13A:

- Expression: this gene is expressed both in the central and the peripheral nervous system, though not at higher level than the other organs (NCBI Unigene, GNF SymAtlas v1.2.4).
- Studies of animal models have shown that ankyrins are expressed in the peripheral nervous system, especially in axons, and along with other proteins participate in the axonal and dendritic morphogenesis (Yamamoto, Ueda et al. 2006). Ankyrins also interact with other genes involved in diseases affecting the nervous system in animal models (Zhou, Opperman et al. 2008).

FLJ40142

The genomic region of the FLJ40142 gene is 26518 bp long leading to a 1946 bp long mRNA. This gene codes for 135 amino acids long protein but has no known function (Entrez Gene, NCBI).

Arguments for FLJ40142:

- Expression: this gene has its highest expression in the nervous system (Unigene: NCBI, GNF SymAtlas v1.2.4).

Other genes of interest including ARPC3, ANAPC7, UBE3B, ATP2A2 and KCTD10 were considered after the first set.

3.2.4 Mutation detection by Sanger sequencing

The coding regions of selected candidate genes, including the likeliest candidates, were sequenced, and no significant sequence variants have been seen. We then proceeded with sequencing the coding region of all the remaining genes within the region of interest. Forward and reverse primers were designed for the remaining exons, and set in 96-well plates for a faster PCR processing.

We found two heterozygous sequence variants in the exon number 5 of the *TRPV4* gene. The first change is a cytosine to tyrosine transition, and was seen in family F1 at coding position 805 (c.805C>T) (Figure 23a). This change leads to the amino acid substitution arginine to cysteine at position 269 (R269C). Next, we sequenced the rest of the family members, and found that all the affected individuals carried the sequence variant, and none of the unaffected individuals, except the two who carry the disease-haplotype, had it. The second change, seen in family F2, is a guanine to adenine transition at coding position 806 (c.806G>A) (Figure 23b). This sequence variation gives the amino acid substitution arginine to histidine at position 269 (R269H). Here also we screened all available family members for this mutation, and found that all the affected had the sequence change and none of the unaffected individuals showed it. Family F4 did not show any significant sequence change in the *TRPV4* gene nor in any of the other genes within the linked region; pointing toward a genetic heterogeneity which is a characteristic feature of Charcot-Marie-Tooth diseases.

After these findings we have screened families F3 and F5 for the *TRPV4* gene, and found no significant sequence variants. We subsequently screened 132 patients for this gene, and two heterozygote sequence variants have been found in two patients. The first one lies at the end of exon number 4 at coding position 694, and is a cytosine to tyrosine transition (c.694C>T) (Figure 23c), leading to the amino acid substitution arginine to cysteine at position 232 (R232C). Additional exploration of the family history showed that the patient had an affected father. The second change, located in the C-terminal region of the gene, was found in the exon number 16 at coding position 2560, and is an Adenine to Guanine transition (c.2560G>A) (Figure 23d).

This missense nucleotide variant gives the amino acid change aspartic acid to asparagine at position 854 (D854N).

The R269 residue lies at the tip of the 3rd ankyrin repeat domain (ANK) of the chicken TRPV4 ankyrin repeats domain structure. The R269 residue is conserved in a wide range of species from human to fish. Moreover, the R269 residue constitutes the first arginine of one of the four TRPV4 endoplasmic reticulum (ER) retention motifs (RGR).

The R232 residue is located in the second ankyrin repeat domain. This residue is also highly conserved in different species from human to fish, and is in a predicted exon splicing enhancer (ESE) SR protein binding site (SF2/ASF (IgM-BRCA1)), and the R232C change destroys this site with a score above the threshold.

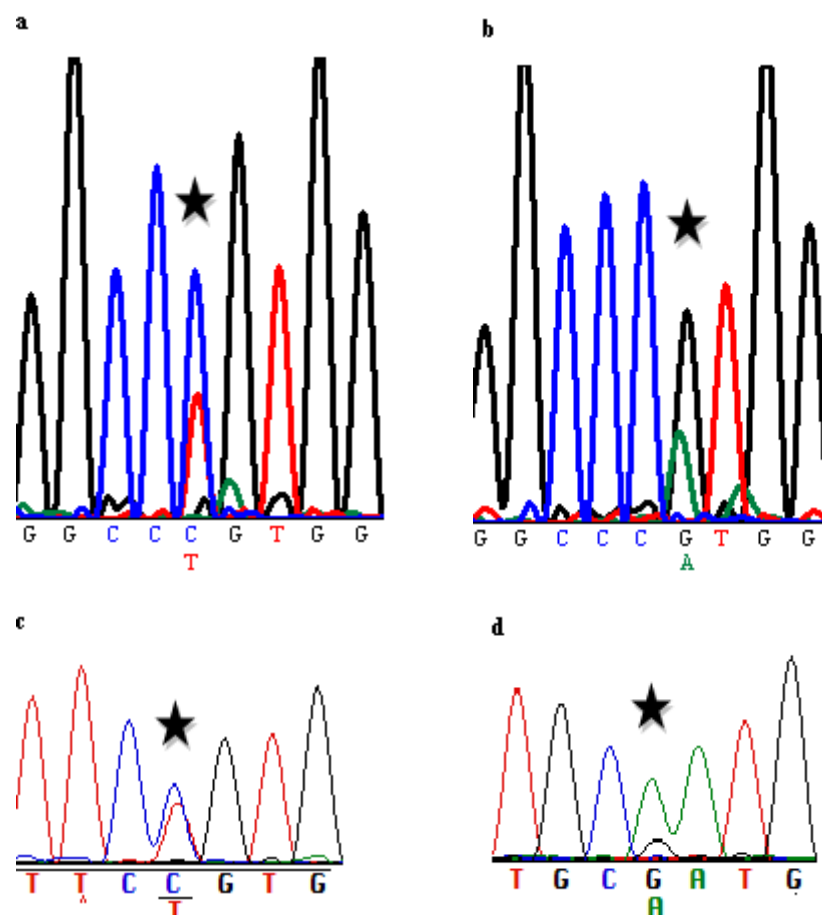


Figure 23 Chromatographs representing the mutations found by Sanger sequencing. Asterisks are showing: a) heterozygous sequence variant c.805C>T in family F1, b) heterozygous sequence variant c.806G>A in family F2, c) heterozygous sequence variant c.694C>T from the CMT2 cohort study, d) heterozygous sequence variant c.2560G>A from the CMT2 cohort study

3.2.5 Exome sequencing

Because screening of family F3 and F4 for the *TRPV4* gene was negative we performed whole exome sequencing using one affected individual in each family. We first excluded all known CMT-causing genes and analyzed the rest of the data. Although not perfect because it does not cover the whole coding genome, exome sequencing has become a useful tool in identifying mutation in small families with suspected hereditary disorders. This sequencing revealed a single nucleotide sequence variant in the *TRPV4* gene in family F3. The sequence variant is located in the exon number 3 at the coding nucleotide position 557, and is a transition of guanine to adenine (c.557G>A) (Figure 24a). This missense mutation leads to the substitution of arginine to glutamine at the amino acid position 186 (R186Q). This variant was missed by previous Sanger sequencing because it was at background noise level (Figure 24b). We have designed new primers to amplify and sequence the exon 3 to confirm this change and check for segregation. All affected individuals in family F4 had the sequence variant which was not seen in the unaffected individuals. Individual III.5 does not have the mutation (Figure 24c), confirming that he is not affected with CMT2C, though he presented some subtle symptoms.

The R186 residue lies at the end of the first ankyrin repeat domain, and the R to Q change is non conservative. Unlike R269, R186 is not part of an ER retention motif.

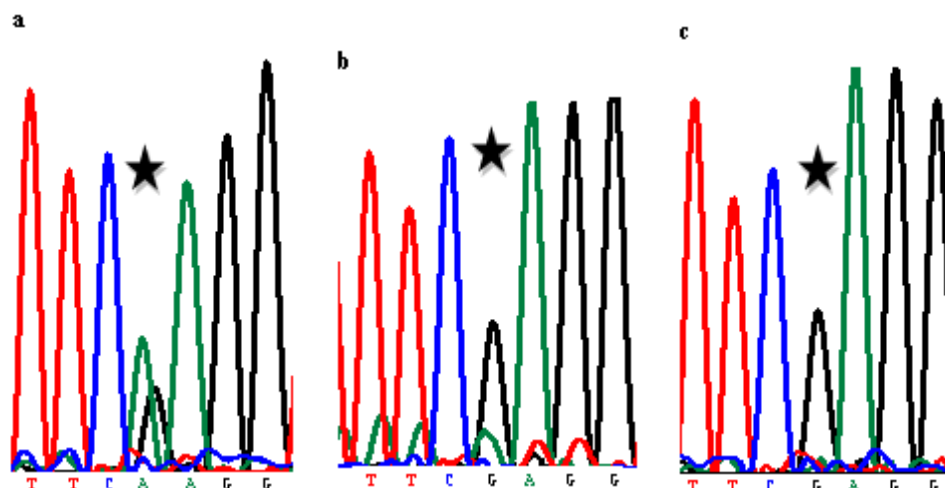


Figure 24 Chromatographs showing the mutation missed by Sanger sequencing and found by exome sequencing.

a) heterozygous sequence variant c.557G>A clearly visible when primers that do not contain SNP were used to amplify the genomic DNA, b) the sequence variant is not apparent (the “A” variant peak is comparable to the background noise), c)

chromatograph of individual III.5 (the sequence variant is not seen). Note that primers used in Figures 24a and 24c are same and different from Figure 24b.

3.3 Functional studies

3.3.1 Expression analysis

Quantitative RT-PCR

Expression of TRPV4 was shown in ventral horn and dorsal root ganglia nerves and in cartilage. In order to confirm the presence of TRPV4 in these tissues, we quantified TRPV4 transcript by qRT-PCR in human spinal cord ventral and dorsal horn, tracheal cartilage, and knee cartilage primary chondrocytes (Figure 25a). TRPV4 transcript was expressed in all of these tissues but the expression level was much higher in cartilaginous tissues.

Five TRPV4 splice variants were cloned in human tracheal and bronchial epithelial cells (Arniges, Fernandez-Fernandez et al. 2006), although two of them were already described (the full-length TRPV4 cDNA called isoform A; GenBank number NM_021625 and the TRPV4 cDNA lacking exon number 7 called isoform B, GenBank number NM_147204; Δ 384–444 amino acids). The other three are the TRPV4-C variant which lacks exon 5 (number DQ59644; Δ 237–284 amino acids), TRPV4-D that presents a short deletion inside exon 2 (number DQ59645; Δ 27–61 amino acids), and TRPV4-E (number DQ59646; Δ 237–284 and Δ 384–444 amino acids) that is produced by double alternative splicing lacking exons number 5 and number 7. Although distinct TRPV4 transcript isoforms lacking exon number 5 and/or exon number 7 have been described (Arniges, Fernandez-Fernandez et al. 2006), we detected no evidence of variable expression of spliced isoforms lacking exon number 5 or number 7 in the different tissues.

To confirm these results, we performed a regular PCR using cDNA from different human tissues, including brain, spinal cord, trachea, liver, pancreas, kidney, and primers located within exon number 4 and number 8 of the TRPV4 cDNA to amplify exon 5 and 7. PCR products were visualized on agarose gel. In all lanes, two bands were identified (Figure 25b). Sequencing of these bands revealed the full length transcript and the one lacking exon number 7 in all tissues. No other deletion was seen elsewhere in the cDNA sequence. However, the band corresponding to the transcript

lacking exon number 7 seemed stronger than the full length in the nervous system tissues. The variant lacking exon 5 was not seen.

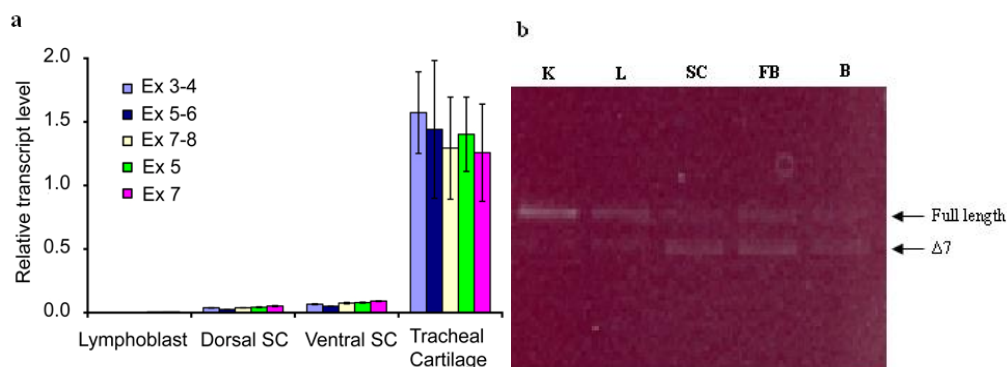


Figure 25 Quantification of TRPV4 transcript by quantitative RT-PCR.

a) in control human lymphoblast lines (n=4), human dorsal spinal cord (n=3), ventral spinal cord (n=3), and tracheal cartilage (n=3) using qRT-PCR primers specific for following exon regions: exons 3–4, exons 5–6, exons 7–8, exon 5, and exon 7. There was no evidence of variable expression of TRPV4 transcript isoforms containing exon 5 or exon 7 in spinal cord compared to cartilage tissues. Values are normalized to the first tracheal cartilage sample. Data is averaged; error bars, s.e.m. b) amplification of TRPV4 full-length cDNA from kidney (K), lung (L), spinal cord (SC), foetal brain (FB), and brain (B). Arrows denote full length TRPV4 and $\Delta 7$ TRPV4. Note that $\Delta 7$ TRPV4 appears stronger in nervous system tissues.

Immunohistochemistry (IHC)

TRPV4 has been shown to be expressed in DRG neurons where it is postulated to play a role in nociception. The expression and function of TRPV4 in motor neurons has not been previously well characterized. One previous study reported TRPV4 immuno-reactivity in human spinal cord motor neurons and ventral root (Facer, Casula et al. 2007). In addition, in situ hybridization indicates that TRPV4 mRNA is expressed in large ventral horn neurons of the adult mouse spinal cord (see Allen Institute for Brain Science Spinal Cord Atlas:

<http://mouse spinal.brain-map.org/imageseries/show.html?id=100017703>). We further examined the expression of TRPV4 protein in mouse spinal cord and DRGs by IHC. TRPV4 protein was expressed in ChAT positive spinal motor neurons, but was absent in TRPV4 knock-out mice tissues (Suzuki, Mizuno et al. 2003) confirming the specificity of the staining.

These data indicate that full-length TRPV4 are expressed in both sensory and motor neurons (Figure 26).

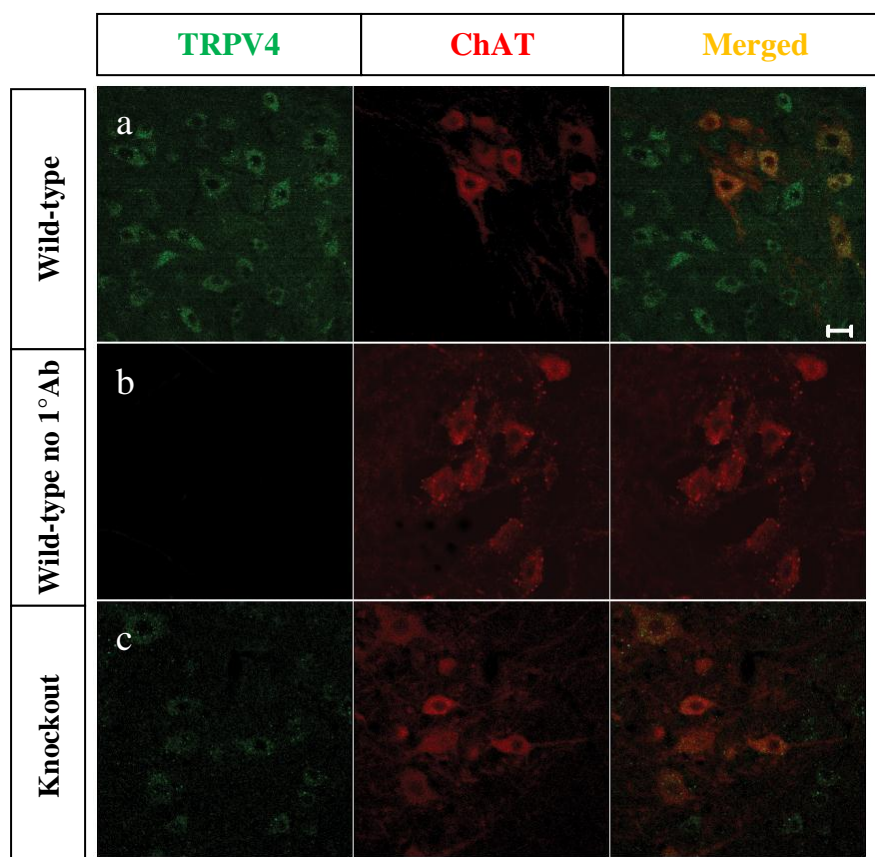


Figure 26 TRPV4 expression in mouse spinal cord ventral horn motor neuron.

TRPV4 is expressed at low level in mouse spinal cord ventral horn motor neuron. a) TRPV4 staining is evident in ChAT-positive motor neurons in WT mice. b) TRPV4 is absent when immunostaining is performed under identical conditions, except that TRPV4 primary antibody is omitted. c) Reduced TRPV4 staining is evident in knockout mice. Scale 20 μ m.

3.3.2 Analysis of WT and mutant TRPV4 in transfected mammalian cells

Cell surface localization

Full-length TRPV4, TRPV4-A, and the one lacking a portion of exon 2, TRPV4-D, were shown to traffic to the surface membrane while TRPV-B, TRPV4-C, and TRPV4-E, that all have deletion of part of the ankyrin repeat domains were retained in the ER (Arniges, Fernandez-Fernandez et al. 2006). The ankyrin domain of the TRPV4 protein has been hypothesized to be important for normal TRPV4 protein tetramerization and cellular trafficking by same investigators (Arniges, Fernandez-

Fernandez et al. 2006). Biogenesis of TRPV4 involves oligomerization in the ER and transfer to the Golgi for subsequent maturation. In order to evaluate whether the R269C and R269H mutants altered the normal trafficking of TRPV4, we transfected different mammalian cell lines with WT and mutant TRPV4, and examined the distribution of TRPV4 protein by IHC. In HeLa cells, mouse WT, R269C, and R269H TRPV4 were all expressed predominantly in the cell cytoplasm and at the cell surface membrane with no differences seen between WT and mutant forms of TRPV4 (Figure 27). In cells, expressing high levels of transfected protein, TRPV4 was present in small, rounded inclusions in the cell cytoplasm which partially co-localized with EEA1, an early endosome marker (Figure 28). When stained with the Golgi marker, GM130, we have seen the same result (Figure 28). These inclusions appeared more abundant and bigger in mutant TRPV4-transfected cells. In HEK 293 cells, human WT and mutant TRPV4 was predominantly present in the cell cytoplasm with surface localization less prominent than in HeLa cells (Figure 27). In order to check whether mutant TRPV4 was retained in the ER or in the Golgi, we stained cells with ER markers. There was little co-localization with the ER marker, calnexin. This indicates that mutant TRPV4 was not sequestered in the ER or in the Golgi. In DRG neurons, TRPV4 was prominently localized to the distal neurites of these cells, but again no difference was seen in cells expressing WT or mutant forms of the protein.

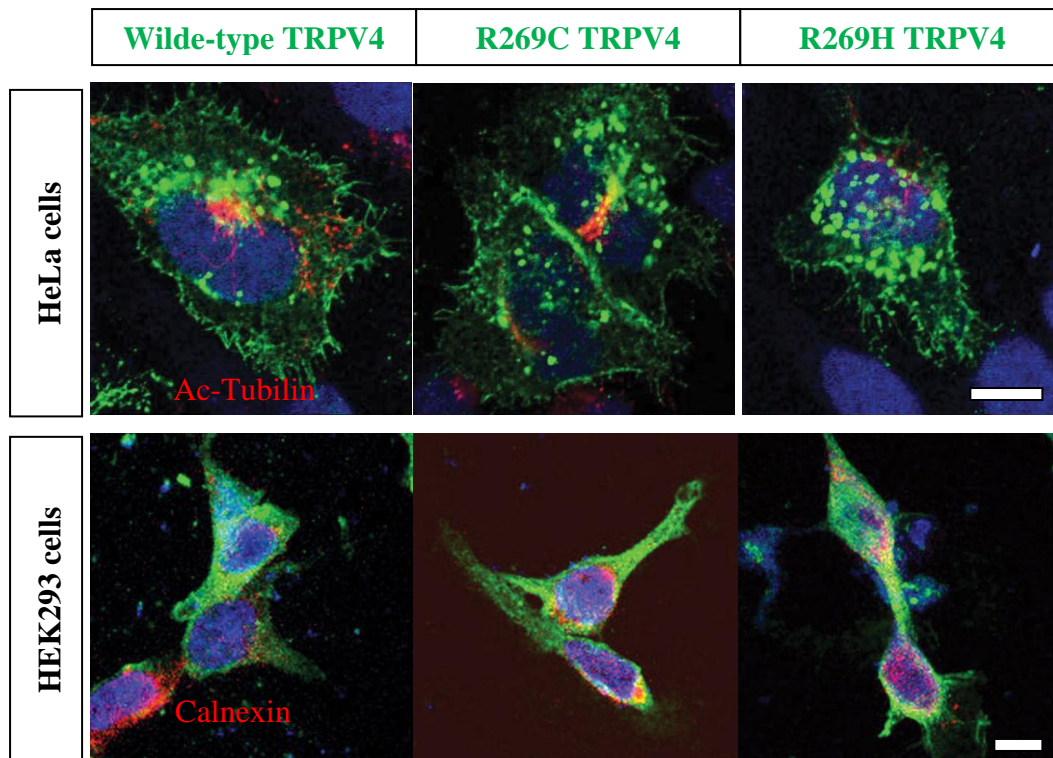


Figure 27 The CMT2C mutations do not change TRPV4 trafficking.

In HeLa and HEK293 cells, WT, R269C, and R269H are localized to the cell cytoplasm and cell surface membrane. Note the inclusions in both wild-type and mutant TRPV4 expressing cells. Both WT and mutant TRPV4 show little co-localization with the endoplasmic reticulum (ER) marker, calnexin, and the Golgi marker, GM130, and there was no difference in cell surface localization. Scale bars 10 μm .

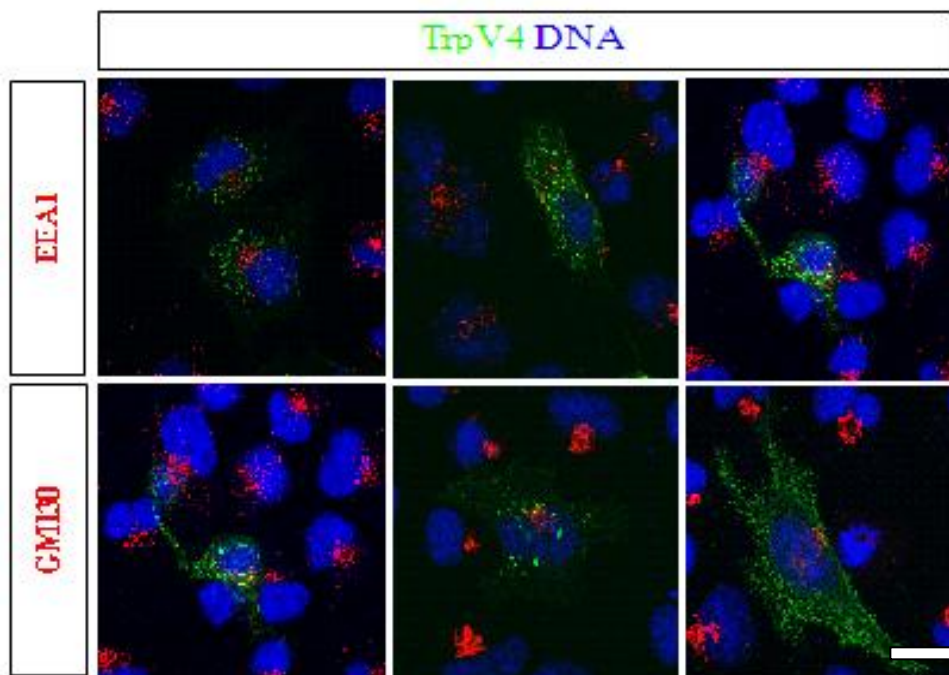


Figure 28 Staining of transfected HeLa cells with ER and Golgi markers.

Note that there is little or no co-localization between TrpV4 and ER (EEA1) and Golgi (GM130) markers. Scale bar 10 μm .

Cell surface biotinylation

In order to further examine the association of WT and mutant TRPV4 with the cell plasma membrane, we isolated cell surface biotinylated proteins from HeLa cells expressing mouse WT, R269C, or R269H TRPV4. Immunodetection of TRPV4 proteins showed appropriately sized bands for TRPV4 in 10 % of whole cell extract inputs and extracts after streptavidin isolation. Protein loading was controlled by immunodetection of β -actin, which showed appropriate depletion after isolation of the membrane fraction. No differences were seen in the amount of TRPV4 expressed at the cell surface membrane in cells expressing WT or mutant forms of TRPV4 (Figure 29). Similar results were seen in HEK 293 cells expressing human WT and mutant forms of TRPV4 (data not shown).

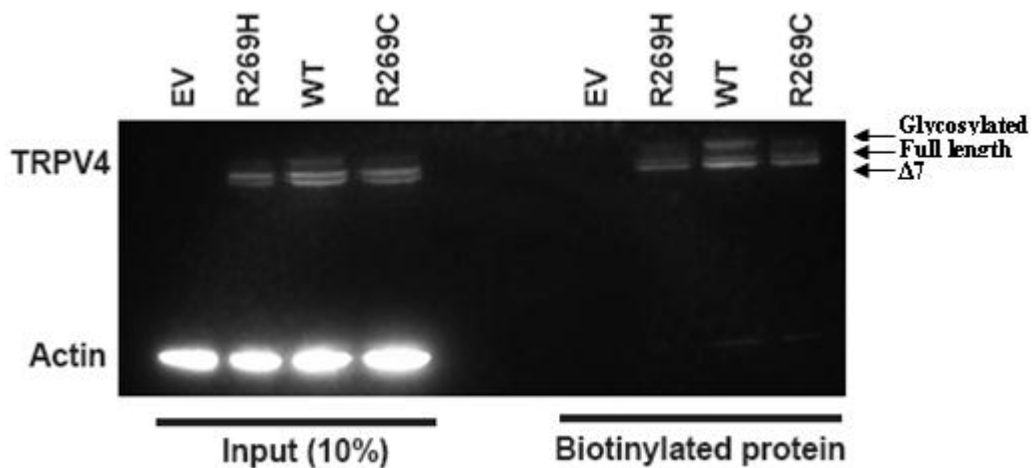


Figure 29 Immunodetection of TRPV4 proteins in HeLa cells.

Immunodetection of TRPV4 proteins shows appropriately sized bands for TRPV4 in 10 % of whole cell extract inputs and the biotinylated fraction. Arrows denote glycosylated, full length and $\Delta 7$ TRPV4. There was no difference in the amount of wild-type compared to mutant TRPV4 in the membrane fraction (biotinylated fraction). However, the glycosylation pattern is slightly different (the upper band, which correspond to the glycosylated protein is stronger in wild-type. Shown is one representative blot of four independent experiments.

Endoplasmic Reticulum stress

To further investigate mutants TRPV4 cellular localization, we checked levels of genes activated during sequestration of genes in the ER. There was no increase in the expression of these genes in HEK 293 cells expressing mutant TRPV4 (Figure 30). This confirms that mutants TRPV4 are not retained in the ER, as shown by previous experiments.

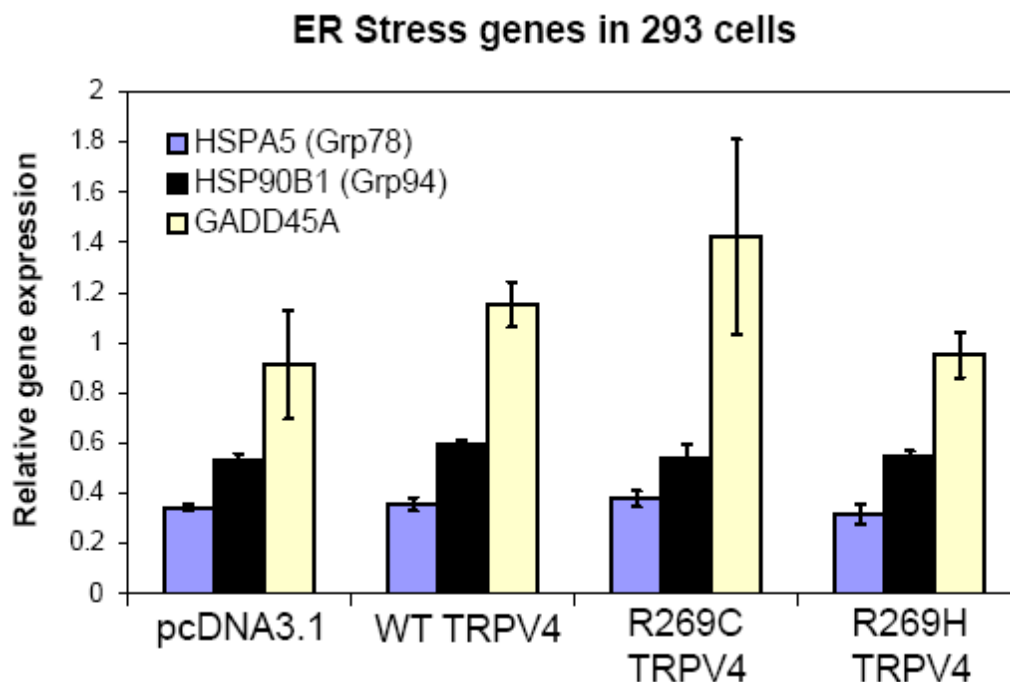


Figure 30 Mutant TRPV4 is not retained in the ER.

The ER stress genes HSPA5, HSP90B1, and GADD45A were measured by qRT-PCR in HEK 293 cells expressing empty vector, WT TRPV4, and mutant forms of TRPV4 for 48 hours. Data are normalized to the GADD45A pcDNA3.1 value. No difference in expression of ER stress genes is seen in cells expressing mutant forms of TRPV4 protein.

Cell death assays

Because TRPV4 is calcium permeable ion channel and Ca^{2+} overload is known to cause cell death, we performed cell death assays to assess the effect of mutants TRPV4 in cell viability. Although R269C and R269H TRPV4 showed no abnormalities of intracellular trafficking or cell surface expression, HEK 293T cells expressing mutant human TRPV4 showed evidence of cellular toxicity and death that increased with time (Figure 31a). At 24 hours, the percentage of dead cells was 4.0 % in WT TRPV4 expressing cells, but 11.0 % for R269C TRPV4 ($p < 0.01$) and 11.4 % for R269H TRPV4 ($p < 0.01$). By 48 hours, 1.8 % were dead in WT TRPV4-expressing cells, 29.3 % dead for R269C ($p < 0.0001$), and 24.9 % dead for R269H ($p < 0.0001$). The addition of ruthenium red (RR), a non-specific TRP channels inhibitor, completely blocked this toxicity (Figure 31b) suggesting that cell toxicity relates to abnormal function of the TRPV4 channel. The same toxicity was seen in DRGs (Figure 31c).

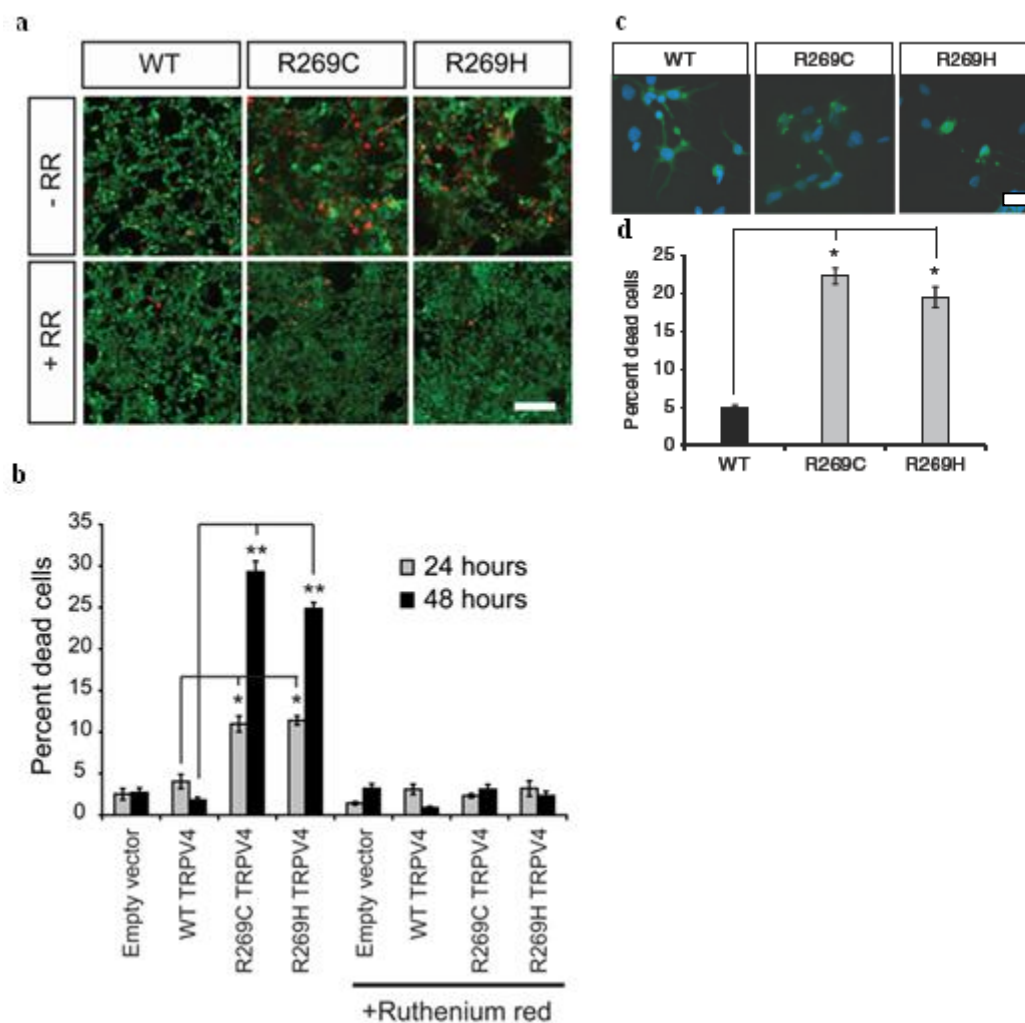


Figure 31 Mutant TRPV4 causes cell toxicity in non-neuronal and in neuronal cells.

a) HEK293 cells expressing R269C and R269H mutants show an increase in the number of dead cells (red channel is EthD-1 stain) at 48 h; this increase is prevented by the TRP channel blocker ruthenium red (RR). Green channel is calcein-AM stain for live cells. Scale bar, 200 μm . b) Quantification of cell death in HEK293 cells indicates a time-dependent increase in cell death that is blocked by the TRP channel blocker ruthenium red (RR). * $P < 0.01$, ** $P < 0.001$. Data in (a) and (b) are averaged from three independent experiments; error bars, s.e.m. c) DRG neurons were transfected with wild-type and mutant forms of TRPV4 (green). At 16 h, some cells expressing mutant forms of TRPV4 show evidence of early cellular toxicity with a collapsed cytoplasm. The nuclear DAPI stain is blue. Scale bar, 40 μm . d) Quantification of propidium iodide uptake in DRG neurons expressing wild-type and

mutant TRPV4 reveals a marked increase of cell toxicity in mutant expressing cells at 48 h. * $P < 0.0001$.

To further evaluate TRPV4 hyperactivity and cell death we used two TRPV4 specific blockers: a genetic modification in the transmembrane domain and a chemical compound (Figure 32). A TRPV4 pore mutation, M680K, was shown to reduce or block TRPV4 Ca^{2+} permeability. HEK 293 cells transfected with constructs containing both M680K and R269C or R269H variants showed less toxicity (Figure 32a). Moreover, relative fluorescent units were reduced (Figure 32c), supporting less calcium entry into the cell. RN1734 is a chemical compound that was recently identified as specific TRPV4 inhibitor. When used, this compound also had a similar effect as the M680K mutant (Figure 32b and 32d).

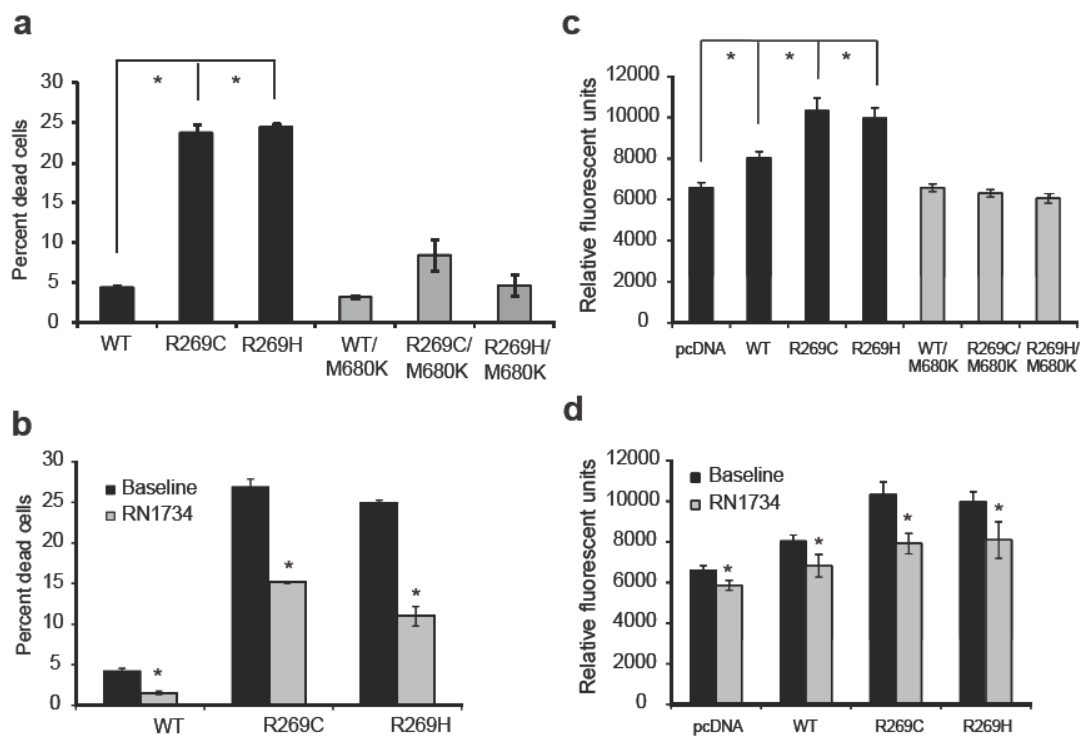


Figure 32 CMT2C mutations cause cell death that is prevented by TRPV channel blockers.

Increased cell death and intracellular calcium levels caused by the CMT2C mutations are mitigated by the TRPV4 inactivating channel pore mutation, M680K, and the TRPV4 channel inhibitor, RN1734. Quantification of cell death in HEK293 cells at 48 hours in WT, R269C, or R269H TRPV4-expressing cells compared to a) WT/M680K, R269C/M680K, or R269H/M680K TRPV4-expressing cells and b) TRPV4-expressing cells treated with the TRPV4 inhibitor, RN1734 at 10 μM . * $p < 0.001$.

Quantification of intracellular calcium levels by Fluorometric Imaging Plate Reader (FLIPR) in HEK293 cells expressing the TRPV4 mutants c) and treated with RN1734 for 24 hours d). * $p < 0.05$. Data in a, b are averaged from three independent transfections, data in c, d are averaged from 4 independent transfections, error bars, s.e.m.

Xenopus oocytes expressing mutants TRPV4 also showed toxicity. When we expressed TRPV4 in *Xenopus* oocytes incubated in normal frog's Ringer solution, mutant forms of TRPV4 caused obvious toxicity within 12 hours with characteristic pigmentation of the vegetal pole (Figure 33). This was observed in WT-expressing oocytes occasionally, but appeared more frequently and earlier in mutant-expressing oocytes. Overt oocyte cell death was witnessed at 48 hours for WT and mutants, but not water-injected oocytes. Although WT TRPV4 was toxic to the cells, this toxicity was much less than in mutants-transfected cells. Incubation of TRPV4-expressing oocytes in a Ca^{+2} -free solution prevented obvious cell toxicity. This toxicity was reversed when oocytes were exposed to ruthenium red (Figure 33).

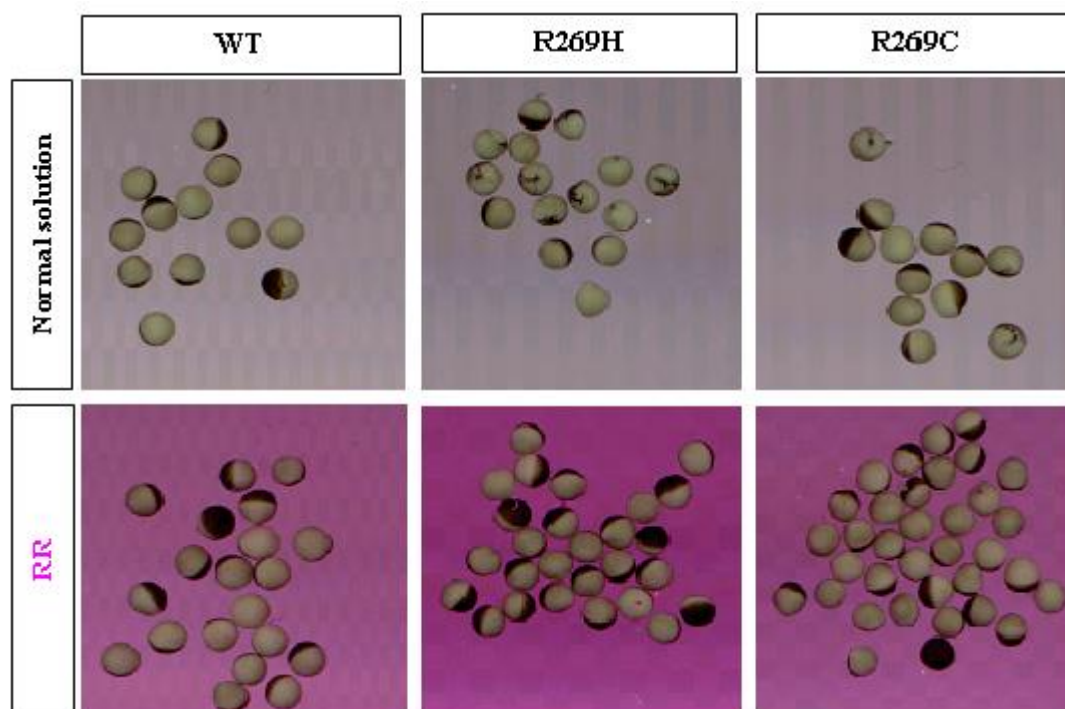


Figure 33 Mutant TRPV4 toxicity in *Xenopus* oocytes is blocked by ruthenium red. Note the characteristic black pigmentation (vegetale pole) in R269H and R269C transfected oocytes in normal solution but absent when oocytes are exposed to ruthenium red (RR).

3.3.3 Electrophysiology

Because TRPV4 is an ion channel, we wanted to evaluate the effect of R269C and R269H mutants in the channel function. As stated above, when we expressed TRPV4 in *Xenopus* oocytes incubated in normal frog's Ringer solution, mutant forms of TRPV4 caused obvious toxicity within 12 hours making electrophysiological studies difficult. We then incubated TRPV4-expressing oocytes in a Ca^{+2} -free solution that prevented obvious cell toxicity and thus subsequent electrophysiology experiments were therefore performed in Ca^{+2} -free solution. Whole cell currents measurement of oocytes expressing R269C and R269H TRPV4 showed a 2.5 fold increase in channel currents compared to WT under resting conditions (18 °C) (Figure 34a). Addition of ruthenium red at 10 μM significantly reduced wild-type, R269H and R269C currents by 53 %, 52 % and 48 %, respectively ($P < 0.05$). TRPV4 is a heat activated ion channel (Watanabe, Vriens et al. 2002). We measured heat-activated mutant and wild-type expressing oocytes and measured currents. In the heat-activated state (38 °C), both wild-type and mutant TRPV4 channel currents increased 2-3 fold above their constitutive levels, with mutant channel currents remaining 2-3 fold higher than wild-type (Figure 34a). It was also known that 4 α -phorbol didecanoate (4 α -PDD) is a specific agonist of TRPV4 (Watanabe, Davis et al. 2002). When the TRPV4 channels were activated by 4 α -PDD, currents were increased by 3.1 fold in mutant-expressing oocytes compared to WT expressing oocytes (Figure 34b & c). Increasing temperature in the oocytes pre-incubated with 4 α -PDD resulted in a further increase in channel activity (Figure 34b & c).

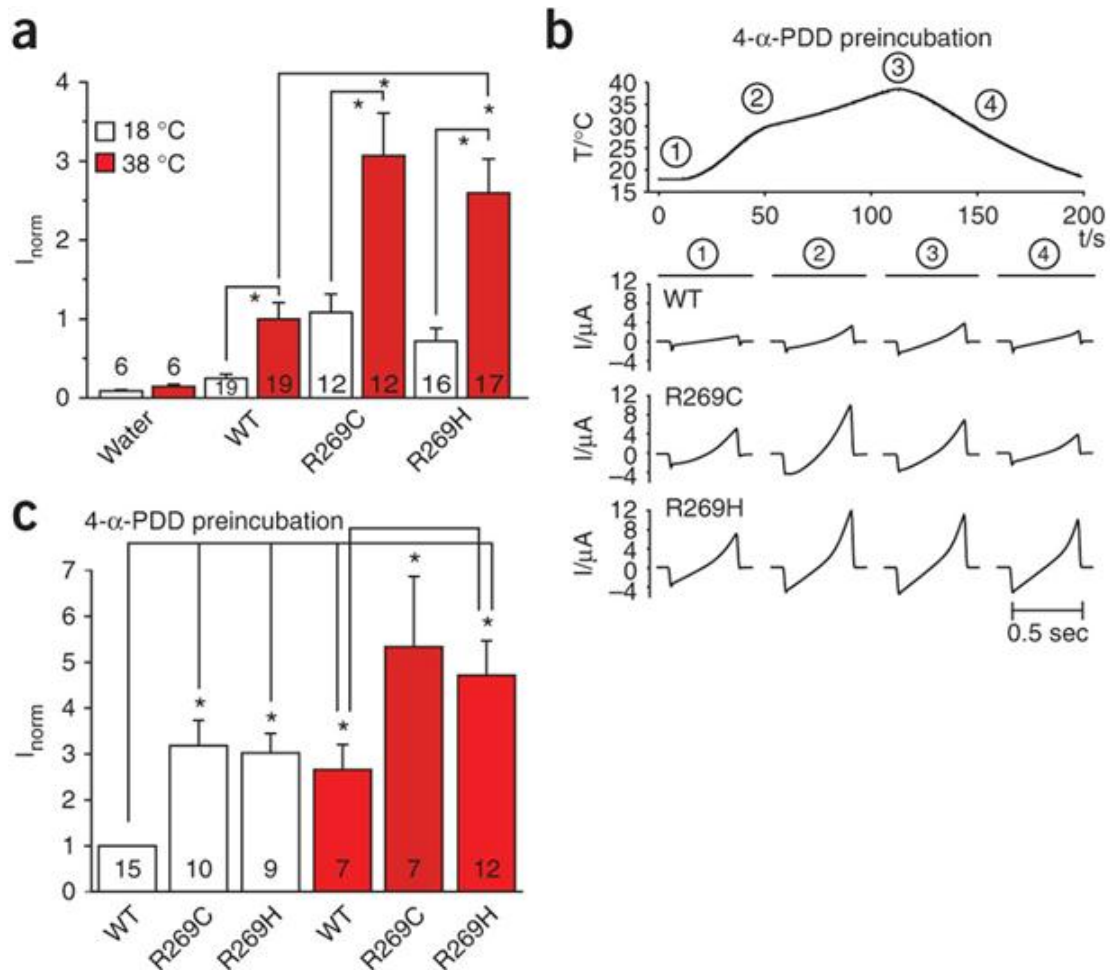


Figure 34 The R269C and R269H mutations cause increased TRPV4 channel activity in *Xenopus* oocytes.

a) Wild-type and mutant TRPV4 were expressed in *Xenopus* oocytes, and currents were measured at 18 °C and after heating to 38 °C. Currents obtained at -100 mV were normalized to currents in wild-type at 38 °C. Basal and stimulated channel activities of both mutants were significantly increased compared to wild-type ($P < 0.006$). Data are averaged from the number of experiments per condition shown in the columns; error bars, s.e.m. $*P < 0.006$. **b)** Representative current ramps obtained after preincubation in 5 μ M 4 α PDD (obtained from clamping cells from -100 to $+100$ mV in 500 ms). **c)** Summary of the data obtained in b. Currents obtained at -100 mV were normalized to wild-type at 18 °C. $*P < 0.05$.

To confirm these electrophysiological results in mammalian cells, we transfected HEK 293 cells with human wild-type and mutants TRPV4 constructs. As seen in *Xenopus* oocytes, higher basal currents were observed in HEK293 cells transfected with R269C or R269H mutants as compared to wild type (Figure 35). Here also, HEK

293 cells were activated by 4 α -PDD before currents measurement, and enhanced responses were observed in R269C and R269H expressing cells. Hypotonicity was also shown to activate TRPV4 channel (Liedtke, Choe et al. 2000). In addition to using 4- α -PDD to activate mutants and wild-type expressing HEK 293 cells, we used hypotonic stimulation, and saw greater currents in mutants TRPV4 expressing cells as compared to wild-type.

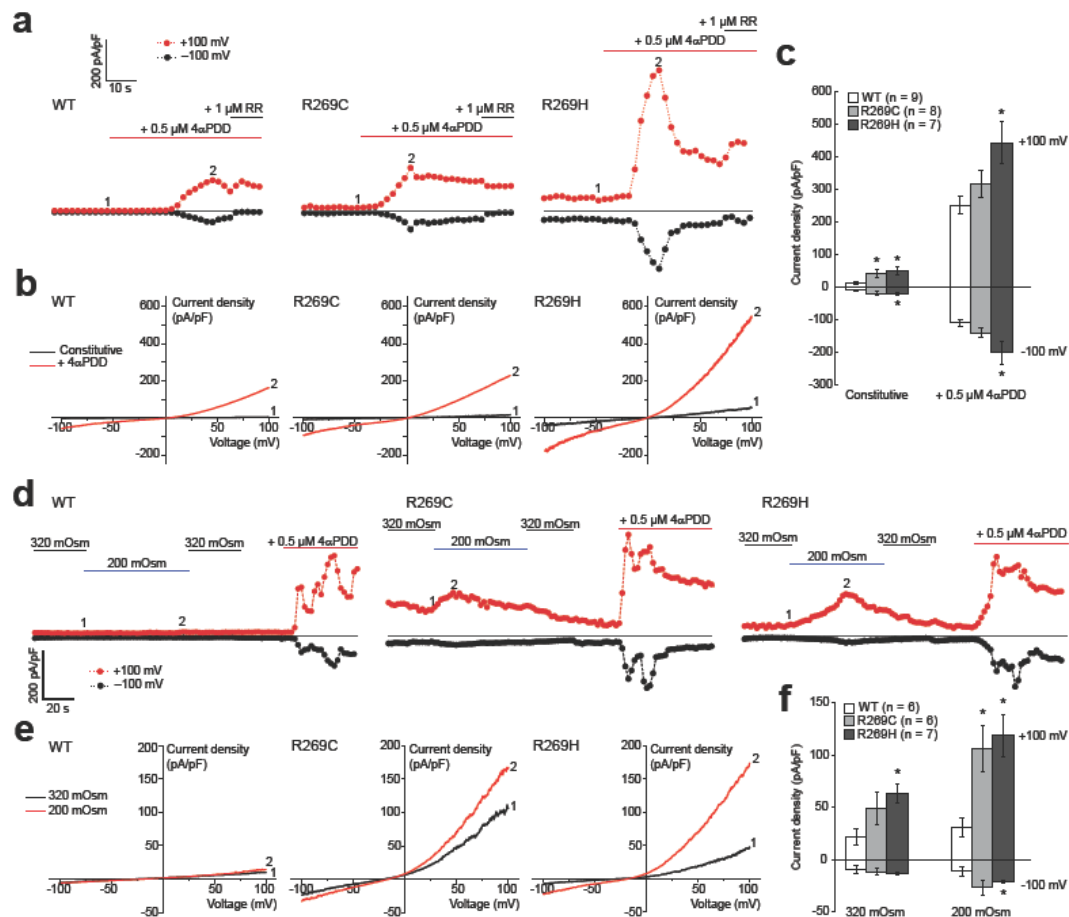


Figure 35 The R269C and R269H mutants cause increased TRPV4 channel activity in HEK293 cells.

Constitutive, 4 α PDD-, and hypotonicity-activated currents in HEK293 cells expressing R269C or R269H TRPV4 are higher than in wildtype. **a**) Time courses showing constitutive currents, stimulation with 4 α PDD (red bar) and inhibition with ruthenium red (RR; black bar). Reductions of >50% are observed in -100 mV currents before and after RR application (WT, 50%; R269C, 53%; R269H, 64%; all are significant $p < 0.05$). **b**) Current-voltage relationship of constitutive (1) and 4 α PDD-activated (2) currents from time courses in (a). **c**) Summarized data from constitutive

and 4 α PDD-activated currents. R269C showed greater variability in current values and a trend to larger currents than WT TRPV4. **d)** Time courses showing constitutive currents, stimulation with hypotonic solution (200 mOsm, blue bar), and 4 α PDD (red bar). **e)** Current-voltage relationship of constitutive (1) and hypotonicity-activated (2) currents from time courses in (d). **f)** Summarized data from constitutive and hypotonicity-activated currents. In (a) and (d), currents at -100 (black) and $+100$ mV (red) were obtained from voltage ramps applied every 2 s. In (c) and (f), means \pm s.e.m are shown and compared with WT values (*, $p < 0.05$; number of cells (n) in legend). For (d-f), whole-cell configuration was established in standard extracellular solution, then exchanged to 320 mOsm solution, which has the ionic strength of 200 mOsm solution but osmolality of standard solution, causing a negative shift of junction potential (-12.6 ± 0.3 and -16.0 ± 0.2 mV in 320 and 200 mOsm solutions, respectively (n=5)), and negative shift of reversal potential in (e). Untransfected HEK293 cells show endogenous volume-regulated anion channel (VRAC) activity, which develops and recovers slowly (several minutes) and is down-regulated by TRPV4 over-expression (1). To minimize possible contamination by remaining VRAC activity, hypotonic stimulation was limited to 60 sec and TRPV4 expression was confirmed by 4 α PDD stimulation.

3.3.4 Cell calcium measurement

As Ca^{2+} -permeable channel, TRPV4 hyperactivation would lead to cell Ca^{2+} overload and cause cell death. In fact, studies have associated TRPV4 hyperactivity to intracellular calcium increase (Krakow, Vriens et al. 2009). We therefore performed calcium measurement using two techniques. Intracellular calcium levels were elevated in the mutant TRPV4 compared to the WT (Figure 36a & b). This calcium uptake caused by the *TRPV4* mutations was inhibited by the inactivating pore domain mutation, M680K, and by the TRPV4 specific blocker, RN1734 (Figure 36a & c).

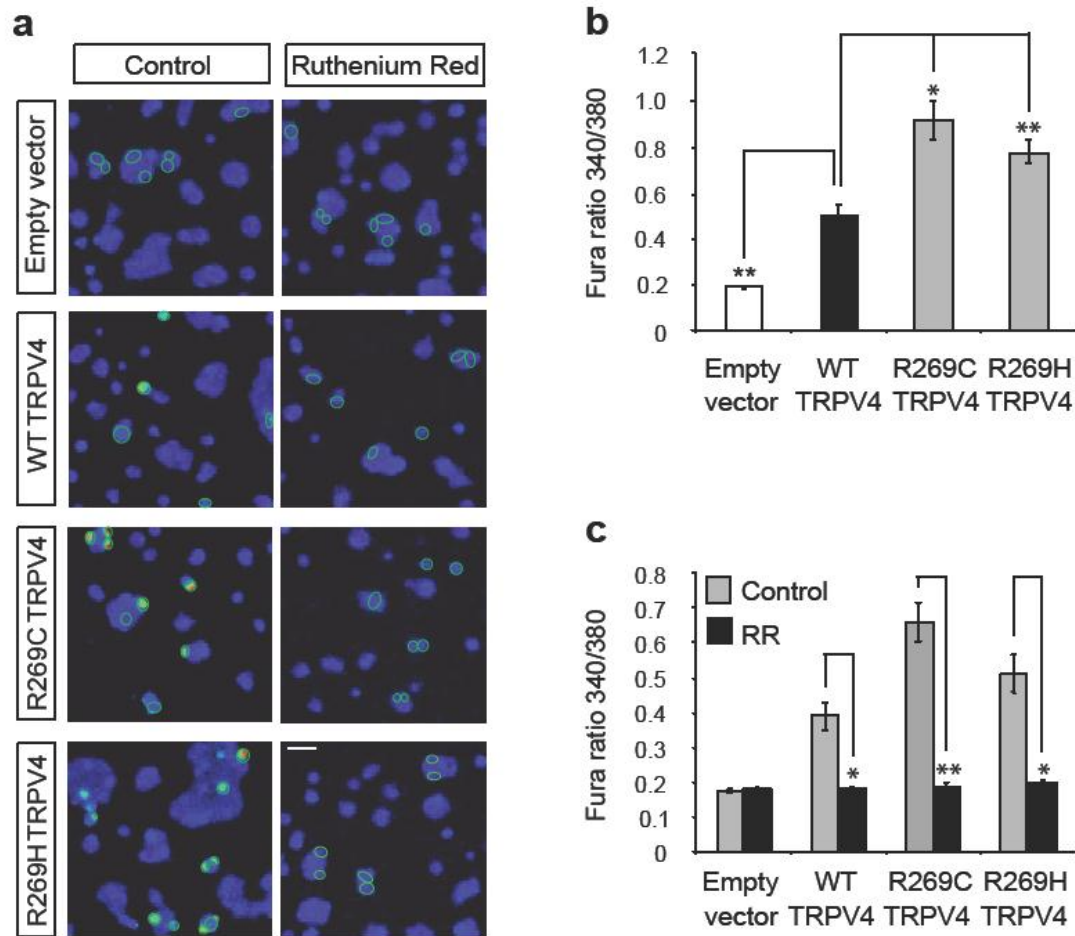


Figure 36 HEK293 cells expressing mutant TRPV4 have higher basal calcium levels than WT expressing cells.

a) Representative images of transfected HEK293 cells (circled) loaded with the fluorescent calcium indicator, Fura 2. Transfected cells were identified by their expression of the fluorescent marker mCherry. Under basal conditions, when cells were perfused with standard extracellular buffer, TRPV4- transfected cells had elevated intracellular calcium concentrations, as demonstrated by an increased Fura ratio. Furthermore, cells expressing the mutant TRPV4 channels, R269C and R269H, had higher levels of intracellular calcium when compared to cells transfected with WT TRPV4. When transfected cells were incubated in the presence of 10 μ M of the TRP channel blocker ruthenium red (RR), the TRPV4-mediated increase in calcium concentration was blocked. Scale bar = 50 μ m. b) Quantification of baseline Fura ratios in TRPV4- or vector-transfected HEK293 cells. $n = 7-10$ coverslips from three independent transfections. c) Quantification of baseline Fura ratios in the presence or absence of ruthenium red. $n = 5$ coverslips. Error bars s.e.m. * $p < 0.01$, ** $p < 0.001$.

3.3.5 Chicken TRPV4-ARD structure determination

This was performed using data collection and refinement statistics in the table below (Table 7). The 2.3-Å crystal structure of the chicken Trpv4 ankyrin repeat domain (ARD) (Figure 37) shows a typical hand-shaped structure with a concave palm surface formed by inner helices and fingers and a convex surface representing the back of the hand. Arg269 is located at the base of finger 3 on the convex surface. In addition, the Arg269 residue side chain is exposed and well positioned to mediate protein-protein interactions that may be critical to TRPV4 function.

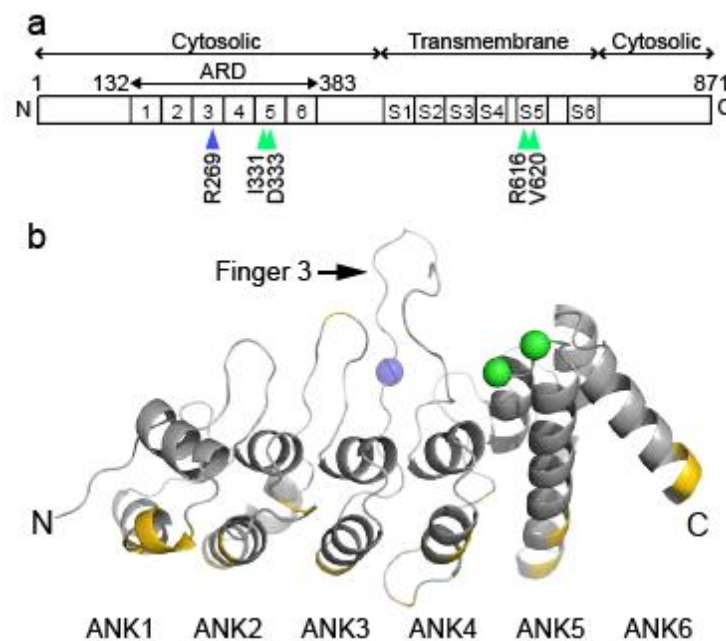


Figure 37 Localization of CMT2C and skeletal dysplasia TRPV4 mutations in the chicken Trpv4 ankyrin repeat domain crystal structure.

The R269C and R269H substitutions are located in the ankyrin repeat domain (ARD) of the TRPV4 protein. a) Primary structure of the TRPV4 protein, with the positions of the CMT2C-associated (Arg269; blue arrowhead) and skeletal dysplasia-associated (Krakow, Vriens et al. 2009) (green arrowheads) mutations indicated below. b) Ribbon diagram of the chicken Trpv4 ARD, with the location of the Arg269 residue (Arg255 in chicken sequence) depicted as a blue sphere and the Ile331 and Asp333 residues (Ile317 and Asp319 in chicken sequence, respectively) previously shown to be mutated in skeletal dysplasia as green spheres.

3.3.6 Protein binding assays and co-immunoprecipitation

One study has shown that PACSINs (1, 2, and 3) bind to TRPV4, and that PACSIN 3 affects the endocytosis of TRPV4 (Cuajungco, Grimm et al. 2006). Therefore, we completed co-immunoprecipitation studies with wild-type and mutant TRPV4. HEK293 cells were co-transfected with PACSIN1, PACSIN2, or PACSIN3 and either FLAG-WT TRPV4, FLAG-R269C TRPV4, FLAG-R269H TRPV4. After immunoprecipitation (IP) using anti-FLAG antibody, bound proteins were separated by SDS-PAGE and analyzed by immunoblotting with antibodies to PACSIN1, 2, or 3. The TRPV4 IP was verified by immunoblotting with anti-FLAG antibody. We found that there is no change in interaction between all PACSINs and mutant TRPV4 (Figure 38a, b & c).

Another study has shown TRPV4 interaction with calmodulin through its ARD (Phelps, Wang et al. 2010). We performed binding assays, and found no disruption in interaction between calmodulin and CMT2C mutant TRPV4 compared to skeletal dysplasias mutant TRPV4 or wild-type TRPV4 (Figure 38d).

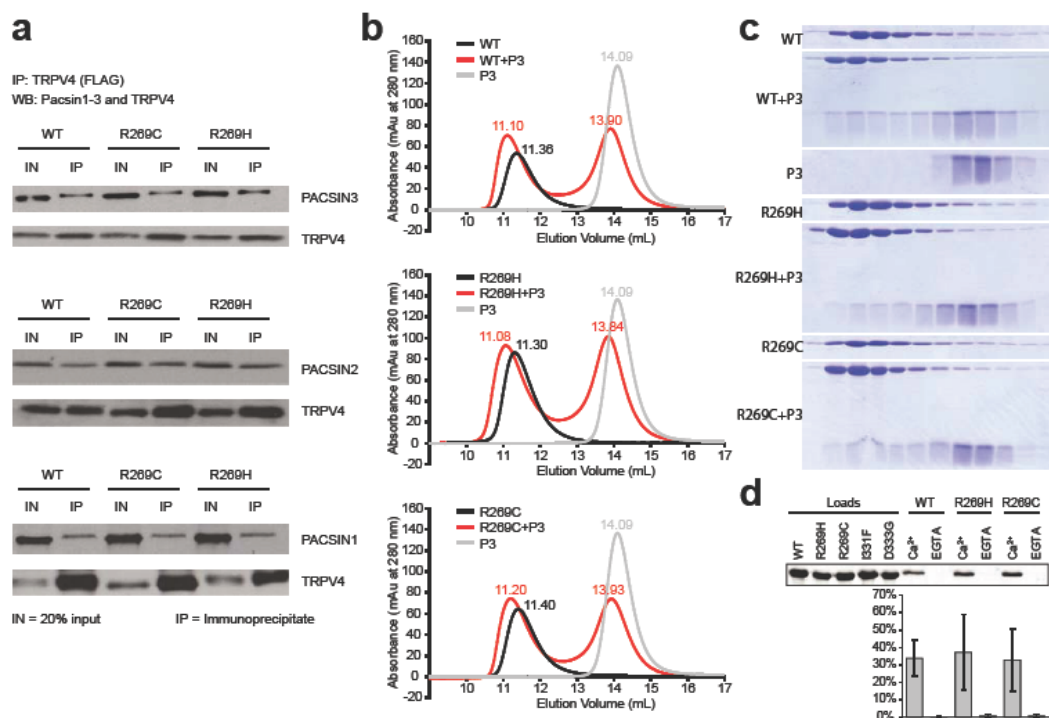


Figure 38 The CMT2C TRPV4 mutations do not influence TRPV4 interaction with PACSINs 1-3 or Ca²⁺-calmodulin.

a) The CMT2C mutations do not reduce co-immunoprecipitation of TRPV4 with PACSINs1-3. (b,c) Interactions of isolated TRPV4-ARD with the isolated PACSIN3 SH3 are unchanged by CMT2C mutations. b) Representative size exclusion

chromatography traces of PACSIN3 SH3 domain alone (grey; the same trace is shown on all graphs for reference), HsTRPV4-ARD alone (black) or the HsTRPV4-ARD/PACSIN3-SH3 mixture (red). Elution volumes for each peak are indicated. Traces are representatives of at least two experiments. c) Coomassie-stained SDS-PAGE gels of the elution fractions (elution volumes 10.1 to 16.1 ml) of the chromatography experiments shown in (b). d) Coomassie-stained gel shows wildtype and mutant TRPV4-ARD loaded (left) and bound to calmodulin-agarose in the presence of Ca^{2+} or EGTA. The normalized amount of protein recovered (average \pm standard deviation) is plotted below, from three independent experiments, showing no significant differences between WT and the mutants.

4 Discussion

4.1 Clinical and laboratory findings

Patients with CMT2C present with axonal-type features with high variability in age of onset and disease course.

CMT2C is a peripheral neuropathy characterized by distal muscle wasting and weakness, mild sensory impairment and prominent vocal fold and diaphragm involvement (Dyck, Litchy et al. 1994). We report five families presenting with clinical, electrophysiological and laryngoscopical features of CMT2C including distal more than proximal limb muscle weakness and atrophy, sensory loss, reduced to absent tendon reflexes, and laryngeal and diaphragmatic muscles weakness. In addition to these previously described findings, sensorineural hearing loss and urinary incontinence were observed in many patients in families F1, F2 and F3. However, sensorineural hearing loss and urinary incontinence were not reported in any patient of families F4 and F5. Moreover family F4 showed subtle or no sensory involvement and no diaphragmatic involvement during NCS; suggesting that these two families may be different clinical entities or manifesting the variability seen in the CMT2C sub-type.

Ages of disease onset were highly variable, ranging from 1 to 53 years. Although the variability in the age of onset and disease severity seen in this study is seen in other types of CMT patients, this pattern seems to occur frequently in CMT2C. Other studies also emphasized the variability in the disease progression and expression as a key feature of CMT2C (Dyck, Litchy et al. 1994). This variability between generations does not reflect the anticipation pattern seen in nucleotide repeat disorders like polyglutamine diseases or fragile X or myotonic dystrophy because some patients in the younger generations (family F1 V.8) appeared to be less affected than their parents (family F1 IV.3). Two patients did not report any symptoms. The first patient, a 71-year old mother of three affected sibs was found to have absent tendon reflexes throughout, and mild husky voice when evaluated at 53 years. The second patient (Family F1, V.2) is a son of an affected woman and brother of two affected young ladies. He was not complaining of any symptom related to CMT2C. When examined he had hammer toes and slight pes cavus, reflexes were absent in ankle and reduced in

knees, and vibration sense was slightly decreased in lower limbs. Although NCS and laryngological studies were not performed, he was found to have the TRPV4 mutation running in his family.

His cousin (Family F1, V.8), although suffering from early laryngeal muscle paralysis, showed few signs when examined 18 years later, suggesting that the disease may be generally milder in men or supporting the characteristic clinical variability seen in previously reported CMT2C families. Other CMT2C studies reported individuals with no complaints, but were found to be affected during clinical examination. Dyck P. J. *et al.* (Dyck, Litchy *et al.* 1994) reported an 80 year-old female with no complaints but who had weakness and atrophy in hand, legs and feet, and decreased to absent reflexes on examination. She also manifested hoarse voice at times after lengthy talk. In addition her NCS was abnormal.

On the opposite side, a 54-year old male (Family F3, III.5), although having no major complaints, was suspected to be affected because his medical history was consistent with long standing high arches, cramps and fasciculations in calves, and recently sleep apnoea for which he is seeing a doctor. Moreover, his neurological examination revealed subtle distal sensory loss, and chest X-rays showed hemidiaphragm paralysis while NCS, especially the phrenic nerve, and EMG did not reveal any sign of chronic neuropathy but median nerve entrapment, making the diaphragmatic paralysis unlikely to be of neurodegenerative origin. Although these findings are subtle, there was still a possibility that he may be affected, but, as discussed below, he did not have mutation in the TRPV4 gene as his affected family members.

The clinical and electrophysiological examination of the youngest patient in family F1 showed little signs of worsening since his first months of life. This is consistent with results from some studies which report that some patients with CMT stabilize over years (Pareyson, Scaiola *et al.* 2006).

Vocal fold and diaphragm paralysis are characteristic and most common features in CMT 2C patients.

Stridor, breathing difficulties on exertion, and hoarseness of voice were the most frequent initial and predominant symptoms and were present in almost all patients. But, ultimately, all these symptoms were present at the late stage of their disease. Laryngeal paralysis primarily involving abductor muscles (opening) leads to air obstruction that manifests symptomatically by stridor (Holinger, Vuckovich *et al.*

1979; Young and Harper 1980). On the other hand, laryngeal paralysis involving adductor muscles (closing) leads to breathing difficulties and risk for aspiration (Mace, Williamson et al. 1978; Pridmore, Baraitser et al. 1992), and hoarseness of voice. Although breathing difficulties can be due to laryngeal adductor muscles paralysis, diaphragmatic and intercostal muscles paralysis seen in this disease can also cause this symptom. Another symptom that may cause breathing difficulties is severe thoracic deformity that may be seen in CMT patients.

Although an unusual clinical feature, vocal fold paralysis has been described in other hereditary motor and sensory neuropathy sub-types. Axonal neuropathies caused by mutations in the *GDAP1* gene (CMT4A and CMT2K) are associated with vocal fold paralysis (Baxter, Ben Othmane et al. 2002; Cuesta, Pedrola et al. 2002; Birouk, Azzedine et al. 2003; Stojkovic, Latour et al. 2004). These CMT sub-types, unlike CMT2C, are autosomal recessive, although some CMT2K cases are autosomal dominantly inherited (Chung, Kim et al. 2008). Symptoms linked to vocal fold paralysis were also reported in some demyelinating CMT sub-types, including CMT1A, CMT2A2, HNPP-PMP22, and CMT1D (Thomas, Marques et al. 1997; Pareyson, Taroni et al. 2000).

But in all these CMT variants, symptoms related to vocal fold paralysis appear in few patients only whereas in CMT2C vocal fold paralysis is a central clinical feature present in all patients. In addition, symptoms are not limited to hoarseness of voice, albeit respiratory difficulties appeared in the third decade in some families (Stojkovic, Latour et al. 2004). Except in two of these families (Azzedine, Bolino et al. 2003; Stojkovic, Latour et al. 2004), diaphragm paralysis was not associated with these diseases, and in one of them the diaphragm paralysis was not symptomatic. Sensorineural hearing loss was reported in several patients in these diseases but urinary incontinence was absent.

Stridor and breathing difficulties were reported in other hereditary neurological disorders. In distal spinal and bulbar motor neuropathy (dSBMA) caused by mutations in the *Dynactin 1* (DCTN1) gene (Puls, Jonnakuty et al. 2003; Puls, Oh et al. 2005), stridor and breathing difficulties are first and predominant symptoms. However, CMT2C and dSBMA have several clinical and laboratory differences. Distal spinal and bulbar muscular atrophy is an autosomal dominant hereditary motor neuropathy in which the disease starts later, ranging from 23 to 39 years. Although ages of onset are highly variable in CMT2C, in most cases the disease starts within the first decade.

In dSBMA, limb weakness starts with hands, and lower limbs are usually affected several years later. While bulbar involvement is a prominent symptom in dSBMA, only one patient in the families studied here, the most affected, presented with subtle facial weakness. In addition, there is no sensory loss in dSBMA, nor were reported diaphragm paralysis, bilateral hearing loss or urinary incontinence.

Dyspnoea on effort and hoarseness of voice were reported in another large kindred affected with distal motor neuropathy (HMN7A) (Young and Harper 1980). In this family, the disease usually started with hand weakness, and progressed to lower limbs years later. Laryngeal symptoms appeared later in the disease course, but in some cases they preceded limb weakness. The gene for this disease was mapped to chromosome 2q14 (McEntagart, Norton et al. 2001), but the disease-causing gene is still not identified. Although CMT2C and HMN7A share some clinical features, there is no urinary incontinence in HMN7A, and sensation is normal.

Patients with CMT2C, like in most CMT variants, have normal life expectancy. But these symptoms, air obstruction and breathing difficulties, are potentially life-threatening, and shorten patients' life expectancy. In fact, a 46-year old patient in family F1 has died of respiratory failure whereas her 77-year old affected mother who has less laryngeal muscle paralysis is still alive. This shortened life expectancy was also seen in other neurological diseases with vocal fold involvement discussed above (Puls, Oh et al. 2005). Patients with severe respiratory difficulties underwent surgery. Tracheostomy was performed in few of them after they lived a better life. Vocal fold tie back or arytenoidectomy were usually performed to liberate air way. This procedure was beneficial to all it was performed on. In fact one of our patients who underwent surgery was playing French horn when we last saw him, 17 years after his surgery.

Limb weakness and atrophy, and not facial involvement, are also common signs in CMT 2C.

Foot weakness and walking difficulties were the second most reported symptoms in the families we investigate here. One patient who had noisy breathing within his first year of life presented minimal foot weakness when evaluated at age 18. In the classical CMT presentation, foot weakness and walking difficulties are first and most common symptoms. However, in some CMT sub-types, including the autosomal dominant CMT2D due to the *GARS* gene mutation, symptoms start with hand

weakness. As in the classical CMT presentation, distal lower limb weakness worsened over time in the patients described here, and upper limbs became affected later in the disease course. Skeletal deformities consistent with pes cavus, hammer toes, and scoliosis were reported in several patients, mostly in patients with very early onset. However, some patients with early onset presented mild or no skeletal deformities, supporting the variability in the disease severity in this disease. These symptoms are characteristic of the classical CMTs, and inversely correlated to the age of disease onset.

Several patients reported worsening of muscle weakness in the cold (“cold paralysis”), which is an intriguing symptom given that TRPV4 is known to be activated by increased temperature.

This symptom could relate to motor neuronal function or possibly to abnormalities of vasoregulation known to be controlled in part by TRPV4.

Sensory loss is a characteristic feature of CMT. Almost all patients studied here presented with some sensory loss. While most patients had minimal sensory loss, few had mild to moderate sensory loss, and only one was moderately affected. Two patients in family F1 had no sensory loss. In general, sensory loss seen in the classical CMT is more pronounced than what we have seen in the patients studied here, and decreased or absent vibration sense was the predominant sensory loss.

Facial weakness, seen in some previous CMT 2C reports (Dyck, Litchy et al. 1994), was not apparent in our study; except in the most affected patient in family F1 (IV.4) who presented minimal facial weakness. Although rarely seen in CMT cases, facial weakness was reported in some CMT variants such as CMT 4G (Rogers, Chandler et al. 2000). But it is in dSBMA that facial weakness represents a characteristic feature present in all patients (Puls, Oh et al. 2005).

Patients with CMT2C also present with sensorineural hearing loss and urinary incontinence.

Several patients from three families studied here had hearing loss and urinary incontinence. The hearing loss was documented by ENT examination, and showed that patients with hearing impairment had a bilateral sensorineural hearing loss. These are distinctive features since there were not reported in previous CMT2C reports (Dyck, Litchy et al. 1994; Donaghy and Kennett 1999; Santoro, Manganelli et al.

2002; McEntagart, Reid et al. 2005). Hearing loss can be due to the auditory nerve dysfunction secondary to the degeneration of all peripheral nerves as it is reported in several CMT sub-types (CMT1D, CMT1E, CMT2E/CMT1F, CMT1X, CMT2A2, and HMSNIV). But in CMT2C, this symptom may also relate to TRPV4 dysfunction because TRPV4 has been shown to express in hair cells, spiral ganglion, and stria vascularis in the cochlea (Liedtke, Choe et al. 2000). In these tissues, TRPV4 may be involved in transduction of acoustic stimuli (Kim, Chung et al. 2003; Mutai and Heller 2003; Nilius, Vriens et al. 2004). Moreover, *TRPV4* knockout mouse have bilateral sensorineural hearing loss (Suzuki, Mizuno et al. 2003). Urinary incontinence was not reported in other CMT variants. Thomas P. K. *et al.* (Thomas, Marques et al. 1997) have reported CMT1A patients with weakness of the pelvic floor muscles resulting in faecal incontinence. However, there was no urinary incontinence, and none of the patients studied here reported faecal incontinence.

Some patients presented unilateral hearing loss, and audiological examination showed features consistent with tympanic injury or other causes unrelated to their neurological disease.

Urinary incontinence is also likely secondary to TRPV4 dysfunction as TRPV4 is expressed in bladder epithelium (Yamada, Ugawa et al. 2009). Studies have suggested that TRPV4 may play a role in sensing of bladder pressures (Gevaert, Vriens et al. 2007). In addition, impairments of bladder voiding was shown in the knockout mouse (Suzuki, Mizuno et al. 2003; Tabuchi, Suzuki et al. 2005; Gevaert, Vriens et al. 2007).

Electrophysiological studies in CMT 2C patients show axonal-type findings with often phrenic nerve involvement.

NCS were consistent with an axonal-type involvement. Motor and sensory, conduction velocities were normal, especially the median nerve (>38 m/s) whereas compound motor action potentials were low. This was in contrast with demyelinating-type CMT in which conduction velocities were generally low. However, in some mildly affected patients, NCS were normal or minimally disturbed. This is another distinctive feature of CMT1 because in this form of CMT NCS show almost always abnormalities, and can appear years before first symptoms appear (Pareyson, Scaiola et al. 2006). The peroneal nerve was the most affected consistent with the CMT distribution; which was first called peroneal muscular atrophy. One patient had prolonged distal latency and slow conduction velocity with normal amplitude of the

left median motor and sensory nerve, respectively. This pattern is not characteristic of CMT2. Her medical history revealed symptoms in her left hand consistent with a median nerve entrapment explaining the NCS results in that side. Phrenic nerve involvement was seen in all but one affected patients in families F1, F2, and F3. In addition to the slight phenotypic difference, NCS of some patients in family F4 was not quite typical of what is seen in CMT2C. In fact, NCS in family F4, although raised the possibility of an increased susceptibility to physical injury such as seen in more diffuse polyneuropathies, was significant for the presence of bilateral asymmetric and probably of a different nature peroneal nerve abnormalities; which could be supportive of bilateral focal peroneal nerve lesions. In addition, NCS family F4 did not show phrenic involvement. All these together may raise the possibility of family F4 being a different peripheral neuropathy entity, at least from CMT2C. In family F5, though, phrenic nerve compound motor action potentials (CMAPs) were not recorded. Phrenic nerve involvement was reported in other CMT variants (CMT1E, and CMT4A) (Sevilla, Cuesta et al. 2003), but no symptoms related to phrenic nerve dysfunction were seen albeit abnormal NCS. Stojkovic *et al.* (Stojkovic, Latour et al. 2004) reported two affected individuals with hemi-diaphragm paralysis but phrenic nerve action potentials were not recorded. EMG showed muscle membrane instability and motor unit remodelling even in the mildly affected individuals suggesting a chronic muscle denervation and reinnervation.

Quantitative sensory testing performed in one patient showed a decrement in CMAP after cooling. This pattern is suggestive of a channelopathy consistent with the genetic and electrophysiological findings discussed below.

Vocal fold paralysis in CMT 2C shows a length-dependent pattern with left muscles being more affected in the beginning of the disease.

Laryngoscopy was done in few of our patients, and showed laryngeal muscles paralysis with the left laryngeal muscles being more affected. In patients evaluated at earlier stage of their disease, left laryngeal muscles were only affected. This pattern of vocal fold paralysis evolution was seen in the previously reported CMT2C families (Dyck, Litchy et al. 1994; Donaghy and Kennett 1999; Santoro, Manganelli et al. 2002; McEntagart, Reid et al. 2005). The presence of bilateral laryngeal muscle paralysis of both abductor and adductor muscles could explain the stridor and hoarseness of voice present in these patients, except in family F4 where only abductor

muscle paralysis was seen. CMT2C is a length-dependent axonal neuropathy. In neurodegenerative diseases in which symptoms appear in length-dependent pattern, muscles innervated by longer nerves appear to be first affected. Therefore, left laryngeal muscles were often first paralyzed because the left recurrent nerve, which innervates those muscles, is longer than the right side nerve. This pattern of left laryngeal muscles being more affected than the right ones at the early stage of the disease is seen in other neurodegenerative diseases, including the distal hereditary motor neuropathy (HMN7A) (Young and Harper 1980). However, in the distal spinal and bulbar muscular atrophy (dSBMA) (Puls, Oh et al. 2005), there is an early bilateral laryngeal paralysis.

Vocal fold paralysis is seen in other CMT sub-types, including CMT2K, CMT4A, CMT1A, CMT2A2, HNPP-PMP22, and CMT1D, but this symptom appears in few patients only whereas in CMT2C vocal fold paralysis is a core symptom present in all patients, and sometimes is the only symptom. In addition, vocal fold paralysis is unilateral and rarely involves both sides.

CMT2C patients show skeletal deformities and diaphragm paralysis.

Spinal radiographs showed skeletal deformities in some patients. This symptom appears generally in CMT patients with early onset. However, not all patients who presented symptoms at early age had spinal deformity; supporting the clinical variability seen in this disease. However there were no bone morphology or density abnormalities. Chest X-rays showed asymmetric diaphragm in few patients due to the phrenic nerve paralysis. This symptom is common in CMT2C families as it was reported in previous studies (Dyck, Litchy et al. 1994; Santoro, Manganelli et al. 2002). Other hereditary neurological disorders including the autosomal recessive CMT 2 due to the *GDAP1* gene reported this symptom in two patients (Azzedine, Bolino et al. 2003; Stojkovic, Latour et al. 2004).

Mutations in TRPV4 were shown to cause bone diseases including autosomal dominant Brachyolmia and Spondylometaphyseal Dysplasia, Kozlowski Type (SMDK) and Metatropic Dysplasia (Rock, Prenen et al. 2008; Krakow, Vriens et al. 2009). Others have later reported TRPV4 mutations in skeletal dysplasias families (Camacho, Krakow et al. 2010).

The brachyolmias are a heterogeneous group of skeletal dysplasias of unknown aetiology that primarily affect the spine. At least three types of brachyolmia have been described (Shohat, Lachman et al. 1989) with different pattern of inheritance. The Type 1 (Hobaek and Toledo forms) and Type 2 (Maroteaux type) brachyolmias are inherited in an autosomal recessive fashion (Fontaine, Maroteaux et al. 1975; Toledo, Mourao et al. 1978; Horton, Langer et al. 1983; Shohat, Lachman et al. 1989). Type 1 brachyolmia forms are characterized by scoliosis, platyspondyly with rectangular and elongated vertebral bodies, overfaced pedicles and irregular, narrow intervertebral spaces. In addition, the Toledo form has characteristic features such as corneal opacities and precocious calcification of the costal cartilage. Type 2 brachyolmia is distinct from type 1 by rounded vertebral bodies and less overfaced pedicles. Type 3 brachyolmia is an autosomal dominant form with severe kyphoscoliosis and flattened, irregular cervical vertebrae (Gardner and Beighton 1994). SMDK is primarily characterized by postnatal short stature and significant kyphoscoliosis leading to progressive deformity. Other clinical findings include normal facies, a short neck, pectus carinatum, and genu varus (Nural, Diren et al. 2006). The radiographic phenotype includes odontoid hypoplasia, platyspondyly with vertebral bodies described as resembling an “open staircase,” overfaced vertebral pedicles, short square ilia, flat acetabular roofs, wide proximal femoral epiphyseal plates, metaphyseal irregularities, and markedly delayed carpal bone ossification (Lachman 2007).

First described in 1966 (Maroteaux, Spranger et al. 1966), metatropic dysplasia often present with shortened limbs and a long, narrow trunk in the newborn period that evolves into a severe, progressive kyphoscoliosis (Leet, Sampath et al. 2006). Affected individuals have a distinctive facies with a prominent forehead and squared-off jaw (Kannu, Aftimos et al. 2007). The radiographic findings in metatropic dysplasia are characteristic and include wafer-like vertebral bodies in newborns, a halberd-shaped pelvis, irregular calcanei and tali, brachydactyly with delayed carpal ossification, and flared or “mushroomed” proximal and distal metaphyses of the femora leading to a “dumbbell-shaped bone” (Lachman 2007). Cervical myelopathy, and stenosis leading to significant neurologic sequelae were reported in metatropic dysplasia patients (Shohat, Lachman et al. 1989; Leet, Sampath et al. 2006), but these result in symptoms consistent with upper motor neurons involvement that clinically differ to peripheral neuropathy. Although some CMT sub-types present with

pyramidal signs, these were not reported in the families we studied here or in the other CMT2C families described elsewhere. Interestingly, some of these patients present with respiratory difficulties and sensorineural deafness (Kannu, Aftimos et al. 2007; Genevieve, Le Merrer et al. 2008). These symptoms are also seen in CMT2C patients but the physiopathology, at least for the breathing difficulties, may be different. The respiratory difficulties in metatropic dysplasia are due to the kyphoscoliosis and narrowed thorax whereas in CMT2C this symptom result from diaphragmatic and/or the accessory respiratory muscles paralysis. In CMT2C hearing loss occurs probably because of intrinsic auditory nerve degeneration while in metatropic dysplasia it may be due to stapedial bone deformity compressing the acoustic nerve. However, both can have the same physiopathology because of the expression of TRPV4 in hair cells. No bone deformities or cartilage abnormalities comparable to those seen in brachyolmia and other skeletal dysplasias caused by TRPV4 mutations (Rock, Prenen et al. 2008; Krakow, Vriens et al. 2009) were seen in the patients we studied here. Skeletal deformities seen in CMT families including the ones studied here are not due to abnormal bone morphology; rather they are due to muscle weakness that fails to sustain joints. Nonetheless, there is a possibility of overlap between these two entities as shown in two studies that reported cases of CMT2-type peripheral neuropathy associated with skeletal dysplasia-type symptoms (Chen, Sul et al. 2010; Zimon, Baets et al. 2010).

The mutation identified in this single case was reported to cause autosomal dominant brachyolmia (V620I) (Rock, Prenen et al. 2008). This residue lies on the pore domain of TRPV4, where most of the brachyolmia and spondylometaphyseal dysplasia, Kozlowski type (SMDK) and Metatropic Dysplasia mutations clustered. In addition, a recent study reported two CMT2C families with short stature in which they identified TRPV4 mutations. Interestingly, the family with mild neuropathy and pronounced short stature had mutation in the pore domain of TRPV4 (S542Y) while the family with severe neuropathy and less remarkable short stature had a mutation in the ankyrin repeat domain (R315W) (Chen, Sul et al. 2010). The latter mutation was also previously reported in a CMT2C family (Auer-Grumbach M., 2010).

Mutations in TRPV4 were described in other neurological disorders including congenital distal spinal muscular atrophy (SMA) and scapulo-peroneal SMA (SPSMA) in two independent studies (Auer-Grumbach, Olschewski et al. 2010; Deng,

Klein et al. 2010). Although these disorders share some features with CMT2C, these neuropathies are phenotypically different. Congenital distal SMA is characterized by more proximal than distal muscle weakness and atrophy with minimal or no sensory symptoms. However, laryngeal muscle and diaphragm involvement are not features seen in congenital distal SMA, although some studies reported congenital SMA with diaphragm paralysis (Bertini, Gadisseux et al. 1989). SPSMA is characterized by a scapulo-peroneal distribution of weakness and atrophy, congenital absence of muscles, and laryngeal palsy as seen in CMT2C. The latter symptom is a characteristic feature that is present in all CMT2C patients, while congenital absence of muscles, specifically the deltoid, was reported in only few patients (Dyck, Litchy et al. 1994; McEntagart, Reid et al. 2005). None of our patients reported congenital absence of muscles.

But, urinary incontinence and hearing loss were not reported in these diseases.

How do mutations in the same gene causes defects in different selected parts of the nervous system needs to be addressed in future studies.

4.2 Genetic analysis

CMT 2C is genetically heterogeneous

The gene for CMT2C was mapped to chromosome 12q23-24 (Klein, Cunningham et al. 2003), and this locus was later confirmed and narrowed by another study (McEntagart, Reid et al. 2005). The genetic analysis of families studied here also found evidence for linkage in this locus with a cumulative LOD score of about 10. By combining linkage data from all families we were able to reduce the region of interest from 3.9 Mb to 2.6 Mb.

From the haplotype reconstruction it appears that all the affected individuals in families F1, F2, and F4 have the disease-bearing allele. Three supposedly unaffected individuals in family F1 (the mother of the founder II.2 and her 71 year-old sister III.4 and son IV.6) also carry the disease-related allele, although the genotype for the founder's mother was inferred. Family members F1 III.4 and F1 IV who were seen in this study had no complaints, and their clinical examination was completely normal, although electrophysiological and laryngological studies were not done on them. This may be due to an incomplete penetrance or the high variability in the age of onset and the severity seen in this disease. In their studies, Dyck P. J. *et al.* (Dyck, Litchy et al.

1994) and Klein C. J. *et al.* (Klein, Cunningham *et al.* 2003) reported similar pattern. They also reported about an asymptomatic individual with a normal clinical and laboratory examination but had the disease-bearing allele. But, another likely explanation could be that this may be a new mutation arising between the affected founder (Fig. 1, individual III.2) and her mother. This is consistent with the family history because no information was gotten from family members suggesting that one of the affected founder's parents or other relatives in the older generations were affected. However, the founder's mother was reported to have absent reflexes, and her EMG showed peroneal involvement at age 71. Based on these findings, it cannot be ruled out that she was not affected due the high variability seen in other families. The haplotype reconstruction in the family F1 was most helpful because it narrowed down the previous region of linkage due to the recombination that took place in the telomeric border of the region of interest. This recombination excluded about 26 genes including the ATXN2 gene from the last mapping study in this locus (McEntagart, Reid *et al.* 2005).

The haplotype reconstruction matched well the disease status in the other two linked families. Linkage analysis done in family F5 excluded the 12q24.11 locus, suggesting genetic heterogeneity within the CMT2C sub-type.

The chromosome 12q24 locus is a “hot-spot” for many neurological disorders.

Scapuloperoneal muscular dystrophy (SPMD) is an autosomal dominant neurodegenerative disorder characterized by a myopathic syndrome. Symptoms develop in the legs first, and manifest with foot-drop and a gait disturbance, and shoulder girdle weakness develops at a later stage of the disease. Mild facial muscles weakness may develop in some patients (Todman and Cooke 1984). Wilhelmsen K. C. *et al.* have mapped the gene causing scapuloperoneal muscular dystrophy in a large family to chromosome 12q21-22 (Wilhelmsen, Blake *et al.* 1996).

Scapuloperoneal muscular atrophy (SPSMA) is the neurogenic form of the syndrome described above. SPSMA is an autosomal dominant disorder characterized congenital absence of muscles, progressive scapular and peroneal atrophy, laryngeal palsy, and progressive distal weakness and atrophy (DeLong and Siddique 1992). The gene for SPSMA was mapped to chromosome 12q24.1-24.31 (Isozumi, DeLong *et al.* 1996), and the disease-causing gene was identified recently (Deng, Klein *et al.* 2010).

Distal hereditary motor neuropathy type II (dHMNII) is an autosomal dominant neuropathy characterized by weakness and atrophy in distal lower limbs but upper limbs can be affected later. This disease is close to CMT1 or CMT2 but there is no or little sensory loss (Timmerman, Raeymaekers et al. 1992). The gene for dHMNII was mapped to chromosome 12q24 (Timmerman, De Jonghe et al. 1996), and the disease-causing gene was identified later by same group (Irobi, De Jonghe et al. 2004).

Congenital distal spinal muscular atrophy (SMA) is an autosomal dominant non-progressive SMA characterized by weakness and atrophy in distal limbs, but proximal limbs can be affected in the severely affected individuals (Fleury and Hageman 1985). The gene for this disorder was mapped to chromosome 12q (van der Vleuten, van Ravenswaaij-Arts et al. 1998), and the gene was recently found (Auer-Grumbach, Olschewski et al. 2010).

Spinocerebellar ataxia type 2 (SCA2) is an autosomal dominant disorder that manifests with cerebellar ataxia, Parkinsonian symptoms and oculomotor impairment. Gispert, S. *et al.* mapped the gene for SCA2 to chromosome 12q24 (Gispert, Twells et al. 1993). Three years later, Pulst S. M. *et al.* identified CAG repeats in the *ATXN2* gene in this locus (Pulst, Nechiporuk et al. 1996).

Recently, an autosomal dominant hereditary spastic paraplegia (SPG36) was mapped to chromosome 12q23-24 (Schule, Bonin et al. 2009). Hereditary spastic paraplegias are characterized by spasticity mostly in lower leading gait difficulties, but can be complicated by other features including urinary dysfunction, ocular impairment and mental disability. In SPG36, the clinical presentation can be complicated by peripheral neuropathy.

SCA2 and SPG36 affect the central nervous system, but some degree of peripheral nervous system involvement is seen as well. Because all these diseases are linked to chromosome 12q, this region might be important in the development or function of the nervous system. Further studies of this region could prove useful in determining its role in the neurogenesis, especially the peripheral nervous system.

4.3 Gene sequencing

TRPV4 is mutated in CMT 2C

Sequencing of candidate genes selected within the region of interest failed to identify any significant sequence variant. This selection was based on function and expression

of the genes. We then undertook sequencing all the genes within that region, and identified two sequence variants in the *TRPV4* gene. *TRPV4* is expressed at low level in neurons but was found to be mutated in three of the five CMT2C families studied here and in two non characterized CMT2 index patients. This proves that, although this method has worked in other cases, gene expression level in targeted tissues may not be the appropriate way to select for candidate genes in a linked region. Two missense mutations characterized here were located in the same codon but predict different amino acid substitutions, R269C and R269H, respectively. This residue is located in the third ankyrin repeat in the intracellular N-terminal region of the TRPV4 protein, and may play a specific role in TRPV4 function. Screening of the two supposedly unaffected individuals in family F1 revealed that they carried the mutation. This makes it less likely that this mutation be a new mutation in this family. Sequencing of TRPV4 in families F3, F4 and F5 did not show any significant sequence variant, supporting the possible genetic heterogeneity in this disease as suggested above. However, exome sequencing revealed a single nucleotide change in the TRPV4 gene in family F3, R186Q. With standard Sanger sequencing we could not first see this sequence variant. A review of the chromatographs showed a very low peak of the mutant variant at the level of the background noise. This is likely due to the fact that primers used to amplify this region of the gene contained SNPs, with one having a frequency of 0.049. It was shown that when a primer that contains SNP is used to amplify a region it can lead to monoallelic amplification. This emphasizes the advantage of the technique used by exome sequencing. In fact there were 131 reads across the sequence variant with 79 reads for the wild-type allele and 52 for the mutant allele. When this region of TRPV4 was amplified with different primers, the mutation appeared well, and segregated with disease status in the family (Family F3). However, individual III.5 did not have the mutation. This is possible because he did not have any clear clinical or laboratory findings in favour of CMT. Although his chest X-rays showed hemi-diaphragmatic paralysis, his phrenic nerve conduction velocity and amplitude were normal, suggesting that his sleep apnoea may be of different origin. The R186 is also located in an ankyrin repeat domain, at the end of the first ARD.

Only about 1 % of genome is translated into protein, and the majority of Mendelian disorders are caused by mutations in this part of the genome. In recent years,

researchers have developed a technique that capture and sequence this part of the genome, making discovery of monogenic diseases mutations easier. Our study emphasizes the importance of targeted capture sequence, and has added to growing list of mutations found by exome sequencing. However, this technique also has its limitations. Not all the exome is covered, leaving the possibility of false negative findings. As in Sanger sequencing, G-C rich regions are hard to sequence using the targeted capture sequencing, and repeat regions are not sequenced at all. With the technology improving and the cost of exome sequencing going down, high throughput capture sequencing will be a valuable tool to uncover new genes and establish diagnosis of genetic disorders.

Screening of 132 families with unspecified CMT2 revealed two other sequence variants in TRPV4 (R232C and D854N), suggesting that mutations in this gene are not as uncommon as one would expect. Further cohort studies may reveal new mutations in this gene.

Other researchers have reported TRPV4 mutations in CMT2C families and other neurodegenerative diseases including scapuloperoneal spinal muscular atrophy (SPSMA), and congenital spinal muscular atrophy (Auer-Grumbach, Olschewski et al. 2010; Chen, Sul et al. 2010; Deng, Klein et al. 2010; Zimon, Baets et al. 2010) discussed below.

TRPV4 mutations also cause skeletal dysplasias

Mutations in the *TRPV4* gene have been previously associated with autosomal dominant skeletal dysplasias. Brachyolmia is caused by R616Q and V620I mutations (Rock, Prenen et al. 2008), and later, the D333G and I331F mutations have been identified in the 5th ankyrin repeat in single patients with spondylometaphyseal dysplasia Kozlowski type and metatropic dysplasia, respectively (Krakow, Vriens et al. 2009).

More recently, other TRPV4 mutations were reported in other metatropic dysplasias families (Camacho, Krakow et al. 2010).

Of the 11 mutations identified in 19 families with skeletal dysplasia, only three are located in the ankyrin repeat domains (Krakow, Vriens et al. 2009; Camacho, Krakow et al. 2010) while only two of the mutations identified in CMT2C/SPSMA/SMA families are localized in the transmembrane domain (Chen, Sul et al. 2010; Zimon,

Baets et al. 2010), and those families with transmembrane domain mutations have some symptoms related to bone abnormalities.

Several cases of single gene mutations causing different diseases, in some cases in different organ systems, were reported in the literature. We will discuss some of them here.

ANO5 mutations cause Gnathodiaphyseal dysplasia and limb-girdle muscular dystrophy and Myoshi muscular dystrophy 3.

Gnathodiaphyseal dysplasia (GDD) is an autosomal dominant disease characterized by frequent bone fractures in adolescence and purulent osteomyelitis of jaws during adult life (Akasaka, Nakajima et al. 1969). This disease was found to be caused by mutations in the *ANO5* gene in 2004 by Tsutsumi *et al.* (Tsutsumi, Kamata et al. 2004). Recently, other researchers identified mutations in the *ANO5* gene in consanguineous families with limb-girdle muscular dystrophy type 2L (LGMD2L) and distal Myoshi muscular dystrophy 3 (MMD3) (Bolduc, Marlow et al. 2010). LGMD2L is an autosomal recessive LGMD characterized by prominent asymmetrical quadriceps femoris and biceps brachii weakness and atrophy. Symptoms start between 11 and 50 years, and the disease severity is variable. MMD3 is characterized by asymmetric distal weakness in lower limbs; mostly calf muscles leading to the inability to stand on tiptoes. While mutations in the N-terminal tail of *ANO5* were seen in LGMD2L and MMD3 only, mutations of the transmembrane domain were seen in ganthodysphyseal dysplasia, and LGMD2L and MMD3.

ANO5 is a calcium-activated chloride channel with unknown function. Although functional analyses showing the effect of these mutations on the channel function are not available, it is still striking that mutations in the same gene cause diseases in different organ systems. Further experiments may be needed to differentiate the effect of the mutations in the channel function or its interaction with other proteins.

Dynactin 1 mutations in distal hereditary motor neuropathy type VIIB and in Perry syndrome. Distal hereditary motor neuropathy type VIIB (dHMNVIIB) is an autosomal dominant motor neuron disease characterized by an adulthood onset of breathing difficulties due to vocal fold paralysis, progressive facial weakness, and weakness and atrophy in hands. Lower limb weakness and atrophy develop later in the disease course. There is no sensory involvement. Puls I. *et al.* found mutations in

the dynactin 1 (*DCTN1*) gene in a large family afflicted with dHMNVIIB (Puls, Jonnakuty et al. 2003).

Perry syndrome is an autosomal dominant neuropsychiatric disorder that starts in the late fifties. The disease starts with psychiatric symptoms including mental depression, sleep disorder, exhaustion and severe weight loss. Later, Parkinsonian symptoms develop. Death occurs by respiratory failure (Perry, Bratty et al. 1975). In 2009, Farrer M. J. *et al.* (Farrer, Hulihan et al. 2009) identified five heterozygous mutations in the *DCTN1* gene in eight Perry syndrome families.

Although both dHMNVIIB and Perry syndrome present with symptoms involving the nervous system, these two diseases are separate because they affect different parts of the nervous system; dHMNVIIB affects peripheral nerves while Perry syndrome affects the central neurons system. In vitro functional expression studies in both disorders indicated that mutations in *DCTN1* resulted in decreased microtubule binding and intracytoplasmic inclusions. However, how mutations in *DCTN1* cause both diseases is still not clear.

Sodium channel, voltage-gated, type IX, alpha subunit (*SCN9A*) mutations cause primary erythralgia, paroxysmal extreme pain disorder, and congenital indifference to pain.

Primary erythralgia is an autosomal dominant disorder characterized by childhood onset of episodic symmetrical red congestion, vasodilatation, and burning pain of the feet and lower legs provoked by exercise, long standing, and exposure to warmth (Mandell, Folkman et al. 1977). Relief is obtained with cold (Michiels, te Morsche et al. 2005). In 2004, Yang F. *et al.* (Yang, Wang et al. 2004) identified mutations in the *SCN9A* gene in affected members of a Chinese family with primary erythralgia and in a sporadic case. Other researchers reported mutations in other families, later (Dib-Hajj, Rush et al. 2005; Michiels, te Morsche et al. 2005).

Paroxysmal extreme pain disorder (PEXPD), formerly known as familial rectal pain, is characterized by paroxysms of rectal, ocular, or submandibular pain with flushing (Fertleman, Baker et al. 2006). Fertleman C. R. *et al.* have identified eight missense mutations in the *SCN9A* gene in 11 families and two sporadic cases of PEXPD (Fertleman, Baker et al. 2006).

Although these two entities are characterized by pain and are allelic, Fertleman C. R. *et al.* suggested that they have distinct underlying biophysical mechanisms.

Carbamazepine is a drug that is efficient in PEXPD but not in primary erythermalgia. Moreover, *in vitro* electrophysiological studies have shown that carbamazepine selectively block persistent current associated with PEXPD mutants but not primary erythermalgia mutants, confirming that each of these disorders represents separate class of peripheral neuronal sodium channelopathy.

Congenital indifference to pain also called 'channelopathy-associated insensitivity to pain' is characterized by painless injuries beginning in infancy but otherwise normal sensory modalities. Perception of passive movement, joint position, and vibration are normal, as are tactile thresholds and light touch perception. Reflexes and autonomic responses are also normal. The first case was described in 1932 (Dearborn 1932). Cox J. J. *et al.* first identified three distinct homozygous mutations in the SCN9A gene in three Pakistani families with congenital indifference to pain (Cox, Reimann *et al.* 2006). Subsequently, Goldberg Y. P. *et al.* (Goldberg, MacFarlane *et al.* 2007) identified 10 homozygous mutations in nine families. *In vitro* functional expression studies have shown that the mutations in congenital indifference to pain cause loss of function.

Although these diseases affect the same organ system, it is still striking that mutations in the same gene cause different diseases, especially in the case of primary erythermalgia or paroxysmal extreme pain disorder and congenital indifference to pain.

Lamin A/C (LMNA) mutations cause Charcot-Marie-Tooth type 2B1, limb-girdle muscular dystrophy type 1B, autosomal dominant Emery-Dreifuss muscular dystrophy (EDMD), and mandibuloacral dysplasia with type A lipodystrophy (MADA).

As described above, Charcot-Marie-Tooth type 2B1 is an axonal neuropathy characterized by distal lower limb muscles weakness and atrophy, but in some cases proximal muscles are affected (Bouhouche, Benomar *et al.* 1999). In 2002, De Sandre-Giovannoli *et al.* (De Sandre-Giovannoli, Chaouch *et al.* 2002) identified a homozygous mutation in the *LMNA* gene in three consanguineous families.

Limb-girdle muscular dystrophy type 1B (LGMD1B) is an autosomal dominant muscular dystrophy associated with cardiomyopathy (van der Kooi, Ledderhof *et al.* 1996). The disease is characterized by symmetrical weakness in the proximal lower

then upper limb muscles. Muchir A. *et al.* identified mutations in the LMNA gene in three LGMD1B families (Muchir, Bonne *et al.* 2000).

The classic EDMD is an X-linked disorder caused by mutations in the emerin gene (Emery 1989), and characterized by myopathic changes in certain skeletal muscles and early contractures at the neck, elbows, and Achilles tendons, as well as cardiac conduction defects. Autosomal dominant EDMD is characterized by slowly progressive muscle weakness with scapulo-ilio-peroneal distribution and late-onset cardiomyopathy. Bonne G. *et al.* have identified mutations in the LMNA gene in five families with autosomal dominant EDMD (Bonne, Mercuri *et al.* 2000).

Mandibuloacral dysplasia with type A lipodystrophy (MADA) is an autosomal recessive disorder characterized by growth retardation, craniofacial anomalies with mandibular hypoplasia, skeletal abnormalities with progressive osteolysis of the distal phalanges and clavicles, and pigmentary skin changes (Young, Radebaugh *et al.* 1971). Novelli G. *et al.* (Novelli, Muchir *et al.* 2002) first identified homozygous mutations in the LMNA gene in nine families with MADA.

Although LGMD1B and EDMD are due to muscle involvement, CMT2B1, and MADA more, are diseases of different organ systems. But yet mutations in the LMNA gene are associated with all these diseases.

Other disorders as diverse as dilated cardiomyopathy type 1A (CMD1A), familial partial lipodystrophy type 2 (FPLD2), Hutchinson-Gilford progeria syndrome (HGPS), Slovenian type heart-hand syndrome, and LMNA-related congenital muscular dystrophy can be also due mutations in the *LMNA* gene.

This chapter underscores the complexity of gene regulation and expression in the different organ systems, a process that is still not well known.

4.4 Functional studies

TRPV4 is expressed in peripheral nerves.

TRPV4 is a non selective cation channel that was shown to be expressed in the nervous system. Studies have reported TRPV4 to be expressed in motor neurons (Facer, Casula *et al.* 2007), ventral root (Facer, Casula *et al.* 2007), and dorsal root ganglion (DRG) neurons (Liedtke, Choe *et al.* 2000). In addition, *in situ* hybridization studies show *Trpv4* mRNA expression in ventral and dorsal horn neurons of adult mouse spinal cord tissue (Allen Institute for Brain Science Spinal Cord Atlas). We

have confirmed TRPV4 expression in the spinal cord using *Trpv4* knockout (Suzuki, Mizuno et al. 2003) and wild type mice by immunohistochemistry (IHC), and in human adult dorsal and ventral spinal cord, and in tracheal cartilage. Furthermore, quantitative RT-PCR showed TRPV4 expression in the nervous system. However, compared to cartilage, TRPV4 was about 95 % less expressed in the nervous system. This high expression in cartilage was shown by previous studies (Rock, Prenen et al. 2008).

To date, all the genes implicated in CMTs have been shown to play a major role in the peripheral nerve structure or function. To our knowledge, *TRPV4* is the second ion channel reported to cause CMT. *KCC3*, a potassium chloride cotransporter was reported to cause hereditary motor and sensory neuropathy associated with agenesis of the corpus callosum (Uyanik, Elcioglu et al. 2006). *KCC3* was localized in the brain and the spinal cord, and *KCC3* knockout mouse showed peripheral nerves hypomyelination. Although the function of TRPV4 in the nervous system is not known, as a calcium channel, TRPV4 may play a role in the axonal degeneration; a process that implicates calcium influx. In addition, as discussed below, dysregulation of calcium homeostasis has been implicated in some neurodegenerative disorders.

TRPV4Δ7 expresses more in the nervous system by RT-PCR but qRT-PCR found no difference in exon 7 levels in different tissues

At least five TRPV4 splice variants cloned in human tracheal and bronchial epithelial cells have been reported in the literature (Arniges, Fernandez-Fernandez et al. 2006). Quantitative RT-PCR using cDNA using primers flanking TRPV4 exon 7 did not show any differential expression in tissues including cartilage, spinal cord, peripheral nerves, and kidney. When we amplified TRPV4 cDNA from different human tissues including brain, spinal cord, trachea, liver, and kidney, only two bands were visualized in each. There was no difference in size between tissues. Moreover, sequencing of these bands revealed that the smaller band lacked exon number 7 while exon number 5 was present in all. However, the band corresponding to the splice variant lacking exon 7 was stronger in tissues from the nervous system. It is possible that the mutations we describe here impact more TRPV4Δ7 function, which is more expressed in neurons. Although a weak argument, this difference could account for TRPV4 mutations causing diseases in different organ systems. Heterologous experiments described here were conducted using TRPV4 full-length. It will be

interesting to perform experiments with the shorter splice variant, and compare mutations described here to those found in bone diseases.

CMT 2C mutations lead to increased channel activity

TRPV4 is a non-selective cation channel that lets Ca^{2+} into cell. Ca^{2+} is an essential intracellular signal in neurons regulating neurite outgrowth, synaptogenesis, synaptic transmission, and plasticity, but excessive influx of Ca^{2+} has also long been associated with neurodegeneration (Mattson 2007). The mutations found here were shown to cause increased channel activity leading to calcium overload. This calcium overload likely causes cell toxicity as shown in different cell models including *Xenopus* oocytes, HEK293 cells, and, most importantly, dorsal root ganglia. Although TRPV4 is expressed at rather low level in nerve tissues, in vitro functional expression studies have shown that abnormal TRPV4 function could still cause neuronal cell death as evidenced by DRG toxicity. When exposed to ruthenium red, mutants and wild-type expressing oocytes showed reduced currents up to 53 %. In the presence of ruthenium red, increased calcium levels and cell death were blocked, suggesting that calcium overload and cell death was due to TRPV4 hyperactivity. However, because ruthenium red is non-specific TRP channels blocker, its blocking activity may not be limited to TRPV4 channel only. In addition, ruthenium red can also be toxic to cells. To investigate the specificity of TRPV4 currents and exclude ruthenium red for causing cell death, we used the specific TRPV4 inhibitor RN-1734, and found that calcium overload and cell death were reversed, confirming the specificity of TRPV4 currents. In addition, the TRPV4 pore-inactivating substitution M680K, which is known to reduce calcium entry into the cell (Voets, Prenen et al. 2002) also reduced cell calcium content and cell death when co-expressed with mutant TRPV4.

Together, these data indicate that cell calcium overload and cell death is due to aberrant activity of the TRPV4 channel. However, as discussed below, increased channel activity could not be accounted for by changes in TRPV4 channel subcellular localization as shown by analysis of surface incorporation of TRPV4 by cell surface biotinylation and wild-type and mutant TRPV4 expressed in cells from the HeLa and HEK293 lines that showed similar spatial distributions.

Mutant TRPV4 display similar cellular localization compared to wild-type, and is not retained in the ER.

TRPV4 protein contains four endoplasmic reticulum (ER) retention or retrieval motifs, two in the intracellular N-terminal region (¹²²RWR and ²⁶⁹RGR) and two in the C-terminal tail (⁸¹⁶RLR and ⁸¹⁹RDR). The R269 residue constitutes the first arginine of the second motif as seen above. These motifs are known to play a role in protein trafficking from the endosome to the membrane (Zerangue, Schwappach et al. 1999). In fact, Zerangue N. *et al.* have shown in ATP-sensitive K⁺ channels that ER retention or retrieval motif is required at multiple stages of K_{ATP} assembly to restrict surface expression to fully assembled and correctly regulated octameric channels. They have shown that when tetrameric channels assemble, ER retention or retrieval motifs are internalized, thus leading these channels to traffic to the cell membrane. When assembly is prevented, ER retention or retrieval motifs are exposed; therefore channel subunits are retained in the ER leading to low expression of these channels.

TRPV4 channels form a functional homotetrameric channel. Assembly occurs in the ER, and the channel is trafficked to the Golgi where it undergoes further maturation (Arniges, Fernandez-Fernandez et al. 2006). Arniges M. *et al.* have shown that when they delete part of TRPV4 ankyrin repeat domains, the protein remains in the ER, and mutation of the first arginine of any of the four ER motifs did not modify the localization of TRPV4, to say TRPV4 was retained in the ER (Arniges, Fernandez-Fernandez et al. 2006).

In addition, ER markers did not show any overexpression suggestive of ER stress. Although different in design, our results are consistent with those of Arniges *et al.* in that ER motif mutation did not modify the cellular localization TRPV4. Based on the results Arniges *et al.* found, we can extrapolate that the mutations we found here did not disturb the ankyrin repeat domains in such a way to disturb TRPV4 assembly and cell surface localization.

TRPV4 mutations are also found in bone diseases.

During our study, mutations in TRPV4 were reported in patients with bone disease (Rock, Prenen et al. 2008; Krakow, Vriens et al. 2009; Camacho, Krakow et al. 2010; Dai, Kim et al. 2010; Nishimura, Dai et al. 2010). Some of these mutations were shown to increase basal and stimulated channel activity, perhaps via direct alteration

of the S5 pore domain (Rock, Prenen et al. 2008). TRP channels operate within macromolecular complexes (Clark, Middelbeek et al. 2008), and the ankyrin motifs are likely critical mediators of protein-protein interactions that regulate TRP channel localization and activity. The R269 residue localized to the convex face of the TRPV4-ARD may mediate distinct interactions with yet-to-be identified regulatory partners particularly important for TRPV4 function in peripheral neurons. Although the R232C and R186C mutations were not studied functionally, R232 and R186 along with the other residues mutated in other neurological disorders (Auer-Grumbach, Olschewski et al. 2010; Deng, Klein et al. 2010) are located on the same face as R269 in the chicken Trpv4 ARD structure, suggesting that they may also play a role in TRPV4 interaction with other proteins important for the nervous system. Moreover, the R232 lies in a splicing enhancer site where the R232C may disrupt splicing and disorganize the ankyrin repeat domain, thus disrupting TRPV4 assembly or activity. The D854 residue is located in the C-terminal part of the protein, a region that has been shown to play a role in the plasma membrane localization of the TRPV4 (Becker, Muller et al. 2008). In fact, their study, Becker D et al. showed that deletion of the C-terminal part of TRPV4 protein up to the 844th amino acid did not traffic to the membrane but a deletion to the 855th amino acid of TRPV4 protein did. Mutation at residue D854 may lead to untrafficked TRPV4, therefore causing toxicity to neuronal cells and CMT2C phenotype. No other mutation has been found in this region, raising the possibility that this sequence variant may not be disease-causing. Heterologous expression studies of the D854N mutation in cell models could give insights into its impact in TRPV4 function.

TRPV4 mutations in CMT 2C lie on the opposite face of that of skeletal dysplasias mutations in the chicken TRPV4 ankyrin repeat domain crystal structure.

The TRPV4 protein has distinct domains, including six transmembrane segments with a putative ion pore region between S5 and S6, an intracellular N-terminal domain containing six ankyrin repeats and an intracellular C-terminal domain. Ankyrin repeat motif is a short sequence of about 33 amino acids residues which forms an anti-parallel helix-turn-helix structure followed by a β -hairpin loop. Often, more than three repeats are found in tandem and stack together to yield a hand-shaped domain with a concave palm surface formed of the inner helices and fingers, and a convex surface analogous to the back of the hand (Gaudet 2008).

Ankyrin repeats mediate protein-protein interactions, some of which have been shown to modulate TRPV4 activity (Phelps, Wang et al. 2010). The 2.3-Å crystal structure of the chicken Trpv4 ankyrin repeat domain (ARD) shows the typical hand-shaped structure with a concave palm surface formed by inner helices and fingers, and a convex surface representing the back of the hand. Arg269 is located at the base of finger 3 on the convex surface, opposite the palm surface harbouring all described skeletal dysplasia mutations in the ARD (Krakow, Vriens et al. 2009) (Figure 39a). Most convincingly, all reported TRPV4 mutations found in CMT2C or SPSMA or congenital SMA (Auer-Grumbach, Olschewski et al. 2010; Chen, Sul et al. 2010; Deng, Klein et al. 2010; Landouere, Zdebik et al. 2010) are located in the opposite side of those identified in bone diseases (Krakow, Vriens et al. 2009; Camacho, Krakow et al. 2010) (Figure 39b). Other non-reported TRPV4 mutations found in distal SMA patients also localize to same face as R269, R186, R315, and R316. This may suggest that residues on these faces may play an important role in TRPV4 interaction with proteins important for the nervous system or the skeleton.

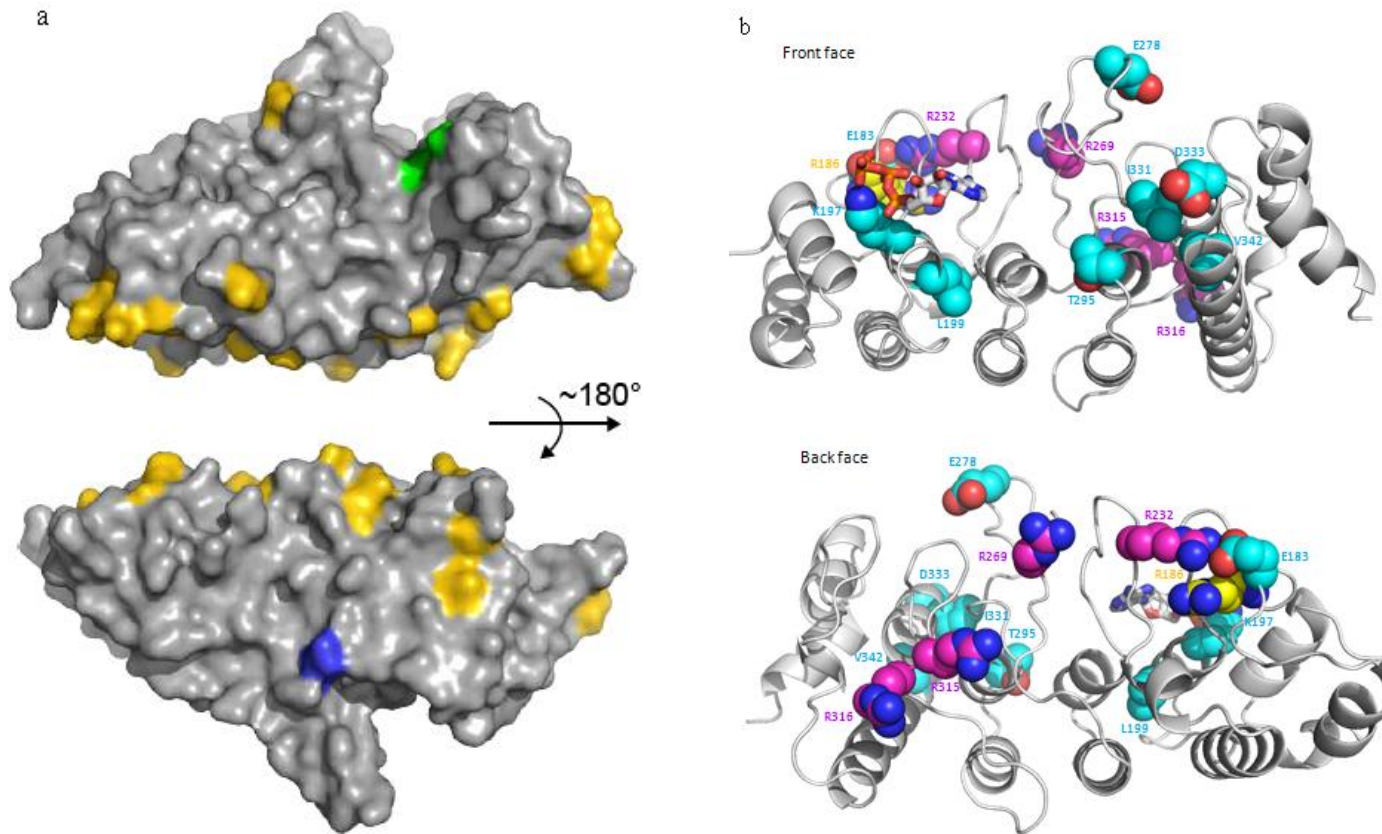


Figure 39 Surface representation of the chicken TRPV4 ARD showing neurological and bone diseases mutations.

a) Arg269 in blue and Ile331 and Asp333 in green. Residues that differ between chicken and human TRPV4 are yellow, demonstrating that the palm and finger regions are conserved. **b)** Green and represent mutations in bone diseases and blue and purple represent mutations in neurological disorders. Note that they are in opposite faces.

CMT 2C mutations do not disrupt TRPV4 protein folding or its interaction with PACSIN 1, 2, and 3.

When compared, the TRPV1, TRPV2 and TRPV6 structures (Jin, Touhey et al. 2006; Lishko, Procko et al. 2007; Phelps, Huang et al. 2008) show a conserved backbone structure at the position Arg269, although the arginine residue is not conserved in other TRPV channels (Figure 40). This suggests that the R269C and R269H substitutions are unlikely to disrupt the protein folding, but the Arg269 side chain is exposed and well positioned to mediate protein-protein interactions that may be critical to TRPV4 function. The cytoskeletal modulating proteins, PACSINs 1-3, have been shown to bind the N-terminus of TRPV4 and modulate its membrane localization and function. When interaction with PACSIN 3 is disrupted, TRPV4 shows increased channel activity (Cuajungco, Grimm et al. 2006). PACSIN 1 is nervous system-specific (Modregger, DiProspero et al. 2002) and altered interaction with this or another such factor could account for the tissue specificity of the CMT2C phenotype. ATP and calmodulin have been shown to bind to TRPV4 through a conserved binding site in the ARD, and that ATP and calmodulin participate in the sensitivity and adaptation profiles of TRPV4 (Phelps, Wang et al. 2010).

However, binding assays and co-immunoprecipitation experiments did not show changes in the interaction of mutant TRPV4 with known protein partners such as calmodulin and PACSIN 1, 2, and 3, confirming that the CMT2C-associated mutations do not grossly disrupt TRPV4 protein folding. Further experiments are needed to define whether specific intermolecular or intramolecular interactions are affected by the Arg269 substitution.

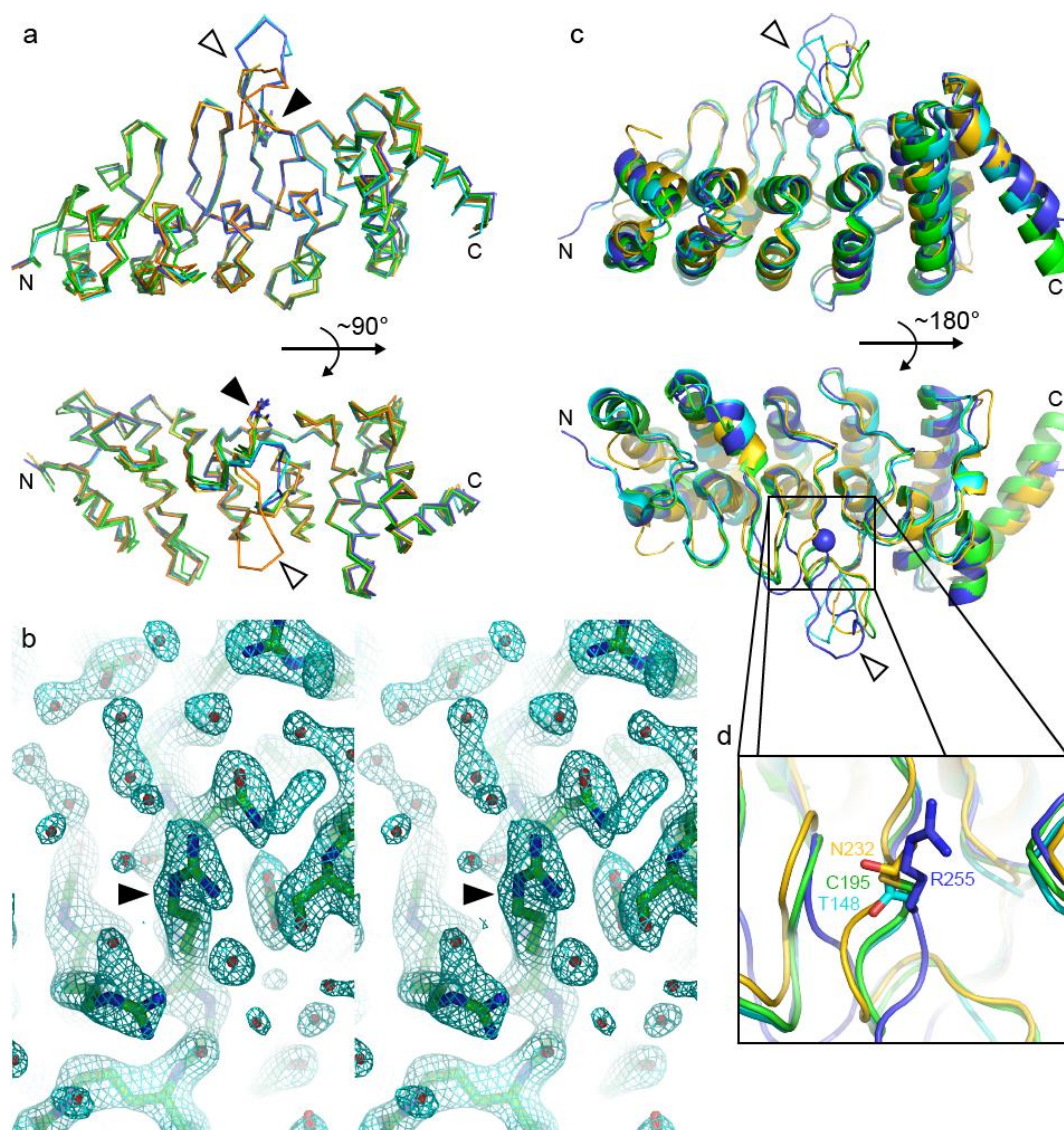


Figure 40 Comparisons of the chicken TRPV4 ARD structures to that of other TRPV proteins.

a) Carbon α traces of the superimposed TRPV4 ankyrin repeat domain structures, Chains A (blue), B (cyan), C (light green), D (dark green) of crystal form I and A (orange) and B (yellow) of crystal form II. They superimpose readily with pairwise root mean squared deviations (rmsd) ranging from 0.31 to 0.71. The largest differences are in the tip of finger 3 (white arrowhead) as observed in TRPV218. The side chain of R255 (R269 in human TRPV4) is shown (black arrowhead). **b)** Stereodiagram of the weighted $2F_o - F_c$ electron density map in proximity to R255 (R269 in human TRPV4; arrowhead) of chain A. **c)** Ribbon diagram of the superimposed structures of chicken TRPV4 (blue; carbon α of R255 shown as a sphere), rat TRPV1 (yellow; 2PNN16), rat TRPV2 (green; 2ETB18) and mouse TRPV6 (cyan; 2RFA19). Again, the largest observed structural differences are at the

tip of finger 3 (white arrowhead). **d)** Zooming into the base of finger 3 at the convex face of the molecule. The backbone positions of residues structurally equivalent to R255 (R269 in human TRPV4) are conserved, although the side chains of these residues differ. Colouring is the same as in (c).

Activating TRPV4 mutations cause other neurological disorders

In SPSMA TRPV4 mutations caused increased channel activity and calcium overload (Deng, Klein et al. 2010). In this study, HEK293 cells were used for both electrophysiological and cell calcium measurement experiments. However, in the other study that reported congenital distal SMA and CMT2C (Auer-Grumbach, Olschewski et al. 2010) there was a decreased channel activity and calcium uptake, and TRPV4 mutants proteins surface localization was reduced. This study used HeLa cells that do not have endogenous TRPV4. TRP channels are known to interact with PIP2 (Nilius, Owsianik et al. 2008). PIP2 is a recruiter of TRPV4 and an inhibitor of its activity. Because ankyrin repeat domain are typical PIP2 binding sites, ankyrin domain mutations diminish the channel's ability to interact with the phospholipid. In HeLa and other cells that lack endogenous TRPV4, the transfected mutant protein is unable to find the membrane without binding PIP2, and thus remains in the cytoplasm. The lack of trafficking of TRPV4 to the membrane can explain its loss of function seen in the second study. On the other side cell types such as HEK293 cells contain endogenous wild-type TRPV4, and the mutant and wild-type proteins sometimes may come together in mixed tetramers. The interaction of wild-type TRPV4 and PIP2 is sufficient to recruit the complex to the plasma membrane. In this case the PIP2 cannot bind to the mutant channel meaning that it does not effectively inhibit TRPV4 mutant, thus causing the gain of channel function. Another possible explanation of the discrepancies can be the difference in the compensatory mechanisms of the different cell types.

4.5 Calcium and neurodegeneration

Several studies have demonstrated the role of calcium ions in several cellular processes including muscle contraction, transmitter release, cell proliferation, gene transcription, and cell death (Berridge, Bootman et al. 2003). In neurons, under physiological conditions, Ca^{2+} plays an important role in the regulation of neurite

outgrowth and synaptogenesis, synaptic transmission and plasticity, and cell survival. Neurons are excitable cells that rapidly transfer electrochemical signals in a highly controlled spatio-temporal manner. Ca^{2+} is critical in mediating many intracellular physiological responses of neurons to chemical and electrical stimulation. TRPV4 is ligand-gated channel, and the influx of Ca^{2+} through ligand-gated channels in the plasma membrane is a critical signal for the release of neurotransmitter from presynaptic terminals and for responses of the postsynaptic neuron (Hartmann and Konnerth 2005). In normal conditions, intracellular Ca^{2+} concentration increases only transiently, second to a few minutes. This transient increase does not affect neurons. However, in pathological conditions such as in neurodegenerative disorders, neurons can no longer control Ca^{2+} fluxes and recover from Ca^{2+} overload, leading to their damage. Two organelles play a critical role in the Ca^{2+} homeostasis; endoplasmic reticulum (ER) and mitochondria are sites of Ca^{2+} regulation.

The role of dysregulation of calcium homeostasis in the pathogenesis of slow progressing neurodegenerative diseases was shown in different studies. We will talk about diseases that are clinically and physiopathologically close to CMTs.

Huntington's disease: Huntington's disease (HD) is an autosomal dominant neurodegenerative disease characterized by motor and psychiatric symptoms. The age of onset ranges from 20 to 50 years, and symptoms manifest as chorea and dementia due to a selective and progressive loss of medium spiny neurons in the striatum. HD is caused by a dominant negative effect the abnormal expansion of Huntingtin protein (Ht). Some studies have shown that mutant Ht disrupts mitochondrial Ca^{2+} homeostasis (Panov, Gutekunst et al. 2002), and associates directly with the inositol triphosphate receptor (IP3R) in the ER and is able to sensitize this receptor to its activation by IP3R (Tang, Tu et al. 2003). Other studies have implicated mutant Ht in N-methyl-D-aspartate receptors (NMDARs) hypersensitivity and an increase in Ca^{2+} influx (Sun, Savanenin et al. 2001). All these lead to Ca^{2+} accumulation over time that can eventually trigger the opening of the permeability transition pore in mitochondria and neuronal death.

Other hereditary neurological disorders in which Ca^{2+} signalling play a role in the pathogenesis are autosomal dominant spino-cerebellar ataxias (SCA). SCAs are neurodegenerative disorders that start between 30 and 50 years, and are characterized by cerebellar ataxia associated with pyramidal and extrapyramidal signs and symptoms, dementia, ophthalmoplegia and pigmentary retinopathy, and peripheral

neuropathy (Zoghbi 2000). These symptoms progress slowly over years. Signs of Ca^{2+} involvement in the pathogenesis of SCAs are downregulation of several neuronal genes highly expressed in Purkinje cells and involved in Ca^{2+} signalling or homeostasis in SCA-1 mutant mice. Among these genes are the calbindin-D28k and paralbumin (Vig, Subramony et al. 2000), and IP3R and SERCA2 (Lin, Antalffy et al. 2000). Another Ca^{2+} channel associated with Purkinje cells degeneration is the voltage-operated Ca^{2+} channel *CACNA1A* gene (Pietrobon 2002).

The closest disease to CMTs in which Ca^{2+} dyshomeostasis was shown to play a role in the pathogenesis is the amyotrophic lateral sclerosis (ALS). ALS is characterized by loss of cortical, spinal and bulbar motor neurons. Symptoms include muscle weakness, breathing and swallowing difficulties, and limbs spasticity (Rowland and Shneider 2001). Only 10 % of ALS cases have a genetic component, and the superoxide dismutase gene (*SOD1*) is most commonly mutated gene in this neurodegenerative disorder (Strong and Gordon 2005). Although the mechanism leading to degradation of motor neurons in this disease is not established, intracellular Ca^{2+} dysregulation was suggested by different studies. Glutamate excitotoxicity, Ca^{2+} dependent formation of protein aggregates, and Ca^{2+} -evoked mitochondrial dysfunction are believed to play a role in the mechanism (Van Den Bosch, Van Damme et al. 2006). Studies have shown that spinal motor neurons do not express the Ca^{2+} binding proteins parvalbumin and calbindin D28k that are Ca^{2+} sequestrators (Ince, Stout et al. 1993) and that they have a high proportion of α -amino-3-hydroxy-5-methylisoxazole-4-propionate acid receptors (AMPA receptors), receptor-operated channels, lacking the GluR2 subunit. This favours Ca^{2+} permeability of these channels (Carriedo, Yin et al. 1996), making these motor neurons highly sensitive to any potential excitotoxicity by either exogenous or endogenous factors.

The role of Ca^{2+} dyshomeostasis was shown in other chronic neurological or neuropsychiatric diseases, including Alzheimer's disease, Parkinson's disease, glaucoma, epilepsy, and schizophrenia.

Dysregulation in Ca^{2+} signalling was also shown to play a role in acute neurodegenerative diseases, including traumatic brain injury, brain stroke, and HIV dementia.

In our study, we have proven that Ca^{2+} overload was toxic to HEK293 and HeLa cells, dorsal root ganglia (DRG) neurons, and *Xenopus* oocytes. TRPV4 channel hyperactivity was shown in *Xenopus* oocyte and HEK293 cells currents measurement.

The sustained TRPV4 channel hyperactivity may cause chronic increased Ca^{2+} entry into the neuronal cells that cannot handle it over a long period of time, leading to their destruction. But the mechanistic process by which hyperactivity of this channel become toxic to neuronal cells while it was showed to cause bone diseases in other studies is not fully understood. The only difference found, as stated earlier, is that skeletal dysplasias mutations mostly cluster in the transmembrane domain of the protein, and while CMT2C and other neurological disorders mutations cluster in the ankyrin repeat domain. Although some skeletal dysplasia mutations localize to the ARD, they lie in opposite face of that of neurological disorders mutations. This can lead to disruption of interaction with specific proteins important for each organ system.

4.6 TRP channels and diseases

TRP channels were discovered just over a decade ago, but there is an increased evidence of their implication or association in the genesis of diseases or pathological processes.

Since their discovery, TRP channel have improved our understanding of molecular processes mediating Ca^{2+} entry into cells. As developed in their description above, TRP channels play a role in the cytosolic free Ca^{2+} concentration. Ca^{2+} signalling is very important in all cell types, thus dysfunctions in Ca^{2+} channels cause or are associated with the pathogenesis of several diseases.

Channelopathies are diseases caused by defect in genes encoding ion channels. The prevalence of monogenic channelopathies in neurology is 35:100,000 (Jurkat-Rott, Lerche et al. 2010). However, this number increases when susceptibility-related mutations are considered. To date, mutations in several TRP channels have been identified to cause disease. In addition, dysregulations of physiological functions mediated by ion channels that can contribute to the genesis of diseases or contribute to the progression of the disease have been described in the literature.

Focal segmental glomerulosclerosis

Focal segmental glomerulosclerosis (FSGS) is a human proteinuric kidney disease in which the podocyte foot processes and glomerular slit diaphragms of the glomerular filter lose their integrity between childhood and adulthood. Mutations in the TRPC6

gene were shown to be linked to FSGS (Kriz 2005; Winn, Conlon et al. 2005). Heterologous expression studies revealed an enhanced activity of three of the six mutants TRPC6. In the nephron, TRPC6 was shown to be expressed in the podocytes in the kidney glomerular filter (Reiser, Polu et al. 2005). Podocyte foot processes and the glomerular slit diaphragm form the glomerular filter and are an essential part of the permeability barrier in the kidney, which is defective in FSGS, making defects in TRPC6 a likely cause of this disease (Kriz 2005). Enhanced TRPC6 activity leads to Ca^{2+} overload of the podocyte that initiates cell death by apoptosis, or causes dysregulation that compromises the integrity of the permeability barrier (Reiser, Polu et al. 2005).

Hypomagnesaemia with secondary hypocalcaemia

Hypomagnesaemia with secondary hypocalcaemia (HSH) is an autosomal recessive disorder characterized by very low serum levels of Mg^{2+} and Ca^{2+} . HSH occurs because of impaired intestinal Mg^{2+} absorption associated with renal Mg^{2+} leak. Mutations in the *TRPM6* gene were shown to cause HSH disease. Heterologous experiment have shown that TRPM6 protein forms a Mg^{2+} -permeable channel, and is expressed in the brush-border membrane of the small intestine and in the apical membrane of renal distal convoluted tubule, both containing highly specialized cells responsible for Mg^{2+} absorption and reabsorption (Voets, Nilius et al. 2004).

Autosomal dominant polycystic kidney disease

Polycystic kidney diseases are characterized by progressive development of large fluid-filled cysts that can occupy much of the mass of the abnormally enlarged kidneys, compressing and destroying normal renal tissue and impairing kidney function. Mutations in *TRPP1* or *TRPP2* genes lead to polycystic kidney disease. Under normal conditions, phosphorylated TRPP2 associates with TRPP1 and prevents nuclear translocation of Id2 which is a crucial regulator of cell proliferation and differentiation. TRPP1/TRPP2 mutations allow Id2 to translocate in the nucleus where it binds to E-proteins, switching off the activity of growth suppression proteins. This explains the hyperproliferative feature of autosomal dominant polycystic kidney disease (Li, Luo et al. 2005).

Mucopolidosis type IV

Mucopolidosis type IV (MLIV) is an autosomal recessive neurodegenerative lysosomal storage disease. The disease manifests with severe psychomotor retardation, corneal opacity, retinal degeneration, strabismus, agenesis of corpus callosum, blood iron deficiency, and achlorohydria (Bach, Webb et al. 2005). MLIV is caused by mutations in the TRPML1 gene. The pathological mechanism of MLIV is not still fully understood. Electron microscopy visualization of late endosomes and lysosomes showed abnormal storage of amphiphilic lipids and membranous materials in multiconcentric lamella together with granulated, water soluble substances (Bach 2001). Heterologous experiments have shown that mutant TRPML1 channels retain physiological function, but are not affected by pH changes (Raychowdhury, Gonzalez-Perrett et al. 2004). In addition, mutant TRPML1 channels induce changes in the endocytotic transport of membrane components, including block to endocytotic route to final lysosome. Disturbed Ca^{2+} homeostasis has also been described in MLIV patient cells (LaPlante, Ye et al. 2004).

Guamanian amyotrophic lateral sclerosis (ALS-G) and Guamanian Parkinsonism dementia (PD-G)

As they are called, these diseases are seen with a relatively higher incidence on the Pacific Islands of Guam and Rato. These diseases are related and have features of ALS, Parkinson's disease and dementia. Mutations in the TRPM7 gene were found in 25 % of the ALS-G/PD-G patients. The aetiology of ALS-G and PD-G is not elucidated but genetic and environmental factors seem to play a role in their occurrence. Interestingly, the incidence of these diseases is higher in environments that are deficient in Ca^{2+} and Mg^{2+} , like the West Pacific. TRPM7 is ubiquitously distributed in most cells, and provides a pathway for Mg^{2+} , Ca^{2+} , and trace metal ions entry into the cell (Monteilh-Zoller, Hermosura et al. 2003). Studies have shown the important role of Mg^{2+} in cell progression and proliferation (Rubin 2005). The suggested mechanism for these diseases is an aggravation of the Mg^{2+} homeostasis by an increased sensitivity of TRMP7 to inhibition by Mg^{2+} in an Mg^{2+} -deficient environment. This leads to decreased intracellular Mg^{2+} that may in turn contribute to the aetiology of the neurodegenerative diseases (Hermosura, Nayakanti et al. 2005).

Complete congenital stationary night blindness

Congenital stationary night blindness (CSNB) is caused by defective signalling from photoreceptors to bipolar cells, and is characterized by a reduced or absent b-wave and a normal a-wave in the electroretinogram (ERG). Two types can be distinguished, the type 1 where there is a complete absence of rod pathway function (cCSNB) and the type 2 characterized by an impaired rod and cone pathway function (icCSNB). Mutations in the nyctalopin (NYX) and the metabotropic glutamate receptor 6 (GRM6) genes were implicated in cCSNB. Postsynaptic defects in depolarizing or ON bipolar cell signalling was shown to cause cCSNB. TrpM1 was shown to be essential for the ON bipolar cell function, and had expression pattern similar to that of nyctalopin. In addition, screening of patients with cCSNB who are negative for NYX and GRM6 mutation revealed mutations in the TrpM1 gene (van Genderen, Bijveld et al. 2009).

Another recent study has shown an association of loss-of-function nonsynonymous polymorphism in the *TRPV4* gene with human hyponatraemia (Tian, Fu et al. 2009). Hyponatraemia is a disorder linked to disturbances in water balance. TRPV4 is involved in the osmoregulation and is activated by extracellular hypotonicity. As such, changes in TRPV4 structure or function may lead to diseases such as hyponatraemia.

TRP channels are also involved in the mechanism of several pathological conditions. Pain is a pathological entity in which many TRP channels have been implicated. Pain is an unpleasant sensory and emotional experience associated with actual, or potential, tissue damage or described in terms of such damage (International Association for the Study of Pain: IASP). Pain is classified as nociceptive, neuropathic, and psychological depending on the origin.

Several studies have shown the role of members of the TRP superfamily in the detection of acute noxious thermal, mechanical, and chemical stimuli. TRPV1 is the first TRP channels member to be implicated in the genesis of pain. Because of its expression in DRG, trigeminal ganglia, and nodose ganglia, in addition to its activation by heat, acid and pungent vanilloid compounds, TRPV1 have been shown to be a strong candidate for the detection and integration of noxious stimuli. In addition, TRPV1 knockout mice showed reduced response to noxious heat stimuli and complete indifference to pungent vanilloids (Caterina, Leffler et al. 2000). Other TRP

channel knockout mice, including TRPV3, TRPV4, and TRPA1 have shown reduced perception to noxious heat and cold (Moqrich, Hwang et al. 2005; Alessandri-Haber, Dina et al. 2006; Kwan, Allchorne et al. 2006).

Neuropathic pains occur in chronic disease such as trigeminal neuralgia, diabetic neuropathy, post-herpetic neuralgia, late-stage cancer, amputation, or physical nerve damage. Members of the TRP channels superfamily were shown to be involved in the aetiology of neuropathic pain. Among these, TRPV1 and TRPV4 are most studied. Hypersensitivity of TRPV1 leads to thermal allodynia and hyperalgaesia. Another TRP member involved in neuropathic pain is TRPA1 which appears to be overexpressed in inflammation and nerve injury (Katsura, Obata et al. 2006).

Itch is another symptom in which TRP channels are implicated. Itch is an irritating skin sensation causing the desire to scratch. This symptom is seen in several skin disorders, including psoriasis, eczema, and scabies. Some studies have shown the role of TRPV1 in the initiation of itch (Mohapatra, Wang et al. 2003). Other studies have shown that itching sensation may be due to activation of other temperature-sensitive TRP channels expressed in skin, keratinocytes, and sensory fibres including TRPV2, TRPV3, TRPV4, TRPA1, and TRPM8. It has also been shown that pruritogenic compounds such as eicosanoids can potently activate TRPV1 and TRPV4 (Watanabe, Vriens et al. 2003).

TRP channels have been implicated in the pathophysiology of different systemic disorders. Activation of TRP channels can cause firing of action potentials in sensory fibres that is relayed to the spinal cord and can trigger efferent signals, such as autonomous reflexes. Activation of sensory fibres can also be directly translated via axon reflexes into vegetative responses, such as vasodilatation. Thus TRP channels can interfere via multiple pathways with organ function (Nilius 2007). Several TRP channel, especially TRPC and TRPM subfamilies, are involved in the inflammatory process.

The study we present here adds to the growing list of diseases caused by ion channel dysfunction now recognized under channelopathies. We have shown functional evidences that R269C and R269H disrupted TRPV4 channel function, and caused intracellular calcium overload which led to cellular toxicity and death.

4.7 Channelopathies and therapeutic future

Ion channels are proteins involved in many pathological processes. Their function can be regulated by different stimuli, mechanical, environmental or chemical. Therefore, it may be possible to reverse the effect of dysfunctional ion channel in organ systems by using the appropriate regulator. To date, several studies have demonstrated the positive effect of inhibiting or stimulating dysfunctional ion channels.

Different studies have demonstrated the calming role of capsaicin in chronic pain, including post-herpetic neuralgia (Backonja, Wallace et al. 2008) and distal sensory polyneuropathy due to HIV infection (Simpson, Brown et al. 2008). The analgesic action of capsaicin is considered to be the consequence of its inhibitory effect on TRPV1, known to mediate pain. More recently, an oral administration of a novel compound (AS1928370) that is a TRPV1 antagonist was shown to reduce neuropathic pain in rats (Watabiki, Kiso et al. 2010) by inhibiting capsaicin-mediated inward currents.

TRPA1 is also known to mediate pain, and is overexpressed in neighbouring uninjured nerves after nerve injury. An *in vivo* study has shown that a knock down of TRPA1 alleviates cold hyperalgesia after spinal nerve ligation (Katsura, Obata et al. 2006).

Recently, it has been shown that activation of TRPM8 in sensory afferents of neuropathic and chronic pain rat models by either cutaneous or intrathecal application of pharmacological agents or by modest cooling causes inhibition of sensitized pain responses.

In our study, mutations were shown to cause TRPV4 hyperactivation. A recent study has shown the inhibitory role of a small interfering RNA (siRNA) of mRNA levels, protein expression, and function of TRPV4 in DRG (Liu, Bi et al. 2010). Although the study did not investigate the clinical effect of TRPV4 inhibition, the use of synthesized siRNA could serve as potential treatment of TRPV4-related pathological conditions. A previous study had shown that painful peripheral neuropathy induced by taxol can be treated by gene silencing of TRPV4 (Alessandri-Haber, Dina et al. 2004). Another potential compound to try in animal model is RN1734 which is a specific TRPV4 antagonist that we showed block cell toxicity caused by TRPV4 hyperactivation.

To date more than 35 % of marketed drugs target ion channels (Jurkat-Rott, Lerche et al. 2010), therefore, there is a high chance to identify or investigate known TRPV4-blockers that may counteract the effects of the mutations we found here.

4.8 Conclusion

We characterized the clinical, electrophysiological, and pathological features of CMT2C in five families and confirmed the previously reported linkage by performing fine mapping. We were able to narrow down the region of linkage for this disorder from 3.9 Mb to 2.6 Mb. We excluded deletions or duplications in this region by SNP array analysis in three families. We identified five sequence variants in the TRPV4 gene, three in three of the families described here, and two in CMT2-type cohort screening. Heterologous expression studies of two of the variants showed that mutants TRPV4 enhance channel activity leading to intracellular Ca^{2+} overload and cell death. TRPV4 is a cation channel known to play a role in fundamental cellular processes such as osmosensation, temperature sensation and mechanosensation. In this study, we have shown that CMT2C is associated with substitutions at the Arg269, Arg232, and Arg186 residues in the ankyrin repeat domain of the TRPV4 protein.

This work uncovers a previously unrecognized role for TRPV4 in neurons and highlights the importance of this ion channel in normal peripheral nerve function. Together with the observations that disruption of TRPML1 causes the central nervous system lysosomal-storage disease mucopolipidosis type IV (Venkatachalam, Long et al. 2008), and that mutation of Trpc3 causes degeneration of cerebellar neurons in mice (Becker, Oliver et al. 2009), this study emphasizes the importance of TRP channels in the pathogenesis of neurodegenerative diseases. Most surprisingly, our data indicate that distinct alterations in this important ion channel result in strikingly different phenotypes that involve separate organ systems.

To date, there is no disease modifying treatment for CMT 2C or any other hereditary neurological disorder. Identifying new proteins will improve our understanding of common pathways involved in CMTs, and will ultimately provide a basis to finding treatment for these diseases. Because treatment of pain targeting TRPV1 channels is showing satisfactory results, the future is promising for TRPV4-related diseases because several agents that have been shown to modulate TRPV4 function can be studied and tested for therapeutic effects.

4.9 Future directions

Here we describe families with Charcot-Marie-Tooth type 2C that have mutations in the transient receptor potential vanilloid, superfamily, member 4 (*TRPV4*). Many questions remain and future and ongoing studies are focused in the following areas:

1. What is the spectrum of neurological disease caused by *TRPV4* mutations? Since our original study, several groups have reported other mutations in *TRPV4* in both peripheral nerve disease and bone diseases. We have continued to evaluate other individuals who present with forms of CMT2 or distal SMA in order to further define the phenotypic spectrum of disorders associated with *TRPV4* mutations.
2. Why do some *TRPV4* mutations cause peripheral nerve disease and others cause bone disease? Different mutations in *TRPV4* cause forms of inherited skeletal dysplasia and inherited neuropathy, disorders affecting distinct organ systems. However, to date, all the described *TRPV4* mutations appear to cause a gain of protein function resulting in increased constitutive and activated ion channel activity. The observation that the mutations cluster in particular anatomical locations of the *TRPV4* protein suggest that there may be specific interactors and regulators important for *TRPV4* channel activity in each of these organ systems. Our future objectives are to find potential interactors by performing co-immunoprecipitation studies and mass spectrometry.
3. What is the normal function of *TRPV4* in motor neurons?
4. Does *TRPV4* mutation result in peripheral nerve degeneration in animal models and does pharmacological inhibition of *TRPV4* ameliorate these defects? *TRPV4* is an ion channel that is modulated by different stimuli, some of which inhibit its activity. Because the mutations found here lead to *TRPV4* hyperactivation, we plan to test the inhibitory effect of some *TRPV4*-antagonists in CMT2C transgenic animals. For this, we plan to generate a fly and mouse model. Animal models have been used to better understand the pathogenesis of human diseases and to develop treatments for those diseases. To date, many compounds that are used to treat human diseases were developed from animal studies. This allowed researchers to test toxicity of drugs, and check their effect in reversing the disease or some symptoms without harm to human. Successful testing of these compounds in animal models may open the road towards clinical trials with the final objective of therapeutic intervention at patient level.

5 References

- Abu-Elheiga, L., M. M. Matzuk, et al. (2001). "Continuous fatty acid oxidation and reduced fat storage in mice lacking acetyl-CoA carboxylase 2." Science **291**(5513):2613-2616.
- Adams, R. D., Victor, M. (1993). "Diseases of the peripheral nerves." *In: Raymond D. Adams, Maurice Victor, eds, Principles of neurology, 5th edition, McGraw-Hill, Inc.:* pp 408-420.
- Akasaka, Y., T. Nakajima, et al. (1969). "[Familial cases of a new systemic bone disease, hereditary gnatho-diaphyseal sclerosis]." Nippon Seikeigeka Gakkai Zasshi **43**(5):381-394.
- Alessandri-Haber, N., O. A. Dina, et al. (2006). "A transient receptor potential vanilloid 4-dependent mechanism of hyperalgesia is engaged by concerted action of inflammatory mediators." J Neurosci **26**(14):3864-3874.
- Alessandri-Haber, N., O. A. Dina, et al. (2004). "Transient receptor potential vanilloid 4 is essential in chemotherapy-induced neuropathic pain in the rat." J Neurosci **24**(18):4444-4452.
- Antonellis, A., R. E. Ellsworth, et al. (2003). "Glycyl tRNA synthetase mutations in Charcot-Marie-Tooth disease type 2D and distal spinal muscular atrophy type V." Am J Hum Genet **72**(5):1293-1299.
- Arnaud, E., J. Zenker, et al. (2009). "SH3TC2/KIAA1985 protein is required for proper myelination and the integrity of the node of Ranvier in the peripheral nervous system." Proc Natl Acad Sci U S A **106**(41):17528-17533.
- Arniges, M., J. M. Fernandez-Fernandez, et al. (2006). "Human TRPV4 channel splice variants revealed a key role of ankyrin domains in multimerization and trafficking." J Biol Chem **281**(3):1580-1586.
- Audo, I., S. Kohl, et al. (2009). "TRPM1 is mutated in patients with autosomal-recessive complete congenital stationary night blindness." Am J Hum Genet **85**(5):720-729.
- Auer-Grumbach, M., A. Olschewski, et al. (2010). "Alterations in the ankyrin domain of TRPV4 cause congenital distal SMA, scapulooperoneal SMA and HMSN2C." Nat Genet **42**(2):160-164.
- Azzedine, H., A. Bolino, et al. (2003). "Mutations in MTMR13, a new pseudophosphatase homologue of MTMR2 and Sbf1, in two families with an autosomal recessive demyelinating form of Charcot-Marie-Tooth disease associated with early-onset glaucoma." Am J Hum Genet **72**(5): 1141-1153.
- Bach, G. (2001). "Mucopolipidosis type IV." Mol Genet Metab **73**(3):197-203.
- Bach, G., M. B. Webb, et al. (2005). "The frequency of mucopolipidosis type IV in the Ashkenazi Jewish population and the identification of 3 novel MCOLN1 mutations." Hum Mutat **26**(6):591.
- Backonja, M., M. S. Wallace, et al. (2008). "NGX-4010, a high-concentration capsaicin patch, for the treatment of postherpetic neuralgia: a randomised, double-blind study." Lancet Neurol **7**(12):1106-1112.
- Bargal, R., N. Avidan, et al. (2000). "Identification of the gene causing mucopolipidosis type IV." Nat Genet **26**(1):118-123.
- Barhoumi, C., R. Amouri, et al. (2001). "Linkage of a new locus for autosomal recessive axonal form of Charcot-Marie-Tooth disease to chromosome 8q21.3." Neuromuscul Disord **11**(1):27-34.

- Baxter, R. V., K. Ben Othmane, et al. (2002). "Ganglioside-induced differentiation-associated protein-1 is mutant in Charcot-Marie-Tooth disease type 4A/8q21." *Nat Genet* **30**(1):21-22.
- Becker, D., M. Muller, et al. (2008). "The C-terminal domain of TRPV4 is essential for plasma membrane localization." *Mol Membr Biol* **25**(2):139-151.
- Becker, E. B., P. L. Oliver, et al. (2009). "A point mutation in TRPC3 causes abnormal Purkinje cell development and cerebellar ataxia in moonwalker mice." *Proc Natl Acad Sci U S A* **106**(16):6706-6711.
- Beech, D. J., K. Muraki, et al. (2004). "Non-selective cationic channels of smooth muscle and the mammalian homologues of Drosophila TRP." *J Physiol* **559**(Pt 3):685-706.
- Bergoffen, J., S. S. Scherer, et al. (1993). "Connexin mutations in X-linked Charcot-Marie-Tooth disease." *Science* **262**(5142):2039-2042.
- Berridge, M. J., M. D. Bootman, et al. (2003). "Calcium signalling: dynamics, homeostasis and remodelling." *Nat Rev Mol Cell Biol* **4**(7):517-529.
- Bertini, E., J. L. Gadioux, et al. (1989). "Distal infantile spinal muscular atrophy associated with paralysis of the diaphragm: a variant of infantile spinal muscular atrophy." *Am J Med Genet* **33**(3):328-335.
- Bienfait, H. M., F. Baas, et al. (2007). "Phenotype of Charcot-Marie-Tooth disease Type 2." *Neurology* **68**(20):1658-1667.
- Birouk, N., H. Azzedine, et al. (2003). "Phenotypical features of a Moroccan family with autosomal recessive Charcot-Marie-Tooth disease associated with the S194X mutation in the GDAP1 gene." *Arch Neurol* **60**(4):598-604.
- Boerkoel, C. F., H. Takashima, et al. (2002). "Charcot-Marie-Tooth disease and related neuropathies: mutation distribution and genotype-phenotype correlation." *Ann Neurol* **51**(2):190-201.
- Bolduc, V., G. Marlow, et al. (2010). "Recessive mutations in the putative calcium-activated chloride channel Anoctamin 5 cause proximal LGMD2L and distal MMD3 muscular dystrophies." *Am J Hum Genet* **86**(2):213-221.
- Bolino, A., M. Muglia, et al. (2000). "Charcot-Marie-Tooth type 4B is caused by mutations in the gene encoding myotubularin-related protein-2." *Nat Genet* **25**(1):17-19.
- Bonne, G., E. Mercuri, et al. (2000). "Clinical and molecular genetic spectrum of autosomal dominant Emery-Dreifuss muscular dystrophy due to mutations of the lamin A/C gene." *Ann Neurol* **48**(2):170-180.
- Bouhouche, A., A. Benomar, et al. (1999). "A locus for an axonal form of autosomal recessive Charcot-Marie-Tooth disease maps to chromosome 1q21.2-q21.3." *Am J Hum Genet* **65**(3):722-727.
- Boulay, G., D. M. Brown, et al. (1999). "Modulation of Ca(2+) entry by polypeptides of the inositol 1,4, 5-trisphosphate receptor (IP3R) that bind transient receptor potential (TRP): evidence for roles of TRP and IP3R in store depletion-activated Ca(2+) entry." *Proc Natl Acad Sci U S A* **96**(26):14955-14960.
- Boulay, G., X. Zhu, et al. (1997). "Cloning and expression of a novel mammalian homolog of Drosophila transient receptor potential (Trp) involved in calcium entry secondary to activation of receptors coupled by the Gq class of G protein." *J Biol Chem* **272**(47):29672-29680.
- Brust, J. C., R. E. Lovelace, et al. (1978). "Clinical and electrodiagnostic features of Charcot-Marie-Tooth syndrome." *Acta Neurol Scand Suppl* **68**:1-142.

- Bush, E. W., D. B. Hood, et al. (2006). "Canonical transient receptor potential channels promote cardiomyocyte hypertrophy through activation of calcineurin signaling." J Biol Chem **281**(44):33487-33496.
- Camacho, N., D. Krakow, et al. (2010). "Dominant TRPV4 mutations in nonlethal and lethal metatropic dysplasia." Am J Med Genet A **152A**(5):1169-1177.
- Carriedo, S. G., H. Z. Yin, et al. (1996). "Motor neurons are selectively vulnerable to AMPA/kainate receptor-mediated injury in vitro." J Neurosci **16**(13):4069-4079.
- Caterina, M. J., A. Leffler, et al. (2000). "Impaired nociception and pain sensation in mice lacking the capsaicin receptor." Science **288**(5464):306-313.
- Caterina, M. J., M. A. Schumacher, et al. (1997). "The capsaicin receptor: a heat-activated ion channel in the pain pathway." Nature **389**(6653):816-824.
- Charcot, J.-M., Marie, P. (1886). "Sur une forme particulière d'atrophie musculaire progressive, souvent familiale, débutant par les pieds et les jambes, et atteignant plus tard les mains." Revue Med.:97-138.
- Chen, D. H., Y. Sul, et al. (2010). "CMT2C with vocal cord paresis associated with short stature and mutations in the TRPV4 gene." Neurology **75**(22):1968-1975.
- Chow, C. Y., Y. Zhang, et al. (2007). "Mutation of FIG4 causes neurodegeneration in the pale tremor mouse and patients with CMT4J." Nature **448**(7149):68-72.
- Chubanov, V., S. Waldegger, et al. (2004). "Disruption of TRPM6/TRPM7 complex formation by a mutation in the TRPM6 gene causes hypomagnesemia with secondary hypocalcemia." Proc Natl Acad Sci U S A **101**(9):2894-2899.
- Chung, K. W., S. M. Kim, et al. (2008). "A novel GDAP1 Q218E mutation in autosomal dominant Charcot-Marie-Tooth disease." J Hum Genet **53**(4):360-364.
- Clark, K., J. Middelbeek, et al. (2008). "Interplay between TRP channels and the cytoskeleton in health and disease." Eur J Cell Biol **87**(8-9):631-640.
- Colomer, J., R. Gooding, et al. (2006). "Clinical spectrum of CMT4C disease in patients homozygous for the p.Arg1109X mutation in SH3TC2." Neuromuscul Disord **16**(7):449-453.
- Cox, J. J., F. Reimann, et al. (2006). "An SCN9A channelopathy causes congenital inability to experience pain." Nature **444**(7121):894-898.
- Crossman, A. R., Neary D. (2010a). "Cells of the nervous system. *In* Neuroanatomy: An illustrated colour text 4th ed, eds Alan R. Crossman and David Neary, Churchill Livingstone Elsevier, London." pp 29-32.
- Crossman A. R., Neary D. (2010b). "Introduction and overview. *In* Neuroanatomy: An illustrated colour text 4th ed, eds Alan R. Crossman and David Neary, Churchill Livingstone Elsevier, London." pp 1-28.
- Crossman, A. R., Neary D. (2010c). "Spinal cord. *In* Neuroanatomy: An illustrated colour text 4th ed, eds Alan R. Crossman and David Neary, Churchill Livingstone Elsevier, London." pp 67-86.
- Cuajungco, M. P., C. Grimm, et al. (2006). "PACSINs bind to the TRPV4 cation channel. PACSIN 3 modulates the subcellular localization of TRPV4." J Biol Chem **281**(27):18753-18762.
- Cuesta, A., L. Pedrola, et al. (2002). "The gene encoding ganglioside-induced differentiation-associated protein 1 is mutated in axonal Charcot-Marie-Tooth type 4A disease." Nat Genet **30**(1):22-25.

- Dai, J., O. H. Kim, et al. (2010). "Novel and recurrent TRPV4 mutations and their association with distinct phenotypes within the TRPV4 dysplasia family." J Med Genet **47**(10):704-709.
- Davis, C. J., W. G. Bradley, et al. (1978). "The peroneal muscular atrophy syndrome: clinical, genetic, electrophysiological and nerve biopsy studies. I. Clinical, genetic and electrophysiological findings and classification." J Genet Hum **26**(4):311-349.
- De Sandre-Giovannoli, A., M. Chaouch, et al. (2002). "Homozygous defects in LMNA, encoding lamin A/C nuclear-envelope proteins, cause autosomal recessive axonal neuropathy in human (Charcot-Marie-Tooth disorder type 2) and mouse." Am J Hum Genet **70**(3):726-736.
- Dearborn, G. V. (1932). "A case of congenital general pure analgesia." J Nerv Ment Dis **75**:612-615
- Déjérine J., S. J. (1893). "Sur la névrite: interstitielle, hypertrophique et progressive de l'enfance." C. R. Soc. Biol. (Paris) **43**:63.
- Delague, V., A. Jacquier, et al. (2007). "Mutations in FGD4 encoding the Rho GDP/GTP exchange factor FRABIN cause autosomal recessive Charcot-Marie-Tooth type 4H." Am J Hum Genet **81**(1):1-16.
- Delany, N. S., M. Hurlle, et al. (2001). "Identification and characterization of a novel human vanilloid receptor-like protein, VRL-2." Physiol Genomics **4**(3):165-174.
- Delmas, P. (2004). "Polycystins: from mechanosensation to gene regulation." Cell **118**(2):145-148.
- DeLong, R. and T. Siddique (1992). "A large New England kindred with autosomal dominant neurogenic scapulo-peroneal amyotrophy with unique features." Arch Neurol **49**(9):905-908.
- Deng, H. X., C. J. Klein, et al. (2010). "Scapulo-peroneal spinal muscular atrophy and CMT2C are allelic disorders caused by alterations in TRPV4." Nat Genet **42**(2):165-169.
- Dib-Hajj, S. D., A. M. Rush, et al. (2005). "Gain-of-function mutation in Nav1.7 in familial erythromelalgia induces bursting of sensory neurons." Brain **128**(Pt 8):1847-1854.
- Dietrich, A., M. Mederos y Schnitzler, et al. (2003). "N-linked protein glycosylation is a major determinant for basal TRPC3 and TRPC6 channel activity." J Biol Chem **278**(48):47842-47852.
- Donaghy, M. and R. Kennett (1999). "Varying occurrence of vocal cord paralysis in a family with autosomal dominant hereditary motor and sensory neuropathy." J Neurol **246**(7):552-555.
- Dubourg, O., S. Tardieu, et al. (2001). "Clinical, electrophysiological and molecular genetic characteristics of 93 patients with X-linked Charcot-Marie-Tooth disease." Brain **124**(Pt 10):1958-1967.
- Duncan, L. M., J. Deeds, et al. (1998). "Down-regulation of the novel gene melastatin correlates with potential for melanoma metastasis." Cancer Res **58**(7):1515-1520.
- Dyck P.J., C. P., Lebo R., and Carney J.A. (1993). "Hereditary motor and sensory neuropathies." In Dyck PJ, Thomas PK, Griffin JW, Low PA, Poduslo JF, eds., Peripheral Neuropathy, 3rd ed., WB Saunders, Philadelphia: pp 1094-1136.
- Dyck P.J., C. P., Lebo R., Carney J.A. (1993). "Hereditary motor and sensory neuropathies." In Dyck PJ, Thomas PK, Griffin JW, Low PA, Poduslo JF,

- eds., Peripheral Neuropathy, 3rd ed., WB Saunders, Philadelphia: pp 1094-1136.
- Dyck, P. J. and E. H. Lambert (1968). "Lower motor and primary sensory neuron diseases with peroneal muscular atrophy. I. Neurologic, genetic, and electrophysiologic findings in hereditary polyneuropathies." Arch Neurol **18**(6):603-618.
- Dyck, P. J., W. J. Litchy, et al. (1994). "Hereditary motor and sensory neuropathy with diaphragm and vocal cord paresis." Ann Neurol **35**(5):608-615.
- Emery, A. E. (1989). "Emery-Dreifuss syndrome." J Med Genet **26**(10):637-641.
- England, A. C. and D. Denny-Brown (1952). "Severe sensory changes, and trophic disorder, in peroneal muscular atrophy (Charcot-Marie-Tooth type)." AMA Arch Neurol Psychiatry **67**(1):1-22.
- Estacion, M., S. Li, et al. (2004). "Activation of human TRPC6 channels by receptor stimulation." J Biol Chem **279**(21):22047-22056.
- Everett, K. V., B. A. Chioza, et al. (2009). "Infantile hypertrophic pyloric stenosis: evaluation of three positional candidate genes, TRPC1, TRPC5 and TRPC6, by association analysis and re-sequencing." Hum Genet **126**(6):819-831.
- Evgrafov, O. V., I. Mersiyanova, et al. (2004). "Mutant small heat-shock protein 27 causes axonal Charcot-Marie-Tooth disease and distal hereditary motor neuropathy." Nat Genet **36**(6):602-606.
- Facer, P., M. A. Casula, et al. (2007). "Differential expression of the capsaicin receptor TRPV1 and related novel receptors TRPV3, TRPV4 and TRPM8 in normal human tissues and changes in traumatic and diabetic neuropathy." BMC Neurol **7**:11.
- Farrer, M. J., M. M. Hulihan, et al. (2009). "DCTN1 mutations in Perry syndrome." Nat Genet **41**(2):163-165.
- Felten D. L., S. A. N. (2010). "Peripheral nervous system." In: David L. Felten, Anil N. Shetty, eds, Netter's Atlas of Neuroscience, 2nd edition, Saunders, Philadelphia: pp 135-206.
- Fertleman, C. R., M. D. Baker, et al. (2006). "SCN9A mutations in paroxysmal extreme pain disorder: allelic variants underlie distinct channel defects and phenotypes." Neuron **52**(5):767-774.
- Fleury, P. and G. Hageman (1985). "A dominantly inherited lower motor neuron disorder presenting at birth with associated arthrogryposis." J Neurol Neurosurg Psychiatry **48**(10):1037-1048.
- Flockerzi, V. (2007). "An introduction on TRP channels." In Transient Receptor Potential (TRP) channels, eds. Veit Flockerzi and Bernd Nilius, Springer Berlin Heidelberg New York: pp 1-19.
- Fontaine, G., P. Maroteaux, et al. (1975). "[Pure spondylar dysplasia or brachyolmy. Apropos of a case]." Arch Fr Pediatr **32**(8):695-708.
- Gabreels-Festen, A., S. van Beersum, et al. (1999). "Study on the gene and phenotypic characterisation of autosomal recessive demyelinating motor and sensory neuropathy (Charcot-Marie-Tooth disease) with a gene locus on chromosome 5q23-q33." J Neurol Neurosurg Psychiatry **66**(5):569-574.
- Garcia, C. A., R. E. Malamut, et al. (1995). "Clinical variability in two pairs of identical twins with the Charcot-Marie-Tooth disease type 1A duplication." Neurology **45**(11):2090-2093.
- Gardner, J. and P. Beighton (1994). "Brachyolmia: an autosomal dominant form." Am J Med Genet **49**(3):308-312.

- Gaudet, R. (2008). "TRP channels entering the structural era." *J Physiol* **586**(Pt 15):3565-3575.
- Gemignani, F. and A. Marbini (2001). "Charcot-Marie-Tooth disease (CMT): distinctive phenotypic and genotypic features in CMT type 2." *J Neurol Sci* **184**(1):1-9.
- Genevieve, D., M. Le Merrer, et al. (2008). "Revisiting metatropic dysplasia: presentation of a series of 19 novel patients and review of the literature." *Am J Med Genet A* **146A**(8):992-996.
- Gevaert, T., J. Vriens, et al. (2007). "Deletion of the transient receptor potential cation channel TRPV4 impairs murine bladder voiding." *J Clin Invest* **117**(11):3453-3462.
- Gingras, H., O. Cases, et al. (2005). "Biochemical characterization of the mammalian Cux2 protein." *Gene* **344**:273-285.
- Gispert, S., R. Twells, et al. (1993). "Chromosomal assignment of the second locus for autosomal dominant cerebellar ataxia (SCA2) to chromosome 12q23-24.1." *Nat Genet* **4**(3):295-299.
- Goldberg, Y. P., J. MacFarlane, et al. (2007). "Loss-of-function mutations in the Nav1.7 gene underlie congenital indifference to pain in multiple human populations." *Clin Genet* **71**(4):311-319.
- Gomez, T. S., M. J. Hamann, et al. (2005). "Dynamin 2 regulates T cell activation by controlling actin polymerization at the immunological synapse." *Nat Immunol* **6**(3):261-270.
- Grandis, M., T. Vigo, et al. (2008). "Different cellular and molecular mechanisms for early and late-onset myelin protein zero mutations." *Hum Mol Genet* **17**(13):1877-1889.
- Guilak, F., H. A. Leddy, et al. (2010). "Transient receptor potential vanilloid 4: The sixth sense of the musculoskeletal system?" *Ann N Y Acad Sci* **1192**:404-409.
- Guilbot, A., A. Williams, et al. (2001). "A mutation in periaxin is responsible for CMT4F, an autosomal recessive form of Charcot-Marie-Tooth disease." *Hum Mol Genet* **10**(4):415-421.
- Guillet, V., N. Gueguen, et al. (2010). "Adenine nucleotide translocase is involved in a mitochondrial coupling defect in MFN2-related Charcot-Marie-Tooth type 2A disease." *Neurogenetics* **11**(1):127-133.
- Guler, A. D., H. Lee, et al. (2002). "Heat-evoked activation of the ion channel, TRPV4." *J Neurosci* **22**(15):6408-6414.
- Hardie, R. C. and B. Minke (1993). "Novel Ca²⁺ channels underlying transduction in Drosophila photoreceptors: implications for phosphoinositide-mediated Ca²⁺ mobilization." *Trends Neurosci* **16**(9):371-376.
- Harding, A. E. and P. K. Thomas (1980). "The clinical features of hereditary motor and sensory neuropathy types I and II." *Brain* **103**(2):259-280.
- Hartmann, J. and A. Konnerth (2005). "Determinants of postsynaptic Ca²⁺ signaling in Purkinje neurons." *Cell Calcium* **37**(5):459-466.
- Hayasaka, K., M. Himoro, et al. (1993). "Charcot-Marie-Tooth neuropathy type 1B is associated with mutations of the myelin P0 gene." *Nat Genet* **5**(1):31-34.
- Hermosura, M. C., H. Nayakanti, et al. (2005). "A TRPM7 variant shows altered sensitivity to magnesium that may contribute to the pathogenesis of two Guamanian neurodegenerative disorders." *Proc Natl Acad Sci U S A* **102**(32):11510-11515.
- Hirano, R., H. Takashima, et al. (2004). "SET binding factor 2 (SBF2) mutation causes CMT4B with juvenile onset glaucoma." *Neurology* **63**(3):577-580.

- Hoefen, R. J. and B. C. Berk (2006). "The multifunctional GIT family of proteins." J Cell Sci **119**(Pt 8):1469-1475.
- Hofmann, T., A. G. Obukhov, et al. (1999). "Direct activation of human TRPC6 and TRPC3 channels by diacylglycerol." Nature **397**(6716):259-263.
- Hofmann, T., M. Schaefer, et al. (2000). "Cloning, expression and subcellular localization of two novel splice variants of mouse transient receptor potential channel 2." Biochem J **351**(Pt 1):115-122.
- Holinger, P. C., D. M. Vuckovich, et al. (1979). "Bilateral abductor vocal cord paralysis in Charcot-Marie-Tooth disease." Ann Otol Rhinol Laryngol **88**(2 Pt 1):205-209.
- Horton, W. A., L. O. Langer, et al. (1983). "Brachyolmia, recessive type (Hobaek): a clinical, radiographic, and histochemical study." Am J Med Genet **16**(2):201-211.
- Huttner, I. G., M. L. Kennerson, et al. (2006). "Proof of genetic heterogeneity in X-linked Charcot-Marie-Tooth disease." Neurology **67**(11):2016-2021.
- Ince, P., N. Stout, et al. (1993). "Parvalbumin and calbindin D-28k in the human motor system and in motor neuron disease." Neuropathol Appl Neurobiol **19**(4):291-299.
- Ionasescu, V. V., J. Trofatter, et al. (1991). "Heterogeneity in X-linked recessive Charcot-Marie-Tooth neuropathy." Am J Hum Genet **48**(6):1075-1083.
- Irobi, J., P. De Jonghe, et al. (2004). "Molecular genetics of distal hereditary motor neuropathies." Hum Mol Genet **13 Spec No 2**:R195-202.
- Isozumi, K., R. DeLong, et al. (1996). "Linkage of scapuloperoneal spinal muscular atrophy to chromosome 12q24.1-q24.31." Hum Mol Genet **5**(9):1377-1382.
- Jacobsen, N. J., G. Elvidge, et al. (2001). "CUX2, a potential regulator of NCAM expression: genomic characterization and analysis as a positional candidate susceptibility gene for bipolar disorder." Am J Med Genet **105**(3):295-300.
- Jin, X., J. Touhey, et al. (2006). "Structure of the N-terminal ankyrin repeat domain of the TRPV2 ion channel." J Biol Chem **281**(35):25006-25010.
- Jordanova, A., P. De Jonghe, et al. (2003). "Mutations in the neurofilament light chain gene (NEFL) cause early onset severe Charcot-Marie-Tooth disease." Brain **126**(Pt 3):590-597.
- Jordanova, A., J. Irobi, et al. (2006). "Disrupted function and axonal distribution of mutant tyrosyl-tRNA synthetase in dominant intermediate Charcot-Marie-Tooth neuropathy." Nat Genet **38**(2):197-202.
- Jordanova, A., F. P. Thomas, et al. (2003). "Dominant intermediate Charcot-Marie-Tooth type C maps to chromosome 1p34-p35." Am J Hum Genet **73**(6):1423-1430.
- Jurkat-Rott, K., H. Lerche, et al. (2010). "Hereditary channelopathies in neurology." Adv Exp Med Biol **686**:305-334.
- Kalaydjieva, L., D. Gresham, et al. (2000). "N-myc downstream-regulated gene 1 is mutated in hereditary motor and sensory neuropathy-Lom." Am J Hum Genet **67**(1):47-58.
- Kannu, P., S. Aftimos, et al. (2007). "Metatropic dysplasia: clinical and radiographic findings in 11 patients demonstrating long-term natural history." Am J Med Genet A **143A**(21):2512-2522.
- Katsura, H., K. Obata, et al. (2006). "Antisense knock down of TRPA1, but not TRPM8, alleviates cold hyperalgesia after spinal nerve ligation in rats." Exp Neurol **200**(1):112-123.

- Kedei, N., T. Szabo, et al. (2001). "Analysis of the native quaternary structure of vanilloid receptor 1." *J Biol Chem* **276**(30):28613-28619.
- Kennerson, M. L., D. Zhu, et al. (2001). "Dominant intermediate Charcot-Marie-Tooth neuropathy maps to chromosome 19p12-p13.2." *Am J Hum Genet* **69**(4):883-888.
- Kessali, M., R. Zemmouri, et al. (1997). "A clinical, electrophysiologic, neuropathologic, and genetic study of two large Algerian families with an autosomal recessive demyelinating form of Charcot-Marie-Tooth disease." *Neurology* **48**(4):867-873.
- Kim, H. J., K. M. Sohn, et al. (2007). "Mutations in PRPS1, which encodes the phosphoribosyl pyrophosphate synthetase enzyme critical for nucleotide biosynthesis, cause hereditary peripheral neuropathy with hearing loss and optic neuropathy (cmtx5)." *Am J Hum Genet* **81**(3):552-558.
- Kim, J., Y. D. Chung, et al. (2003). "A TRPV family ion channel required for hearing in *Drosophila*." *Nature* **424**(6944):81-84.
- Klein, C. J., J. M. Cunningham, et al. (2003). "The gene for HMSN2C maps to 12q23-24: a region of neuromuscular disorders." *Neurology* **60**(7):1151-1156.
- Kleopa, K. A., E. Zamba-Papanicolaou, et al. (2006). "Phenotypic and cellular expression of two novel connexin32 mutations causing CMT1X." *Neurology* **66**(3):396-402.
- Kottgen, M., B. Buchholz, et al. (2008). "TRPP2 and TRPV4 form a polymodal sensory channel complex." *J Cell Biol* **182**(3):437-447.
- Kovach, M. J., J. P. Lin, et al. (1999). "A unique point mutation in the PMP22 gene is associated with Charcot-Marie-Tooth disease and deafness." *Am J Hum Genet* **64**(6):1580-1593.
- Krajewski, K. M., R. A. Lewis, et al. (2000). "Neurological dysfunction and axonal degeneration in Charcot-Marie-Tooth disease type 1A." *Brain* **123**(Pt 7):1516-1527.
- Krakow, D., J. Vriens, et al. (2009). "Mutations in the gene encoding the calcium-permeable ion channel TRPV4 produce spondylometaphyseal dysplasia, Kozłowski type and metatropic dysplasia." *Am J Hum Genet* **84**(3):307-315.
- Kriz, W. (2005). "TRPC6 - a new podocyte gene involved in focal segmental glomerulosclerosis." *Trends Mol Med* **11**(12):527-530.
- Kruglyak, L., M. J. Daly, et al. (1996). "Parametric and nonparametric linkage analysis: a unified multipoint approach." *Am J Hum Genet* **58**(6):1347-1363.
- Kruse, M., E. Schulze-Bahr, et al. (2009). "Impaired endocytosis of the ion channel TRPM4 is associated with human progressive familial heart block type I." *J Clin Invest* **119**(9):2737-2744.
- Kwan, K. Y., A. J. Allchorne, et al. (2006). "TRPA1 contributes to cold, mechanical, and chemical nociception but is not essential for hair-cell transduction." *Neuron* **50**(2):277-289.
- Lachman, R. S. (2007). "Metabolic disorders and Skeletal dysplasias." *In Taybi and Lachman's radiology of syndromes* Fifth Edition, St Louis: Mosby-Year Book: pp 1080-1081.
- Landoure, G., A. A. Zdebik, et al. (2010). "Mutations in TRPV4 cause Charcot-Marie-Tooth disease type 2C." *Nat Genet* **42**(2):170-174.
- LaPlante, J. M., J. Falardeau, et al. (2002). "Identification and characterization of the single channel function of human mucolipin-1 implicated in mucopolipidosis type IV, a disorder affecting the lysosomal pathway." *FEBS Lett* **532**(1-2):183-187.

- LaPlante, J. M., C. P. Ye, et al. (2004). "Functional links between mucolipin-1 and Ca²⁺-dependent membrane trafficking in mucopolidosis IV." Biochem Biophys Res Commun **322**(4):1384-1391.
- Latour, P., C. Thauvin-Robinet, et al. (2010). "A major determinant for binding and aminoacylation of tRNA(Ala) in cytoplasmic Alanyl-tRNA synthetase is mutated in dominant axonal Charcot-Marie-Tooth disease." Am J Hum Genet **86**(1):77-82.
- Launay, P., A. Fleig, et al. (2002). "TRPM4 is a Ca²⁺-activated nonselective cation channel mediating cell membrane depolarization." Cell **109**(3):397-407.
- Leal, A., K. Huehne, et al. (2009). "Identification of the variant Ala335Val of MED25 as responsible for CMT2B2: molecular data, functional studies of the SH3 recognition motif and correlation between wild-type MED25 and PMP22 RNA levels in CMT1A animal models." Neurogenetics **10**(4):375-376.
- Leal, A., B. Morera, et al. (2001). "A second locus for an axonal form of autosomal recessive Charcot-Marie-Tooth disease maps to chromosome 19q13.3." Am J Hum Genet **68**(1):269-274.
- Leet, A. I., J. S. Sampath, et al. (2006). "Cervical spinal stenosis in metatropic dysplasia." J Pediatr Orthop **26**(3):347-352.
- Lewis, R. A., A. J. Sumner, et al. (2000). "Electrophysiological features of inherited demyelinating neuropathies: A reappraisal in the era of molecular diagnosis." Muscle Nerve **23**(10):1472-1487.
- Li, X., Y. Luo, et al. (2005). "Polycystin-1 and polycystin-2 regulate the cell cycle through the helix-loop-helix inhibitor Id2." Nat Cell Biol **7**(12):1202-1212.
- Li, Z., P. I. Sergouniotis, et al. (2009). "Recessive mutations of the gene TRPM1 abrogate ON bipolar cell function and cause complete congenital stationary night blindness in humans." Am J Hum Genet **85**(5):711-719.
- Liapi, A. and J. N. Wood (2005). "Extensive co-localization and heteromultimer formation of the vanilloid receptor-like protein TRPV2 and the capsaicin receptor TRPV1 in the adult rat cerebral cortex." Eur J Neurosci **22**(4):825-834.
- Liedtke, W., Y. Choe, et al. (2000). "Vanilloid receptor-related osmotically activated channel (VR-OAC), a candidate vertebrate osmoreceptor." Cell **103**(3):525-535.
- Lin, X., B. Antalffy, et al. (2000). "Polyglutamine expansion down-regulates specific neuronal genes before pathologic changes in SCA1." Nat Neurosci **3**(2):157-163.
- Lishko, P. V., E. Procko, et al. (2007). "The ankyrin repeats of TRPV1 bind multiple ligands and modulate channel sensitivity." Neuron **54**(6):905-918.
- Liu, T. T., H. S. Bi, et al. (2010). "Inhibition of the expression and function of TRPV4 by RNA interference in dorsal root ganglion." Neurol Res **32**(5):466-471.
- Loftus, T. M., D. E. Jaworsky, et al. (2000). "Reduced food intake and body weight in mice treated with fatty acid synthase inhibitors." Science **288**(5475):2379-2381.
- Lu, G., D. Henderson, et al. (2005). "TRPV1b, a functional human vanilloid receptor splice variant." Mol Pharmacol **67**(4):1119-1127.
- Lupo, V., M. I. Galindo, et al. (2009). "Missense mutations in the SH3TC2 protein causing Charcot-Marie-Tooth disease type 4C affect its localization in the plasma membrane and endocytic pathway." Hum Mol Genet **18**(23):4603-4614.

- Lupski, J. R., R. M. de Oca-Luna, et al. (1991). "DNA duplication associated with Charcot-Marie-Tooth disease type 1A." Cell **66**(2):219-232.
- Luzio, J. P., V. Poupon, et al. (2003). "Membrane dynamics and the biogenesis of lysosomes." Mol Membr Biol **20**(2):141-154.
- Mace, M., E. Williamson, et al. (1978). "Autosomal dominantly inherited adductor laryngeal paralysis--a new syndrome with a suggestion of linkage to HLA." Clin Genet **14**(5):265-270.
- Mandell, F., J. Folkman, et al. (1977). "Erythromelalgia." Pediatrics **59**(1):45-48.
- Maroteaux, P., J. Spranger, et al. (1966). "[Metatrophic dwarfism]." Arch Kinderheilkd **173**(3):211-226.
- Massion-Verniory L, D. E., and Potvin A. M (1946). "Rétinite pigmentaire familiale compliquée d'une amyotrophie neurale." Rev. Neurol. (Paris) **78**:561.
- Mattson, M. P. (2007). "Calcium and neurodegeneration." Aging Cell **6**(3):337-350.
- McEntagart, M., N. Norton, et al. (2001). "Localization of the gene for distal hereditary motor neuronopathy VII (dHMN-VII) to chromosome 2q14." Am J Hum Genet **68**(5):1270-1276.
- McEntagart, M. E., S. L. Reid, et al. (2005). "Confirmation of a hereditary motor and sensory neuropathy IIC locus at chromosome 12q23-q24." Ann Neurol **57**(2):293-297.
- McLaughlin, H. M., R. Sakaguchi, et al. (2010). "Compound heterozygosity for loss-of-function lysyl-tRNA synthetase mutations in a patient with peripheral neuropathy." Am J Hum Genet **87**(4):560-566.
- Meier, C., R. Dermietzel, et al. (2004). "Connexin32-containing gap junctions in Schwann cells at the internodal zone of partial myelin compaction and in Schmidt-Lanterman incisures." J Neurosci **24**(13):3186-3198.
- Michailov, G. V., M. W. Sereda, et al. (2004). "Axonal neuregulin-1 regulates myelin sheath thickness." Science **304**(5671):700-703.
- Michiels, J. J., R. H. te Morsche, et al. (2005). "Autosomal dominant erythromelalgia associated with a novel mutation in the voltage-gated sodium channel alpha subunit Nav1.7." Arch Neurol **62**(10):1587-1590.
- Mochizuki, T., G. Wu, et al. (1996). "PKD2, a gene for polycystic kidney disease that encodes an integral membrane protein." Science **272**(5266):1339-1342.
- Modregger, J., N. A. DiProspero, et al. (2002). "PACSIN 1 interacts with huntingtin and is absent from synaptic varicosities in presymptomatic Huntington's disease brains." Hum Mol Genet **11**(21):2547-2558.
- Mohapatra, D. P., S. Y. Wang, et al. (2003). "A tyrosine residue in TM6 of the Vanilloid Receptor TRPV1 involved in desensitization and calcium permeability of capsaicin-activated currents." Mol Cell Neurosci **23**(2):314-324.
- Monteilh-Zoller, M. K., M. C. Hermosura, et al. (2003). "TRPM7 provides an ion channel mechanism for cellular entry of trace metal ions." J Gen Physiol **121**(1):49-60.
- Montell, C. and G. M. Rubin (1989). "Molecular characterization of the *Drosophila* trp locus: a putative integral membrane protein required for phototransduction." Neuron **2**(4):1313-1323.
- Moqrich, A., S. W. Hwang, et al. (2005). "Impaired thermosensation in mice lacking TRPV3, a heat and camphor sensor in the skin." Science **307**(5714):1468-1472.

- Movahed, P., B. A. Jonsson, et al. (2005). "Endogenous unsaturated C18 N-acylethanolamines are vanilloid receptor (TRPV1) agonists." J Biol Chem **280**(46):38496-38504.
- Muchir, A., G. Bonne, et al. (2000). "Identification of mutations in the gene encoding lamins A/C in autosomal dominant limb girdle muscular dystrophy with atrioventricular conduction disturbances (LGMD1B)." Hum Mol Genet **9**(9):1453-1459.
- Mutai, H. and S. Heller (2003). "Vertebrate and invertebrate TRPV-like mechanoreceptors." Cell Calcium **33**(5-6):471-478.
- Nakamura, M., R. Sanuki, et al. (2010). "TRPM1 mutations are associated with the complete form of congenital stationary night blindness." Mol Vis **16**:425-437.
- Nauli, S. M., Y. Kawanabe, et al. (2008). "Endothelial cilia are fluid shear sensors that regulate calcium signaling and nitric oxide production through polycystin-1." Circulation **117**(9):1161-1171.
- Nelis, E., J. Berciano, et al. (2004). "Autosomal dominant axonal Charcot-Marie-Tooth disease type 2 (CMT2G) maps to chromosome 12q12-q13.3." J Med Genet **41**(3):193-197.
- Nelis, E., S. Erdem, et al. (2002). "Mutations in GDAP1: autosomal recessive CMT with demyelination and axonopathy." Neurology **59**(12):1865-1872.
- Nelis, E., C. Van Broeckhoven, et al. (1996). "Estimation of the mutation frequencies in Charcot-Marie-Tooth disease type 1 and hereditary neuropathy with liability to pressure palsies: a European collaborative study." Eur J Hum Genet **4**(1):25-33.
- Niemann, A., M. Ruegg, et al. (2005). "Ganglioside-induced differentiation associated protein 1 is a regulator of the mitochondrial network: new implications for Charcot-Marie-Tooth disease." J Cell Biol **170**(7):1067-1078.
- Niemann, S., M. W. Sereda, et al. (2000). "Uncoupling of myelin assembly and schwann cell differentiation by transgenic overexpression of peripheral myelin protein 22." J Neurosci **20**(11):4120-4128.
- Nilius, B. (2007). "TRP channels in disease." Biochim Biophys Acta **1772**(8):805-812.
- Nilius, B., G. Droogmans, et al. (2003). "Transient receptor potential channels in endothelium: solving the calcium entry puzzle?" Endothelium **10**(1):5-15.
- Nilius, B. and G. Owsianik (2010). "Channelopathies converge on TRPV4." Nat Genet **42**(2):98-100.
- Nilius, B., G. Owsianik, et al. (2008). "Transient receptor potential channels meet phosphoinositides." EMBO J **27**(21):2809-2816.
- Nilius, B., J. Prenen, et al. (2003). "Voltage dependence of the Ca²⁺-activated cation channel TRPM4." J Biol Chem **278**(33):30813-30820.
- Nilius, B., J. Prenen, et al. (2005). "Regulation of the Ca²⁺ sensitivity of the nonselective cation channel TRPM4." J Biol Chem **280**(8):6423-6433.
- Nilius, B., J. Prenen, et al. (2001). "Differential activation of the volume-sensitive cation channel TRP12 (OTRPC4) and volume-regulated anion currents in HEK-293 cells." Pflugers Arch **443**(2):227-233.
- Nilius, B., K. Talavera, et al. (2005). "Gating of TRP channels: a voltage connection?" J Physiol **567**(Pt 1):35-44.
- Nilius, B., J. Vriens, et al. (2004). "TRPV4 calcium entry channel: a paradigm for gating diversity." Am J Physiol Cell Physiol **286**(2):C195-205.

- Nishimura, G., J. Dai, et al. (2010). "Spondylo-epiphyseal dysplasia, Maroteaux type (pseudo-Morquio syndrome type 2), and parastremmatic dysplasia are caused by TRPV4 mutations." Am J Med Genet A **152A**(6):1443-1449.
- Novelli, G., A. Muchir, et al. (2002). "Mandibuloacral dysplasia is caused by a mutation in LMNA-encoding lamin A/C." Am J Hum Genet **71**(2):426-431.
- Nural, M. S., H. B. Diren, et al. (2006). "Kozlowski type spondylometaphyseal dysplasia: a case report with literature review." Diagn Interv Radiol **12**(2):70-73.
- Ola H Skjeldal, O. S., Sigvald Refsum (1993). "Phytanic acid storage disease." In Dyck PJ, Thomas PK, Griffin JW, Low PA, Poduslo JF, eds., Peripheral Neuropathy, 3rd ed., WB Saunders, Philadelphia: pp 1149-1160.
- Omori, Y., M. Mesnil, et al. (1996). "Connexin 32 mutations from X-linked Charcot-Marie-Tooth disease patients: functional defects and dominant negative effects." Mol Biol Cell **7**(6):907-916.
- Owsianik, G., K. Talavera, et al. (2006). "Permeation and selectivity of TRP channels." Annu Rev Physiol **68**:685-717.
- Panov, A. V., C. A. Gutekunst, et al. (2002). "Early mitochondrial calcium defects in Huntington's disease are a direct effect of polyglutamines." Nat Neurosci **5**(8):731-736.
- Parent, A. (1996). "Spinal nerves and peripheral innervation." In: André Parent, Carpenter's Human Neuroanatomy, ninth edition, Patricia Coryell, ed, Williams & Wilkins, Philadelphia.: pp 262-292.
- Pareyson, D. (1999). "Guidelines for the diagnosis of Charcot-Marie-Tooth disease and related neuropathies. Ad hoc Working Group of the Peripheral Nervous System Study Group, Italian Neurological Society." Ital J Neurol Sci **20**(4):207-216.
- Pareyson, D. (2003). "[Diagnosis of hereditary neuropathies in adult-subjects]." Minerva Med **94**(5):301-317.
- Pareyson, D. (2004). "Differential diagnosis of Charcot-Marie-Tooth disease and related neuropathies." Neurol Sci **25**(2):72-82.
- Pareyson, D., V. Scaiola, et al. (2006). "Clinical and electrophysiological aspects of Charcot-Marie-Tooth disease." Neuromolecular Med **8**(1-2):3-22.
- Pareyson, D., F. Taroni, et al. (2000). "Cranial nerve involvement in CMT disease type 1 due to early growth response 2 gene mutation." Neurology **54**(8):1696-1698.
- Passage, E., J. C. Norreel, et al. (2004). "Ascorbic acid treatment corrects the phenotype of a mouse model of Charcot-Marie-Tooth disease." Nat Med **10**(4):396-401.
- Patzko, A. and M. E. Shy (2011). "Update on Charcot-Marie-Tooth disease." Curr Neurol Neurosci Rep **11**(1):78-88.
- Pentao, L., C. A. Wise, et al. (1992). "Charcot-Marie-Tooth type 1A duplication appears to arise from recombination at repeat sequences flanking the 1.5 Mb monomer unit." Nat Genet **2**(4):292-300.
- Peral, B., V. Gamble, et al. (1995). "Splicing mutations of the polycystic kidney disease 1 (PKD1) gene induced by intronic deletion." Hum Mol Genet **4**(4):569-574.
- Perry, T. L., P. J. Bratty, et al. (1975). "Hereditary mental depression and Parkinsonism with taurine deficiency." Arch Neurol **32**(2):108-113.
- Peters, D. J. and L. A. Sandkuijl (1992). "Genetic heterogeneity of polycystic kidney disease in Europe." Contrib Nephrol **97**:128-139.

- Phelps, C. B., R. J. Huang, et al. (2008). "Structural analyses of the ankyrin repeat domain of TRPV6 and related TRPV ion channels." Biochemistry **47**(8):2476-2484.
- Phelps, C. B., R. R. Wang, et al. (2010). "Differential regulation of TRPV1, TRPV3, and TRPV4 sensitivity through a conserved binding site on the ankyrin repeat domain." J Biol Chem **285**(1):731-740.
- Philipp S, W. U., Flockerzi V. (2000). "Molecular biology of calcium channels." In: Calcium Signaling, edited by Putney JWJ. Boca Raton, FL: CRC: pp 321-342.
- Pietrobon, D. (2002). "Calcium channels and channelopathies of the central nervous system." Mol Neurobiol **25**(1):31-50.
- Pridmore, C., M. Baraitser, et al. (1992). "Distal spinal muscular atrophy with vocal cord paralysis." J Med Genet **29**(3):197-199.
- Priest, J. M., K. H. Fischbeck, et al. (1995). "A locus for axonal motor-sensory neuropathy with deafness and mental retardation maps to Xq24-q26." Genomics **29**(2):409-412.
- Puls, I., C. Jonnakuty, et al. (2003). "Mutant dynactin in motor neuron disease." Nat Genet **33**(4):455-456.
- Puls, I., S. J. Oh, et al. (2005). "Distal spinal and bulbar muscular atrophy caused by dynactin mutation." Ann Neurol **57**(5):687-694.
- Pulst, S. M., A. Nechiporuk, et al. (1996). "Moderate expansion of a normally biallelic trinucleotide repeat in spinocerebellar ataxia type 2." Nat Genet **14**(3):269-276.
- Qian, F., F. J. Germino, et al. (1997). "PKD1 interacts with PKD2 through a probable coiled-coil domain." Nat Genet **16**(2):179-183.
- Quaggin, S. E., G. B. Heuvel, et al. (1996). "Primary structure, neural-specific expression, and chromosomal localization of Cux-2, a second murine homeobox gene related to Drosophila cut." J Biol Chem **271**(37):22624-22634.
- Raychowdhury, M. K., S. Gonzalez-Perrett, et al. (2004). "Molecular pathophysiology of mucopolidosis type IV: pH dysregulation of the mucolipin-1 cation channel." Hum Mol Genet **13**(6):617-627.
- Reiser, J., K. R. Polu, et al. (2005). "TRPC6 is a glomerular slit diaphragm-associated channel required for normal renal function." Nat Genet **37**(7):739-744.
- Reiter, J. F. and W. C. Skarnes (2006). "Tectonic, a novel regulator of the Hedgehog pathway required for both activation and inhibition." Genes Dev **20**(1):22-27.
- Riazanova, L. V., K. S. Pavur, et al. (2001). "[Novel type of signaling molecules: protein kinases covalently linked to ion channels]." Mol Biol (Mosk) **35**(2):321-332.
- Rock, M. J., J. Prenen, et al. (2008). "Gain-of-function mutations in TRPV4 cause autosomal dominant brachyolmia." Nat Genet **40**(8):999-1003.
- Rogers, T., D. Chandler, et al. (2000). "A novel locus for autosomal recessive peripheral neuropathy in the EGR2 region on 10q23." Am J Hum Genet **67**(3):664-671.
- Rosenberg, R. N. and A. Chutorian (1967). "Familial opticoacoustic nerve degeneration and polyneuropathy." Neurology **17**(9):827-832.
- Rowland, L. P. and N. A. Shneider (2001). "Amyotrophic lateral sclerosis." N Engl J Med **344**(22):1688-1700.
- Rubin, H. (2005). "Central roles of Mg²⁺ and MgATP²⁻ in the regulation of protein synthesis and cell proliferation: significance for neoplastic transformation." Adv Cancer Res **93**:1-58.

- Russell, J. W., A. J. Windebank, et al. (1995). "Treatment of stable chronic demyelinating polyneuropathy with 3,4-diaminopyridine." Mayo Clin Proc **70**(6):532-539.
- Ryazanova, L. V., M. V. Dorovkov, et al. (2004). "Characterization of the protein kinase activity of TRPM7/ChaK1, a protein kinase fused to the transient receptor potential ion channel." J Biol Chem **279**(5):3708-3716.
- Saito, M., Y. Hayashi, et al. (1997). "Linkage mapping of the gene for Charcot-Marie-Tooth disease type 2 to chromosome 1p (CMT2A) and the clinical features of CMT2A." Neurology **49**(6):1630-1635.
- Sakaguchi, H., S. Yamashita, et al. (2010). "A novel GJB1 frameshift mutation produces a transient CNS symptom of X-linked Charcot-Marie-Tooth disease." J Neurol **258**(2):284-290.
- Santel, A. and M. T. Fuller (2001). "Control of mitochondrial morphology by a human mitofusin." J Cell Sci **114**(Pt 5):867-874.
- Santoro, L., F. Manganelli, et al. (2002). "Charcot-Marie-Tooth disease type 2C: a distinct genetic entity. Clinical and molecular characterization of the first European family." Neuromuscul Disord **12**(4):399-404.
- Schlingmann, K. P., S. Weber, et al. (2002). "Hypomagnesemia with secondary hypocalcemia is caused by mutations in TRPM6, a new member of the TRPM gene family." Nat Genet **31**(2):166-170.
- Schule, R., M. Bonin, et al. (2009). "Autosomal dominant spastic paraplegia with peripheral neuropathy maps to chr12q23-24." Neurology **72**(22):1893-1898.
- Senderek, J., C. Bergmann, et al. (2003). "Mutations in a gene encoding a novel SH3/TPR domain protein cause autosomal recessive Charcot-Marie-Tooth type 4C neuropathy." Am J Hum Genet **73**(5):1106-1119.
- Senderek, J., C. Bergmann, et al. (2003). "Mutation of the SBF2 gene, encoding a novel member of the myotubularin family, in Charcot-Marie-Tooth neuropathy type 4B2/11p15." Hum Mol Genet **12**(3):349-356.
- Sereda, M., I. Griffiths, et al. (1996). "A transgenic rat model of Charcot-Marie-Tooth disease." Neuron **16**(5):1049-1060.
- Sevilla, T., A. Cuesta, et al. (2003). "Clinical, electrophysiological and morphological findings of Charcot-Marie-Tooth neuropathy with vocal cord palsy and mutations in the GDAP1 gene." Brain **126**(Pt 9):2023-2033.
- Shohat, M., R. Lachman, et al. (1989). "Brachyolmia: radiographic and genetic evidence of heterogeneity." Am J Med Genet **33**(2):209-219.
- Shy, M. E., A. Jani, et al. (2004). "Phenotypic clustering in MPZ mutations." Brain **127**(Pt 2):371-384.
- Simpson, D. M., S. Brown, et al. (2008). "Controlled trial of high-concentration capsaicin patch for treatment of painful HIV neuropathy." Neurology **70**(24):2305-2313.
- Skre, H. (1974). "Genetic and clinical aspects of Charcot-Marie-Tooth's disease." Clin Genet **6**(2):98-118.
- Smith, G. D., M. J. Gunthorpe, et al. (2002). "TRPV3 is a temperature-sensitive vanilloid receptor-like protein." Nature **418**(6894):186-190.
- Snipes, G. J., U. Suter, et al. (1992). "Characterization of a novel peripheral nervous system myelin protein (PMP-22/SR13)." J Cell Biol **117**(1):225-238.
- Sobel, E., H. Sengul, et al. (2001). "Multipoint estimation of identity-by-descent probabilities at arbitrary positions among marker loci on general pedigrees." Hum Hered **52**(3):121-131.

- Stojkovic, T., P. Latour, et al. (2004). "Vocal cord and diaphragm paralysis, as clinical features of a French family with autosomal recessive Charcot-Marie-Tooth disease, associated with a new mutation in the GDAP1 gene." Neuromuscul Disord **14**(4):261-264.
- Street, V. A., C. L. Bennett, et al. (2003). "Mutation of a putative protein degradation gene LITAF/SIMPLE in Charcot-Marie-Tooth disease 1C." Neurology **60**(1):22-26.
- Strong, M. J. and P. H. Gordon (2005). "Primary lateral sclerosis, hereditary spastic paraplegia and amyotrophic lateral sclerosis: discrete entities or spectrum?" Amyotroph Lateral Scler Other Motor Neuron Disord **6**(1):8-16.
- Strotmann, R., C. Harteneck, et al. (2000). "OTRPC4, a nonselective cation channel that confers sensitivity to extracellular osmolarity." Nat Cell Biol **2**(10):695-702.
- Strümpell, A. (1883). "Zur Kenntniss der multiplen degenerativen Neuritis." Arch Psychiatr Nervenkr **14**:339.
- Sun, Y., A. Savanenin, et al. (2001). "Polyglutamine-expanded huntingtin promotes sensitization of N-methyl-D-aspartate receptors via post-synaptic density 95." J Biol Chem **276**(27):24713-24718.
- Suzuki, M., A. Mizuno, et al. (2003). "Impaired pressure sensation in mice lacking TRPV4." J Biol Chem **278**(25):22664-22668.
- Tabuchi, K., M. Suzuki, et al. (2005). "Hearing impairment in TRPV4 knockout mice." Neurosci Lett **382**(3):304-308.
- Tang, B. S., G. H. Zhao, et al. (2005). "Small heat-shock protein 22 mutated in autosomal dominant Charcot-Marie-Tooth disease type 2L." Hum Genet **116**(3):222-224.
- Tang, T. S., H. Tu, et al. (2003). "Huntingtin and huntingtin-associated protein 1 influence neuronal calcium signaling mediated by inositol-(1,4,5) triphosphate receptor type 1." Neuron **39**(2):227-239.
- Thiemann, A., S. Grunder, et al. (1992). "A chloride channel widely expressed in epithelial and non-epithelial cells." Nature **356**(6364):57-60.
- Thomas, P. K., D. B. Calne, et al. (1974). "Hereditary motor and sensory polyneuropathy (peroneal muscular atrophy)." Ann Hum Genet **38**(2):111-153.
- Thomas, P. K., W. Marques, Jr., et al. (1997). "The phenotypic manifestations of chromosome 17p11.2 duplication." Brain **120** (Pt 3):465-478.
- Tian, W., Y. Fu, et al. (2009). "A loss-of-function nonsynonymous polymorphism in the osmoregulatory TRPV4 gene is associated with human hyponatremia." Proc Natl Acad Sci U S A **106**(33):14034-14039.
- Timmerman, V., P. De Jonghe, et al. (1996). "Distal hereditary motor neuropathy type II (distal HMN II): mapping of a locus to chromosome 12q24." Hum Mol Genet **5**(7):1065-1069.
- Timmerman, V., P. Raeymaekers, et al. (1992). "Linkage analysis of distal hereditary motor neuropathy type II (distal HMN II) in a single pedigree." J Neurol Sci **109**(1):41-48.
- Todman, D. H. and R. A. Cooke (1984). "Scapuloperoneal myopathy." Clin Exp Neurol **20**:169-174.
- Toledo, S. P., P. A. Mourao, et al. (1978). "Recessively inherited, late onset spondylar dysplasia and peripheral corneal opacity with anomalies in urinary mucopolysaccharides: a possible error of chondroitin-6-sulfate synthesis." Am J Med Genet **2**(4):385-395.

- Tooth, H. (1886). "Two peroneal types of progressive muscular atrophy." Lewis London.
- Tsutsumi, S., N. Kamata, et al. (2004). "The novel gene encoding a putative transmembrane protein is mutated in gnathodiaphyseal dysplasia (GDD)." Am J Hum Genet **74**(6):1255-1261.
- Uyanik, G., N. Elcioglu, et al. (2006). "Novel truncating and missense mutations of the KCC3 gene associated with Andermann syndrome." Neurology **66**(7):1044-1048.
- Van Den Bosch, L., P. Van Damme, et al. (2006). "The role of excitotoxicity in the pathogenesis of amyotrophic lateral sclerosis." Biochim Biophys Acta **1762**(11-12):1068-1082.
- van der Kooi, A. J., T. M. Ledderhof, et al. (1996). "A newly recognized autosomal dominant limb girdle muscular dystrophy with cardiac involvement." Ann Neurol **39**(5):636-642.
- van der Vleuten, A. J., C. M. van Ravenswaaij-Arts, et al. (1998). "Localisation of the gene for a dominant congenital spinal muscular atrophy predominantly affecting the lower limbs to chromosome 12q23-q24." Eur J Hum Genet **6**(4):376-382.
- van Genderen, M. M., M. M. Bijveld, et al. (2009). "Mutations in TRPM1 are a common cause of complete congenital stationary night blindness." Am J Hum Genet **85**(5):730-736.
- Vassilev, P. M., L. Guo, et al. (2001). "Polycystin-2 is a novel cation channel implicated in defective intracellular Ca(2+) homeostasis in polycystic kidney disease." Biochem Biophys Res Commun **282**(1):341-350.
- Vazquez, G., B. J. Wedel, et al. (2004). "The mammalian TRPC cation channels." Biochim Biophys Acta **1742**(1-3):21-36.
- Venkatachalam, K., A. A. Long, et al. (2008). "Motor deficit in a Drosophila model of mucopolysaccharidosis type IV due to defective clearance of apoptotic cells." Cell **135**(5):838-851.
- Vergarajauregui, S. and R. Puertollano (2006). "Two di-leucine motifs regulate trafficking of mucopolysaccharidase-1 to lysosomes." Traffic **7**(3):337-353.
- Verhoeven, K., M. Villanova, et al. (2001). "Localization of the gene for the intermediate form of Charcot-Marie-Tooth to chromosome 10q24.1-q25.1." Am J Hum Genet **69**(4):889-894.
- Vig, P. J., S. H. Subramony, et al. (2000). "Relationship between ataxin-1 nuclear inclusions and Purkinje cell specific proteins in SCA-1 transgenic mice." J Neurol Sci **174**(2):100-110.
- Vincent, F., A. Acevedo, et al. (2009). "Identification and characterization of novel TRPV4 modulators." Biochem Biophys Res Commun **389**(3):490-494.
- Vizioli (1889). "Dell'atrofia progr. Nervosa." Boll R Acad Medico-chir Napoli.
- Voets, T., B. Nilius, et al. (2004). "TRPM6 forms the Mg²⁺ influx channel involved in intestinal and renal Mg²⁺ absorption." J Biol Chem **279**(1):19-25.
- Voets, T., J. Prenen, et al. (2002). "Molecular determinants of permeation through the cation channel TRPV4." J Biol Chem **277**(37):33704-33710.
- Wang, C., H. Z. Hu, et al. (2004). "An alternative splicing product of the murine trpv1 gene dominant negatively modulates the activity of TRPV1 channels." J Biol Chem **279**(36):37423-37430.
- Warner, L. E., P. Mancias, et al. (1998). "Mutations in the early growth response 2 (EGR2) gene are associated with hereditary myelinopathies." Nat Genet **18**(4):382-384.

- Watabiki, T., T. Kiso, et al. (2010). "Amelioration of Neuropathic Pain by Novel Transient Receptor Potential Vanilloid 1 Antagonist AS1928370 in Rats without Hyperthermic Effect." *J Pharmacol Exp Ther* **336**(3):743-750.
- Watanabe, H., J. B. Davis, et al. (2002). "Activation of TRPV4 channels (hVRL-2/mTRP12) by phorbol derivatives." *J Biol Chem* **277**(16):13569-13577.
- Watanabe, H., J. Vriens, et al. (2003). "Anandamide and arachidonic acid use epoxyeicosatrienoic acids to activate TRPV4 channels." *Nature* **424**(6947):434-438.
- Watanabe, H., J. Vriens, et al. (2002). "Heat-evoked activation of TRPV4 channels in a HEK293 cell expression system and in native mouse aorta endothelial cells." *J Biol Chem* **277**(49):47044-47051.
- Wilhelmsen, K. C., D. M. Blake, et al. (1996). "Chromosome 12-linked autosomal dominant scapuloperoneal muscular dystrophy." *Ann Neurol* **39**(4):507-520.
- Winn, M. P., P. J. Conlon, et al. (2005). "A mutation in the TRPC6 cation channel causes familial focal segmental glomerulosclerosis." *Science* **308**(5729):1801-1804.
- Wissenbach, U., M. Bodding, et al. (2000). "Trp12, a novel Trp related protein from kidney." *FEBS Lett* **485**(2-3):127-134.
- Wrabetz, L., M. D'Antonio, et al. (2006). "Different intracellular pathomechanisms produce diverse Myelin Protein Zero neuropathies in transgenic mice." *J Neurosci* **26**(8):2358-2368.
- Wrabetz, L., M. L. Feltri, et al. (2000). "P(0) glycoprotein overexpression causes congenital hypomyelination of peripheral nerves." *J Cell Biol* **148**(5):1021-1034.
- Xu, H., Y. Fu, et al. (2006). "Glycosylation of the osmosensitive transient receptor potential channel TRPV4 on Asn-651 influences membrane trafficking." *Am J Physiol Renal Physiol* **290**(5):F1103-1109.
- Xu, X. Z., F. Moebius, et al. (2001). "Regulation of melastatin, a TRP-related protein, through interaction with a cytoplasmic isoform." *Proc Natl Acad Sci U S A* **98**(19):10692-10697.
- Yamada, T., S. Ugawa, et al. (2009). "Differential localizations of the transient receptor potential channels TRPV4 and TRPV1 in the mouse urinary bladder." *J Histochem Cytochem* **57**(3):277-287.
- Yamamoto, M., R. Ueda, et al. (2006). "Control of axonal sprouting and dendrite branching by the Nrg-Ank complex at the neuron-glia interface." *Curr Biol* **16**(16):1678-1683.
- Yang, Y., Y. Wang, et al. (2004). "Mutations in SCN9A, encoding a sodium channel alpha subunit, in patients with primary erythromalgia." *J Med Genet* **41**(3):171-174.
- Yiangou, Y., P. Facer, et al. (2001). "Vanilloid receptor 1 immunoreactivity in inflamed human bowel." *Lancet* **357**(9265):1338-1339.
- Young, I. D. and P. S. Harper (1980). "Hereditary distal spinal muscular atrophy with vocal cord paralysis." *J Neurol Neurosurg Psychiatry* **43**(5):413-418.
- Young, L. W., J. F. Radebaugh, et al. (1971). "New syndrome manifested by mandibular hypoplasia, acroosteolysis, stiff joints and cutaneous atrophy (mandibuloacral dysplasia) in two unrelated boys." *Birth Defects Orig Artic Ser* **7**(7):291-297.
- Yu, Y., S. H. Keller, et al. (2009). "A functional single-nucleotide polymorphism in the TRPC6 gene promoter associated with idiopathic pulmonary arterial hypertension." *Circulation* **119**(17):2313-2322.

- Zerangue, N., B. Schwappach, et al. (1999). "A new ER trafficking signal regulates the subunit stoichiometry of plasma membrane K(ATP) channels." Neuron **22**(3):537-548.
- Zhang, L. and D. Saffen (2001). "Muscarinic acetylcholine receptor regulation of TRP6 Ca²⁺ channel isoforms. Molecular structures and functional characterization." J Biol Chem **276**(16):13331-13339.
- Zhao, C., J. Takita, et al. (2001). "Charcot-Marie-Tooth disease type 2A caused by mutation in a microtubule motor KIF1Bbeta." Cell **105**(5):587-597.
- Zhou, S., K. Opperman, et al. (2008). "unc-44 Ankyrin and stn-2 gamma-syntrophin regulate sax-7 L1CAM function in maintaining neuronal positioning in *Caenorhabditis elegans*." Genetics **180**(3):1429-1443.
- Zimon, M., J. Baets, et al. (2010). "Dominant mutations in the cation channel gene transient receptor potential vanilloid 4 cause an unusual spectrum of neuropathies." Brain **133**(Pt 6):1798-1809.
- Zoghbi, H. Y. (2000). "Spinocerebellar ataxias." Neurobiol Dis **7**(5):523-527.
- Zuchner, S., P. De Jonghe, et al. (2006). "Axonal neuropathy with optic atrophy is caused by mutations in mitofusin 2." Ann Neurol **59**(2):276-281.
- Zuchner, S., I. V. Mersiyanova, et al. (2004). "Mutations in the mitochondrial GTPase mitofusin 2 cause Charcot-Marie-Tooth neuropathy type 2A." Nat Genet **36**(5):449-451.
- Zuchner, S., M. Nouredine, et al. (2005). "Mutations in the pleckstrin homology domain of dynamin 2 cause dominant intermediate Charcot-Marie-Tooth disease." Nat Genet **37**(3):289-294.

6 Publications that have arisen from the thesis

- ***Landouré G**, *Zdebik AA, Martinez TL, Burnett BG, Stanescu HC, Inada H, Shi Y, Taye AA, Kong L, Munns CH, Choo SS, Phelps CB, Paudel R, Houlden H, Ludlow CL, Caterina MJ, Gaudet R, *Kleta R, *Fischbeck KH, *Sumner CJ. Mutations in TRPV4 cause Charcot-Marie-Tooth disease type 2C. **Nature Genetics**, **2010**;42(2):170-174.

*contributed equally

- Zimoń M, Baets J, Auer-Grumbach M, Berciano J, Garcia A, Lopez-Laso E, Merlini L, Hilton-Jones D, McEntagart M, Crosby AH, Barisic N, Boltshauser E, Shaw CE, **Landouré G**, Ludlow CL, Gaudet R, Houlden H, Reilly MM, Fischbeck KH, Sumner CJ, Timmerman V, Jordanova A, Jonghe PD. Dominant mutations in the cation channel gene transient receptor potential vanilloid 4 cause an unusual spectrum of neuropathies. **Brain** **2010**;133(6):1798-1809.